Fire Performance of a Laterally Loaded Light Timber-framed Compartment

By Daniel Jessop

Supervised by

Associate Professor Michael Spearpoint

Dr Anthony Abu

Hans Gerlich

Colleen Wade

A thesis submitted in partial fulfilment of the requirements for the degree of Master of Engineering in Fire Engineering

Department of Civil and Natural Resources Engineering

University of Canterbury

Private Bag 4800

Christchurch, New Zealand

March 2016

The work reported here was funded by BRANZ from the Building Research Levy

Abstract

The New Zealand Building Code (NZBC) deemed to satisfy solution for houses and small multi-unit dwellings requires external walls within 1 m of and at angles less than 90° to a property boundary to be fire-rated to a minimum 30-min fire resistance rating (FRR). The NZBC also requires structural building systems to remain stable during and after fire when subjected to a uniformly distributed horizontal face load of 0.5 kPa 'in any direction'. This research investigated the fire performance of laterally loaded light timber-framed compartments, to assess their suitability under the NZBC requirements for residential buildings.

The research involved a full-scale standard furnace experiment and a full-scale compartment fire experiment. The building design was based on common New Zealand residential building construction for a light timber-frame building with compartment dimensions of 4.33 m × 3.35 m and stud height of 2.4 m. One of the 4.33 m walls was 30-min fire-rated and the other building elements were of typical non-fire-rated construction. Internal wall and ceiling linings were 10 mm thick standard grade plasterboard, except for the fire-rated wall which had 10 mm fibre-reinforced plasterboard on both sides of the timber framing. The external cladding and roof consisted of light-weight sheet materials except for the fire-rated wall which had no additional covering. The fire-rated wall was subjected to a lateral load applied at the top plate equivalent to a 0.5 kPa face load. The roof truss system was an integral component in providing lateral support to the fire-rated wall and each roof truss spanned between the fire-rated wall and the parallel 4.33 m wall. Each roof truss was designed with a splice in the centre of the bottom chord, connected by toothed metal connector plates.

In the furnace experiment the compartment was heated to the ISO 834 standard time-temperature curve, failure of the roof truss system at the truss connector plate was observed after 30.5 min, causing failure of the roof resulting in lateral deflection of the loaded fire-rated wall. It was found there was non-uniform temperature distribution in the compartment. An analysis of the failure taking into consideration temperature distribution in the compartment suggests that the roof truss system with splice supporting the fire-rated wall would fail in lateral stability after 26 min if the furnace had been driven to achieve the ISO 834 time-temperature relationship at ceiling level. An analysis of expected performance of an unlined compartment predicts a lateral stability failure time of 19.5 min if exposed to the ISO 834 standard time-temperature curve.

The compartment experiment was a natural fire with a fixed initial ventilation and fuel load consisting of wood cribs. The roof truss design incorporated specific protection of the splice using blocks of timber. The wall system failed in lateral stability after 28 min and before all the fuel in the compartment was consumed. Applying a time equivalence method suggests that the fire-rated wall restraint system performance would be the equivalent of 33.5 min in a standard fire resistance test for the compartment. Comparing the results for Experiments #1 and #2, the protection added to the splice improved the performance of the lateral load restraint system from 26 min to 33.5 min. An analysis of expected performance of an unlined compartment predicts a lateral stability failure time of 26 min if exposed to the ISO 834 standard time-temperature curve.

UNIVERSITY OF CANTERBURY
Te Whare Wānanga o Waitaha
CHRISTCHURCH NEW ZEALAND

Deputy Vice-Chancellor's Office
Postgraduate Office

Co-Authorship Form

This form is to accompany the submission of any thesis that contains research reported in co-authored work that has been published, accepted for publication, or submitted for publication. A copy of this form should be included for each co-authored work that is included in the thesis. Completed forms should be included at the front (after the thesis abstract) of each copy of the thesis submitted for examination and library deposit.

Please indicate the chapter/section/pages of this thesis that are extracted from co-authored work and provide details of the publication or submission from the extract comes:
Some of the content of Chapter 5 in the thesis was used to prepare a co-authored paper for the 9th International Conference on Structures in Fire: Jessop D, Abu A, Wade C, Spearpoint M, Gerlich H, Buchanan A. Full-scale fire test of a laterally loaded light timber-framed compartment.

Please detail the nature and extent (%) of contribution by the candidate:
All of the research, analysis and discussion in Chapter 5 of the thesis was prepared by the candidate, except where cited. The co-authored paper was developed with 70% contribution by the candidate and 30% by the co-authors.

Certification by Co-authors:
If there is more than one co-author then a single co-author can sign on behalf of all
The undersigned certifys that:

- The above statement correctly reflects the nature and extent of the Master candidate's contribution to this co-authored work
- In cases where the candidate was the lead author of the co-authored work he or she wrote the text

Name: *Michael Spearpoint (on behalf of all co-authors)* Signature: *M Spearpoint* Date: *18 Mar 2016*

Acknowledgements

First and foremost I would like to thank my supervisors:

- Associate Professor Michael Spearpoint *(UC)* – Your vision and expertise in experimental research has been of exceptional benefit to this research, not to mention the support and guidance you provided to me throughout my time in the Fire Engineering programme for which I am very grateful.
- Dr Anthony Abu *(UC)* – Your creative thinking and problem solving approach to the project helped me rationalise the research approach and was immensely helpful during the analysis. I also wish to thank you for the support during my time in the Fire Engineering programme.
- Hans Gerlich *(Fi-St Consulting)* – Without your enthusiasm and vision the project would have never got off the ground. I am fortunate to have had the opportunity to carry out unique experimental work and thank you for this.
- Colleen Wade *(BRANZ)* – Your guidance and input throughout the project has been exceptionally valuable. Your expertise made it possible to carry out two very challenging full-scale fire experiments and you were always willing to provide help, advice and guidance.

The experimental research was carried out at the Building Research Association of New Zealand (BRANZ), Porirua. I would like to thank all the staff at BRANZ for making me feel welcome and for taking time to provide advice and guidance. In particular thanks to Peter Whiting, Paul Chapman, Peter Collier, Patricia Shaw, Haejun Park and Ed Soja. A special thanks to the lab technicians Lukas Hersche, Rik Engel, Norm Wood, Peter Stewart and Howard Harman for the time spent building, instrumenting, and running the experiments.

I would like to extend my thanks to Grant Dunlop from the University of Canterbury for the time and effort spent preparing equipment for the experimental work.

Versatile Homes & Buildings – A generous thank you for material supply, advice, enthusiasm and support of project. Without your support this project would not have been possible. In particular I would like to thank Jon-Paul Ferris and Dean Murphy for your time and effort that went into supporting the project.

Winstone Wallboards Ltd (GIB®) – Thank you for the materials, labour and support of the research.

Thank-you to the New Zealand Fire Service Commission for their continued support of the Fire Engineering programme at the University of Canterbury. Thanks also to the NZFS for their support in Experiment #2.

I would like to thank my employer, Cosgroves Ltd, for the leave of absence and the company's continued support of my studies, in particular Brady Cosgrove, Barbara Crestani, and the Fire Team. Without your support this would not have been possible. Also special thanks to Dr Dennis Pau for guidance provided throughout my Fire Engineering studies.

Lastly, I would like to thank my friends and family for their understanding during what has been an exceptionally busy year for me. Special thanks to Rhys, Muriel and Chris for opening their home to me in Wellington and making me feel comfortable during all three of my visits while I was away from home carrying out experimental work.

Contents

List of Figures

List of Tables

Nomenclature

Symbol	Description	Units
A	Cross-section area of structural member	m^2
A_f	Floor area of compartment or space being considered	m^2
A_h	Area of horizontal openings in the roof	m^2
A_r	Timber section lost in charring due to corner rounding on one corner	m^2
A_v	Area of vertical vent openings in compartment	m^2
d	Distance from the top of a structural section to the bottom of the design tension zone (commonly height or depth of member)	m
d_i	Distance between truss T_i and $F_{applied}$	m
$d_c(t)$	Depth of char and is a function of time	mm
D	Width and height of each stick in the crib	m
D_A	Depth (height) of timber member section	mm
E	Modulus of elasticity (Young's modulus)	Pa
e_f	Fuel load energy density and may be modified for sprinklered firecells and certain structural elements – for this research no modification factor is applied	$MJ.m^{-2}$
E	Cumulative radiant energy on the assembly over a period of time	$J.m^{-2}$
F	Tension force in the member	N
F_i	Tension force in truss T_i	N
$F_{applied}$	Force applied to the member spanning between truss T_1 and T_2	N
g	Acceleration due to gravity, taken to be 9.81	$m.s^{-2}$
h_i	Height at position *i* relative to a reference point	m
h_p	Thickness of plasterboard layer	mm
h_v	Weighted average height of vertical openings in the compartment	m
H	Average height of the space	m
k_b	A factor taking into account the thermal inertia of different lining materials	-
k_m	A structural material factor and is taken to be 1.0 for protected steel, reinforced concrete, timber or a mix of protected/unprotected steel. For	-

	unprotected steel a different value is calculated based on the area and height of vertical openings, and the floor area.	
L	Span of a member	m
m	Mass of crib remaining (a time-dependent variable)	kg
$\dot{m}_p$	Instantaneous mass loss rate of wood from a crib	$kg.s^{-1}$
M_0	Initial mass of the combustible material in a crib	kg
n	Number of layers of sticks in a crib	-
p_i	Pressure at position *i*	Pa
$\dot{Q}''$	Instantaneous radiant heat flux incident upon an assembly	$W.m^{-2}$
r	Radius of corner rounding due to charring, equals the calculated depth of charring	mm
S	Clear spacing between sticks in a crib	m
t	Time	s
t_{ig}	Time since ignition of crib	s
t_{ins}	Basic insulation value, the fire resistance of a single layer of plasterboard without influence of any adjacent materials	min
t_{min}	Time from ISO-834 furnace test start	min
t_{prot}	Basic protection value, based on an average temperature rise over the unexposed surface of a plasterboard lining being limited to 250°C, and a maximum temperature rise at any one point of no more than 270°C.	min
t_0	Time for flame spread to reach edge of a crib for a centre ignited crib	s
T	Temperature	K
T_0	Ambient temperature	°C
V_i	Velocity at position *i*	ms^{-1}
W_A	Width of timber member section	mm
Δl	Elongation of member	m
ε	Strain	mm/mm
ε_f	Emissivity of fire gases	-
ρ	Density (of air)	$kg.m^{-3}$
σ	Stress	Pa

σ_f	Stefan-Boltzmann constant, 5.67×10^{-8}	$W.m^{-2}.K^{-4}$
v_p	Regression velocity of a crib; a material dependent parameter	$m.s^{-1}$

1 Introduction

1.1 Background

The New Zealand Building Code (NZBC) Acceptable ("deemed to satisfy") Solution for houses and small multi-unit dwellings requires external walls within 1 m of and at angles less than 90° to a property boundary to be fire-rated to a minimum 30-min fire resistance rating (FRR) as shown in Figure 1-1. The NZBC also requires structural building systems to remain stable during and after fire. The associated New Zealand design standards have various provisions for strength and stability assessment of structures at the ultimate limit state. For post-fire structural stability the NZBC Verification Method B1/VM1 simplifies this requirement to the provision of sufficient resistance to ensure that a fire-rated structure does not collapse when subjected to a uniformly distributed horizontal face load of 0.5 kPa 'in any direction'. For residential buildings this 0.5 kPa load is typically applied to fire-rated external walls only.

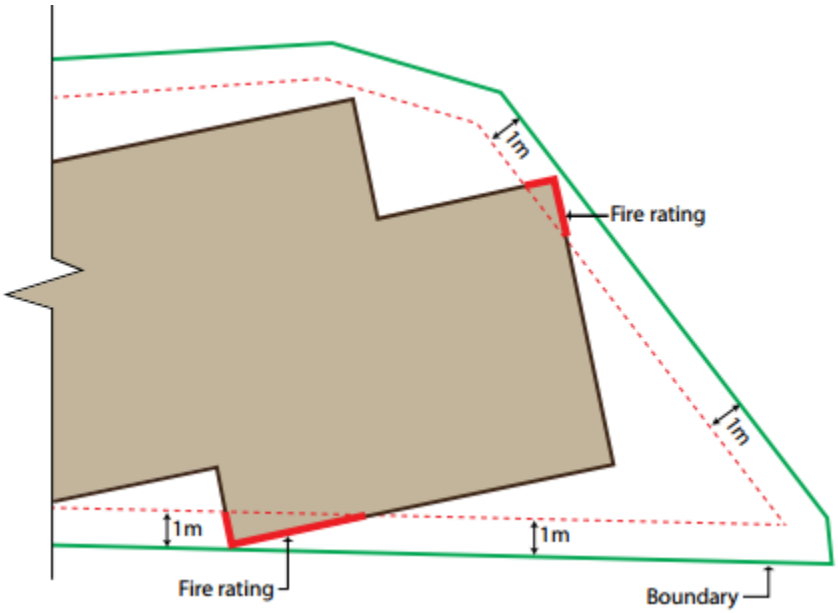

Figure 1-1 – Excerpt from Acceptable Solution C/AS1 (MBIE, 2014c)

Common design methods assume that non-fire-rated elements of buildings fail and do not provide any support to fire-rated elements at the fire limit state. As such, fire-rated external walls of residential buildings are designed to be self-supporting with full fixity at their bases as shown in Figure 1-2. For timber-framed walls this requirement is usually achieved with wider timber framing and additional fixings. These details use the wider foot-print of 140 mm timber framing held down by steel hold-down brackets, screwed into the timber studs and bottom plate, and anchored through the bottom plate into a concrete floor slab beneath.

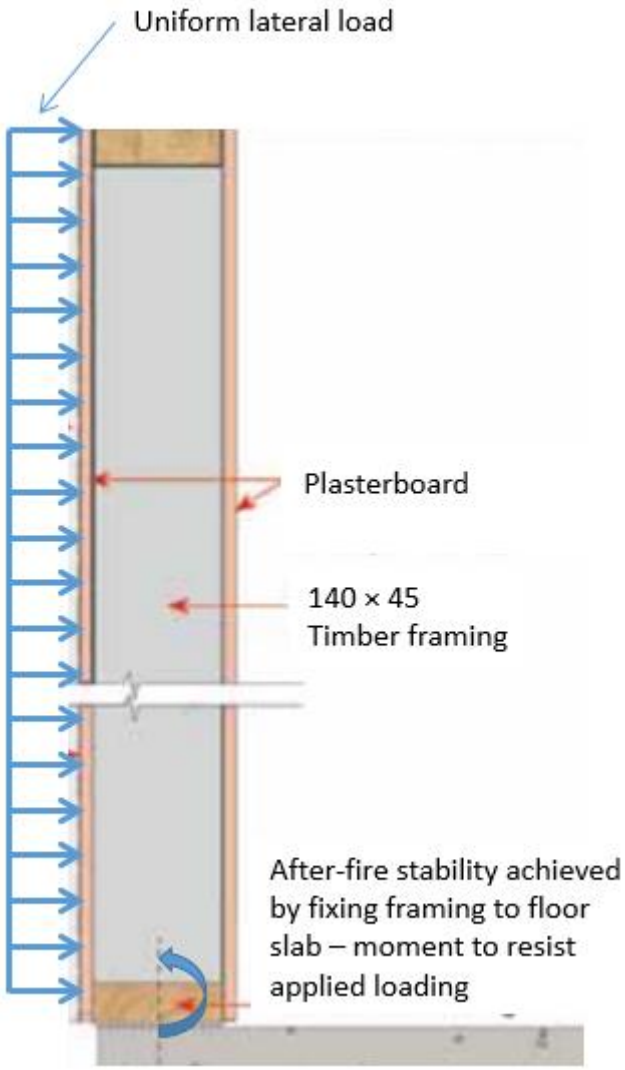

Figure 1-2 – Section showing typical timber wall framing construction for fire-rated external walls in residential buildings (Adapted from Winstone Wallboards (2012))

The use of the wider wall framing and fixing details may be an unnecessary cost. In simple single-storey buildings, support provided by non-fire-rated roof truss systems and non-fire-rated walls may be able to provide sufficient restraint for the lateral load resistance required by the NZBC. However this needs to be ascertained, as the performance of typical non-fire-rated wall and roof truss systems in fire-exposed laterally loaded light timber-framed buildings is not known.

1.2 Research Approach

This research therefore investigates the fire performance of laterally loaded light timber-framed compartments to assess their suitability under the NZBC requirements for residential buildings. It involved two full-scale fire experiments of such a compartment in comparison to analytical predictions of its behaviour. The building design was based on common New Zealand residential building construction details and was designed to fit on the BRANZ fire resistance furnace in its horizontal orientation. This furnace was used for the first experiment in which the compartment was heated to the ISO 834 standard time-temperature curve. The second experiment was a compartment burn experiment with a fixed fuel load and fixed initial ventilation openings.

The compartment dimensions were 4.33 m × 3.35 m with nominal stud height of 2.4 m as shown in Figure 1-3. One of the 4.33 m walls was 30-min fire-rated. The building was lined with 10 mm thick standard grade plasterboard, except for the fire-rated wall which had 10 mm thick fibre-reinforced plasterboard on both sides of the timber framing. The external cladding consisted of light-weight sheet materials to the roof and walls, except for the fire-rated wall which had no additional covering. Five roof trusses spanned between the fire-rated wall and the non-rated long wall. These roof trusses were of timber construction. A splice and truss connector plate connection located mid-span of the bottom chord was included in the experimental setup to assess the performance of such connections, as would commonly be found in trusses spanning greater than 6 m.

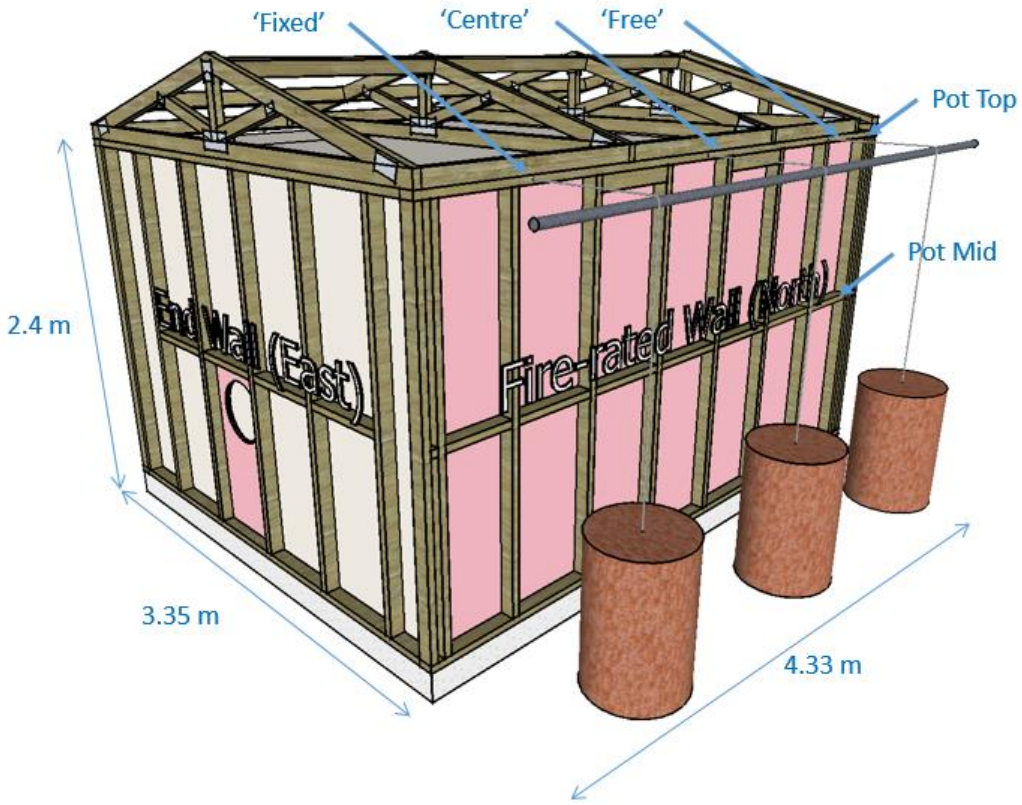

Figure 1-3 – Image of light timber-framed building designed for experimental research

A lateral load was applied at the top of the fire-rated wall to simulate the required 0.5 kPa load as specified in NZBC Verification Method B1/VM1. This was achieved by suspending three water-filled steel drums spaced to distribute equal forces along the top plate of the fire-rated wall via a pulley system. A dummy chord with an array of twelve thermocouples was installed in the roof space of the compartment, at the same height and similar location to the bottom chords of the roof trusses. These temperature readings provided data on the charring rates. Surface temperatures and adiabatic surface temperature measurements were also recorded at a number of locations on the internal walls. The deflection of the laterally loaded fire-rated wall was also measured at various locations during the experiments.

1.3 Thesis Overview

This thesis describes the research carried out, including an investigation into the requirement for lateral stability of fire-rated walls, the methods for assessing performance of light timber-framed buildings in fire, and the experimental research carried out. The thesis concludes by summarising the findings of the research and relates these to NZBC requirements.

Chapter 2 *Fire Safety Design for Buildings* provides an overview of the fire safety objectives in the New Zealand Building Code and describes the structure of the regulatory requirements. Relevant information for fire development and the behaviour of compartment fires is described. The concepts of fire resistance, fire severity and equivalent fire severity are introduced and applied to light timber-framed building design.

Chapter 3 *Residential Light Timber-framed Building Design* discusses the key considerations, assumptions and design requirements unique and specific to light timber-framed building design. This includes structural fire objectives, Fire Service intervention, and design for 'after-fire' or 'post-fire' conditions. The basis for requirements to provide fire resistance ratings to building elements is established and there is a discussion regarding lateral stability of fire-rated elements.

Chapter 4 *Light Timber-frame Building Performance in Fire* describes the main construction elements that make up the fabric of a building and their performance in fire, individually and as a system in a light timber-framed building. Specific building elements described include plasterboard linings, timber framing, light weight wall systems, roof trusses and roof truss connector plates.

Chapter 5 *Experiment #1* describes the experiment building configuration including lateral load and furnace experiment methodology. An analysis of the results, comparison to other research and a discussion is presented in the latter part of the chapter.

Chapter 6 *Experiment #2* describes changes to the experiment building configuration compared to Experiment #1 and the design aspects specific to the compartment experiment such as fuel load and ventilation. An analysis of the results for this experiment, comparison to other research and a discussion is presented in the latter part of the chapter.

Chapter 7 *Summary* provides a summary of the analysis presented in Chapter 5 and Chapter 6, comparing the outcome of the assessment for the two experiments with the New Zealand Building Code requirements. This chapter includes a *Conclusions* section that concludes the research, identifies the limitations, makes recommendations and suggests where further research is required.

2 Fire Safety Design for Buildings

2.1 Fire Safety Objectives

Fire safety objectives may be considered in the context of life safety, environmental protection, property protection and business interruption protection. Life safety is the most common objective and this relates to ensuring people have sufficient time for safe evacuation from buildings before being overcome by the effects of fire or smoke. Life safety also considers the safety of firefighters attending a building fire. Environmental protection relates to limiting environmental damage in the event of a fire and may include consideration for gaseous pollutants in smoke and liquid pollutants in firefighting run-off water. Property protection objectives may relate to protecting a building's structure and fabric, the contents and neighbouring buildings or property (Buchanan, 2001).

Fire safety objectives are met by using active and passive fire protection systems. Active fire safety systems are those considered to limit the effects of fire by an action taken by a device or person (Buchanan, 2001). Passive systems are usually built into the structure or fabric of a building and limit the effects of fire intrinsically. Note that many systems are not readily classified and may exhibit behaviour somewhere between that of an active and passive system, for example intumescent paint. This research is mainly concerned with passive systems used to protect the building fabric.

Uncontrolled fires in compartments may reach what is known as a fully developed post-flashover stage, characterised by intense burning and high temperatures within a compartment. Such a fire involving the structure of a building may threaten neighbouring property due to a radiative heat flux from the building involved in fire or failure of building elements that may fall or impact neighbouring property. A post-flashover fire may also threaten firefighters if there is a risk of heavy building elements collapsing on them. This research is being carried out with the primary consideration being property protection of other property such as neighbouring buildings, and also touches on considerations for safety of firefighters. Life safety is not usually of concern in a small single-level single-firecell building after a fire has reached the post-flashover stage and a successful evacuation has occurred. This research focusses on fires that reach the post-flashover stage and therefore threaten building structure.

Fire design is commonly carried out to either prescriptive requirements or performance based design with specific acceptance criteria. Internationally there has been a move from codes with prescriptive requirements to performance based codes in which a design is accepted if it meets the stated performance requirements. Performance based design requires improved science and more detailed calculation methods (Buchanan, 2008). An understanding and quantitative description of building behaviour and performance in fire is required for engineers to carry out performance based design.

2.2 New Zealand Regulatory Context

2.2.1 Overview

The building industry in NZ is governed by the Building Act 2004 (the Act). Within the Act building regulations are made, and Schedule 1 of the Building Regulations 1992 contains the Building Code. All building work in NZ must comply with the Building Code. The NZBC is a performance-based code that

states how a building must perform in its intended use and does not prescribe the building design or construction (New Zealand Government, 2015d).

The NZBC is structured with five levels. The first three levels are the Building Code objectives, functional requirements and performance criteria and these are mandatory. Below this are two means of compliance documents known as the Verification Method and Acceptable Solutions ("deemed to satisfy"). These two compliance documents are non-mandatory and one way of demonstrating compliance with the requirements of the NZBC. The Acceptable Solutions provide a specific prescribed solution, and the Verification Method provides a way of testing or calculation to demonstrate compliance with the NZBC (New Zealand Government, 2015a). The five levels and descriptions for each are summarised in Table 2-1 as presented by the Ministry of Business, Innovation and Employment (New Zealand Government, 2015b).

Table 2-1 – NZBC structure and levels

	Level	**Description**
Building Code (Mandatory)	1. Objective	The social objective the building must achieve.
Building Code (Mandatory)	2. Functional requirement	What the building must do to satisfy the social objective.
Building Code (Mandatory)	3.Performance criteria	Qualitative or quantitative criteria which the building must meet in order to comply.
Means of compliance documents (Non-mandatory)	4. Verification Method	Prescriptive test or calculation method that provides one means of compliance.
Means of compliance documents (Non-mandatory)	5. Acceptable Solution	Prescriptive step-by-step solution that provides one means of compliance.

A design that differs from that described in the compliance documents is known as an alternative solution. An alternative solution approach can be used to demonstrate compliance with the NZBC performance criteria. The performance criteria is what a design is assessed against; if the design meets the performance criteria then it is considered that the functional requirement and objective will be met. This research investigates building performance in the context of the NZBC performance criteria, and the compliance documents.

Standards New Zealand uses committees to produce Standards. These Standards may be cited in full or in part by Acceptable Solutions or Verification Methods, and may also be cited subject to certain modifications (New Zealand Government, 2015c). There are a number of NZ, Australian and other international standards relevant to this research, and these are introduced throughout this report when relevant.

NZBC Clause A3 (New Zealand Government, 2012a) assigns an Importance Level (IL) to a building based on use and function. A building's IL level has an effect on fire safety design requirements. This research considers IL 2 buildings which are considered as being "buildings posing normal risk to human life or the environment, or a normal economic cost, should the building fail"; this classification applies

to residential buildings and is applicable to this research for the building design and performance requirements.

2.2.2 Building Code Clauses C1 – C6

The NZBC Clauses C1-C6 *Protection from Fire* contain the requirements for building design with respect to fire safety, protection of other property and facilitation of firefighting operations. The NZBC does not consider protection of property under the same ownership. Building Code Clause C1 contains the objectives for Clauses C2 – C6, which contain only the functional requirements and performance criteria. The following paragraphs summarise each of the clauses and specific requirements that relate to this research for residential buildings.

Clause C1 *Objectives of Clauses C2 to C6 (Protection from Fire)* has three objectives that are stated as: *(a) safeguard people from an unacceptable risk of injury or illness caused by fire, (b) protect other property from damage caused by fire, and (c) facilitate firefighting and rescue operations* (New Zealand Government, 2012b). Protection of other property and facilitating firefighting and rescue operations are relevant when considering structural stability of fire-rated elements during and after fire. In a compartment involved in a post-flashover fire, any occupants that have not escaped and remain inside the compartment can be considered to have perished due to high temperatures, high concentrations of toxic combustion products and insufficient oxygen (Spearpoint, 2008). The NZBC does not directly consider protection of people close to or intimate with a fire. There is limited provision for the preventing of fire occurring and this is related to requirements for fixed combustion appliances.

Clause C2 *Prevention of fire occurring* has functional requirements and performance criteria for fixed appliances using controlled combustion intended to safeguard people from illness or injury. For a residential building this would apply when a combustion appliance such as a fireplace is installed or a gas hot water system. This does not relate directly to this research and is not discussed further.

Clause C3 *Fire affecting areas beyond the fire source* has functional requirements that include protecting people from the effects of fire that are not close to the fire source, preventing external vertical fire spread in buildings with a height of 10 m or more and ensuring a low probability of fire spread to other property. Clause C3 is relevant to this research as it directs the requirement to fire-rate external walls and provide stability to these walls. Performance criteria include controls on surface finishes to limit the rate of fire spread in the early stages of a fire, restriction on the allowable height of vertical fire spread over external cladding, restriction on the radiative heat fluxes emitted to relevant property boundaries, and restriction on external cladding materials for buildings within a metre of a property boundary.

Clause C4 *Movement to place of safety* has functional requirements and performance criteria intended to safeguard people from injury or illness caused by fire and providing sufficient time for people to escape from a building. As discussed in Section 2.1, this is unlikely to be of concern once a fire has developed to the stage of threatening the building structure.

Clause C5 *Access and safety for firefighting operations* has functional requirements that consider timely and unimpeded access to a building for emergency services personnel and their safety during rescue and firefighting operations.

Clause C6 *Structural stability* has functional requirements relating to structural systems in buildings, requiring them to maintain structural stability during fire so as there is a low probability of injury or illness to occupants and firefighters, and a low probability of damage to adjacent property. There is also a requirement that failure of building elements with a higher fire resistance does not occur due to the collapse of building elements with a lesser fire resistance (C6.4).

From the above requirements, Clauses C3, C5 and C6 are of particular relevance when designing fire-rated external walls for residential buildings close to neighbouring property and this report will examine those aspects. The fire safety aspects for fuel burning appliances and life safety of occupants of a building are beyond the scope of this report. For residential buildings the performance criteria are commonly met by incorporating passive fire protection methods into the building design and construction. Nyman (2002) describes that fire resistance of building elements to prevent fire spread and collapse of structure is the most important element of passive fire protection.

Compliance with NZBC Clauses C1 – C6 can be achieved by alternative solution or applying the available means of compliance documents (i.e. Verification Method or Acceptable Solution). The Acceptable Solutions are usually the most cost-effective way of demonstrating compliance with the NZBC and with respect to NZBC Clauses C1 – C6 this is the most common pathway for demonstrating compliance for simple residential buildings. Verification Method C/VM2 *Framework for Fire Safety Design* (MBIE, 2014e) can be applied to fire designs for most buildings and is usually applied for designs that do not fit within the constraints of the relevant Acceptable Solution.

There are seven Acceptable Solutions for the NZBC 'C' Clauses, these are C/AS1 – C/AS7. Acceptable Solution C/AS1 *Acceptable Solution for Buildings with Sleeping (residential) and Outbuildings (Risk Group SH)* (MBIE, 2014c) is applied for residential buildings with sleeping use and outbuildings. Examples of sleeping (residential) buildings include houses, townhouses and small multi-unit dwellings. C/AS2 *Acceptable Solution for Buildings with Sleeping (non-institutional) (Risk Group SM)* (MBIE, 2014d) is applied for buildings with permanent accommodation such as apartments, temporary accommodation such as motels, hotels, and education accommodation. This research focuses on self-contained residential buildings and therefore C/AS1 is the most relevant Acceptable Solution. For the purposes of informing the reader and providing a comparison, the requirements of C/AS2 are also touched on. Acceptable Solutions C/AS3 to C/AS7 are for other types of buildings that are beyond the scope of this research, such as commercial buildings, health care facilities, retail stores and institutional facilities with sleeping use (e.g. prisons and hospitals).

2.2.3 Building Code Clause B1

NZBC Clause B1 *Structure* contains the requirements for the structural behaviour and performance of buildings. There are three objectives: *(a) safeguard people from injury caused by structural failure, (b) safeguard people from loss of amenity caused by structural behaviour, and (c) protect other property from physical damage caused by structural failure.* The functional requirement is given in B1.2 and requires buildings and building elements to withstand the combination of loads likely to be experienced throughout their lives. The performance criteria specifically requires consideration for conditions likely to affect stability including fire.

B1/VM1 *General* is a compliance document for the design of structures to meet NZBC Clause B1 requirements and is used for residential buildings (among others). The Verification Method B1/VM1 cites a number of Standards which can be used with modifications given in B1/VM1 to design

structures to meet the performance requirements of NZBC Clause B1. The combined Australian and New Zealand Standard AS/NZS 1170 *Structural Design Actions* is cited by B1/VM1 with modifications and consists of five parts. *Part 0: General principles* provides combinations of actions for fire for assessing structural performance at the ultimate limit state during and after fire. This is the most relevant of the five parts to this research.

B1/AS1 *General* is a compliance document for masonry, timber, earth buildings and stucco, drains and glazing. For timber-framed buildings, NZS 3604 is called up as the Acceptable Solution to B1 with a number of modifications. NZS 3604:2011 *Timber-framed buildings* (Standards New Zealand, 2011c) has no requirements for building structure performance during and after fire and the modifications made by B1/AS1 do not add any requirement for stability during and after fire. The only requirement in NZS 3604 relating to fire is in Paragraph 10.1.5.2 requiring that anchorages shall not extend through the wall or reduce the fire integrity rating of the wall.

2.3 Compartment Fires

2.3.1 Fire Development

A fire may go through a number of phases from the time of ignition to the time of extinguishment as described by Spearpoint (2008). These are often labelled as: incipient and ignition, growth, flashover, fully developed and decay as shown in Figure 2-1 for a fire assuming no intervention. Not all fires will follow these phases, some fires may go out naturally in the early phases and these are of no interest to this research. As described in Sections 2.1 and 2.2, this research focusses on fires that threaten building structure and therefore transition to a fully-developed post-flashover phase.

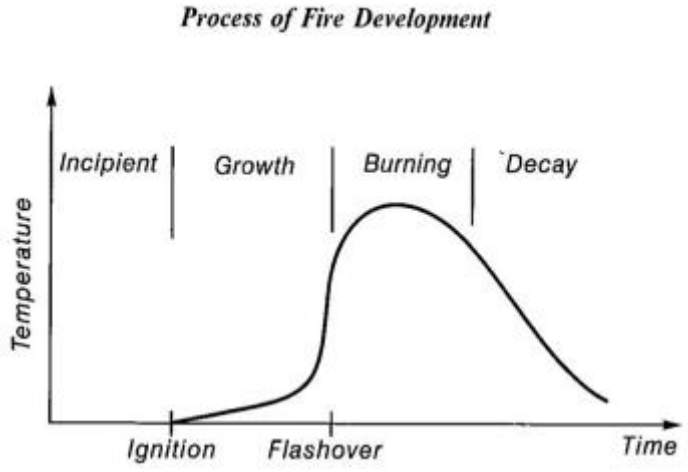

Figure 2-1 – Phases of fire development in terms of compartment temperature for a typical fire, taken from Buchanan (2001)

Flashover is used to describe the demarcation between the pre-flashover and post-flashover stages of the compartment fire (Karlsson & Quintiere, 2000). ISO 13943:2008 *Fire Safety – Vocabulary* (Technical Committee ISO/TC 92, 2008) defines flashover as *"transition to a state of total surface involvement in a fire of combustible materials within an enclosure*". Common criteria for flashover include a compartment temperature of 500-600°C, or radiation to the floor of the compartment at 15

to 20 kW/m^2, or the occurrence of external flaming from enclosure openings (Karlsson & Quintiere, 2000).

The fully developed phase of a compartment fire follows flashover and is often characterised by ventilation-controlled burning due to combustion within the compartment being limited by the availability of oxygen. The energy released from the fire within the room is often at its highest and external flaming may occur at the openings as unburnt gases escape the compartment and meet a fresh supply of oxygen from outside air, resulting in flaming combustion. The energy released within the compartment is governed by the size of compartment openings. Average gas temperatures in a compartment during the fully developed phase of a fire may be in the range 700°C to 1200°C (Karlsson & Quintiere, 2000).

As fuel is consumed and the surface area of fuel available reduces there is a reduction in the burning rate of fuel in the compartment. The fire may become fuel-controlled rather than ventilation-controlled and the average gas temperature in the compartment will decline (Karlsson & Quintiere, 2000). The time following fire transition from ventilation controlled burning to fuel controlled burning is known as the decay phase and this will continue until the fire goes out. England et al (2000) define the decay period as starting when the temperature in the enclosure has reduced to 80% of its peak, and other sources suggest that when 80% of the fuel has been consumed a fire can be considered to be entering the decay phase (Spearpoint, 2008).

The fully developed and decay fire phases are usually of most interest in structural fire engineering (Spearpoint, 2008). The fully developed phase is when the peak compartment temperatures usually occur, and due to thermal inertia effects the peak temperature within an element may occur during the decay phase of the fire.

2.3.2 Quantifying Compartment Fires

Fire engineering design commonly requires quantitative description and prediction of a compartment fire. This is most commonly done in terms of the time-temperature relationship for a compartment and this is an important measure of fire severity (Thomas, 2008). Time-temperature histories for compartments are used as inputs for certain equivalent fire severity methods such as the cumulative radiant energy method as described in Section 2.5.5. There are a number of factors that will influence the temperature rise in a compartment, including:

- Fuel types, quantities, locations, geometry
- Enclosure dimensions
- Enclosure ventilation (types, locations and geometries)
- Enclosure bounding construction materials
- Proportion of fuel actually burned in the enclosure

The temperature in a compartment will be dependent on the heat release rate (HRR) of fuel within the compartment, noting that not all fuel will necessarily burn within the compartment. Thomas (2008) noted that *"no currently available formula provides a satisfactory basis for estimating a universally applicable enclosure temperature-time relationship"*. The HRR will be primarily influenced by the fuel and enclosure ventilation factors listed above. For ventilation controlled burning of wood, experimental investigation showed that the rate of burning $\dot{m}$ [kg/s] in a room with a single opening can be approximated as $\dot{m} = 0.092 A_v \sqrt{H_v}$ (Buchanan, 2001). Many studies have found an empirical

dependence on the term $A_v\sqrt{H_v}$ (Buchanan, 2001). Opening size and location was an important consideration for the compartment experiment of this research, as described in Section 6.3.2.

For many compartments the temperature within the enclosure may vary significantly with location within the compartment. The distribution of temperature will be dependent on the distribution of ventilation openings around the compartment. If the openings are uniformly distributed across the width of an enclosure then the air flows are essentially 2-D changing along the depth of the compartment. In this instance, the depth to width ratio of the compartment has little influence. For the case where there is a single opening, if this opening width is much less than the width of the enclosure, then the flows into/out and within the enclosure can be quite complex, and the depth to width ratio of the compartment becomes important. If the depth to width ratio is >>1 then the flow essentially becomes two dimensional (uniform across the width of the enclosure) at some distance from the opening. It is worth noting that in many 'real' fires the ventilation conditions can be expected to change (Thomas, 2008).

CIB carried out 321 experiments on a number of compartments with depths and widths ranging from 0.5 m to 6 m, and heights from 0.5 to 1.5 m as described by Thomas (2008). Thomas (2008) refers to the "80/30 period", the time from 80% to 30% of fuel mass remaining as the period of steady burning of the fire. The fuel used was wood cribs with the fuel load being 10, 20, 30 or 40 kg/m^2 floor area. Opening size was the full height of the compartment and centrally located; the widths used were one-quarter, one-half, three-quarters or full width. Temperature measurements were taken in two locations at the centre of the compartments: at a quarter and three-quarters of the enclosure height. It is noted that in some instances the lower thermocouple was inside the crib. Thomas (2008) comments that the average temperature of the 80/30 period is "*a very poor representation of the maximum measured temperature"* and the 80/30 mass loss rate *"may not always represent the maximum mass loss rate accurately".* The experiment results show considerable variation in rate of burning for each fixed ventilation parameter, and considerable variation in average gas temperature for each ventilation factor.

British Steel in cooperation with the Fire Research Station at Cardington, United Kingdom (BS/FRS) carried out a number of experiments in an enclosure 22.9 m deep × 5.6 m wide × 2.75 m high as described by Thomas (2008). The enclosure had a single opening in the 5.6 m wall, and the opening size was varied from 1/8th to the full wall area in sizes of 12.5%, 25%, 50% and 100%. The results show comparable maximum temperatures for the 100%, 50% and 25% ventilation cases, and a much lower maximum ventilation for the 12.5% vent area. It was found that different ignition modes resulted in little difference in the maximum temperatures reached or the duration of high temperatures (Thomas, 2008).

2.3.3 Empirical Calculation of Compartment Fires

The parametric time-temperature curve defined in Annex A of Eurocode EN 1991-1-2:2002 (CEN, 2002) is a set of empirical equations that are used to generate gas temperature histories for a fire in a compartment. The method takes into account the thermal properties of the bounding surfaces of the enclosure, ventilation geometry, fuel load and the initial fire growth rate. It can be used for compartments up to 500 m^2 floor area, without openings in the roof and for maximum compartment heights up to 4 m. There is an implicit assumption that the fire load of the compartment is completely burnt out, and the approach is suitable for fire compartments with mainly cellulosic type fire loads,

although fire load densities can be specified to take into consideration the combustion behaviour of the fuel (CEN, 2002).

Kirby (2004) reviewed the Eurocode EN 1991-1-2:2002 parametric curves validation and considered that generally they provided good agreement between predicted and measured temperatures. It was also found that in the instances where they did not agree, the predicted temperatures were on the conservative side.

2.3.4 Computer Modelling using Zone Models

Zone models use numerical simulation to predict average macroscopic features of a compartment fire. They are based on the fundamental principles of mass and energy conservation. The most common model is the 'two-zone' model which splits the gases in a room into an upper and lower layer, each of which is spatially uniform. Differential equations are solved for pressure, upper layer volume, temperature of each layer and the rate of change of mass in the upper and lower layers. The upper layer volume can be used to calculate the layer height, and the rate of change of mass in the layers will take into account fuel mass loss rate, vents and gaseous flows between layers. A single zone model solves the same set of equations except the upper layer volume, flow between layers and layer height equations are not required (Quintiere, 2008).

Wind effects may affect entrainment rates in a plume and this can be taken into account in plume equations solved in a zone model. Zone models commonly assume that the volume of the fire plume is small relative to the zone volume and therefore effects of this are ignored, similarly the heat capacity of the contents of the room are usually ignored. The wall, ceiling and floor thermal properties including heat capacity is usually taken into account when calculating heat losses through the compartment boundaries. Ventilation flow through vertical openings are calculated based on temperature and density differences using orifice flow theory and utilising Bernoulli's equation along a streamline (Quintiere, 2008). The vertical pressure distribution over the height of an opening can also be calculated using basic fluid mechanics.

Most zone models will estimate convective heat transfer to the bounding surfaces of a compartment using empirical correlations for natural convection. Similarly, due to the complexity and insufficient development of appropriate models, radiative heat transfer from flames is usually based on empirical relationships. Radiation from the smoke layer is easier to calculate in principle however there are challenges associated with determining the properties of the smoke particulates and their contribution to the layer radiation (Quintiere, 2008).

The zone model software B-RISK from BRANZ is freely available. This software includes the capability to model compartments as single or two zone spaces, except for the compartment of fire origin which must be two zone, and a post-flashover subroutine based on burning wood cribs (Wade et al., 2013). B-RISK was used to predict compartment temperatures for various fuel and ventilation configurations considered in the Experiment #2 design, as described in Section 6.3.4.

2.4 Fire Resistance

2.4.1 Introduction

The fire resistance of a building element is a property which gives it the ability to withstand a fire of a certain severity. For an element to perform its intended function during and after fire, the fire resistance of that element needs to be greater than the fire severity. Fire resistance is commonly defined in terms of the time for which an element meets a set of criteria when exposed to a standard test furnace fire (Spearpoint, 2008) and is stated as a fire resistance rating (FRR) for that element. Fire resistance can be compared to fire severity in one of three domains; time, temperature or strength. In the time domain, the time to failure is compared to the fire duration. For the temperature domain, the temperature that causes failure for a specified element is compared to the maximum temperature reached in the element during the fire. Lastly, the strength domain compares the applied (design) load during the fire with the load capacity of the element at elevated temperature. Verification of the performance of each element is most commonly carried out in the time domain (Buchanan, 2001).

2.4.2 Test Methods

Testing provides a means of acceptance and can also act as a data source which can be used to support variations by assessment (Collier, 2000). Most countries require full-scale testing in a large furnace because of practical difficulties in calculations and limitations in small-scale tests which may not be representative of full-scale behaviour. Small-scale tests may not capture effects of shrinkage, deflections, connection problems or gaps between panels of lining materials which could occur in real fires or in full-scale tests. The full effects of radiant heat transfer also cannot be captured in small-scale tests. For structural members required to be tested under load, it is difficult to equate loads between small-scale tests and full-scale tests because there is not a linear relationship between the load applied and the bending moment in an element. Small-scale testing is most commonly used to supplement data already gathered from full-scale testing (Buchanan, 2001).

Full-scale testing is also commonly preferred over assessment by calculation. There are practical difficulties in carrying out fire resistance rating calculations. This principally relates to the significant number of unknowns associated with material behaviour in fire, including thermal properties which are temperature dependent, and defining heat transfer coefficients which apply at the boundaries. A good physical understanding of the test scenario is required and for these reasons calculations need to be based on full-scale fire resistance test results of similar assemblies to enable a comparison with a tested assembly to be made (Buchanan, 2001).

In New Zealand the most common method for obtaining FRRs is by full-scale testing (Nyman, 2002). Tests are carried out at the Building Research Association of New Zealand (BRANZ) fire laboratory located in Judgeford, Porirua, New Zealand. The facility has a full-scale furnace that can be orientated either horizontally or vertically. The furnace is capable of testing specimens that fit onto a frame with an opening of approximately 4 m × 3 m and has been used to test floor, wall and door constructions (among others). BRANZ carries out testing to AS 1530 Part 4 (SAA, 2005), ISO 834 (ISO, 1999) or BS 476 Parts 20-23 (BSI, 1987) as required. There is similarity in the methods of testing and requirements of these standards (Nyman, 2002). Figure 2-2 shows the full-scale furnace at BRANZ in the horizontal orientation.

Figure 2-2 – BRANZ furnace in horizontal orientation with burners firing

2.4.3 Fire Resistance Ratings

A fire resistance rating (FRR) is usually expressed in minutes or hours and is the time that the building element can meet a certain set of criteria when exposed to a standard fire test. A constructed system is assigned a FRR based on the time to failure under a standard fire test for one or more of each of the following general failure criteria: structural adequacy, integrity and insulation.

Structural adequacy applies to load-bearing elements and tests the performance under a fixed loading condition during fire. It is of interest to note that AS 1530 Part 4 does not specify a load to use when testing structural adequacy. It is important that regulators and practicing engineers are aware of the load which was applied to a fire rated system in the standard fire resistance test when considering its performance in fire.

Testing standards will often have a limit on deflection or rate of deflection for structural adequacy, so that the test can be stopped before collapse of the specimen occurs, which may cause damage to the furnace (Buchanan, 2001). For horizontal load-bearing elements such as beams and floor systems, deflection is commonly required to be measured at the mid-span of the element and may be measured at other locations where significant deflection is likely to occur during the test (SAA, 2005).

For vertically loaded elements such as a beam or floor system, AS 1530 Part 4 defines two criteria to check for failure; one is a limiting deflection based on the ratio of the span of the element to the depth of the load-bearing part of its structure, and the second is based on the rate of deflection of that same ratio and calculated over 1 min intervals. These criteria for limiting deflection and limiting rate of deflection are shown in Equation 2-1 and Equation 2-2 respectively. The rate of limiting deflection does not apply before a deflection of L/30 is exceeded due to relatively rapid deflections that can occur before stable conditions are reached.

$$Deflection = \frac{L^2}{400d}$$ *Equation 2-1*

$$Rate\ of\ deflection = \frac{L^2}{9000d}$$ *Equation 2-2*

Integrity failure occurs when cracks, fissures or other openings develop that allow the passage of flames or hot gases (SAA, 2005). For a plasterboard lined wall this would occur when a gap forms in the lining or a sheet of plasterboard falls off on the unexposed side of the wall, allowing hot smoke and/or flame to pass through the wall. Failure to properly treat penetrations through a wall could lead to an early failure by this mode. AS 1530 Part 4 (SAA, 2005) provides methods for testing for integrity failure using gap gauges, a cotton pad or visible sustained flaming. Sustained flaming on the surface of the unexposed face for 10 s or more is considered to be an integrity failure. The cotton pad method tests for ignition of a cotton pad held up to the unexposed face, and this method is not appropriate for specimens that do not have an insulation rating as the radiant heat can cause ignition of the cotton pad. Gap gauges are used to measure the size of an opening and if this size exceeds a defined width and length then an integrity failure is considered to have occurred.

Insulation failure occurs when the temperature rise on the unexposed side of the wall exceeds specified criteria. For a test to AS 1530 Part 4 (SAA, 2005) this is an average temperature rise of 140°C, or a peak rise at any thermocouple of 180°C. The temperature rise is referenced against the average temperature measured on the unexposed face of the wall within 5 min before the start of the test.

Fire resistance ratings are assigned to elements in the form of xx/xx/xx where the time of fire resistance in min is assigned in the order of 'structural adequacy/integrity/insulation'. The standard time-temperature relationship for the fire used in AS 1530 Part 4 (SAA, 2005), ISO 834 (ISO, 1999) or BS 476 Parts 20-23 (BSI, 1987) is found in the international standard ISO 834 (ISO, 1999). ISO 834 defines the time-temperature relationship as shown in Equation 2-3.

$$T = 345 \log_{10}(8t_{min} + 1) + T_0$$ *Equation 2-3*

There are differences between the test standards but these can be considered to be relatively insignificant. The differences usually relate to furnace pressure and the method of obtaining furnace temperature measurements. The use of the plate thermometer to measure and control gas temperature in the furnace has improved reproducibility between different test furnaces. However AS 1530 Part 4, which is the standard commonly used in NZ, does not require the use of plate thermometers, this is in contrast to Europe where for example BS EN 1363-1 *Fire resistance tests, General requirements* (BSI, 2012) requires plates to be used (Wade, Gerlich, & Abu, 2014).

One perceived shortfall with furnace testing is that there is no requirement for repeatability in the test regime. A single test only is required, or a number of tests can be carried out for a specimen type and the most favourable result taken (Wade et al., 2014). It is therefore difficult to know how representative a tested system is. For example, in 2009 a round robin of resistance fire tests were carried out by 32 laboratories (Dumont, 2010) according to EN 1364-1:1999 *Fire resistance tests for non-loadbearing elements – Walls* (CEN, 1999). The fire resistance criteria measured were integrity and insulation. The test specimen consisted of a gypsum plasterboard partition with a steel stud frame

and one gypsum plasterboard layer on each side of the frame. The results showed a significant range in both integrity and insulation failure times in the tests. With outliers removed, most of the integrity values fall within a range of 51 to 80 min, and most of the insulation values between 45 and 65 min.

2.5 Fire Severity

2.5.1 Introduction

Fire severity can be considered as the measure of destructive impact of a fire. For real fires it is not appropriate to define this in terms of exposure to the standard fire as real fires will have different characteristics and would only coincidentally be similar to a standard fire (Buchanan, 2001). England et al. (2000) suggest that fire severity is often represented in terms of: time-temp relationship in enclosure, HRR time-temp relationship, heat flux-time relationship, equivalent time of exposure to the standard fire. The fire severity will depend on fuel type and geometry, fire compartment construction and geometry, size and location of ventilation openings and needs to be considered in the context of the element being exposed to the fire.

Five full-scale compartment fire experiments were carried out by Blackmore et al (Blackmore et al., 1999) with compartment dimensions of 3.6 m deep × 3 m wide × 3 m high. There were two openings; a door opening measuring 2 m high × 0.8 m wide located centrally in one of the short walls, and a window measuring 2 m wide × 1.8 m high located centrally in a long wall. There was a false ceiling at 2.4 m above floor level, and the top sill of the window was flush with the ceiling. The average theoretical fire load energy density (FLED) was 808 MJ/m^2. Two different wall constructions were tested; light timber framing with plasterboard and masonry. Experimental results found that in the early stages of the fire within 5 min of ignition, temperatures reached close to 1000°C and 1100°C for the plasterboard and masonry compartments respectively. This is more severe than the standard fire, which after 5 min has a temperature rise of 556°C above ambient temperature. As the compartment fire reached the decay phase and temperatures decay, the temperatures in the standard furnace test become more severe.

Section 2.3.2 described compartment fires and introduced some of the concepts including the factors that affect compartment temperature. Compartments with larger vent openings will usually result in hotter burning fires with a shorter duration, whereas smaller vent areas will result in cooler fires with a longer burning duration. These effects are significant when considering the fire severity experienced by structural elements. Intuitively it may seem that a higher compartment temperature would be more severe, however a longer duration fire has more time for the heat to penetrate building elements. Although the peak fire temperature is not as high. As a result of this longer duration, a compartment fire with a lower maximum temperature may be more severe when considering the effect on structure. These factors were an important consideration for designing Experiment #2, as described in Section 6.3. Figure 2-3 shows an indicative time-temperature curve that compares the standard (ISO 834) fire with possible fires in compartments with relatively small (bold line) and relatively large (thin line) openings.

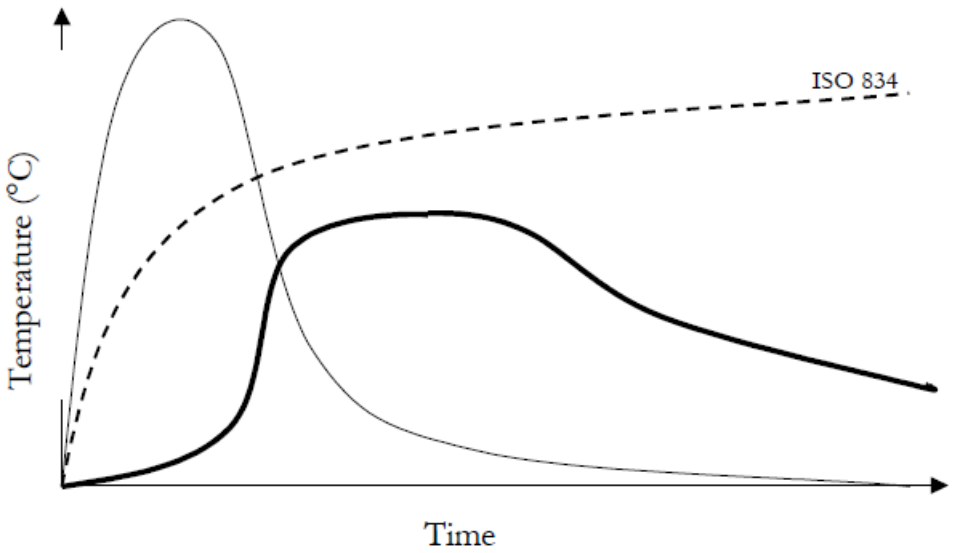

Figure 2-3 – Time-temperature curve for the standard fire, and fires in a compartment with relatively small and relatively large openings (bold and thin lines respectively), taken from Nyman (2002)

2.5.2 Equivalent Fire Severity Concept

Fire resistance ratings for building elements are expressed in terms of exposure to a standard fire. As previously described it is widely recognised that standard fire resistance tests are not representative of real fire exposure, and therefore a method of assessing the performance of a building element or elements when exposed to a realistic fire is required. It is uncommon to calculate performance of elements exposed to non-standard fires from first principles due to an absence of well-developed calculation methods for many materials and systems. In addition to this, although time-temperature curves for real fires can be readily modelled, it is unfeasible to test each construction system against the large variety of possible design fire scenarios (Buchanan, 2001). A method is required for equating predicted real compartment fires with the performance of construction elements based on standard testing.

The concept of "equivalent fire severity" has been developed based on the principle of comparing the time-temperature history of a compartment fire with the standard furnace test. There are two main aspects to the comparative analysis carried out; one is the parameters that are used to determine the expected compartment gas temperatures, and the other is the assessment of the impact of the compartment temperature on the construction elements being considered. This two-step approach was used to compare building performance in Experiment #1 and #2.

The time to failure is likely to be more than the FRR if the actual fire severity is less than that of the ISO-834 furnace test. This would occur for compartments with low fuel loads (MJ/m^2) and/or significant roof venting. If the actual fire severity is greater than that of the ISO-834 test then the time to failure would likely be less than the FRR. Nyman (2002) found that when a light-weight wall assembly is exposed to a fire of higher severity than the standard fire in the early stages, the wall will fail significantly sooner than indicated by the unexposed face temperature profile. In addition to this, the loading conditions on a load-bearing structure may be different to the loads applied in the furnace test and this may affect the failure time for a load-bearing structure.

2.5.3 Equivalent Fire Severity Calculation Methods

There are a number of calculation methods for equivalent fire severity, including the "equal area concept", "maximum temperature concept", "minimum load capacity concept", and "time equivalent formulae" as described by Buchanan (2001). Time equivalence methods are most commonly applied in New Zealand and can be considered to be most useful for determining FRR's when there is limited information about the specific behaviour and response of the construction elements (Wade et al., 2014).

A number of time equivalence methods have been developed based on temperature measurement of unloaded protected steel members. They are based on the premise that a protected steel member can survive compartment burnout if it can sustain the same maximum temperature in a standard furnace test without failure. Experiments were carried out with a number of different ventilation conditions on a limited number of members. The tests are not considered to be indicative of structural performance, but a means by which to compare the temperature recorded in the element during exposure to the standard test fire. Time equivalent methods calculate an equivalent fire resistance rating, that if an element is protected to that rating (or greater) then burnout of a compartment can occur without structural failure (Buchanan, 2001).

Time equivalence methods have been validated for use with reinforced concrete as well as protected steel members, and both these types of members are sensitive to critical temperature. Timber construction materials behave inherently different in fire in that charring of wood may continue even after the fire has exhausted the fuel contents of the compartment, unless the timber has been specifically protected to prevent charring. For these types of members which continue to decay during the cooling phase of the fire, time equivalence methods may not be valid. The continued degradation of such elements may result in eventual failure even after the fuel contents of the compartment have been consumed (Wade et al., 2014).

Although time equivalent formulae were not developed specifically for light timber-frame construction, they can be useful (Buchanan, 2001) particularly if the intent is to use a temperature-based time equivalence method to calculate protection required to prevent a timber element from charring (Wade et al., 2014). They still need to be used with caution as gypsum plasterboard and timber framing elements will continue to decay after the point of maximum temperature has been reached, and a longer cooler fire could be similar or more severe for these elements than a shorter hotter fire that raised a steel element to a higher temperature. The time equivalence approach does not take into account variations in properties of the structure and therefore there is an inherent risk in over-simplification (Wade et al., 2014).

In NZ the most commonly used time equivalence formula and that which is referenced in C/VM2 is the Eurocode formula (CEN, 2002) and as described by Buchanan (2001) is based on a formula published by the CIB W14 group (CIB, 1986) and Law (Law, 1971) formulae, and based on research by Schneider et al. (1994). Kirby et al. (1999) proposed some modifications to the Eurocode values for k_b for large spaces. These modifications are not considered to be required for the size of enclosures being considered in this research.

2.5.4 Eurocode Time Equivalence Formulae

Verification Method C/VM2 (MBIE, 2014e) refers to the Eurocode time equivalence formula as one method to determine fire severity for a full burnout design fire. A fire resistance rating applied to

external walls protecting other property and their support systems and for primary structural elements in buildings >25 m tall is commonly required to be sufficient to withstand burnout of the fuel contents of the compartment. The Eurocode time equivalence method is generally accepted for use with protected steel members and reinforced concrete members. It is not intended for use with light-weight construction and unprotected steel. Research by Thomas (1996) suggests that using the time equivalence formula can be on the un-safe side for many cases. Wade et al. (2014) note that use of time-equivalence methods to specify a fire resistance rating intended to withstand burnout of a firecell will not necessarily provide certainty that the Building Code functional requirements to prevent fire spread or structural collapse will be achieved. The Eurocode time equivalent formula is used in this report is that stated in C/VM2 and is given in Equation 2-4.

$$t_e = e_f k_b k_m w_f \qquad \textit{Equation 2-4}$$

Where: w_f is the ventilation factor that takes into account horizontal and vertical openings and is calculated as:

$$w_f = \left(\frac{6.0}{H}\right)^{0.3}\left[0.62 + \frac{90(0.4-\alpha_v)^4}{1+b_v\alpha_h}\right] \geq 0.5$$

$$\alpha_v = \frac{A_v}{A_f} \quad 0.025 \leq \alpha_v \leq 0.25$$

$$\alpha_h = \frac{A_h}{A_f} \quad \alpha_h \leq 0.20$$

$$b_v = 12.5(1 + 10\alpha_v - \alpha_v^2) \geq 10.0$$

2.5.5 Cumulative Radiant Energy Method

Nyman proposed a method that quantifies fire severity based on the total energy impinging on a surface. Three full-scale tests were carried out by Nyman (2002) with compartments constructed of various light-weight timber and steel-framed walls and ceiling/floor systems. The compartment size was based on an ISO 9705:1993 (ISO, 1993) room with internal dimensions of 3.6 m deep × 2.4 m wide × 2.4 m high and a single opening of 2.0 m high × 0.8 m wide in one of the shorter walls. A number of different assembly types were tested in the standard furnace and also in the compartment, to allow a comparison of failure times. Fires in the compartment were designed to simulate rapid fire growth followed by ventilation controlled burning (Wade et al., 2014).

Babrauskas (1976) states that the predominant mode of heat transfer to an assembly in the post-flashover phase of a fire is by radiation. Radiant heat transfer is a function of the temperature raised to the fourth power and therefore Nyman's approach calculates fire severity based on the area under a plot of emissive power of the compartment gas vs time as shown in Equation 2-5. Emissivity, ε_f, is conservatively taken as 1 to simplify the calculation. Based on the experiments that were carried out, Nyman (2002) found that the time to failure of non-load-bearing drywall assemblies can be predicted to a reasonable level of accuracy by considering the cumulative radiant energy (CRE) the assembly is exposed to. Nyman's method implicitly assumes that the different fires (real and furnace) have the same energy characteristics in that the convective components of the fire's heat transfer to the assembly are of equal proportion to the total energy transferred (Nyman, 2002).

$$E = \int_0^t \dot{Q}'' dt = \varepsilon_f \sigma_f \int_0^t (T^4) dt \qquad [\text{J.m}^{-2}] \qquad \textit{Equation 2-5}$$

Nyman's emissive power of fire gases method can be used to calculate an equivalent fire severity for a building element exposed to a real fire and compare this to the performance observed in a standard fire test. The general concept is that the cumulative radiant energy received during a real fire can be calculated based on a time-temperature curve for gas temperatures in the compartment, and this can be equated to the cumulative radiant energy received during the standard fire test based on the test's time-temperature curve as shown in Figure 2-4. For an assembly with a known failure time when exposed to the ISO curve, the failure time when exposed to a different (i.e. real fire) can be predicted.

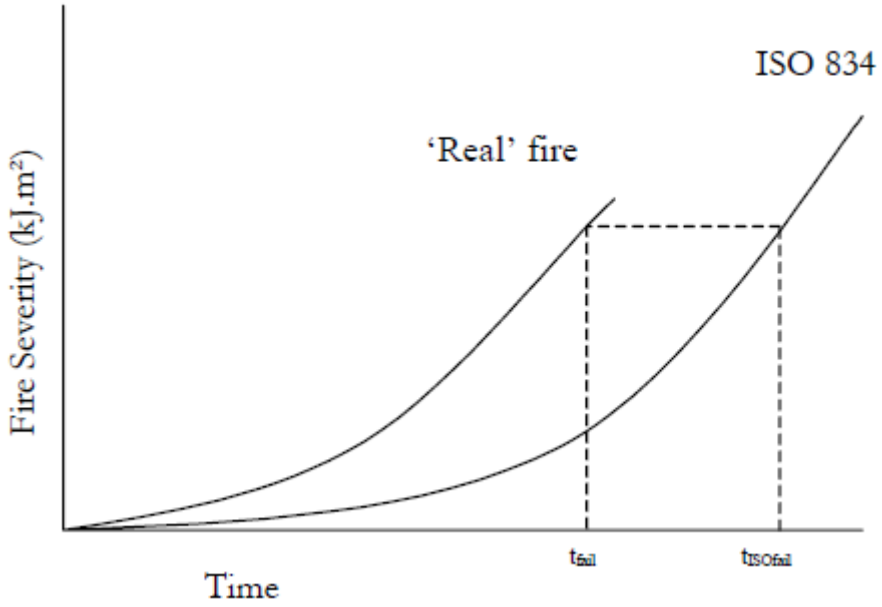

Figure 2-4 – Radiant exposure area concept of equivalent fire severity (taken from Nyman, 2002)

For an assembly of known fire resistance rating Wade et al. (2014) provides a design procedure to predict the time to failure in a compartment fire. The approach is based on equating the cumulative radiant energy a specimen was exposed to before failure in a furnace test, with the cumulative radiant energy the specimen is exposed to in a compartment fire. This approach is used in the analysis of Experiments #1 and #2 as described in Section 5.5.1 and 6.7.2 respectively.

Wade et al. (2014) carried out a number of assessments to validate the performance of the CRE method for predicting fire resistance insulation failure on timber-framed wall systems lined with plasterboard. A finite difference heat transfer model (Collier, 1996; Collier, 2000) was used to calculate the fire resistance rating with respect to insulation failure for two timber-framed wall systems, lined with either 10 mm or 13 mm thick fibre-reinforced gypsum plasterboard on each side. Five different parametric design fire curves and the ISO 834 standard test time-temperature were used to assess each wall system. The assessment found that generally there was good agreement between the results of the CRE method and the finite difference modelling. There were two notable exceptions to this that occurred in the decay phase of Eurocode fires with relatively low FLED to opening factor ratios (FLED/opening factors of 400/0.05 and 800/0.08). These fires were characterised as having a period of rapid burning causing them to enter the decay phase earlier than the other fires.

Research by Barnett (2007) applied the CRE method to a number of compartment time-temperature histories to determine an equivalent fire severity when compared to the standard fire time-temperature curve. He found that the CRE method can be used for different construction assemblies and noted limitations may exist for ceilings and combustible assemblies (Wade et al., 2014).

The CRE method requires the time-dependent compartment gas temperature history to be known. This could be determined by using a fire model, such as a zone model (refer Section 2.3.4), or by using an analytical equation (refer Section 2.3.3).

3 Residential Light Timber-framed Building Design

3.1 Performance Objectives

3.1.1 Protection of Other Property

A fire within a building may present a risk of fire spread to neighbouring buildings due to heat transfer, predominantly by radiation from openings in external walls. To reduce this risk of fire spread, the NZBC limits the allowable radiation flux on and 1 m beyond a property boundary. NZBC performance requirement C3.6 requires that buildings are designed and constructed to limit radiative heat flux to 30 kW/m^2 on a boundary and 16 kW/m^2 at 1 m beyond the boundary. These requirements are commonly achieved for buildings close to boundaries by fire-rating external walls in part or their entirety with a fire resistance rating sufficient to withstand burnout of the enclosure.

Performance requirement C3.7 has specific requirements for external walls of buildings located within 1 m of a boundary. These walls need to be clad with non-combustible materials or with materials that do not ignite for at least 15 min when subjected to a radiant flux of 30 kW/m^2 (for Importance Level 2 buildings). Performance requirement C3.7 is considering the scenario in which a fire has occurred in one building and is providing resistance to ignition of external walls facing the neighbouring building.

The requirements C3.6 and C3.7 work in conjunction with each other. By limiting the ignitability of external walls within 1 m of a boundary, a higher level of radiation can be permitted to be received on the boundary and up to 1 m over the boundary. This approach is based on research and a conference paper by Barnett and Wade (2002) and is known as the limiting distance method. The limiting distance method assumes an emitted heat flux from non-fire-rated external wall areas in the building of fire origin with key assumptions as stated in the C/VM2 Commentary Document (MBIE, 2013b):

- No flame projection from openings
- Cladding properties represent timber with 15% moisture content
- There is limited duration of exposure
- Fire-gas temperatures follow the standard time-temperature curve

The radiation limit on a boundary used in conjunction with limiting combustibility of external surface finishes for 15 min is intended to be sufficient until the Fire Service arrives and is able to provide additional resources to prevent fire spread across the boundary. Similarly, the 16 kW/m^2 heat flux value 1 m from a boundary may not prevent ignition or damage to some cladding systems, but is stated with the expectation of Fire Service intervention to provide a secondary means of preventing fire spread if required. Without intervention the NZBC requirements may not prevent building to building fire spread in all cases (MBIE, 2013b).

The Verification Method C/VM2 (MBIE, 2014e) and Acceptable Solutions C/AS2-C/AS7 (MBIE, 2014d) provide different ways of demonstrating compliance with the NZBC performance requirements for limiting heat flux on a boundary. These methods are all based on the limiting distance method and will require portions of walls to be fire-rated based on their distance, geometry and the fire load energy density (FLED) of the firecell compartment. The method requires walls within 1.0 m of a boundary to be almost completely fire-rated, except for concessions for small limited openings. As the distance between the boundary and the wall increase, the area required to be fire-rated reduces.

The NZBC Acceptable Solution C/AS1 (MBIE, 2014c) for single household unit residential buildings and outbuildings only requires external walls within 1 m at an angle less than 90° to a site title boundary to have a 30-minute FRR, as shown in Figure 3-1. There is no requirement to fire-rate walls that are greater than 1 m from a boundary for single household units.

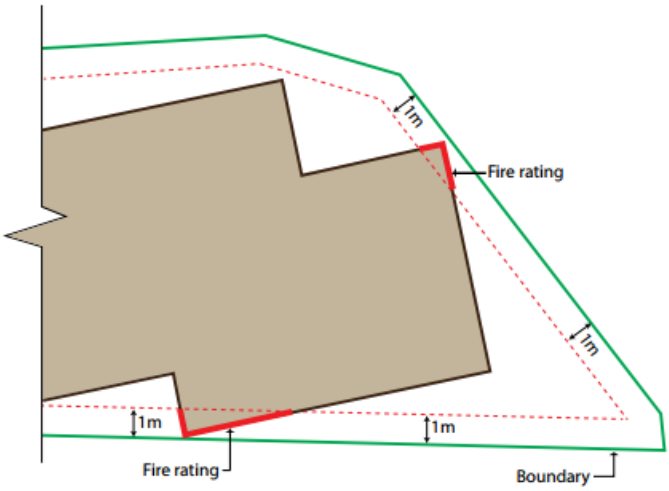

Figure 3-1 – Excerpt from C/AS1 showing external wall fire-rating requirements for residential buildings (MBIE, 2014c)

The C/AS1-C/AS7 Commentary document (MBIE, 2013a) describes that the NZBC requirement to protect other property is achieved for residential buildings designed to C/AS1. In practice there may be many residential building configurations that would not achieve the performance criteria of the NZBC for limiting radiation heat flux on a boundary. This is seemingly implicitly acknowledged in the commentary document with the statement that *"For buildings other than those in risk group SH, fire spread horizontally across a boundary is mitigated by restricting the radiation that might be incident on property on the other side of the boundary"*. It is understood the external wall fire-rating requirements for residential buildings stem back to 1992 and for a number of reasons have remained mostly unchanged.

Areas of external wall required to be fire-rated are commonly assigned a FRR that is intended to be sufficient to withstand burnout of the compartment's fuel contents. The Acceptable Solution prescribes the FRR required to fire-rated external walls based on the building use. The FRR prescribed in the Acceptable Solutions C/AS2-C/AS7 is understood to be based on the Eurocode (CEN, 2002) time equivalence formula described in Section 2.5.4. The NZBC Verification Method C/VM2 refers to a 'full burnout design fire' and requires this to be based on complete burnout of a firecell with no intervention. C/VM2 provides fire engineers with three options for structural design and assessing the performance of structural elements subjected to a full burnout design fire:

a. Use a time-equivalence method to calculate the equivalent fire severity. The fire resistance rating for elements required to withstand a burnout design fire is specified to be at least the equivalent fire severity, with a minimum of 20-min FRR.
b. Use a parametric gas temperature vs time formula (e.g. Eurocode parametric fire as described in Section 2.3.3) to calculate a thermal boundary condition and use this as an input to a suitable structural response model.
c. Construct a heat release rate versus time structural design fire. Then use a suitable fire model or energy conservation equations, taking into account ventilation conditions, to determine suitable boundary conditions for input into a structural response model.

The key take-away in the context of this research is that the Acceptable Solution C/AS1 requirements for fire-rating of external walls are the least onerous, requiring only those walls within 1 m of a relevant boundary and at an angle of less than 90° to be fire rated. Many configurations for buildings designed to C/AS1 may not achieve the limiting radiant heat flux of the NZBC performance criteria. The requirements for other buildings with comparative fuel loads are more onerous with respect to both allowable unprotected areas and FRR required to external walls.

3.1.2 Fire Fighting Operations – Firefighter Safety

The New Zealand Building Act (New Zealand Government, 2004) gives firefighters the authority to enter buildings on fire for the purposes of firefighting and rescue operations. The Fire Service make their own decisions in regards to the circumstances in which they will enter a building. A principle of the Building Act is that firefighters have a reasonable expectations that they should not suffer illness or injury whilst undertaking firefighting and rescue operations (MBIE, 2013b).

In the New Zealand Building Code, performance criteria C5.6 requires building design and construction to allow firefighters to reach the floor of fire origin, search the area of fire origin and protect their means of egress. This performance criteria is stated with consideration for firefighters' personal protective equipment and standard training. The performance criteria also includes requirements for Fire Service vehicle access, a means to deliver firefighting water to all parts of a building, and a means for providing relevant information to firefighters.

As previously discussed (refer Section 2.3.1), building structure is not usually threatened until a fire reaches the post-flashover stage, at which time the space is expected to have been evacuated. On this basis it is reasonable to anticipate that firefighters would not be carrying out search and rescue operations in a compartment that has reached post-flashover, but may be carrying out such operations in other parts of the building. NZBC Clause C6.3 performance criteria require that structural systems providing firefighters with access to floors for firefighting and rescue operations are to remain stable "during and after fire". The requirement here appears to be intended for structural systems supporting upper floors in multi-level buildings and for a single storey residential building there is seemingly no stability expectation in the NZBC of fire-rating walls or roof structure in single-level buildings for the purposes of protecting firefighters.

C/AS1 requires separate household units in multi-unit dwellings to be fire-separated from each other with construction achieving a 30-min FRR. Beyond this there are no requirements to fire-rate structure within a household that supports an upper floor or walls, unless those walls are required to be fire-rated to prevent spread of fire to neighbouring property. There are no additional fire-rating requirements specific to support firefighting operations.

3.2 Design Considerations

3.2.1 Sprinkler Protection

New Zealand has a relatively high reliance on active fire safety systems and in particular sprinkler systems for fire safety design. Sprinkler systems prevent flashover for 95% to 99% of likely fires (Buchanan, 2008) and on the basis of successful operation, one could argue that no specific fire-rated protection would be needed for structural elements. The NZBC C/VM2 and Acceptable Solutions for

non-storage buildings permit up to a 50% reduction in some instances in the fire-resistance rating assigned to structural elements for sprinkler protected buildings. Buchanan (2008) suggests that it is hard to justify a reduction in the design fire load or fire heat release rate if sprinklers are installed given that there remains a low probability that a sprinkler system could fail to control a fire. Sprinklers may fail due to water supply failure, being subjected to a fire beyond their design capability or other reasons. Sprinkler protection in single household residential buildings is relatively uncommon in New Zealand and this research has been limited to non-sprinklered residential buildings.

3.2.2 Fire Service Intervention

It is important to define whether Fire Service intervention is being taken into account in a design. Although it is considered unlikely that Fire Service intervention would prevent growth to flashover due to the time elapsed for fire detection, alerting and travel to the building (Buchanan, 2008), Fire Service intervention may still negate a need to design for full burnout of a compartment if it could be expected there would be timely Fire Service attendance.

Consideration can be given to what is reasonable to expect for an urban environment, and use this to determine a suitable design parameter for intervention. The C/VM2 Commentary document (MBIE, 2013b) describes that the NZFS provides a secondary role in respect to NZBC Clause C1 (b) (protection of other property) and is complementary to C/VM2 Design Scenario HS as described in Section 3.1.1. The Commentary document also notes that timely Fire Service intervention cannot be guaranteed, but refers to data for past fire incidents and states that the risk of fire spread to adjacent property is "small but not insignificant". The NZFS Emergency Incident Statistics 2005-2010 are referred to and the Commentary document states that these show approximately 3% of all structure fires had an occurrence of fire spread to adjacent property.

3.2.3 Defining 'After Fire' and Design for Burnout

An important design consideration is to be able to define what is meant by 'after fire' or 'post fire'. This could mean the time at which the fuel contents of the building are exhausted, the time when the building and its structure has returned to ambient temperature, or the time after which the Fire Service intervene and extinguish the fire thus cooling the structure down. There is no definition in the NZBC compliance documents, handbook or regulations for this, although the term and concept is referred to in a number of places. NZBC Clauses C6.2 and C6.3 require building elements to remain stable "after fire" and is discussed further in Section 3.3. NZBC B1/VM1 provides a combination of loads to test for stability "after the fire until the building is either repaired or demolished", and does not define "after fire".

When considering fire-rating building elements for the purpose of protection of other property, design is commonly intended to be for 'burnout' of the building's contents. An implicit assumption in this design philosophy is that there is no Fire Service intervention. The building elements therefore need to maintain the required performance for the full duration of the fire until the 'after fire' state is reached. Designing timber structures to resist burnout of a compartment is not as simple as structures consisting of non-combustible materials (Buchanan, 2001). Charring of the timber may continue even after the contents of the compartment are extinguished or burnt out (König, 1998). Thus to prevent failure of the charred timber structure there may need to be intervention to remove damaged linings and extinguish any charring occurring, or a design based on preventing charring of timber members.

There is a requirement in some countries such as Norway for light-weight timber buildings to be designed for complete burnout with no intervention from the Fire Service (Buchanan, 2001).

Wade et al. (2014) commented that the concept of withstanding burnout is used quite freely within the NZBC compliance documents and could be interpreted as meaning that the fire-rated construction continues to perform its intended function following exposure to a compartment fire for its full duration. There is no certainty that the functional requirements of the Building Code to prevent fire spread and structural collapse will be achieved through the use of time-equivalence methods to specify a FRR to withstand 'burnout'.

It is worth noting the FLED value used for residential buildings in NZ is lower than specified elsewhere. For example the Eurocode (CEN, 2002) specifies 780 MJ/m^2 average for a dwelling, and Swiss data reproduced by Thomas (1986) as part of a CIB Research Group reported an average FLED of 500 MJ/m^2 for homes. Spearpoint (2008) suggests a 90 % fractile value of between 1.35 to 1.65 times this average value and this equates to between 675 MJ/m^2 and 825 MJ/m^2. The South African National Standard 10400-T:2011 Edition 3 (SANS, 2011) states a design fuel load of 450 MJ/m^2 for domestic residence and detached dwelling house. The time equivalence value calculated using the Eurocode method is directly proportional to the FLED value used. Due to this difference in assumed FLED value, the corresponding time equivalence calculated is lower in NZ than other international jurisdictions.

3.3 Stability

3.3.1 Comparing Stability and Structural Adequacy

Structural adequacy and stability are often incorrectly used interchangeably or considered to be the same (Gerlich, 2015b). It is important the two concepts are understood to be distinct and separate. Structural adequacy is an output of a standard fire test on a single load-bearing specimen, and stability is a function of a building's design and interaction of a number of elements.

Structural adequacy represents the first number in a fire resistance rating (FRR) as described in Section 2.4.3 of this report. It is quantified based on the duration a loadbearing specimen successfully withstands an applied vertical load in the standard furnace test. A non-loadbearing element will not have a vertical load applied during the standard fire test and has no structural adequacy rating.

C/AS1 – C/AS7 defines structural adequacy as being *"in the context of the standard test for fire resistance, is the time in min for which a prototype specimen has continued to carry its applied load within defined deflection limits"* (MBIE, 2014c; MBIE, 2014d). This is consistent with the definition given in the Verification Method C/VM2 (MBIE, 2014e). The Acceptable Solutions also add a comment not found in C/VM2; *"The fire design load should be as specified in B1/VM1"*. This comment may cause confusion as B1/VM1 also specifies loads to test lateral stability of fire-rated systems as well as dead and live loads.

In the context of fire engineering, stability is the support provided to a building element having an FRR. The intent of this is to prevent premature failure of structural elements due to additional loads caused by the fire (Gerlich, 2015b). This stability, also known as lateral stability, is a function of how a building is designed and constructed and is not assessed by the standard furnace test. An

understanding of how elements within the building interact and the effects of fire on the performance of the structure is required to assess (structural) stability (Gerlich, 2015b).

Stability of fire-rated elements is usually a consideration in scenarios where an external wall is required to be fire-rated to protect adjacent property. Elements providing lateral support to the wall are often not fire-rated and therefore not relied on to provide support in the fire condition. This commonly occurs in residential buildings where one external wall is close to a property boundary and the remainder of the walls and support structure are not required to be fire-rated. In this situation it is commonly assumed that the non-fire rated elements have failed in the fire condition and the fire-rated external wall becomes 'free-standing'.

NZBC C/AS1 – C/AS7 defines stability as *"in the context of fire protection is the support provided to a building element having a FRR, intended to avoid premature failure due to structural collapse as a result of applied load, dead and live loads or as a result of any additional loads caused by fire"*. This is seemingly consistent with the design criteria of B1/VM1 which is described further in Section 3.3.6.

For internal fire-rated walls providing separation between firecells, stability of these walls is usually ensured by the support provided by the connected elements in the firecell not affected by fire. It is assumed that a fire occurs in one firecell only at any one time and if the fire separation performs its function of preventing fire spread to the adjacent firecell, there is usually no further analysis required. This scenario is illustrated in Figure 3-2 and is common in multi-unit residential dwelling developments.

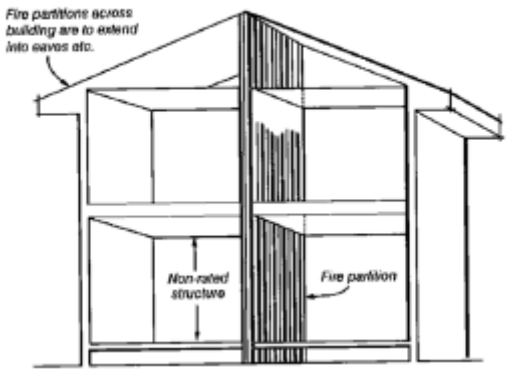

Figure 3-2 – Fire-rated wall between apartments (taken from Buchanan, 2001)

For external walls, proprietary details have been developed for providing lateral stability to fire-rated external walls for single-storey light timber-framed buildings designed within the scope of NZS 3604:2011 *Timber-framed buildings*. These details use the wider foot-print of 140 mm timber framing held down by steel hold-down brackets, screwed into the timber studs and bottom plate, and anchored through the bottom plate into a concrete floor slab beneath. Due to many possible variations, there is no standard solution for complex structures outside the scope of NZS 3604:2011 and specific engineering design is required (Gerlich, 2015b).

3.3.2 NZBC C Clause Requirements

The performance criteria NZBC C6.2 requires that structural systems necessary for stability in fire to remain stable during and after fire. Account needs to be taken of the fire severity, any active fire safety systems in the building that affect fire severity including automatic fire sprinkler systems, and the

likelihood and consequence of failure of these fire safety systems with respect to structural stability. There is specific reference to "systems necessary for structural stability in fire" and the most likely intended interpretation is that stability provisions only apply to elements required to have an FRR (Gerlich, 2015a). NZBC Clause C6.4 requires that elements assigned a certain level of fire resistance are not caused to collapse by elements having a lesser fire resistance.

C/VM2 does not explicitly state requirements for stability of fire-rated elements however there is a requirement that the structural system supporting fire-rated external walls must provide structural adequacy sufficient to keep the external wall in place for the full duration of the fire. The reference to structural adequacy in this context would appear to be an error. The intended reference may have been to stability.

C/AS2 Part 4.3 *Structural stability during fire* Paragraph 4.3.1 requires that "structural stability" of primary building elements that have an assigned FRR be retained for the duration of that FRR. This means that any elements providing support to a fire-rated element, must have the same fire resistance rating. This supports the interpretation that the building code performance clause for stability during fire applies to fire-rated elements only. C/AS2 Part 4.3.2 requires primary elements to resist collapse during a fire when subjected to design dead and live loads required by NZBC B1 and any additional loads caused by the fire. For a discussion of NZBC Clause B1 requirements refer to Section 3.3.3.

A primary element in the context of fire engineering is defined in the NZBC Handbook (MBIE, 2014f) as "a building element providing the basic loadbearing capacity to the structure, and which if affected by fire may initiate instability or premature structural collapse". The definition is followed by a comment stating that suspended floors in a multi-storey building are primary elements. Some structural engineers have commented that in industry "primary element" may have a different meaning in a structural engineering context to fire engineering, and this may be causing further confusion in interpretation of the requirements.

The Acceptable Solution C/AS2 (MBIE, 2014d) also describes specific requirements for vertical and horizontal stability. For vertical stability, Paragraph 4.3.4 requires that primary elements in a vertical orientation (e.g. a wall) are rated for structural adequacy, and primary elements in a horizontal orientation (e.g. a floor) are supported by primary elements with at least an "equivalent" structural adequacy rating. With respect to horizontal stability, Paragraph 4.3.5 requires horizontal stability to be provided to elements assigned an FRR by one of three methods:

a) Cantilevering the member from a structural base that has an FRR the same or greater than that of the member concerned
b) By support provided from another fire-rated element with the same or greater FRR.
c) By support provided from primary elements outside the firecell.

No reference is made to the loads which need to be applied to test for vertical and horizontal stability, however it would seem likely that the intent is that these are in accordance with NZBC Clause B1.

The above paragraphs and description in C/AS2 for "Stability of building elements having an FRR" is not included in C/AS1. It could be interpreted that there is no requirement for structural stability during and after fire for buildings designed to C/AS1. This would apply to common residential housing designs.

3.3.3 NZBC Clause B1 Requirements

NZBC Clause B1 performance criteria B1.3.1 and B1.3.2 require that buildings and building elements have a low probability of becoming unstable or collapsing throughout their lives, and also to have a low probability of causing loss of amenity throughout their lives. Clause B1.3.3 requires buildings and building elements to withstand the combination of loads (vertical and horizontal) likely to be experienced during construction or alteration and throughout their lives considering physical conditions likely to affect stability, including the effects of temperature and fire.

These temperature and fire effects may induce additional loads that occur and could be due to "changes in length or other deformations in building elements as a result of high temperatures" as stated in C/AS2 (MBIE, 2014d). C/AS2 also comments that the effects of temperature on strength reduction need to be taken into account, and this may include consideration for the maximum temperature attained, the heat capacity of the element, loss of cross sectional area, the extent of exposure, the effect of any protective systems and any restraint due to attached structure.

With respect to structural performance during and after fire, AS/NZS 1170 *Part 0: General principles* Clause 4.2.4 provides combinations of actions for fire for confirming the ultimate limit state. These actions consist of 'dead' action, 'live' action and "*thermal actions arising from the fire"*. Section 6 of AS/NZS 1170 Part 0 provides ultimate limit state criteria which includes minimum lateral resistance *"where it is appropriate to consider stability of remaining walls that may collapse outwards after a fire event"*. This implies that inwards collapse of these walls is permissible under the Standard which seems reasonable provided there are no life safety concerns. The words "where it is appropriate" is somewhat ambiguous and common interpretation is that this requirement applies to elements in a building that have been assigned a FRR for the purposes of protecting other property.

B1/VM1 modifies Clause 4.2.4 of AS/NZS 1170.0 to include a combination of actions for during the fire and "after the fire until the building is either repaired or demolished". The combination of actions consist of 'dead' loads, 'live' actions and "*thermal actions arising from the fire"* together with a lateral force. B1/VM1 states that account is to be taken of the effects of the fire on the material properties and geometry of the structure. The lateral force to be applied during the fire is proportional to the dead and live loads; given as 2.5% of the sum of dead load and live load with a suitable modification factor applied to the live load component.

For the after fire case, the lateral force is taken to be the greater of two values, one which is calculated as per the 'during fire' case, and the other being "*a uniformly distributed horizontal face load of 0.5 kPa in any direction"*. This requires prevention of wall collapse inwards or outwards. It is unclear what elements and scenarios this applies to, however common and convenient interpretation in industry is that these requirements apply to fire-rated external walls. Common interpretation is to test the performance of an external fire-rated wall for two-way stability against a 0.5 kPa face loading only.

These requirements in AS/NZS 1170.0 and B1/VM1 are not specified in relation to any particular type of structural material and would appear to apply to steel, concrete, heavy timber and light-weight timber buildings equally. They also do not single out elements having a fire resistance rating and therefore it could be interpreted that structural elements in all buildings must retain post-fire stability until repair or demolition. In practice this would be cost prohibitive to achieve and is unlikely to be the intent of the NZBC. In practice designers will usually refer to the NZBC C Clauses which require post-fire stability of fire-rated elements only (Gerlich, 2015a).

For light timber-framed buildings, NZS 3604:2011 is called up as the Acceptable Solution to NZBC Clause B1 with a number of minor modifications. NZS 3604:2011 has no requirements for building structure performance during and after fire, and the modifications made by B1/AS1 do not add any requirement for stability during and after fire.

3.3.4 Analysis of NZBC Requirements

The previous sections have highlighted some of the key requirements of the NZBC with respect to designing for stability. There would appear to be inconsistencies between the fire performance requirements of structural systems in the NZBC Clause B and C performance requirements, and also in the Verification Methods and Acceptable Solutions. There is a requirement for stability of structural systems during and after fire in both the NZBC Clause B and C performance requirements, however it is not clear whether this applies to all structural elements, only those which are fire rated, or only those which carry out certain functions. The relationship and hierarchy in requirements between Clauses B1 and C6 are particularly ambiguous.

For residential buildings, an alternative compliance path has been suggested by Gerlich (2015a): compliance with B1 by Acceptable Solution B1/AS1 and compliance with C1-C6 by Acceptable Solution C1/AS1. Compliance with these two acceptable solutions by definition satisfies the requirements of the NZBC with respect to stability of fire-rated walls for residential buildings. “This is common sense for simple structures with a 30-min FRR where it is most unlikely that external walls will collapse in such a way as to threaten firefighters or adjacent property” (Gerlich, 2015a).

3.3.5 Exploring the Concept of Stability in Fire

It is important to consider the context in which we are designing for stability to understand how the requirements should be developed and apply. There are a number of different opinions as to what is driving the requirement(s) for stability of buildings and building elements during fire. Some objectives are explicitly stated in the NZBC performance requirements, some are implicit and others are captured in part only. Three ideas that are often raised are: protection of firefighters, protection of other property, and protection of post-fire investigators and the general public.

It would seem intuitive that fire-rated elements need to remain stable at least for the equivalent time in which they are expected to carry out their function. For example, a fire-rated external wall with a 60-min FRR designed for the purpose of protecting neighbouring property from horizontal fire spread, should remain standing for at least the equivalent of its 60-min FRR. To this end, any elements that provide support to this wall should have the same or greater FRR. The requirements of the NZBC are consistent with this.

Another issue often raised is the risk of building collapse on firefighters, this could be walls, floors or roofs. The requirements of NZBC Clause C are reasonably clear with respect to protection of firefighters in multi-level buildings and have been previously described. Firefighter safety is considered, in combination with their standard operating procedures and protective equipment, by fire-rating to prevent floor collapse in multilevel buildings, the duration of which depends on building height. NZBC Clause C appears to place no performance requirement on walls and roofs in single storey buildings for the purposes of protecting firefighters. It would seem therefore, inconsistent to apply a stability requirement to a single fire-rated external wall in a building for the purposes of protecting firefighters. For consistency, at least the remaining walls in the building should achieve the same performance level if indeed this is the intent.

Related to the considerations for protection of firefighters, is the direction of wall collapse. It could be argued that an outward collapsing wall presents a greater risk to life safety for firefighters and observers than an inward collapsing wall. It has previously been described in this report that AS/NZS 1170 seemingly permits inward collapse of walls, and B1/VM1 modifies this to require stability in both directions. The question of collapse direction is important in that for many buildings it is relatively straightforward to design to prevent collapse in one direction only, but more onerous to prevent collapse in two directions. One school of thought is that outward collapse is not permitted due to the risk of damage to neighbouring property if a wall collapses over a site title boundary. Permitting inward collapse and not outward would seem reasonable in this instance. Another reason that the wall needs to remain standing is to limit radiation to the relevant boundary.

There are some structures that present a greater risk than others. For example collapse of a concrete structure is likely to present a greater danger than collapse of a light timber-framed structure. NZS 3101:Part 1:2006 *Concrete Structures Standard* (Standards New Zealand, 2006) identifies a possibility of risk of injury or death to firefighters standing outside a building with concrete wall elements, and requires these to be designed to prevent outward collapse due to fire exposure. A light timber-framed building that has had extended exposure to a post-flashover fire is likely to have severely degraded timber framing, and in the absence of Fire Service intervention there may be little framing and cladding remaining.

For a single-storey building the risks associated with collapse can likely be managed. As buildings become larger and taller, the consequences of sudden collapse are likely to increase. These different risk levels appear to have been captured to some extent by the NZBC C Clause performance requirements, however Clause B1 appears to have the unintended requirement that all structures must remain stable during and after a fire. There are many low rise residential and rural buildings that are remote from site title boundaries and present no spread of fire threat to neighbouring property but if required to be preserved for post-fire investigation would require significant fire rating.

3.3.6 Design for Stability – Lateral Load

The magnitude of the lateral load being designed for needs to be considered. Common interpretation is that the 0.5 kPa load specified in B1/VM1 represents a 'nominal' wind loading. It can be shown using Bernoulli's equation (Equation 3-1) with suitable assumptions that a 0.5 kPa load on the face of the wall equates to a wind speed of approximately 100 km/h, as shown in the calculations below.

$$\frac{V_1^2}{2} + \frac{p_1}{\rho} + gh_1 = \frac{V_2^2}{2} + \frac{p_2}{\rho} + gh_2 \qquad \textit{Equation 3-1}$$

$$\frac{V_1^2}{2} = \frac{p_2}{\rho} \xrightarrow{yields} V_1 = \sqrt{2\frac{p_2}{\rho}}$$

$$V_1 = \sqrt{2\frac{500}{1.23}} = 28.5\ m/s = 103\ km/h$$

It is not unreasonable to expect a 100 km/h wind (or greater) in NZ. NZS 3604:2011 provides ultimate limit state wind speeds ranging from 32 m/s (115 km/h) to 55 m/s (198 km/h). If there is an assumption of no Fire Service intervention and we are considering 'burnout' of the building, then it is likely the

wall's timber framing and plasterboard linings are in a severely degraded state near the end of the specified time of fire resistance for reasons discussed in Section 3.2.3. For a light timber-frame wall weighing approximately 25 kg/m^2 (i.e. 250 N/m^2 = 0.25 kPa) this wind load is approximately 200% of the self-weight of the wall system.

There is a common interpretation that the fire-rated elements in light timber-framed building should be able to withstand a 0.5 kPa lateral load during and after a fire. The context of this on the overall building fire performance needs to be considered. The provisions for prevention of fire spread to neighbouring property make a number of assumptions, including no external flaming from unprotected openings, and a uniform radiant flux from these openings as discussed in Section 3.1.1. If a light timber-frame building has only one external fire-rated wall (a common occurrence), and the remainder are non-fire-rated, and this building is exposed to a 100 km/h wind, then it is very unlikely that the assumptions made in the design to prevent spread of fire to neighbouring property will hold true. There will be hot debris, smoke, ash and embers spread a significant distance from the building of fire origin.

Considering a scenario of timely Fire Service intervention in which the fire-rated wall including its linings remaining intact, then it may be reasonable that a controlled collapse in a safe manner could be initiated by the Fire Service. This could be a 'push' away from neighbouring property, and one could argue that permitting inward collapse for this purpose is safer than leaving a partially degraded structure standing.

4 Light Timber-frame Construction Performance in Fire

4.1 Introduction

4.1.1 Typical Construction

There is an increasing demand for timber as a building material. Benefits of timber structures include high strength to weight ratio, “visual and tactile attractiveness, high energy efficiency, quick erection time and a low carbon footprint” (Werther et al., 2012). Light time frame construction is commonly used in NZ for low-rise buildings and particularly for residential occupancies. Sawn timber is often used as framing for walls, floor joists and roof trusses. Walls and ceilings are typically lined with gypsum plasterboard. Typical construction for a light timber-framed building is shown in Figure 4-1.

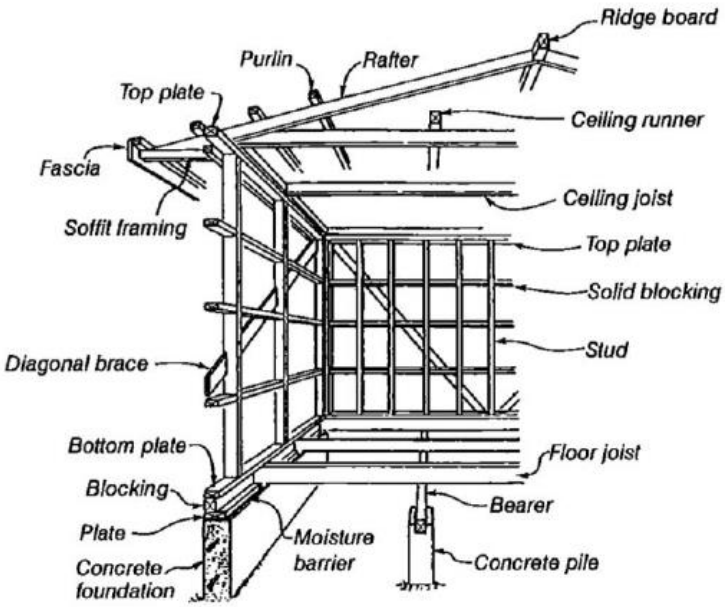

Figure 4-1 – Typical light timber house framing, taken from Buchanan (2001)

The relatively slender timber framing members have little inherent fire resistance. Gypsum plasterboard linings are often used to enclose timber framing, forming a wall or floor/ceiling system with a certain level of fire resistance. Gypsum board is usually fixed directly to timber studs in the case of walls, and either directly to timber joists or more commonly onto metal batten systems for ceilings. Ceilings may be suspended on a steel suspension system to form a ceiling cavity. Fixing methods for gypsum board to timber or ceiling battens include screws, nails or glue adhesive, with screws and glue being the most common in residential buildings.

NZS 3604:2011 *Timber-framed Buildings* describes the requirements for the design and construction of timber-framed buildings without a need for specific engineering design. This is the most common compliance pathway for residential building design in New Zealand. The Standard also refers to other New Zealand Standards with respect to timber properties, durability and performance. Design to NZS 3604:2011 typically dictates stud spacing to be at maximum 600 mm centres, roof truss spacing no greater than 1200 mm, and wall heights from 2400 mm to 3000 mm high. Common residential design is based on 2400 mm stud height for single-storey houses.

4.1.2 Building Performance

There have been a number of full-scale fire tests carried out in light timber-frame buildings, including a three-storey apartment building (Hayashi et al. 1999) and a six-storey building at the Cardington test facility in England (Lennon et al. 2000). These full-scale tests and others have shown that light timber-frame construction can be designed to provide excellent fire resistance. Important findings include the importance of good workmanship in achieving the intended fire resistance, and correct installation of cavity barriers and fire stopping to maintain continuity of fire-rated construction. A high quality gypsum board is also considered to be an important factor (Buchanan, 2001).

4.2 Plasterboard

4.2.1 Introduction

Gypsum plasterboard (or gypsum board) is a rigid board made from predominantly gypsum plaster. In New Zealand it is most commonly sold in sheet sizes measuring 2400 mm × 1200 mm but is available in sizes up to 6000 mm × 1350 mm. It may contain additives to enhance performance in specific areas (e.g. fire, acoustic or structural) such as glass fibre sand, perlite or vermiculite. It is used extensively throughout the New Zealand construction industry for providing fire resistance as part of light-weight wall and floor assemblies. Typical gypsum board has a density of between 550 and 800 kg/m^3 and is produced in thicknesses between 10 mm and 19 mm. The external paper facing provides tensile reinforcing to the board (Buchanan, 2001).

4.2.2 Types of Board and Composition

Gypsum is 21% water by weight and also contains about 3% free water, depending on the ambient conditions. This moisture content is an important aspect of the properties of gypsum board. The heating of gypsum plaster results in a chemical reaction that dehydrates the board as gypsum is converted to a powdery form. Significant energy is required for the solid gypsum to undergo this chemical change which releases water and then also to evaporate the free water. Gypsum board will complete the dehydration process at temperatures between 200°C and 300°C (Buchanan, 2001).

Internationally there are three commonly recognised types of gypsum board, known as regular board, Type X board and special purpose board. Regular board is not required to have a fire resistance rating and usually has a low density core with no reinforcing beyond the paper facing. Type X board is a term used in North America for generic fire resistant gypsum board. Type X boards will usually contain glass fibre reinforcing and other additives to improve its performance in fire. Special purpose boards are proprietary products made by manufacturers to achieve specific performance over the generic and Type X boards (Buchanan, 2001). BS EN 520 *Gypsum plasterboards – Definitions, requirements and test methods* (BSI, 2004) describes performance characteristics for categorising plasterboards; with Type A board being a 'regular' board and Type F being a 'special purpose' fire resisting board.

The minimum requirements for manufacturer of plasterboard in New Zealand are given in AS/NZS 2588:1998 "Gypsum Plasterboard". In New Zealand most plasterboard is manufactured to a higher standard to meet consumer expectations (Buchanan, 2001). Proprietary board products in NZ are designed and manufactured as special purpose boards with enhanced performance for fire, acoustics, structural bracing, wet areas, and use in high impact or x-ray environments.

4.2.3 Behaviour in Fire

The behaviour of plasterboard in fire is well known and follows a typical pattern. As a board is heated from one side, the temperature of the exposed face increases steadily until reaching approximately 100°C, at which it will plateau as free and chemically combined water is driven off. Once the plasterboard is dehydrated the temperature will begin to rise rapidly. There is little residual strength in regular boards after the gypsum has been dehydrated and converted to a powdery form, and at this time it is reliant on glass fibre reinforcing (or similar) to hold it together (Buchanan, 2001). The chemical changes causing dehydration of the plasterboard also affect the thermal properties of gypsum board, and therefore these properties change as a function of temperature.

Research by Sultan (2000) found that the main parameters that have a significant influence on performance of light timber-frame systems lined with gypsum board are: lining type, lining thickness, number of layers, insulation type and width, presence of glass fibre in gypsum board, gypsum density and stud type.

When exposed to higher humidity environments, the feel of plasterboard when handled can be a bit 'dozy'. This exposure to high humidity increases the free moisture content (not crystalline). Crystalline is the bulk of the moisture in the board. Any additional free moisture due to high humidity leading up to a fire is considered unlikely to have a significant effect on the board's performance, however this has not been quantified (seasonal testing has not been carried out).

The fire performance of gypsum board generally improves with increased density. Gypsum board with a greater density will tend to have fewer air voids, a greater quantity of moisture of crystallisation and therefore a greater heat absorbing capacity (Nyman, 2002). A greater heat absorbing capacity will improve the insulating performance of the board which can be used to protect structural members by delaying temperature rise on unexposed surfaces (Buchanan, 2001). Tests carried out found an 8% increase in fire resistance where board density was increased by 6% (Richardson & McPhee, 1996).

Premature failure of regular board can occur due to large cracks resulting in large sections of board falling off walls and ceilings in an unpredictable manner. Glass fibres can be used to control shrinkage and cause a web of fine cracks instead of fewer large cracks and typically melt at a temperature of approximately 700°C. Boards that have closely spaced fixings and glass fibre reinforcing will not usually fall off until the glass fibres melt (Buchanan, 2001). Ostman (2010) refers to research that concluded the critical temperatures for falling-off of glass reinforced board are 600°C for ceiling linings and 800°C for wall linings. Ceiling linings tend to fall off earlier than wall linings simply due to gravity loads acting against them. The extent to which glass fibre reinforcing can hold a board together is considered to be one of the most critical aspects of fire resisting gypsum plasterboard performance. Additives such as vermiculite (among others) can also be used to control shrinkage (Buchanan, 2001).

4.3 Light Timber Framing

4.3.1 Introduction

Light timber framing is the largest single end use of sawn timber in New Zealand. Radiata pine is the predominant type of wood used for light timber framing in NZ. NZS 3602:2003 *Timber and wood-based*

products for use in building (Standards New Zealand, 2003) describes requirements for timber materials and aspects of design and construction that are relevant to ensuring adequate performance.

The main properties that are considered in the requirements for structural framing members are: stiffness, strength, nail holding, fastening, durability, stability and shrinkage. Grading rules are used to control defects and the presence of such defects will affect the properties of the timber, particularly strength and stiffness (NZ Wood, 2016). Timber degrades when exposed to fire or sufficiently high temperatures. Material properties change continuously with temperature and charring of the timber resulting in a changing cross-sectional area.

4.3.2 Properties

Timber material properties have high variability including variations in moisture content, density and modulus of elasticity. Timber members behave differently in each loading direction. Perpendicular to grain its strength and stiffness properties are much lower than in the fibre direction. Timber also has weakness in the cross grain direction where highly brittle tensile failure can occur.

NZS 3604:2011 *Timber-framed Buildings* (Standards New Zealand, 2011c) requires all structural framing to be stress grade (SG) verified. Timber can either be machine stress graded (MSG) or visually stress graded (VSG). Machine stress grading is carried out in accordance with AS/NZS 1748.1:2011 *Timber – Solid – Stress-graded for structural purposes, Part 1: General requirements* (Standards New Zealand, 2011a) and AS/NZS 1748.2:2011 *Timber – Solid – Stress-graded for structural purposes, Part 2: Qualification of grading methods* (Standards New Zealand, 2011b). The Standard requires that each piece of timber pass through a machine that measures its stiffness and it is graded accordingly, assuming a stiffness strength relationship. MSG timber is also visually graded to downgrade pieces with defects such as oversize knots and excessive distortion or warp (ITM, 2012). VSG of timber uses a grader to visually inspect each length of timber and assigns a grade to it using the NZS 3631:1988 New Zealand Timber Grading Rules (Standards New Zealand, 1988). These rules limit the presence and size of defects according to the anticipated mechanical properties (King, 2003). This method is more commonly used by smaller manufacturers.

Both VSG and MSG timber need to be tested to be considered as verified timber. NZS 3622:2004 Verification of Timber Properties (Standards New Zealand, 2004) describes the rules and grade acceptance criteria for verification and is the same process for both MSG and VSG timber. The verification process involves the manufacturer taking random timber samples from a production line and testing the bending stiffness and bending strength. Statistical analysis is used to ensure the population of timber falls within the stated grade criteria. Each grade is assigned an average and minimum modulus of elasticity (stiffness rating).

SG timber is assigned a number classification based on its stiffness, for example SG6 or SG8, with a larger number being a higher stiffness classification/group. SG timber is further defined as either being ‘dry’ or ‘wet’. Dry refers to timber that has been kiln dried and then graded. Wet refers to timber that is graded ‘green’ before drying. The grades of dry timber referred to in NZS 3604:2011 are:

i. SG 6, to meet the properties specified for No. 1 Framing or MSG 6 in NZS 3603;
ii. SG 8, to meet the properties specified for MSG 8 or VSG 8 in NZS 3606; and
iii. SG 10, to meet the properties specified for VSG 10 in NZS 3603.

For light timber-framed building construction SG 8 (dry) is most commonly used for framing and roof trusses. SG 6 (dry) may be used for non-load-bearing elements and web members in roof trusses. NZS 3604:2011 refers to SG timber with modulus of elasticity properties as defined in NZS 3603:1993. NZS 3603:1993 Amendment 4 Tables 2.2 and 2.3 give the characteristic stresses for each species, grade and moisture conditions for design purposes. The characteristic stresses given in NZS 3603:1993 are derived from methodology given in NZS 4063.2:2010 Characterization of structural timber - Determination of characteristic values (Standards New Zealand, 2010).

NZS 3603:1993 modifies the modulus of elasticity to be used for design to take into account the effect of neighbouring elements on deformation behaviour. For MSG timber elements in a system with at least 4 elements, and in which the system constrains them to deformations similar to their neighbours, the modulus of elasticity E is to be taken directly from Table 2.3 of NZS 3603:1993 (Figure 4-2), joisted floors and timber-framed stud walls are examples. For other types of systems then the modulus of elasticity is to be taken based on values of E and E_{lb} as follows:

a) For a system with a single timber element the modulus of elasticity is E_{lb}
b) For a system with two or three elements acting together the modulus of elasticity is $0.5(E+E_{lb})$

1. Moisture condition – Dry (m/c = 16 %)

Species	Grade	Bending strength f_b	Compression strength f_c	Tension strength f_t	Modulus of elasticity E (GPa)	Lower bound modulus of elasticity E_{lb} (GPa)
Radiata pine & Douglas fir	MSG15	41.0	35.0	23.0	15.2	11.5
	MSG12	28.0	25.0	14.0	12.0	9.0
	MSG10	20.0	20.0	8.0	10.0	7.5
	MSG8	14.0	18.0	6.0	8.0	5.4
	MSG6	10.0	15.0	4.0	6.0	4.0

NOTE –

(1) Shear strength for dry Radiata pine shall be taken as f_s = 3.8 MPa. Shear strength for dry Douglas fir shall be taken as f_s = 3.0 MPa.

(2) Compression perpendicular to grain for dry Radiata pine and Douglas fir shall be taken as f_p = 8.9 MPa.

(3) Grades shall be verified as required by NZS 3622.

Figure 4-2 – Characteristic stresses for machine stress graded timber [MPa], an excerpt from NZS 3603:1993

4.3.3 Behaviour at Elevated Temperatures

During the combustion of a timber member, its cross-section constantly changes with time and fire intensity. A charred layer forms rapidly when it is first exposed to the fire, and char formation slows down due to the protective properties of the charred layer. If the residual cross section of the timber member becomes very small, then the charring rate will increase again (Buchanan 2011). The shrinking and cracking of char can increase the charring rate of timber by allowing the passage of combustible gases to the surface (Drysdale, 2011). The char layer itself will not usually burn due to insufficient oxygen at the surface (Buchanan, 2001).

Figure 4-3 shows the main layers or zones that make up a cross section of timber that has been exposed to fire. The exposed surface of the char layer is close to the fire temperature, and there is a

steep thermal gradient through the char to the char base. There is a distinct boundary between the char layer and the remaining wood, this is often considered to correspond to a temperature of 300°C (Buchanan, 2001), which is consistent with EN 1995-1-2:2004 (CEN, 2004). Below this boundary there is a layer of heated wood, the pyrolysis zone is within this layer and is where the wood is undergoing thermal decomposition into gaseous pyrolysis products. This pyrolysis zone is taken to be the part of the layer above 200°C. Below this layer of heated wood the inner core of the timber member remains at ambient temperature (Buchanan, 2001).

Moisture in the wood below the char layer evaporates as this wood is heated above 100°C, with some of it travelling out of the burning face and some deeper into the wood. The result of the moisture travelling into the wood is an increase in moisture content in the heated wood a few centimetres below the char (Friquin). The inner core of a heavy timber member will remain at its initial temperature for some time (Buchanan, 2001).

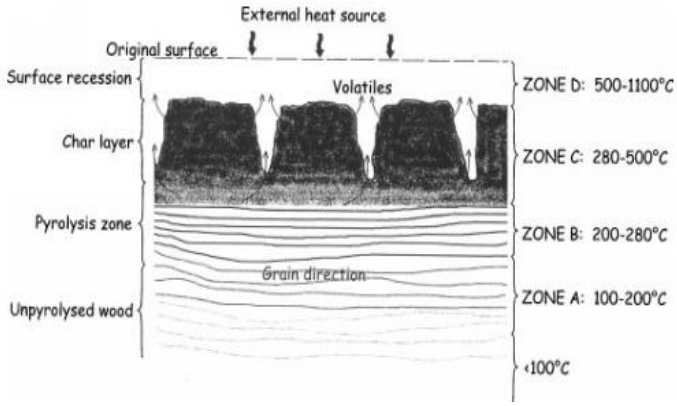

Figure 4-3: Formation of char on a timber member exposed to fire (Friquin, 2011)

In design calculations the charred layer is considered to have no strength, and the basis for common structural design is that residual cross sectional area (i.e. the area below the char) has strength to support loads. In this context for simple calculation methods, there is no requirement for a designer to calculate the temperature profile within the timber member (Buchanan, 2001), only to determine the demarcation between the char layer and the uncharred wood.

4.3.4 Assessing Performance at Elevated Temperature

There are a number of methods for assessing the thermal and structural behaviour of timber exposed to fire, and EN 1995-1-2:2004 provides several calculation methods. Some of the methods available for accounting for reduced strength of heated wood include:

- Effective cross section method – uses a cross section smaller than the actual residual cross section which implicitly assumes a layer of zero strength wood below the char line, and material properties unaffected by temperature. Eurocode 5 gives a 7 mm thickness of zero-strength wood layer for exposure greater than 20 min, and this is reduced linearly to 0 for exposure less than 20 min.
- Reduced properties method – uses the residual cross section dimensions with an average reduction in the material properties over the whole residual cross section, this can take into account the loading and the result is dependent on the residual area and heated perimeter.
- Eurocode 5 design with parametric fire specifies a strength reduction factor based on depth of char and original minimum dimension of cross section. The load capacity of the residual

cross-section exposed to a parametric fire is reduced by a reduction factor based on the ratio of depth of char to the original minimum dimension of the cross-section.

Research by Collier (P. C. R. Collier, 1992) found that timber density and moisture content are the two most important factors affecting the charring rate of solid timber. The char rate may reduce after prolonged fire exposure due to increasing thickness of the insulating layer of char (Buchanan, 2001). Collier (1992) recommended charring rates dependent on the density of the timber, based on timber at 12% moisture content. These were 0.75 mm/min, 0.70 mm/min, and 0.65 mm/min for timber densities of 400 kg/m^3, 500 kg/m^3, and 600 kg/m^3 respectively, based on furnace experiments carried out to AS 1530 Part 4 with specimens exposed to the ISO 834 time-temperature heating regime. Annex A of EN 1995-1-2:2004 provides charring rates for parametric fires that is a function of the ventilation available during the fire.

NZS 3603:1993 (Standards New Zealand, 2005) gives a charring rate of 0.65 mm/min for radiata pine and other timber species with similar density, and allows the charring rate for species with greater density to be established by test or calculation in accordance with BRANZ Study Report No. 42 (P. C. R. Collier, 1992). A method is provided for calculating the residual cross section of a timber element exposed to fire, taking into account the effects of corner rounding. The method is simply to deduct from the original cross section dimensions on each exposed side of the member, a thickness of material calculated as the rate of charring multiplied by the period of exposure, and to further subtract an allowance for corner rounding effects. Figure 4-4 shows a cross-section view of a timber member exposed to fire and the corner rounding effects, and Equation 4-1 is an equation for calculating the area of timber lost due to corner rounding.

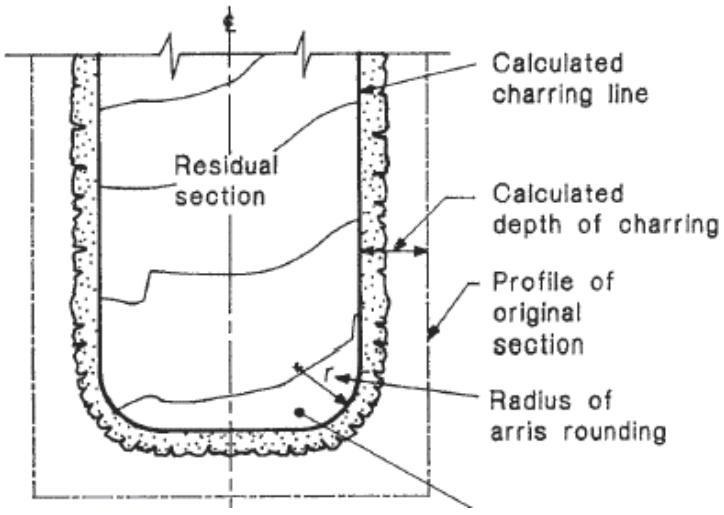

Figure 4-4 - Cross-section view of timber member exposed to fire showing corner rounding effects, taken from NZS 3603:1993 (Standards New Zealand, 2005)

$$A_r = 0.215r^2 \qquad \textit{Equation 4-1}$$

The cross-section area of timber lost due to fire exposure can therefore be calculated based on the depth of charring as shown in Equation 4-2.

$$A(t) = \left(D_A - 2d_c(t)\right) \times \left(W_A - 2d_c(t)\right) - 4A_r \qquad \textit{Equation 4-2}$$

The residual cross-section method with corner rounding has been used to assess performance of the timber members in the experimental work conducted in this research.

Calculation methods for charring rates in heavy timber are typically based on a protective char layer of approximately 25 mm being established on the timber member. These methods are based on research for heavy timber (i.e. those with minimum cross-section dimensions >100 mm), and the behaviour of light timber framing may be substantially different. In small-sized timber framing members such as those commonly found in LTF structures, the timber member may collapse before a protective char layer of 25 mm depth is attained (Ostman, 2010). Due to this inability to build up a protective layer; charring rates in light timber-framed construction are expected to be higher than those for heavy timber.

4.4 Light Timber-frame Systems

4.4.1 Introduction

In New Zealand fire resistance ratings for light timber-framed assemblies lined with plasterboard are manufacturer published proprietary ratings based on systems using their products, as opposed to generically rated systems found in other countries. The compliance documents require construction systems to be assigned an FRR by test to AS 1530 Part 4 (SAA, 2005), or BS 476 Parts 20-24 (BSI, 1987) as applicable. These ratings will be obtained with the systems constructed to specific requirements and these construction requirements are published alongside the fire resistance ratings. It is important the construction details as specified by the manufacturer are followed precisely, with only approved variations.

It is possible to calculate thermal and structural behaviour of light timber-framed wall and other gypsum lined systems such as ceilings in real fires however it can be difficult and recommended for research and development purposes (Buchanan, 2001). In most instances, designers will select an assembly with a listed proprietary FRR that meets the fire resistance rating required by the compliance document or based on a time equivalence calculation.

4.4.2 Behaviour

Adequately constructed light frame construction with suitable materials can have excellent fire behaviour (Buchanan, 2001). Wall systems are predominantly dependent on the performance of the plasterboard linings and their ability to provide protection to the framing behind. Failure of the lining material can result in fire spread or structural collapse of the barrier (Buchanan, 2001).

A complete assembly of light frame construction can be assigned an FRR based on performance in a standard fire test. Note that individual components cannot be assigned an FRR as the performance of the system is dependent on the constructed elements working together as a system. For a LTF wall system, the face of a stud in contact with a fire exposed gypsum board lining will char at the fastest rate, with less charring occurring on the side faces of the studs. There will be no or limited charring on the face of the stud fixed to the unexposed side of the wall. Despite the charring occurring, long periods of fire resistance can be achieved if the lining on the fire side remains in place.

A typical temperature profile for an uninsulated wall during a standard fire test is shown in Figure 4-5. The lengthy plateau at 100°C for the exposed lining is due to the behaviour of plasterboard as

previously described in Section 4.2.3. There is a corresponding plateau at a lower temperature on the cavity side of the exposed lining. The temperature on the exposed face lags behind even further (Ostman, 2010).

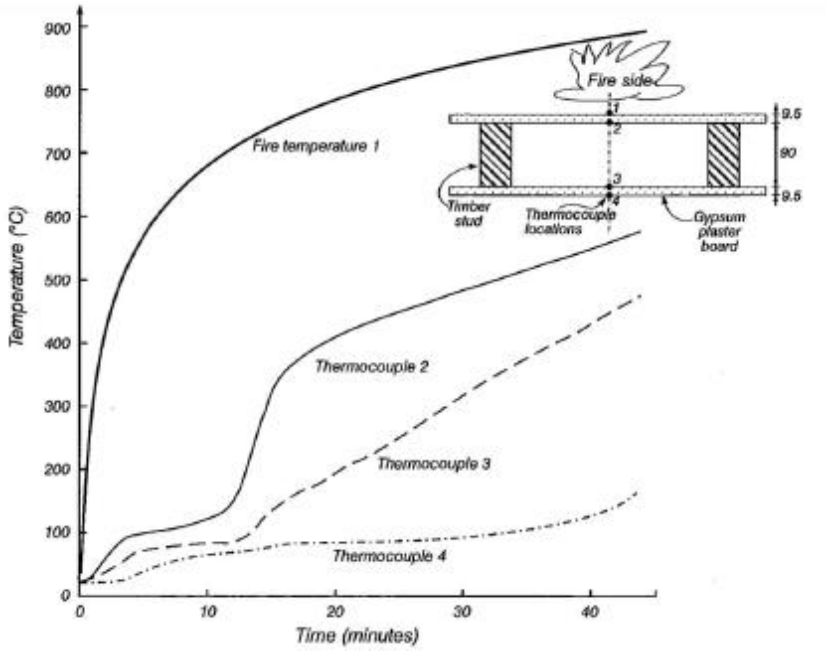

Figure 4-5 – Temperature profiles within a cavity during a standard fire resistance test (taken from Thomas (1996))

For loadbearing light timber-framed walls with an axial load, the assessment of structural fire performance is based on the strength of the residual studs after a period of fire exposure. Typical charring profiles for timber studs in walls with and without insulation in the cavities is shown in Figure 4-6. The type of insulation in the cavity is important; some materials such as polyester insulation will melt and the system will behave similarly to one without insulation, whereas non-combustible mineral fibre insulation will remain in place and provide protection to the sides of the studs. The charring rate on the wide face of the stud facing into the cavity can be taken as being about half that of the edge on the fire exposed side for a wall cavity without insulation (Buchanan, 2001). As previously described, there is no charring on the face of the stud fixed to the unexposed gypsum board.

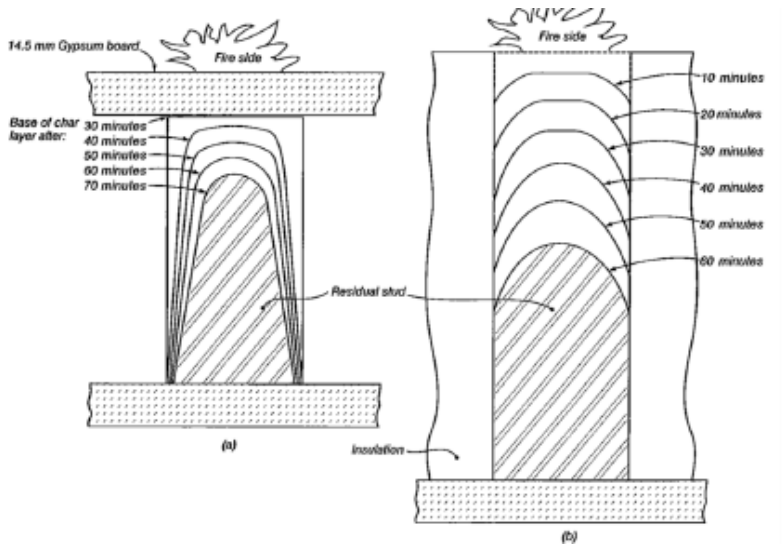

Figure 4-6 – Measured char profiles on timber studs: (a) Stud in empty cavity protected with 14.5 mm gypsum board; (b) Stud in insulated cavity with no protection on the fire-exposed face (taken from Buchanan (2001))

For light timber-framed systems, the component materials and their geometric arrangement will affect the insulating properties of the assembly. For those without insulation in the cavity between framing members, the highest temperature on the unexposed face will occur remote from the studs or joists. Heat transfer from the exposed lining to the unexposed side can be considered one dimensional and the timber stud has no influence on the heat transfer and temperatures. Both radiation and convection contribute to the heat transfer, with the radiation component becoming increasingly significant as temperatures increase. Moisture movement can also contribute to heat transfer through evaporation and condensation mechanisms (Buchanan, 2001). Timber stud walls commonly bow away from the fire due to the drying shrinkage of timber on the fire side.

4.4.3 Fastening

The mechanical fastening of gypsum plasterboard is important to ensure the board performs for the intended time and does not fall off prematurely. An early failure of a sheet will result in the wall framing or floor joists being exposed directly to the fire and result in premature failure of the assembly and a reduced fire resistance rating. Screws generally provide the most secure method of fixing and is the most common in NZ for fire-rated systems. Glue fixing is common for non-fire-rated construction and these adhesives have negligible performance at elevated temperatures and should be considered to have zero fixing strength during and after exposure to elevated temperatures associated with fire (Buchanan, 2001).

The spacing and location of screw or nail fixings is important, the screws must be spaced at relatively close intervals, and far enough away from the edges of sheets to prevent the board from pulling away during a fire. Buchanan (2001) describes that the strength of a cut edge is less than that of a machine finished edge. In industry, screws spacing is specified further from cut edges than machine finished edges because of this. The length of screw or nail fixing needs to be sufficient such that it remains anchored in uncharred wood. Plaster or jointing compound is used to finish butt joints between sheets. Fixing spacing and type becomes especially important for ceiling systems, where gravity loads act to pull the sheet away from its fixings.

4.4.4 Insulation

Improved fire resistance can occur if well-fitting mineral wool insulation is installed in a wall cavity because this protects the studs and the lining on the unexposed face, after the fire-exposed lining falls off. Glass fibre insulation is less beneficial or can lead to reduced fire resistance because the glass melts when exposed to post-flashover temperatures. Generally the main negative effect of insulation is that the gypsum board on the fire-exposed side heats up faster than for an empty cavity, which leads to earlier dehydration and falling off of the board and subsequently a reduced fire resistance (Buchanan, 2001). This research has considered uninsulated wall systems, to reduce the number of variables in the experiment results.

4.4.5 Lining failure and Charring – Calculation Methods

There are a number of calculation methods for ‘failure’ of plasterboard linings and for assessing the protection provided to light timber-framing to allow the timber to continue to perform its intended function. For example, a load-bearing light timber-framed wall that is required to maintain its load carrying capacity for a certain fire duration (FRR).

One calculation method is known as the onset of char method. This is a conservative approach based on protecting the timber members so that no charring occurs during the entire time of fire exposure

(Standards New Zealand, 1991). This design approach can have a number of useful applications if used in conjunction with a realistic assessment of expected fire severity for a burnout fire. By ensuring there is no charring of the structure, structural performance is likely to be unaffected and the structure should continue to perform as intended. In addition to this, the light timber-framed structure should be able to be repaired without need to replace timber members that would have otherwise charred (Buchanan, 2001).

EN 1995-1-2:2004 (CEN, 2004) has some limited information on the start of charring of timber behind protective layers, and for failure time of protective layers when exposed to the standard fire (Ostman, 2010). This includes equations for calculating the onset of charring for timber behind regular gypsum plasterboard Type A, H and F based on an assumed temperature of 300°C; failure time of regular gypsum plasterboard type A; and charring rates of timber behind gypsum plasterboard type F as defined in EN 520 (BSI, 2004).

Ostman (2010) provides equations based on EN 1995-1-2:2004 for calculating basic insulation values and protection values for gypsum plasterboard as shown in Equation 4-3 and Equation 4-4 respectively. The basic insulation value t_{ins} is the fire resistance of a single layer without influence of any adjacent materials, and is based on failure criteria consistent with ISO 834 with initial ambient temperature assumed to be 20°C. The basic protection value t_{prot} is based on an average temperature rise over the unexposed surface of the board being limited to 250°C, and a maximum temperature rise at any one point of no more than 270°C (Ostman, 2010). It is considered that the basic protection value can be used for the purposes of calculating the onset of charring to EN 1995-1-2 requirements (Ostman, 2010).

$$t_{ins} = 24\left(\frac{h_p}{15}\right)^{1.4} \qquad \textit{Equation 4-3}$$

$$t_{prot} = 30\left(\frac{h_p}{15}\right)^{1.2} \qquad \textit{Equation 4-4}$$

Research by fire testing has shown that using the 270°C failure criteria on the unexposed face (of a fire exposed board) as the temperature at which exposed linings fall off is conservative for fibre-reinforced (Type F) gypsum boards (Ostman, 2010). Ostman (2010) suggests that for floor/ceiling systems, fibre-reinforced (Type F) gypsum boards do not fall off until the temperature on the unexposed side of the board reaches 400°C for ceilings and until 600°C for walls.

4.4.6 Roof Trusses

Buchanan (2001) describes that light timber trusses exposed to post flashover fire conditions have little fire resistance. The strength and stiffness of the assembly is predominantly determined by the behaviour of truss plate connections and these are highly vulnerable when exposed to fire conditions. If these trusses are protected by a fire resisting ceiling then a good level of fire resistance can be achieved. Furnace testing has shown that temperatures in ceiling plenums are significantly less than the furnace gas temperatures provided the ceiling system remains in place, typically reaching slightly less than 330°C after 60 min of exposure to an ASTM E119 furnace test (Shrestha, Cramer, & White, 1995).

NZS 3604:2011 (Standards New Zealand, 2011c) includes provision for the use of timber nail-plated roof trusses and these are common in residential buildings in New Zealand (Walker, 2011). NZS 3604:2011 requires specific engineering design for roof trusses, and manufacture must be by an accredited fabricator. Truss members are connected using toothed truss connector plate; a steel plate with multiple spikes or teeth projecting from one face. The connectors are pressed into the timber using hydraulic or pneumatic presses. There are limitations on the truss design so that excessive loads that may have an adverse effect on the building structure do not occur. The key limitations found in NZS 3604:2011 are listed by Walker (2011):

- a span no greater than 12 m,
- eaves overhang shall not exceed 750 mm measured horizontally from the face of the support,
- spacing no greater than:
    - 900 mm for heavy roof claddings
    - 1200 mm for light roof claddings,
- resultant loads not exceeding 16 kN in either an upwards or downwards direction,
- ground snow load may not exceed 2 kPa

Shrestha et al (1994; 1995) carried out research into the structural performance of metal-plate-connected wood trusses under constant loading and at elevated temperatures up to 325°C. The research developed a simplified technique for modelling mechanical properties of metal-plate connectors at temperatures found in the plenum area of a protected roof/floor-ceiling assembly, and did not consider temperatures that would be expected with direct fire exposure. It is noted that at elevated temperatures, the assembly may undergo large deformation before failure. Structural steel loses approximately 30 % of its strength and stiffness by about 500°C, and as temperature continues to increase the loss increases rapidly (Cote et al., 2008). Shrestha et al (1995) comments that sheet metal is expected to exhibit similar characteristics at elevated temperature.

Experimental work (White & Cramer, 1994) at the USDA Forest Products Laboratory showed that metal plates served as a protective layer to the surface of the timber by reflecting some radiation, while the plate teeth conduct thermal energy to a greater depth into the timber. As a consequence of this, the plated surface of the wood showed signs of delayed charring, while higher temperatures were measured at internal cross-section locations were observed in areas covered by a nail plate. There is a truss analysis model, SAWTEF, developed by Cramer et al (1993) that when compared to full scale test results for both trusses and truss plate connected joints gives good agreement (Cramer, 1995). The model is limited to ceiling air temperatures of up to 350°C.

Harman and Lawson (2007) carried out experimental research to study the heat transfer through metal plates into timber members, there were no loads applied to the specimens before, during or after testing. Each specimen was constructed with two 38 mm by 89 mm, 0.30 m long members connected by two 75 mm by 150 mm galvanized steel truss plates of 20 gauge (0.95 mm) with punched teeth approximately 8 mm long. Twelve experiments were carried out, six test specimens with the connector plate teeth completed embedded and six with a 3.2 mm joint gap between the butted ends of the wood members, and a 0.8 mm gap between the face of the metal plate and the surface of the wood. The tests were carried out using a gas fired radiant panel calibrated to expose the wood to a heat flux of 20 kW/m^2.

Figure 4-7 shows where thermocouples were installed on the specimens. Thermocouple A was located on the surface of the timber behind the metal plate (centred), and thermocouple C was on the surface of the timber (centred) 5 mm from the edge of the metal plate. Thermocouples B and D were located in the centre of the timber member directly behind thermocouples A and C respectively. Thermocouple E was located on the surface of the timber approximately 20 mm from the end of the metal plate.

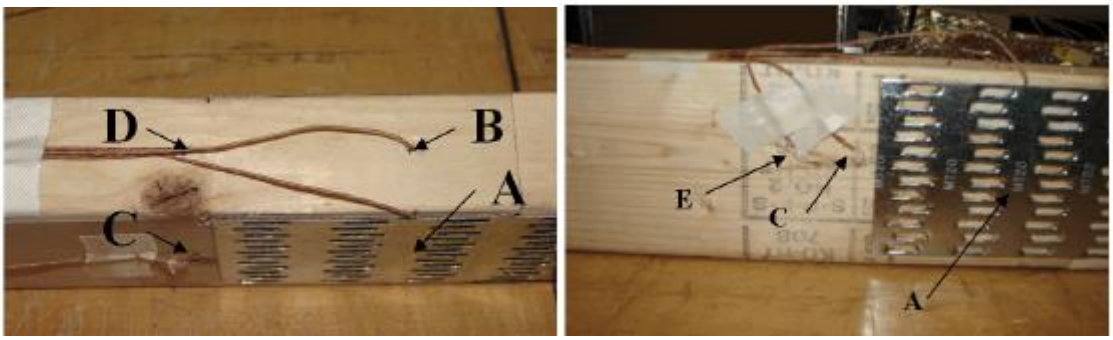

Figure 4-7 – Locations of thermocouples A, B, C, D and E (taken from Harman and Lawson (2007))

The experiments were carried out for a duration of 60 min. Harman and Lawson (2007) found that the results of the twelve test were similar. Figure 4-8 shows average thermocouple temperature measurements for the first six tests, where the metal plates were fully embedded in the timber. The thermocouple directly behind the nail plate (Thermocouple A) exhibits a lower temperature than the temperature measurements on the surface of the wood as measured by Thermocouples C and E. These results are consistent with the USDA testing carried out by White and Cramer (1994).

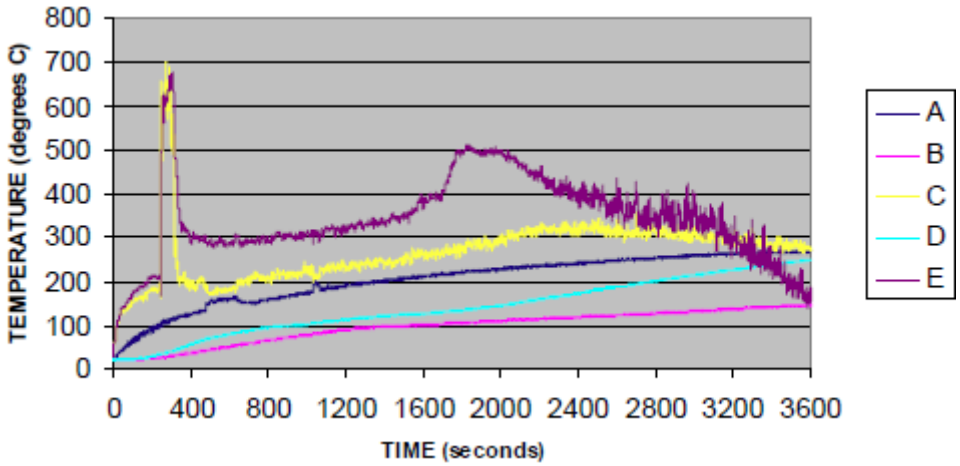

Figure 4-8 – Thermocouple temperature averages of six tests carried out with metal plates fully embedded (taken from Harman and Lawson (2007))

It is interesting to note that the results for the embedded thermocouples show a lower temperature rise at the centre of the timber behind the metal plate (Thermocouple B), than behind the uncovered timber (Thermocouple D). This is a contradictory result to what White and Cramer (1994) found. Harman and Lawson comment that this could be due to differences in experimental methodology, including the single sided exposure in their experiments compared to four-sided exposure in the USDA tests. It was found that having a gap between the metal plate and wood leads to considerable higher temperatures measured in the thermocouple behind the metal plate (Thermocouple A).

5 Experiment #1

5.1 Introduction

As discussed previously in Section 3.1.1, the NZBC Acceptable Solution for houses and small multi-unit dwellings requires external walls within 1 m of and at angles less than 90° to a property boundary to be fire-rated to a minimum 30-min fire resistance rating (FRR). Section 3.3.3 describes the NZBC requirements for structural building systems to remain stable during and after fire. B1/VM1 requires sufficient resistance to ensure that a fire-rated structure does not collapse when subjected to a uniformly distributed horizontal face load of 0.5 kPa.

The first experiment was a full-scale furnace test of a compartment based on a design to NZS 3604:2011 as described in Section 4.1.1 and common New Zealand residential building construction details. The furnace was heated to the ISO 834 standard time-temperature curve. A lateral load was applied at the top of the fire-rated wall to simulate the required 0.5 kPa load as specified in NZBC Verification Method B1/VM1.

5.2 Experiment Design

5.2.1 Building Set-out and Framing

The compartment was designed to fit on the furnace specimen frame for the full-scale furnace at BRANZ. The compartment dimensions were 4.33 m × 3.35 m with nominal stud height of 2.4 m as shown in Figure 5-1. The roof pitched approximately 15° and spanned 3.35 m between the long walls (4.33 m).

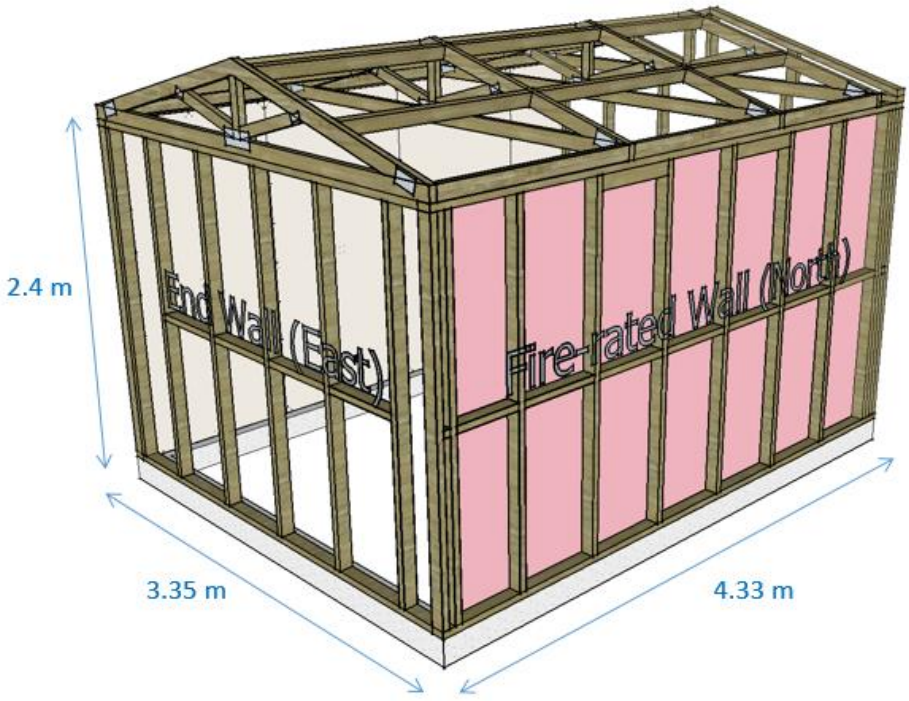

Figure 5-1 – Experiment #1 compartment dimensions

The four walls of the compartment were constructed with nominal 90 mm × 45 mm kiln dried SG8 (machine stress graded to AS/NZS 1748:2006) framing grade Radiata pine for the studs, nogging, top plate and bottom plate. Studs were spaced nominally at 600 mm centres and nogging between studs fixed at approximately 1200 mm above the bottom plate. Figure 5-2 shows the general stud layout for the four walls. The significance of the 'fixed' and 'free' wall labels is described in Section 5.2.2. The top and bottom plates were continuous along the length of each wall.

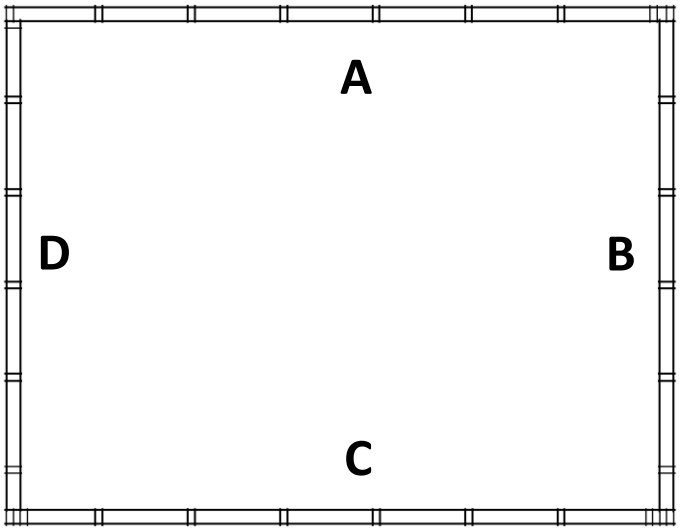

Figure 5-2 – Stud framing set-out. A = non-rated long wall; B = free wall; C = fire-rated wall; D = fixed wall

Figure 5-3 shows a typical section cutting through the long walls (fire-rated and non-rated walls). The studs, bottom plate, top plate and nogging framing members are shown, as are the roof truss purlins. Also visible is the ceiling system consisting of plasterboard fixed to battens and this is described further in Section 5.2.6.

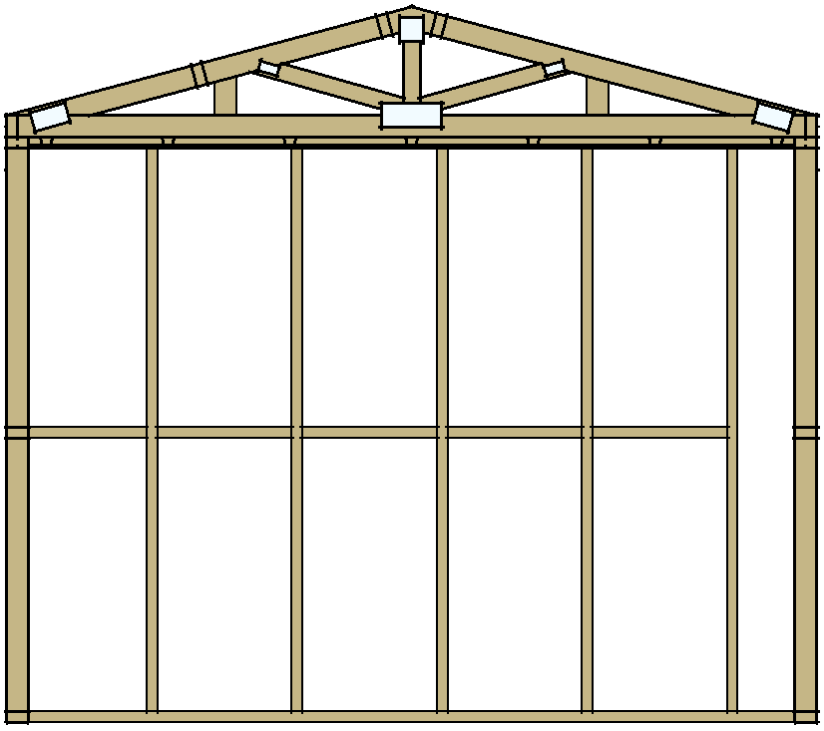

Figure 5-3 – Typical section looking along length of compartment

Studs were fixed to the bottom and top plates with two nails at each end, nailed through from the top/bottom plate side into the stud. Bottom plates were fixed in the corners to adjacent bottom plates using 0.95 mm galvanised steel plates with punched teeth that are hammered into the timber to grip, an illustration of this plate type is shown in Figure 5-4.

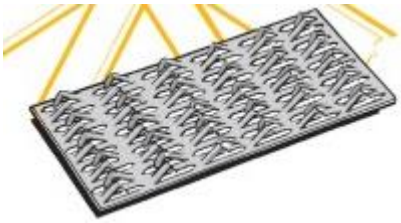

Figure 5-4 – Illustration of galvanised steel plate used to connect bottom plates (taken from MiTek, (2011))

5.2.2 End Wall Fixing Details

The experiment compartment was approximately 4.3 m long. Many residential buildings including garages will have fire-rated walls with a length greater than this. To allow the performance of a wall up to 8 m long to be assessed, one end-wall of the fire-rated boundary wall was disconnected from the end wall, as shown in Figure 5-5.

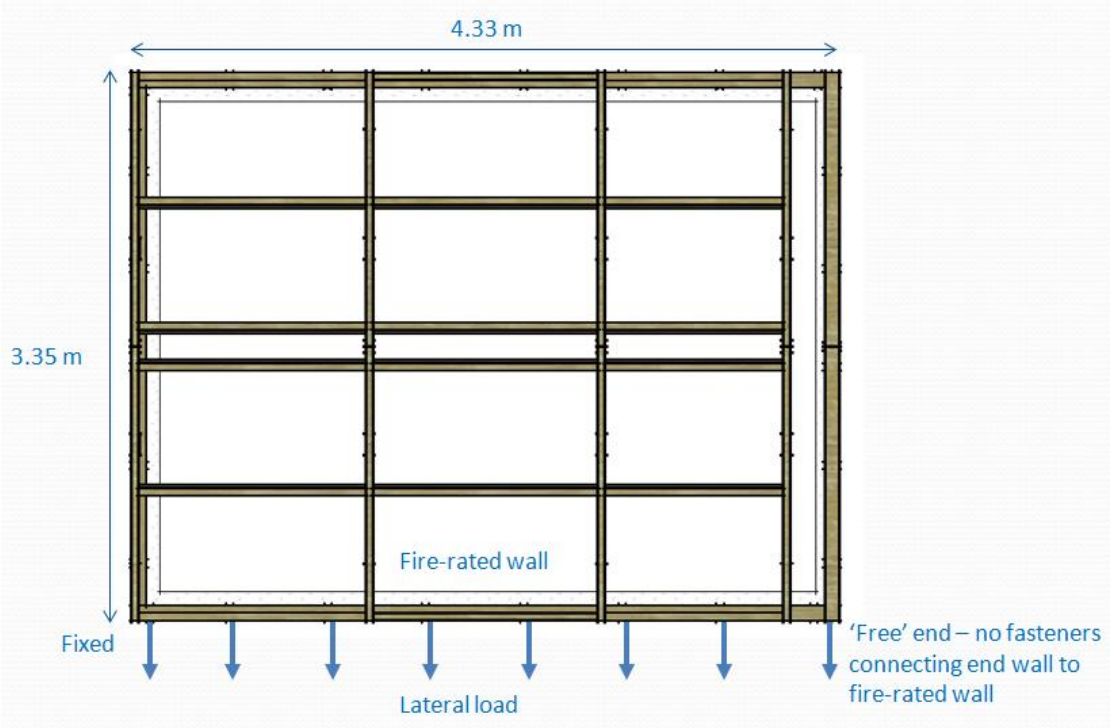

Figure 5-5 – Sketch showing that one end of the fire-rated wall 'disconnected' from the end wall

5.2.3 Roof Truss

Five roof trusses span between the fire-rated wall and the non-rated long wall. Four of these trusses were physically connected to the top plate of the fire-rated wall (T1 – T4), and one was rested on the top of the wall at the 'free' end (T5) with no mechanical fastening. Figure 5-6 shows the roof truss layout for the experiment, with the fire-rated wall at the bottom of the image. Truss spacing was based on a design to NZS 3604:2011 as described in Section 4.1.1. Truss T4 is the load-carrying truss closest to the 'free' end wall. This truss was effectively the outer-most truss (i.e. gable end truss) moved inward by 300 mm. The reason for moving the truss inwards was that if the truss sat on top of the top plate of the end wall, it would be partially protected from the effects of fire, compromising an

assessment of performance of walls spanning greater than 4 m. The intent was to have even spacing between trusses T1-T2, T2-T3 and T3-T4 as indicated by the dashed lines in Figure 5-6, however the as-built layout is as shown.

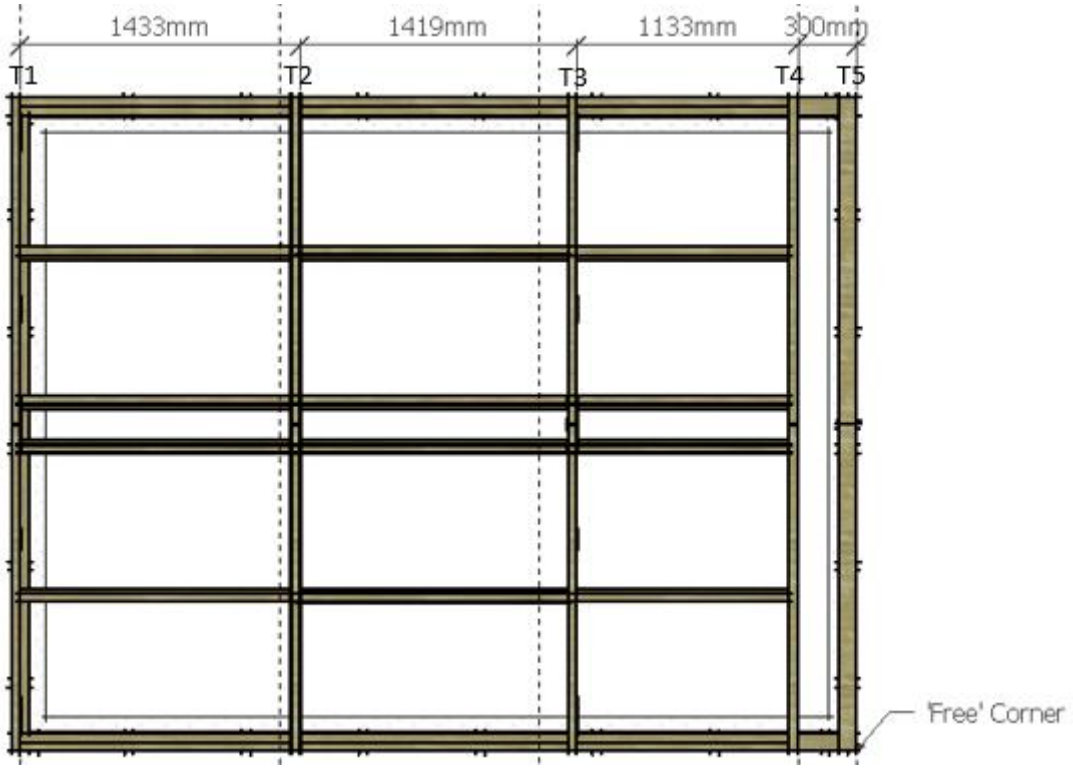

Figure 5-6 – Experiment #1 Roof truss layout

The four fixed roof trusses were of timber construction and consisted of a bottom chord, top chord, and three diagonal members as shown in Figure 5-7. As described in Section 4.4.6, roof trusses are designed to specific engineering design and for the experiment the roof truss was designed using commercial software. The truss top and bottom chord members were nominal 90 mm × 45 mm kiln dried SG8 (machine stress graded to AS/NZS 1748:2006) H1.2 Radiata pine. The webs were nominal 70 mm × 45 mm kiln dried SG8 (machine stress graded to AS/NZS 1748:2006) H1.2 Radiata pine. A splice and truss connector plate connection located mid-span of the bottom chord was included in the experimental setup to assess the performance of such connections, as would commonly be found in trusses spanning greater than 6 m. The fifth truss was built-up for accepting the roof cladding system and was a different construction to the four load-carrying trusses.

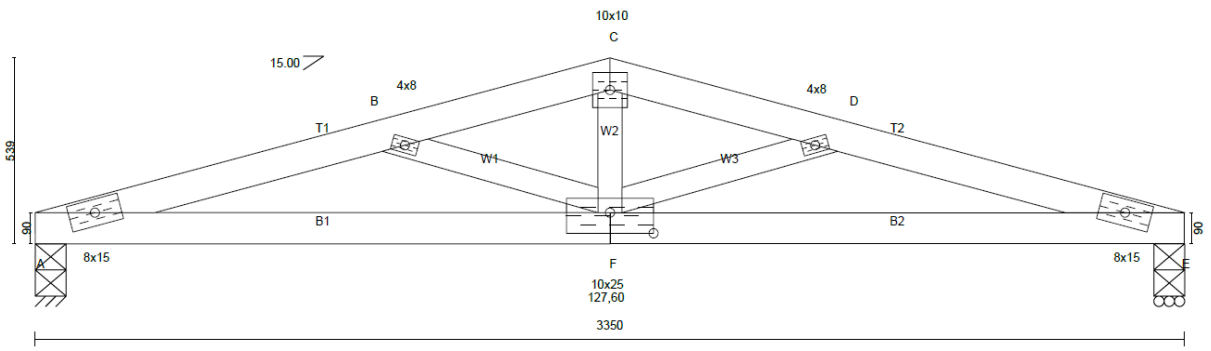

Figure 5-7 – Drawing of roof truss, note the splice at the centre of the bottom chord connected with a truss connector plate

The truss connector plates were manufactured from 1.0 mm thick, G300 grade steel, (galvanised specification Z275) steel strip with teeth punched out to a depth of approximately 8 mm and a typical example is shown in Figure 5-8. A connector plate measuring 100 mm × 250 mm was used to connect the two halves of the bottom chord, and this also connected to the three web members (refer Figure 5-7). Connector plates measuring 80 mm × 150 mm connected the top chords to the bottom chords at each end of the truss members. The sloping web members were connected to the top chords with truss connector plates measuring 40 mm × 80 mm. The top chords were joined at the apex to each other and to the vertical web member with a 100 mm × 100 mm truss connector plate. The roof trusses were assembled off-site by an accredited roof truss manufacturer using typical commercial construction techniques to press the plates into both sides of the timber.

Figure 5-8 – Typical truss connector plate (taken from MiTek (2011))

To aid in the manufacturing process, the timber members of the roof truss are held together with wire dogs prior to having the connector plates pressed in as shown in Figure 5-9. These wire dogs remain embedded in the timber after the manufacturing process is complete.

Figure 5-9 – Example of connection at top chord of truss, embedded wire dogs visible above truss connector plate

Purlins spanned between truss top chords and at both ends of the trusses as shown in Figure 5-10. These were constructed with 90 mm × 45 mm kiln dried SG8 (machine stress graded to AS/NZS 1748:2006) H1.2 Radiata pine at maximum 1000 mm centres. Purlins were fixed to the trusses using three nails at each purlin joint as shown in Figure 5-11.

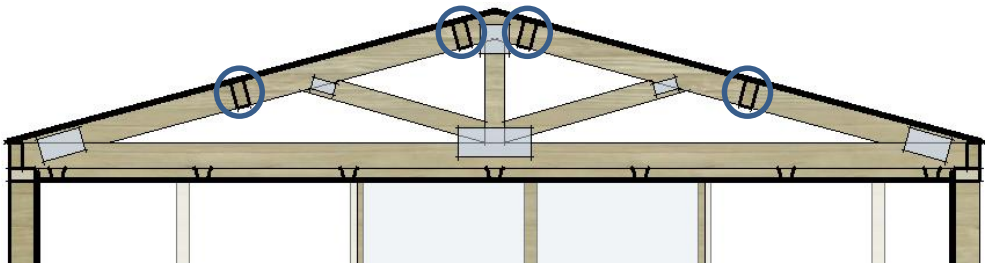

Figure 5-10 – Section showing purlin set-out (purlins circled)

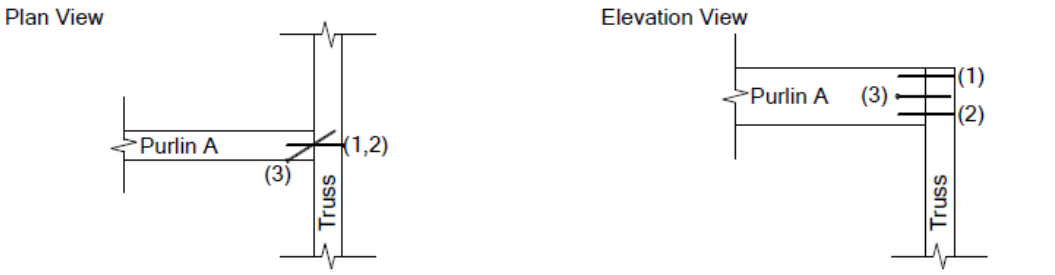

Figure 5-11 – Purlin fixing details (used with permission from Versatile Homes and Buildings)

The trusses were fixed to the top plate of walls using two 1.55 mm thick galvanised steel right angle brackets measuring 40 mm wide with a 28 mm deep bottom face and 85 mm high top face. One bracket was fixed to each side of the truss with four 30 mm x 3.15 mm nails to the truss and two 14g x 35 mm self-tapping drill screws into the top plate as shown in Figure 5-12 and Figure 5-13.

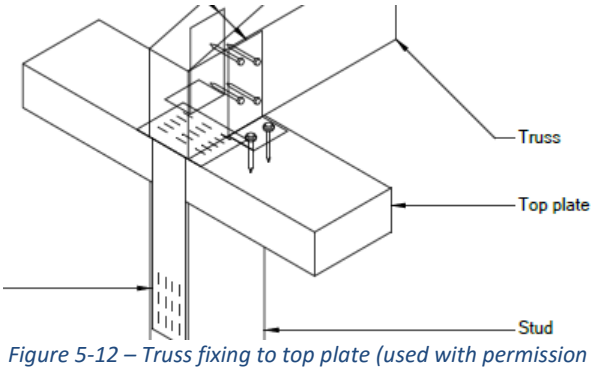

Figure 5-12 – Truss fixing to top plate (used with permission from Versatile Homes and Buildings)

Figure 5-13 – Photo of truss fixing to top plate

5.2.4 Roof Bracing

The roof truss system was braced using metal straps as shown in Figure 5-14 and Figure 5-15. These straps were 0.55 mm thick × 27 mm wide, made of G550 Z275 galvanised steel and laid over the top of purlins and tensioned. Each end was fixed with five 30 mm x 3.15 mm galvanised nails to timber and the crossing point was fixed with two 30 mm x 3.15 mm galvanised nails. The bracing is intended to transfer the load from the roof and roof truss top chords to the top plate of the wall, and then via the top plate into the foundation through the wall bracing system.

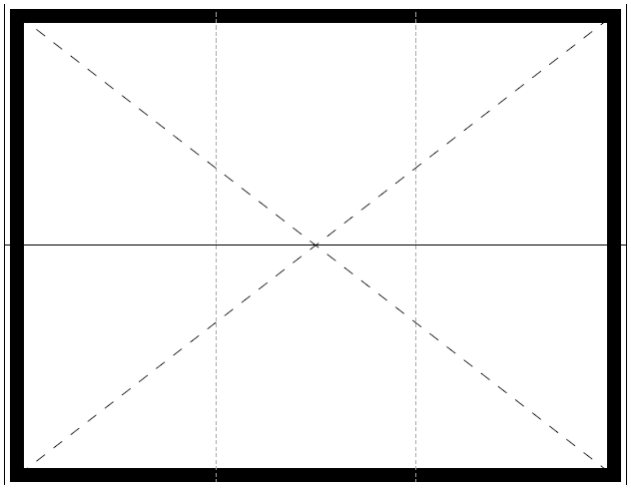

Figure 5-14 – Roof bracing layout, indicated with dashed line (used with permission from Versatile Homes and Buildings)

Figure 5-15 – Photo showing roof bracing

5.2.5 Roofing

The roofing was constructed of 0.35 mm thick mild steel 'roofing iron' with a rib profile, fixed to purlins with 12 mm × 65 mm screws with a set out as shown in Figure 5-16. Bituminous building paper was installed under the roofing and a flashing installed at the ridge of the roof as shown in Figure 5-17. The edge of the roofing overhung the long walls and there was no gutter installed at the edge, as shown in Figure 5-18. Barge flashings were installed at the end of the roofing where it met the short walls. Barges were fixed through the roofing to the top chord of trusses below with 12 mm × 65 mm screws, and nailed into purlins from the ends. Note that at the 'free' end wall, the barge was not fixed through the roofing, instead only fixed to the 'floating' truss on top of the end wall.

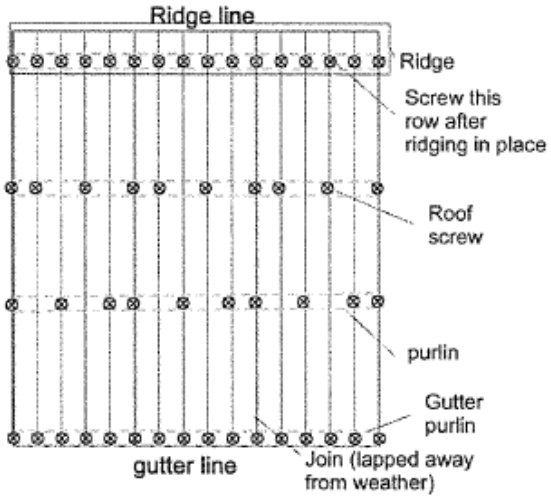

Figure 5-16 – Roof screwing pattern (used with permission from Versatile Homes and Buildings)

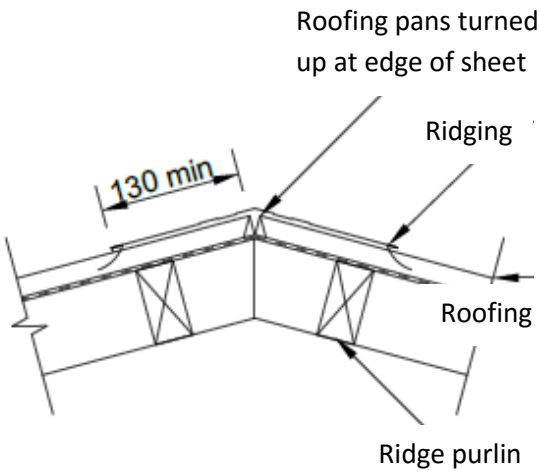

Figure 5-17 – Roof ridging detail (used with permission from Versatile Homes and Buildings)

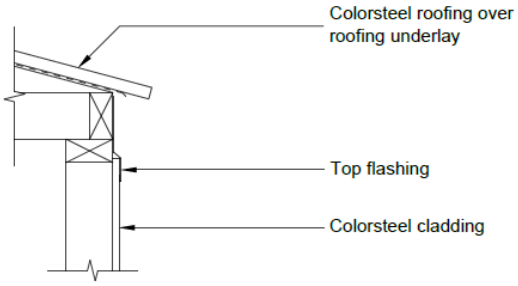

Figure 5-18 – Roof gutter edge detail (used with permission from Versatile Homes and Buildings)

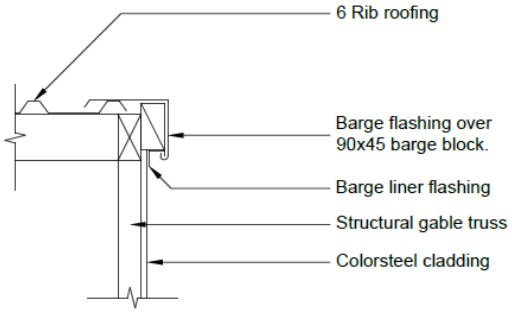

Figure 5-19 – Roof barge detail (used with permission from Versatile Homes and Buildings)

5.2.6 Ceiling System

In common residential construction in NZ, ceiling linings are typically fixed to timber or metal battens, which are either suspended from the roof trusses above or fixed directly to the roof trusses. For this research, metal battens were fixed to the underside of the bottom chord of roof trusses, spanning the long dimension (4.33 m) of the compartment. There were 7 lengths of 35 mm deep battens spaced at approximately 500 mm centres, with the battens closest to the walls being spaced approximately 75 mm from the wall. The layout is shown below in Figure 5-21. The battens were constructed of 0.55 base metal thickness (BMT) steel, and the profile/shape is shown in Figure 5-20. Battens were fixed to each timber truss using 8g × 32 mm wafer head needle tip screws, two per truss fixing. The ends of the battens butting into the short walls were supported with 90° 38 mm × 38 mm knurled finish 0.55 BMT steel fixed into the top of studs in the short wall, as shown in Figure 5-22 and Figure 5-23.

Figure 5-20 – Image and profile of ceiling batten

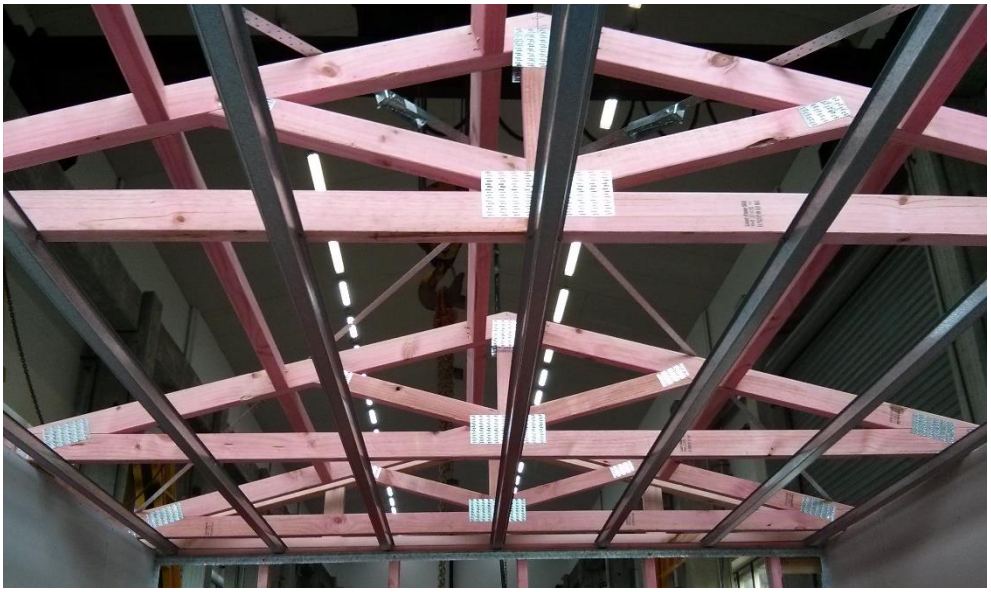

Figure 5-21 – Photo showing ceiling batten layout

Figure 5-22 – Batten and bracket fixing configuration

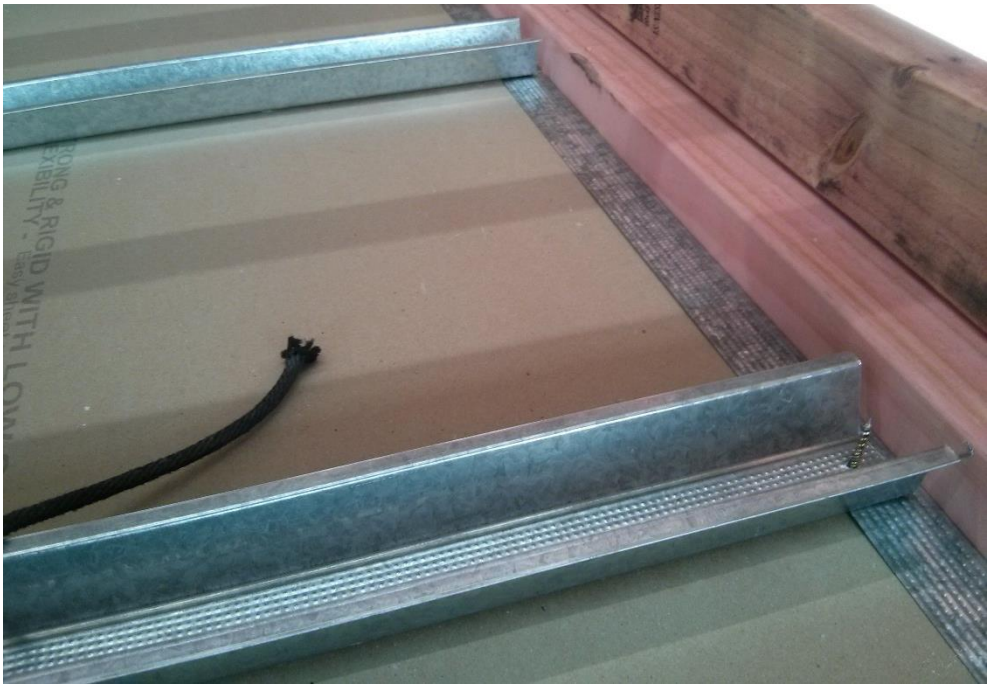

Figure 5-23 – Batten end right angle plate configuration with plasterboard fixed

Sheets of 10 mm standard plasterboard were fixed to the ceiling battens with the long (2400 mm) sheet dimension being perpendicular to the batten direction. Sheet end joints were staggered and all butt joints were formed over ceiling battens. The sheets were fixed at the edges and centre to each

batten with 32 mm dual thread plasterboard screws. At butt ends, screw fixings were spaced at 200 mm along the cut edge of the sheet. Daubs of glue were placed on battens at 200 mm centres between the screw fixings. Figure 5-24 shows a photo of the compartment viewed from above with ceiling linings fixed to metal battens.

Figure 5-24 – Plasterboard ceiling fixed to battens, viewed from above

5.2.7 Wall Linings

Internal linings were 10 mm thick standard grade plasterboard, except for the fire-rated wall which had 10 mm thick fibre-reinforced plasterboard on both sides of the timber framing. Sheets were supplied in 2400 mm × 1200 mm size and cut to suit the framing layout and ceiling height. Sheets were installed in the vertical orientation, i.e. 2400 mm length spanning between the bottom plate and top plate or ceiling. Sheets were touch fitted and installed with a 5 – 10 mm gap between bottom edge of lower sheet and notional floor reference level. The internal faces of all walls were taped and stopped using two coats of a 90-min setting bedding compound and paper reinforcing tape.

The fibre-reinforced plasterboard sheets were fastened to the fire-rated wall framing with 41 mm x 6g gold passivated high thread screws at 300 mm centres on the perimeter of each sheet and along each stud. The fasteners were located approximately 12 mm from bound sheet edges and 18 mm from cut sheet edges. Fasteners in the corners were placed 50 mm from the sheet edge in both directions.

The standard grade plasterboard sheets were fastened to framing with 32 mm × 6g gold passivated high thread screws at 300 mm centres on the perimeter of each sheet. Daubs of adhesive were spaced at 300 mm centres to fix the centre of the sheet to intermediate studs. Fasteners were placed nominally at 12 mm from sheet edges. In the corners they were placed 50 mm from the sheet edge in both directions.

5.2.8 Wall Cladding

The walls were designed as non-fire-rated walls, except for the one long fire-rated wall which was designed to achieve a 30-min FRR using common industry construction details. The external cladding

consisted light-weight sheet materials to the roof and walls, except for the fire-rated wall which had 10 mm thick fibre-reinforced gypsum plasterboard both sides and no additional covering. The non-fire-rated long wall was clad with three different light-weight systems as shown in Figure 5-25: 10 mm standard plasterboard, 7 mm plywood and 6 mm fibre cement board to assist with research being carried out by others. The ply lining consisted of a 1200 mm and 130 mm wide sheets, the plasterboard was a single 1200 mm wide sheet, and the fibre cement consisted of one 1200 mm wide and one 600 mm wide sheet; all sheets were 2400 mm in length.

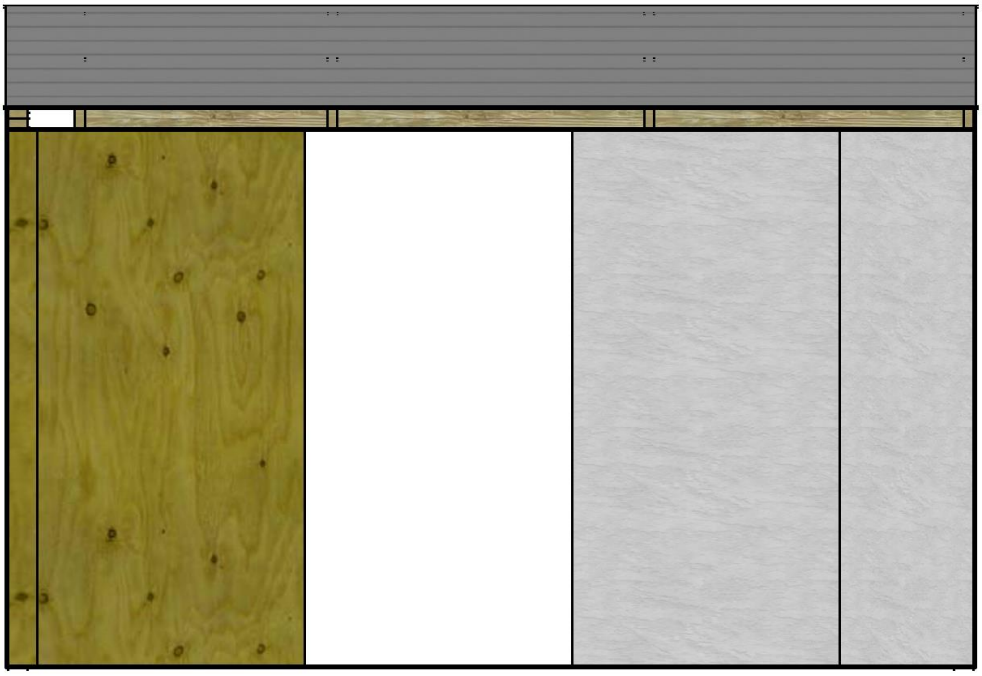

Figure 5-25 – Non-rated long wall cladding systems, from left to right: plywood, plasterboard, fibre cement

The plywood and plasterboard were screw fixed at 300 mm centres around the perimeter of the sheets and along intermediate studs, using 32 mm × 6g gold passivated high thread screws. The fibre cement board was fixed with 40 mm × 2.8 mm nails at 200 mm centres on sheet edges and intermediate framing.

The short 'fixed' and 'free' end walls were clad with 0.35 mm thick mild steel with a zinc/aluminium and paint coating, and a weatherboard appearance achieved by roll-forming. The boards were nailed to timber framing with galvanised flat twisted shank clouts (35 mm × 2.8 mm). The barge end (above the wall) was clad with 0.40 mm thick mild steel with a zinc/aluminium and paint coating, and a board and batten appearance achieved by pressing. The boards were nailed to timber framing with galvanised flat head, twisted shank clouts (35 mm × 2.8 mm). Corners, openings and laps were nailed at approximately 120 mm centres, and internal studs were nailed at approximately 230 mm centres. Figure 5-26 shows the cladding on the fixed end short wall. Also visible is the opening which was later fitted with a fire-resistant glazed viewing panel to complete the compartment enclosure and allow viewing into the compartment during the experiment.

Figure 5-26 – Short wall cladding, prior to roof installation

5.2.9 Lateral Load

A lateral load was designed for the fire-rated wall based on B1/VM1 requirements for a 0.5 kPa face load. This translated to a 0.6 kN.m^{-1} line load at the top of the wall as shown in the calculations below. The load was applied as an 'outward' pulling load on the fire-rated wall rather than a push as this was considered the more onerous scenario for the small compartment. The reason for this is that a pushing load on the fire-rated long wall would be supported by both the end walls, whereas a pulling load requires the support of the roof truss system. Both loads require the long walls to resist bowing due to the lateral load, however the distance between the end walls becomes more important in the pushing scenario, i.e. a longer compartment may perform quite differently. It is recognised that a lateral load on a gable end wall may be more onerous, the research has not set out to assess this.

0.5 kPa $\times$ 2.4 m stud height:
= 1.2 kN.m^{-1} line load at mid height of wall

1.2 kN.m^{-1} line load at mid height of wall:
= 0.6 kN.m^{-1} applied at top and bottom plate of wall

There was no load applied to the bottom plate due to it being fixed to the furnace frame. Any load applied at the bottom plate would not be transferred to the other elements in the building and therefore applying a load at the bottom plate would not affect the experiment. A 0.6 kN.m^{-1} uniformly distributed line load applied at top plate level is considered to be representative of a 0.5 kPa face load. The wall is 4.33 m long and three fixing points were used for the lateral load. The load at each fixing point was determined to be 88.3 kg, as shown in the calculations below.

0.6 kN.m^{-1} $\times$ 4.33 m = 2.60 kN

$$\frac{2600\ \text{N}}{9.81\ \text{ms}^{-2}} = 265\ \text{kg}$$

$$265/3 = 88.3\ \text{kg}$$

This lateral load was achieved by suspending three water-filled steel drums at discrete fixing points, spaced to represent a uniformly distributed load along the top plate of the fire-rated wall. The drums were suspended via a pulley system as shown in Figure 5-27, the steel bar runner was fixed to a custom-built timber support frame. To determine the fixing point locations, the top plate is conceptually split into three even length segments of 1.43 m each, and the midpoint of each of these segments used as the location to fix the load. The loads were fixed at 0.72 m from each end, and one at the centre of the wall. The drums were suspended approximately 100 mm to 150 mm from the ground, which was intended to be sufficient to allow the wall to 'fail' but not fall away entirely from the compartment. Note that the height of the drums could not be accurately set due to the challenges in fixing the cable system. Figure 5-28 shows a photo of the water drums suspended prior to the experiment being carried out.

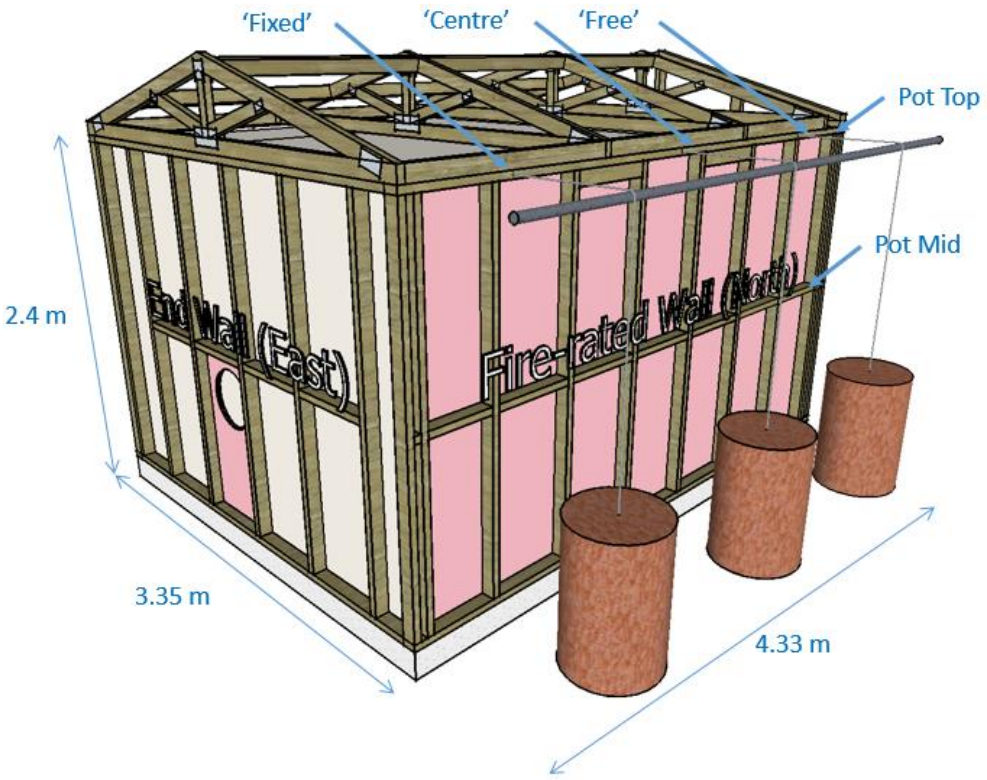

Figure 5-27 – Image illustrating lateral load applied to fire-rated wall of compartment

Figure 5-28 – Experiment #1 photo of water drums used to apply lateral load to fire-rated wall

5.2.10 Expected Behaviour of Laterally Loaded Compartment

The expected behaviour was rationalised by considering the load paths due to the lateral load imposed on the fire-rated wall. The lateral load applied at top plate was expected to impart a tensile load on the bottom chord of the roof trusses that span between the fire-rated wall and non-rated long wall. The compartment is fixed into the furnace specimen frame through the bottom plate, and this prevents the compartment from being accelerated in the direction of the load. The compartment is expected to be kept rigid and square by the end walls resisting the tendency for the non-rated long wall to collapse inward. The end walls therefore end up having an in-plane shearing resistance, to counteract the lateral load applied at the top plate of the fire-rated wall.

Figure 5-29 shows the expected load paths, noting that the magnitudes are not to scale. The expected mode of failure in the fire scenario is at the bottom chord of the roof truss; due to the tensile load and reduced cross-sectional area following fire exposure. The spliced connection at the centre of the truss is expected to have less capacity in fire than the timber truss cross-section.

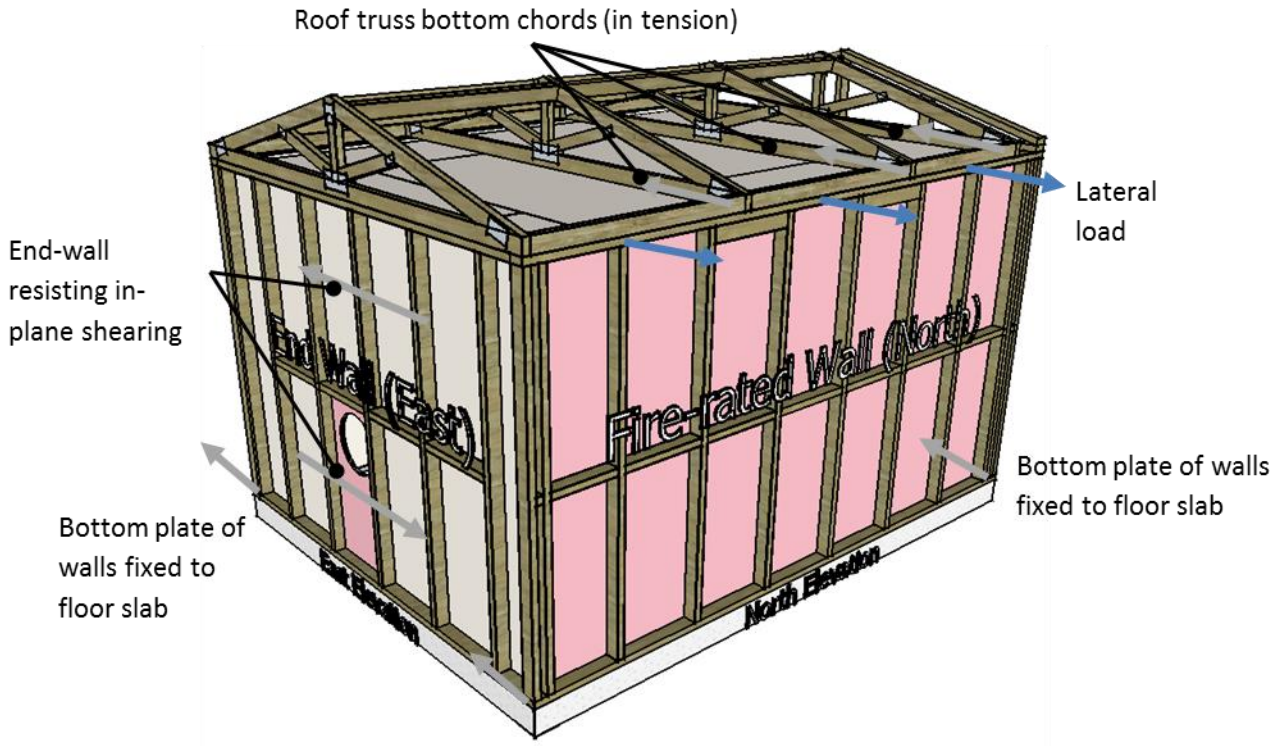

Figure 5-29 – Expected load transfer for laterally loaded compartment

The bracing capacity of the end-walls was not expected to be an issue, as these are commonly designed for much greater loads due to earthquake. This warrants some discussion about the bracing performance of walls. In NZ the bracing performance of walls constructed in accordance with NZS 3604:2011 is determined by test and not calculation of behaviour of components. The test that is used is known as the 'P21 test' and it subjects a specimen to repeated lateral load. The specimen is pushed to a pre-determined deflection and the resistance achieved at this deflection is measured, this is done cyclically. The peak load from the bracing test gives the value for resisting wind loads, and the residual load after a number of cycles gives the earthquake bracing capacity. Earthquake capacity is usually lower than wind. Bracing units are calculated per metre of length for a given wall height. These are multiplied by the length of the wall to calculate the contribution of a particular wall length.

There are no simplified methods for calculating bracing performance of light timber-framed buildings in fire conditions. There will be a complex interaction of degraded linings, framing and cladding and fixings and this is beyond the scope of what this research investigates. Bracing performance during fire is not something that is commonly researched as usually buildings are tested for performance in fire, earthquake, or wind as individual and not concurrent events.

5.3 Instrumentation

5.3.1 Dummy Chord

A dummy chord with an array of twelve thermocouples was installed in the roof space of the compartment, at the same height and similar location to the bottom chords of the roof trusses. The thermocouple layout is shown in Figure 5-30. Mineral insulated metal sheath (MIMS) Type K thermocouples were used. A nail plate was fixed to one side of the dummy chord as shown in Figure

5-34, so that the difference in char rates on timber with and without a nail plate could be compared. The general location of the dummy chord in the ceiling space is shown in Figure 5-31, and a photo of the installed location in Figure 5-33. The dummy chord was suspended from the roof purlins, so as not to impart any additional loading on the ceiling system. The additional load on the roof purlins and trusses was considered negligible in the context of the experiment.

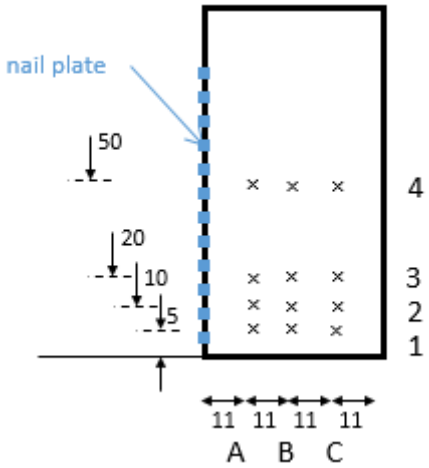

Figure 5-30 – Experiment #1 dummy chord thermocouple layout

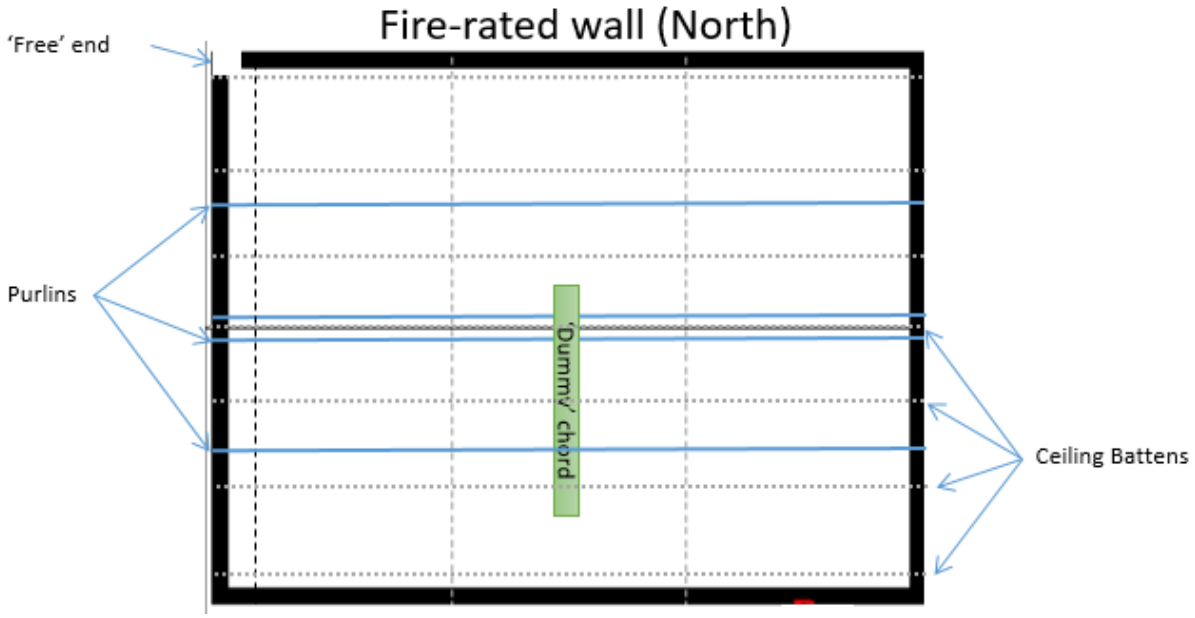

Figure 5-31 – Experiment #1 dummy chord general location

Figure 5-32 – Photo of dummy chord with splice

Figure 5-34 – Experiment #1 photo of dummy chord with splice showing nail-plate

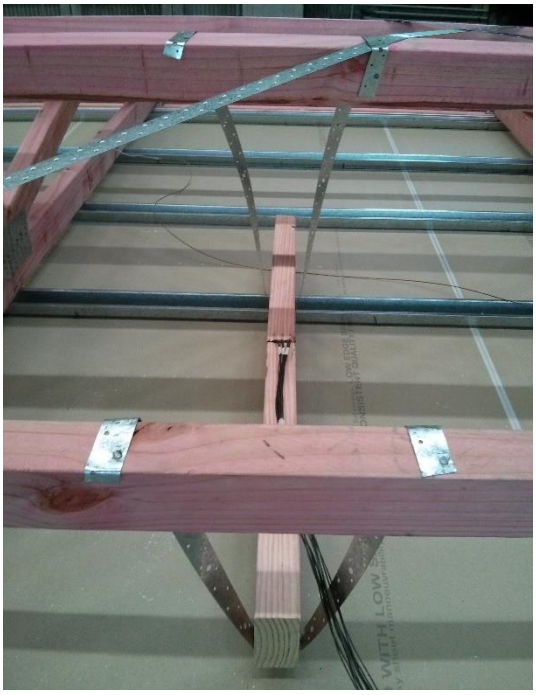

Figure 5-33 – Experiment #1 photo of dummy chord suspended from purlins

5.3.2 Temperature Measurements – Devices

Surface temperatures and adiabatic surface temperature measurements were recorded at a number of locations on the internal walls, ceiling and cladding. The types of devices used to measure temperature are listed in Table 5-1. These temperature readings provided data on the charring rates and the temperatures in the compartment and ceiling spaces. Copper disc thermocouples were chromel-alumel thermocouples mounted on copper discs and covered with insulating pads, in accordance with clause 2.2.3 of AS 1530 Part 4.

Table 5-1 – Measurement device types and descriptions

Device Type	Description
A	The thin steel plate devices consisted of a 75 mm × 75 mm square mild steel plate approximately 0.6 mm thick, painted on the front (fire exposed surface) with high temperature black paint as shown in Figure 5-35. A 24g bare thermocouple wire bead was welded to the centre of the back face of the steel plate (Figure 5-35, Figure 5-36 and Figure 5-37).
B	Thin steel plate with affixed thermocouple and ceramic fibre insulation backing, compressed thickness approximately 10 mm; measuring adiabatic surface temperature of internal linings (Figure 5-38).
C	Plate thermometers constructed in accordance with ISO 834-1 (1999) and EN1363-1 (2012). The plate thermometers are made from a 0.7±0.1 mm thick nickel alloy sheet. The 150 × 100 mm sheet is folded to form a plate thermometer with a face of 100 x 100 mm. A K-type thermocouple was secured to the centre of the back face of the nickel alloy sheet by a small (25 × 6 mm) steel strip and two 2 mm diameter screws. A 97 mm × 97 mm × 10 mm thick) pad of inorganic insulation material was fitted behind the thermocouple; measuring adiabatic surface temperature (Figure 5-39).
D1	Copper disk thermocouple covered by insulated pad; measuring cavity surface temperature of exposed lining.
D2	Copper disk thermocouple covered by insulating pad; measuring cavity surface temperature of unexposed lining or cladding.
E	Fibreglass insulated, Type K, thermocouple wire with twisted ends, measuring air temperature in roof space.
F	Copper disk thermocouple; measuring outside surface temperature of unexposed plasterboard, plywood or fibre cement. Fiberglass insulated, Type K, thermocouple wire with twisted ends used (held with a screw) on metal cladding.
G	Fibreglass insulated, Type K, thermocouple wire with twisted ends. Installed between ceiling lining and underside of bottom chord of roof truss; measuring air temperature in roof space.

Figure 5-35 - Photo of thin steel plate surface temperature measuring device (Type A) (Wade, 2015)

Figure 5-36 shows a section view of a thin steel plate device fixed to a wall, and Figure 5-37 a section of a thin steel plate device fixed to a ceiling.

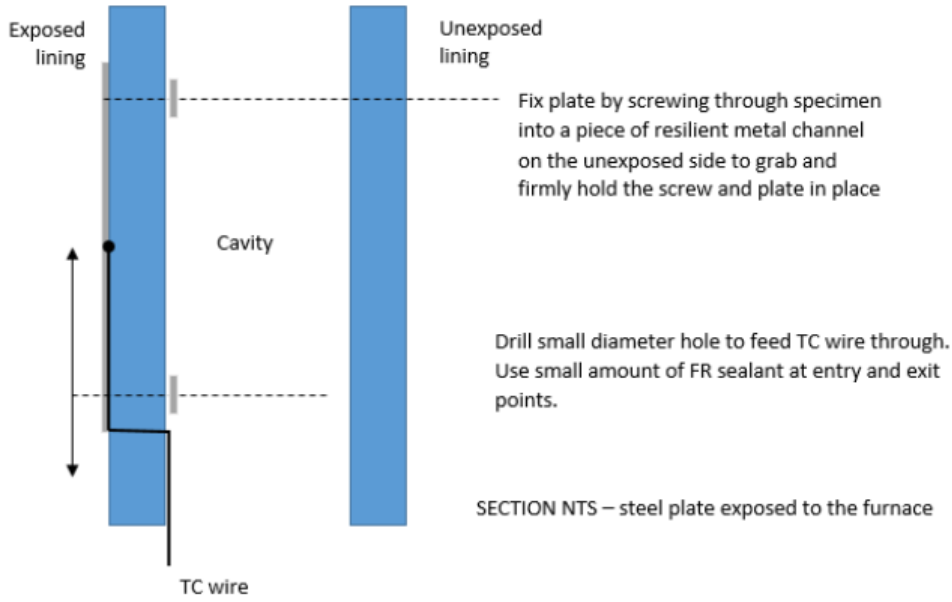

Figure 5-36 – Section through wall showing thin steel plate (Type A) device measuring surface temperature (Wade, 2015)

Figure 5-37 – Section through ceiling showing thin steel plate (Type A) device measuring surface temperature (Wade, 2015)

Figure 5-38 shows a section view of a thin steel plate with insulation backing (Type B) device fixed to a ceiling as used to measure adiabatic surface temperature.

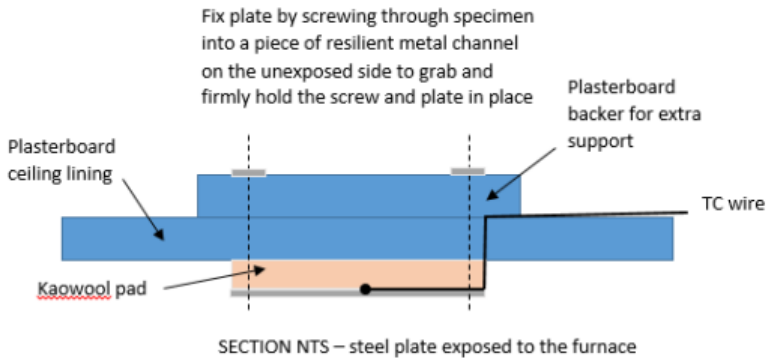

Figure 5-38 – Section through ceiling showing thin steel plate with insulation backing (Type B) device measuring adiabatic surface temperature (Wade, 2015)

Figure 5-39 shows a section view of a plate thermometer (Type C) device fixed to a wall as used to measure adiabatic surface temperature.

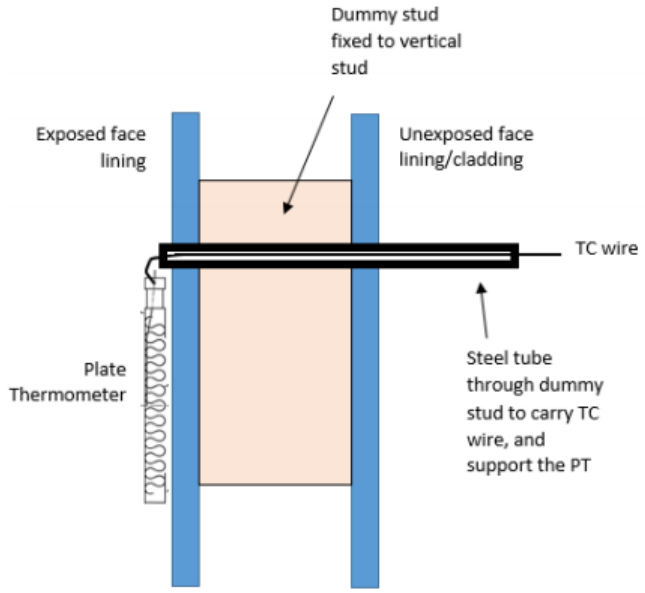

Figure 5-39 – Section through wall showing plate thermometer (Type C) device measuring adiabatic surface temperature (Wade, 2015)

5.3.3 Temperature Measurement – Ceiling and Roof

The surface temperature and adiabatic surface temperature on the exposed side of the ceiling linings were measured with device Type A and B respectively. These devices were located in two places on the ceiling. The surface temperature on the unexposed side of the roof was measured in two places using Type F devices. In locations below these Type F devices, the roof space air temperature was measured with a device suspended from the roof purlins (Type E). Type G devices were installed in the air space between the bottom chord of trusses and the top of ceiling linings. The locations of the devices in a plan and view are shown in Figure 5-40 and Figure 5-41 respectively.

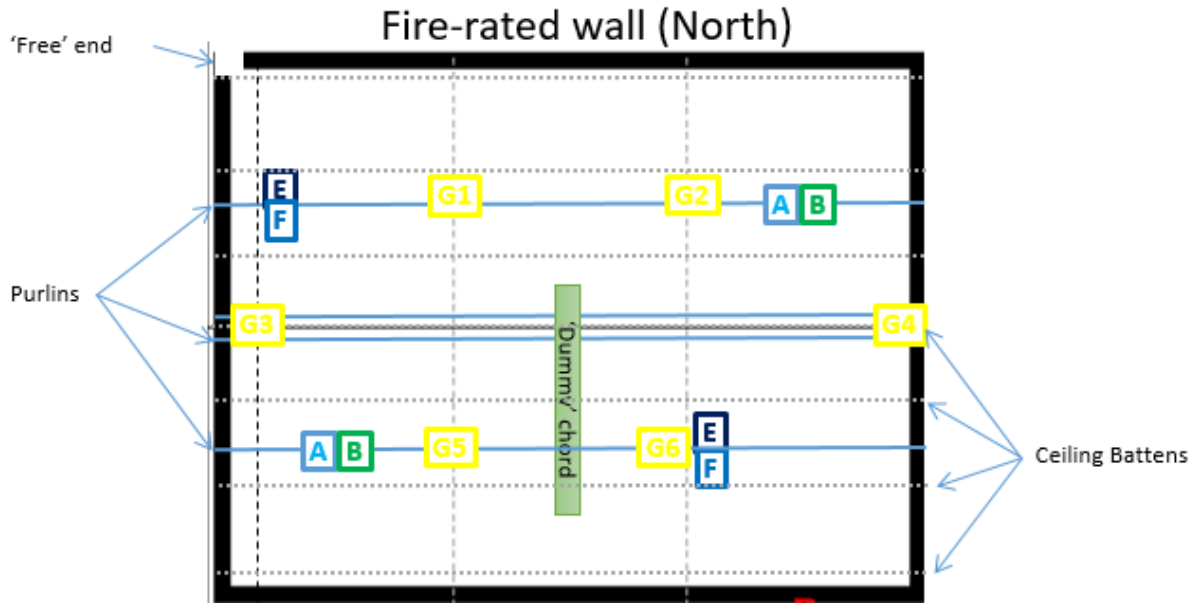

Figure 5-40 – Experiment #1 ceiling and roof device locations, plan view

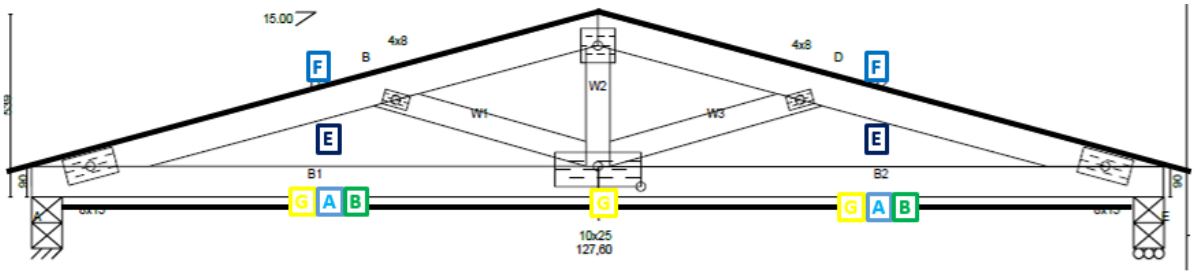

Figure 5-41 – Experiment #1 ceiling and roof device locations, section view

5.3.4 Temperature Measurement – Walls

Temperature measurements were taken at a number of locations on each wall, on the exposed surface, in the cavity and on the outside of the wall. The fire-rated wall had six measurement locations, with various measurements taken in each. The general layout of the devices in relation to the timber framing set-out is shown in Figure 5-42. Devices were installed approximately midway between studs, at approximately one third or two thirds the stud height, referred to as 'high' and 'low' device locations respectively.

Near the centre of the wall the following were measured: exposed lining surface temperature, exposed lining adiabatic surface temperature, exposed and unexposed lining cavity face temperature, and the unexposed lining outside face temperature using Type A, C, D1 and D2 devices respectively. The unexposed lining outside face temperature was measured at five locations using Type F devices; in addition to the aforementioned central location these were at opposing ends of the wall in low and high locations. Exposed and unexposed lining cavity temperature measurements were also taken near the 'free end' of the fire-rated-wall, coincident with the unexposed lining outside face device.

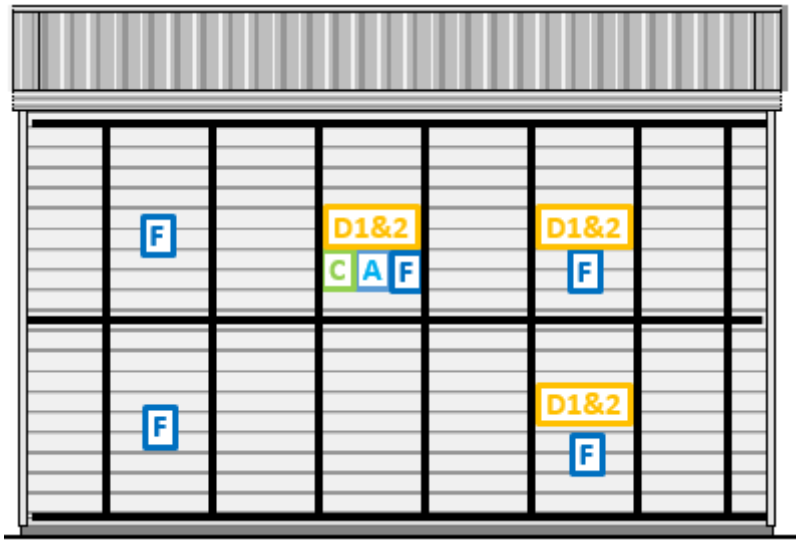

Figure 5-42 – Experiment #1 general layout of devices in fire-rated wall (viewed from outside)

Figure 5-43 shows the general layout of devices in non-rated long wall. Devices were fixed to the outside face of each unexposed cladding type. For the plywood and fibre cement these were installed in the low and high locations, and in the standard plasterboard a single thermocouple was installed at the high location. Devices were installed on the cavity side of both the exposed and unexposed linings at low and high locations for the plywood and fibre cement, and high location only for the standard plasterboard. Thin steel plates (Type A) and plate thermometers (Type C) were installed at high locations on the plywood and fibre cement exposed linings facing the compartment.

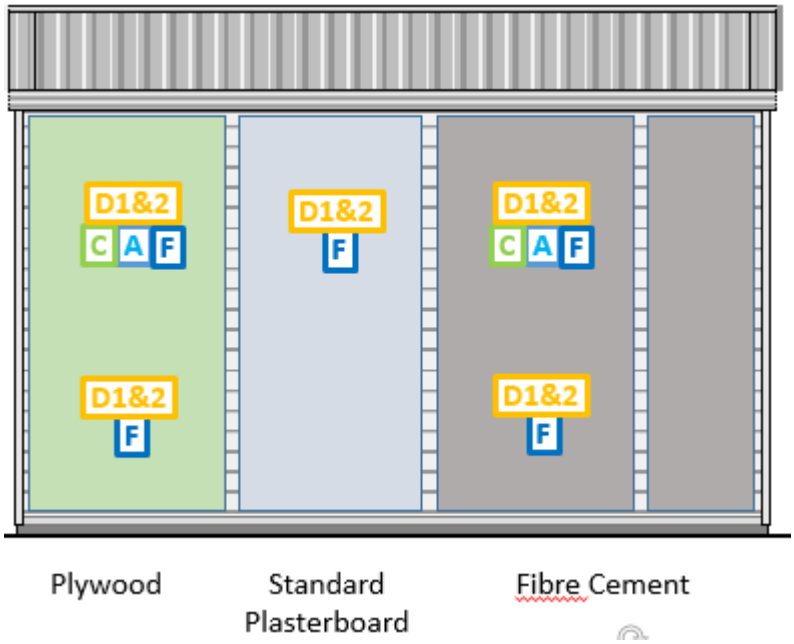

Figure 5-43 – Experiment #1 general layout of devices in non-rated long wall

Devices were installed in both the end walls in the high location. These included Types A, C, D1, D2 and F. Figure 5-44 shows the general layout for the 'fixed' end wall, and this was the same for the 'free' end wall when viewed from the outside.

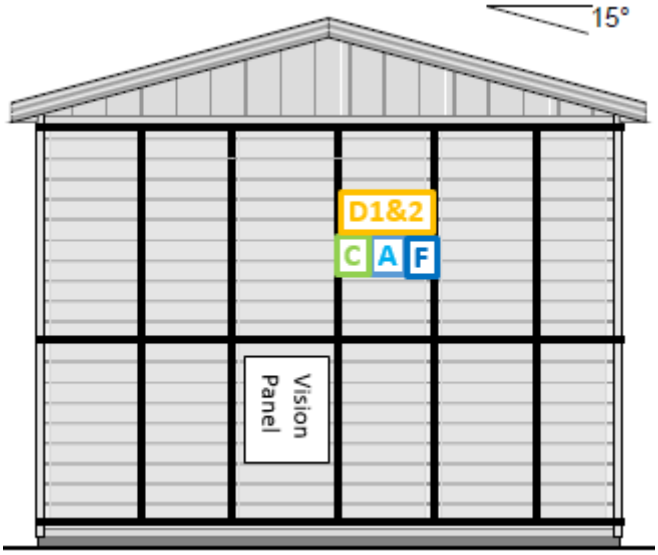

Figure 5-44 – Experiment #1 general layout of devices in fixed end wall

Figure 5-45 – Experiment #1, photo showing 360° view inside the compartment, Type A, B and C devices are visible

5.3.5 Fire-rated Wall Deflection

The deflection of the laterally loaded fire-rated wall was measured at various locations using two methods. One method was a manual measurement of the fall in height of the drums which were suspended from the wall, this gave deflection at the top plate at three locations at 5 min intervals. At the free end of the wall, along the end stud-line, three linear potentiometers were fixed on a frame to measure deflection at the bottom plate, nogging and top plate heights. A photo of the set-out of these potentiometers is shown in Figure 5-46. Ceramic fibre insulation wool was affixed to the outside of the wall and in a gap between the top plate of the wall and the underside of the roof to protect the potentiometers from damage. The bottom plate measurement was not expected to deviate from its initial position, given the bottom plates fixing to the furnace specimen frame.

Figure 5-46 – Experiment #1 photo of linear potentiometers at mid (nogging) and top plate at free end wall

5.3.6 Furnace and Experiment Procedure

The furnace frame consists of a concrete ring beam, fixed to a steel frame used to anchor the specimen into the furnace, shown in Figure 5-47. The bottom plate of the compartment was fixed directly into the concrete frame using M12 bolts at approximately 1200 mm centres to the perimeter of the furnace specimen frame.

Figure 5-47 – Experiment #1 furnace specimen frame

The compartment, attached to the specimen frame was lifted onto the horizontal furnace (Figure 5-48) and the specimen frame fixed to the furnace.

Figure 5-48 – Experiment #1 compartment being lowered onto furnace

The intent was to carry out the experiment in accordance with AS 1530 Part 4 (SAA, 2005) as closely as possible. However there were a number of challenges with the experiment due to the unique case of having a whole building on a furnace. These challenges are discussed throughout the report where relevant. The gas-fired furnace has twelve MIMS chromel-alumel thermocouples uniformly distributed over the plan area of the furnace, at approximately 100 mm below the notional floor level. An average of the temperature reading for all thermocouples at each point in time was used as an input to drive the furnace to follow the ISO 834 time-temperature curve. It can be seen from Figure 5-49 that the temperature measured by the furnace thermocouples closely followed the ISO 834 standard fire curve for the experiment duration of 30.5 min. The furnace temperature, as measured by the furnace thermocouples, was within the tolerances of AS 1530 Part 4 throughout the experiment.

In a common furnace test the thermocouples driving the furnace would be located 100 mm from the face of the test specimen. In this experiment they were all below notional floor level and the compartment extended to more than 2.4 m above this height. Due to heat losses from the perimeter walls and roof of the compartment, it was found there was more variation in temperature over the height of the compartment than in a standard furnace test and this is described further in Section 5.4.5.

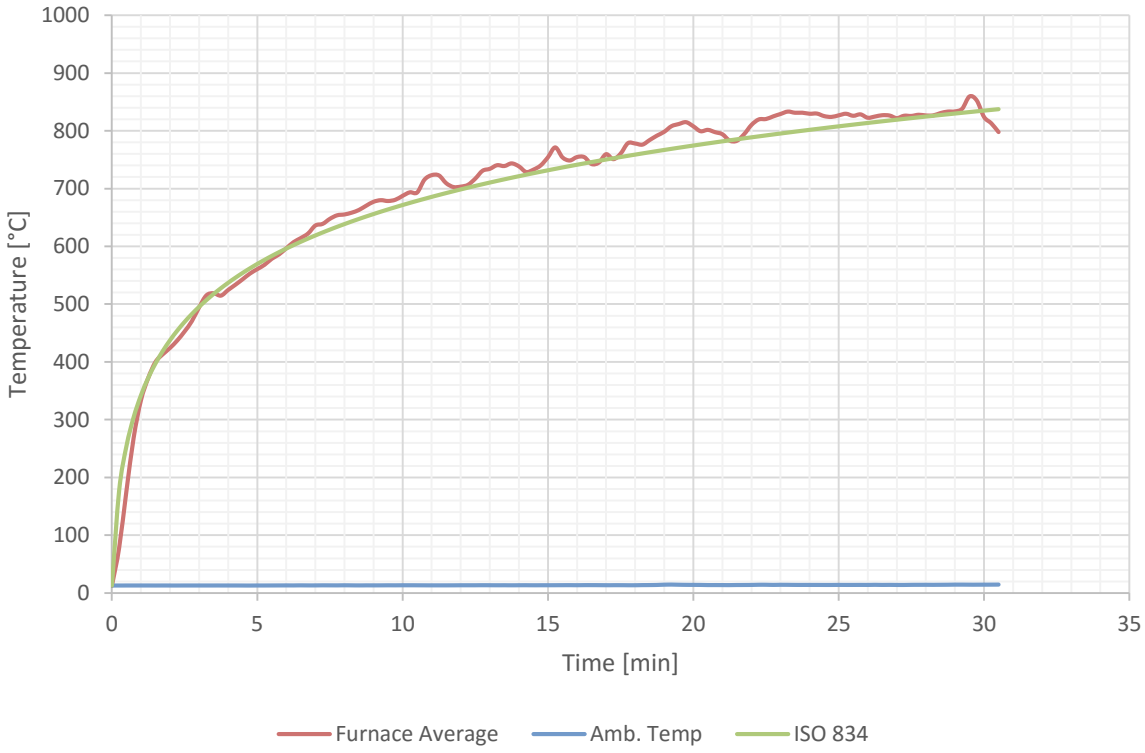

Figure 5-49 – Experiment #1 furnace temperature (average of furnace probes) and ISO 834 time-temperature curve

AS 1530 Part 4 (SAA, 2005) specifies that a furnace pressure of zero is established at a height of 500 mm above the notional floor level for the specimen for vertical elements. An average value of 8.0 Pa pressure change per metre height is given in AS 1530 Part 4 and is used in assessing furnace pressure conditions. The pressure at the sensor is not meant to deviate by more than ±5 Pa for the test time between 5 and 10 min, and not more than ±3 Pa from 10 min into the test onward.

The differential pressure of the furnace above the laboratory atmosphere was controlled to be neutral at 500 mm above the floor level (-6 Pa at the probe). The differential pressure was monitored using a micro-manometer connected to a computer controlled data logging system which recorded the pressure at 15 s intervals. The pressure measured at the probe is shown in Figure 5-50. During the experiment, the laboratory became smoke-logged (see Figure 5-51) and the furnace negative pressure was increased in an attempt to reduce the volume of combustion products escaping from the compartment into the laboratory space. The target pressure was increased to between -20 Pa and -25 Pa which shifted the neutral plane to between 2.3 m and 2.9 m, based on AS 1530 Part 4 parameter of 8 Pa pressure change per metre height. Positive pressure in the furnace is slightly more severe than negative pressure due to pushing hot gases out through gaps in the specimen. The negative pressure will have slightly reduced the fire severity experienced by construction elements during the experiment compared to a standard fire resistance test.

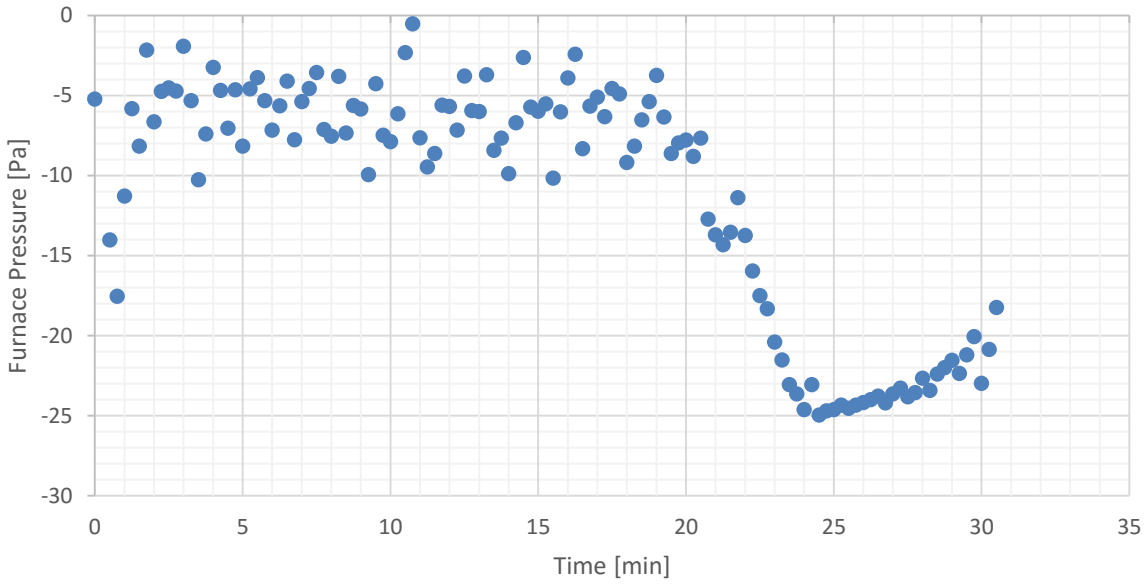

Figure 5-50 – Experiment #1 furnace pressure

Figure 5-51 – Experiment #1 photo of 'free' end wall at approximately 19 min

5.4 Results

5.4.1 Observations

The main observations during the first 10 min of the experiment were increasing quantities of rising steam from the compartment, condensation forming on the outside face of the metal cladding, and no detectable deflection in the fire-rated wall. Approximately 16 min into the experiment, the plasterboard ceiling failed. This was accompanied by significant increases in the quantity of steam and smoke rising from the compartment as shown in Figure 5-52.

Figure 5-52 - Experiment #1 photo of fixed end wall soon after ceiling system failed (approximately 16 min)

The laboratory became smoke-logged approximately 19 min into the experiment due to the extract fans in the roof of the laboratory not being able to keep up with the quantity of smoke and steam gases being released from the test compartment. Just after 20 min the pressure in the furnace is reduced in an attempt to reduce the smoke-logging of the laboratory (see Figure 5-50). A manual measurement of deflections of the top-plate of the fire-rated wall is taken, there are no significant deflections.

After 24 min there is clear evidence of plasterboard wall linings falling away, as there is a visible blackening of the paint on the fixed end wall cladding. Deflections in the order of 10 mm to 15 mm of the top plate of the fire-rated wall are observed. Fire broke through the plywood cladding system after 29 min, and the open area of plywood increased steadily over the next 1.5 min such that the top half of the plywood cladding was mostly burnt away or fallen off. Flaming on the exterior surface of the plywood was manually extinguished.

At 30 min, deflections of the top plate of the wall increased to approximately 20 mm, 30 mm and 40 mm at fixed, central and free load points of the fire-rated wall respectively. The experiment was terminated at 30.5 min.

5.4.2 Roof Space Temperatures

Figure 5-53 shows the roof space temperature measurements during the experiment, measured by the Type G and Type E devices. The time of fall-off of the plasterboard ceiling at approximately 16 min is evident by a rapid increase in temperature readings of the thermocouples in the ceiling space at this time. This failure time is consistent with observations during the experiment.

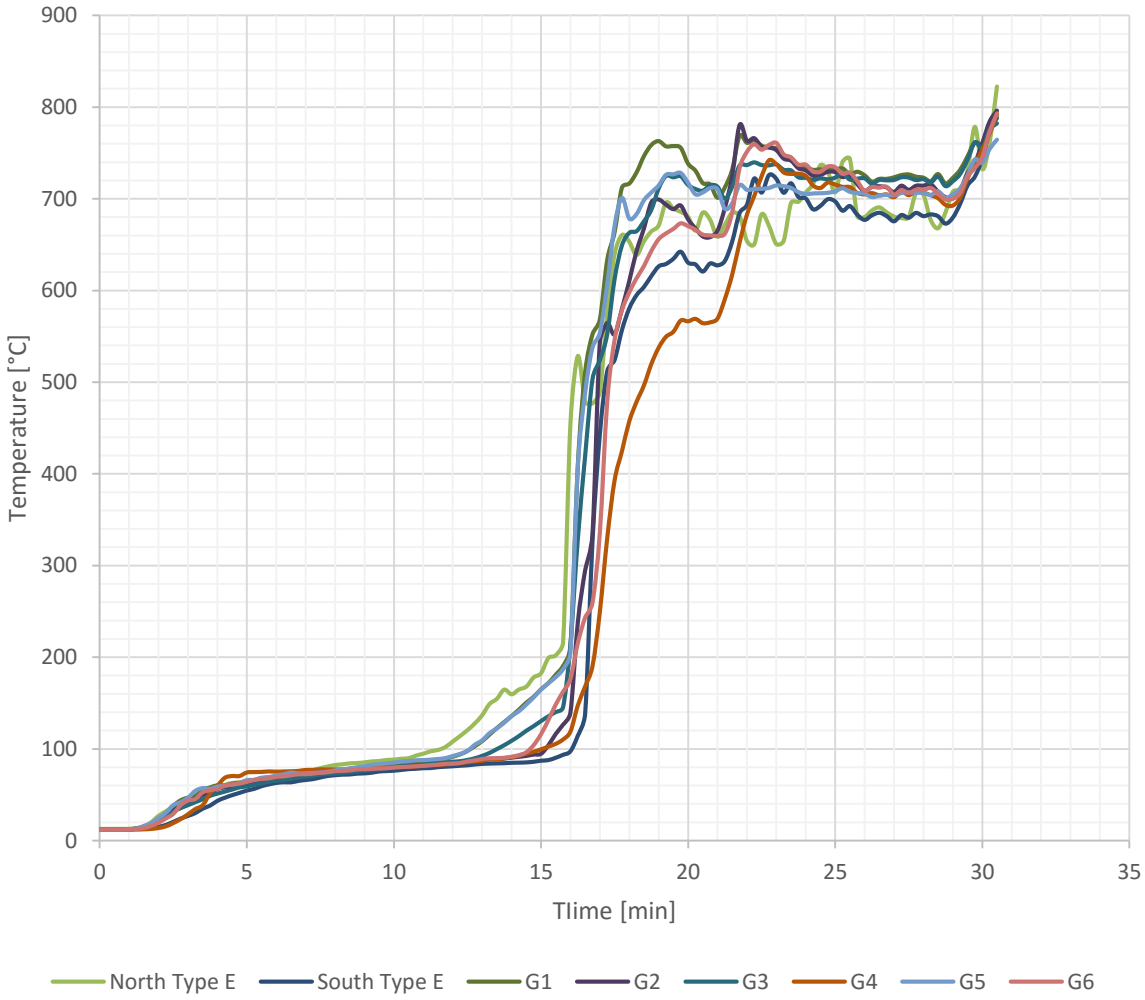

Figure 5-53 – Experiment #1 roof space temperature measurements, Type G and E

5.4.3 Wall Lining Temperatures

Three non-fire-rated walls were lined internally with 10 mm standard plasterboard as described in Section 5.2.7, and each wall would be expected to have a similar failure time. Figure 5-54 compares the fire and cavity side surface temperatures for the exposed standard plasterboard lined walls measured by Type D1 devices. It can be seen from the graph that destructive failure by partial or complete falling off of the wall linings occurred between approximately 27.5 min and 29 min.

Note that based on observations during the experiment, some portions of lining on the lower parts of the end walls failed earlier than 27.5 min. This was evidenced by blackening of the metal cladding at particular locations, from about 24 min onward. An example of what was observed is shown in Figure 5-55. The channel for thermocouple FBC-Low was initially wired in reverse, and this was corrected after 4.5 min; the first 4.5 min of values have been discarded. 'PLY', 'PLB' and 'FBC' refer to the areas of wall clad with plywood, plasterboard and fibre cement respectively. 'High' and 'Low' refers to devices in the upper or lower half of the wall respectively.

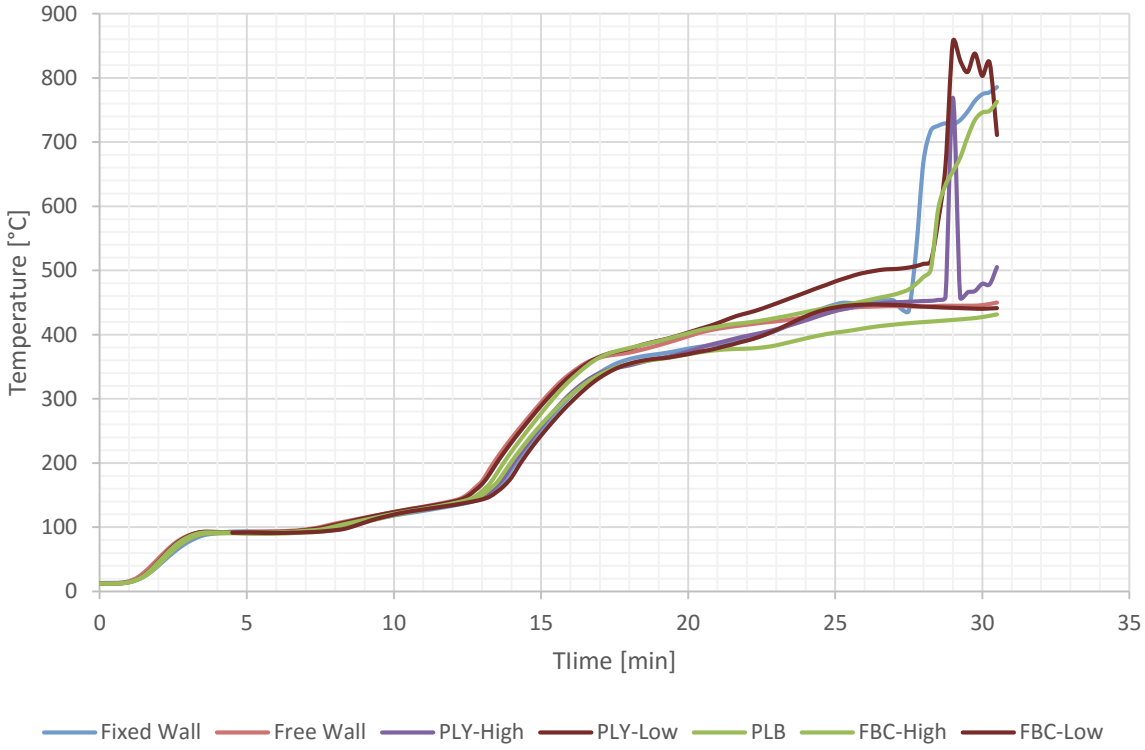

Figure 5-54 – Experiment #1 cavity side temperature of exposed wall linings

Figure 5-55 – Experiment #1 photo showing evidence of lining failure on lower portion of end wall at 25 min

5.4.4 Fire-rated Wall Lining Temperature

Figure 5-56 shows the cavity side temperature measurements for the exposed and unexposed linings of the fire-rated wall lined with 10 mm fibre-reinforced plasterboard as described in Section 5.2.7. There is an initial temperature rise to approximately 100°C of the exposed lining and at this temperature there is a plateau, due to chemical change and moisture removal from the board. The unexposed lining temperature lags behind the exposed lining but exhibits a similar trend. After the last moisture content is driven from the exposed lining at approximately 13 min, the temperature of this lining increases rapidly until reaching approximately 350°C, at which time the temperature increase continues but at a slower rate. The unexposed lining lags behind and its temperature increase is more gradual from 100°C at approximately 13 min to 300°C near the end of the experiment. As discussed in Section 4.4.5, the fall-off time for fibre-reinforced plasterboard is considered to be approximately 600°C. There is no indication from the temperature changes in the board during Experiment #1 that any of the fire-rated linings fell from the timber framing, and it seemed from observation during the experiment that these linings remained in place.

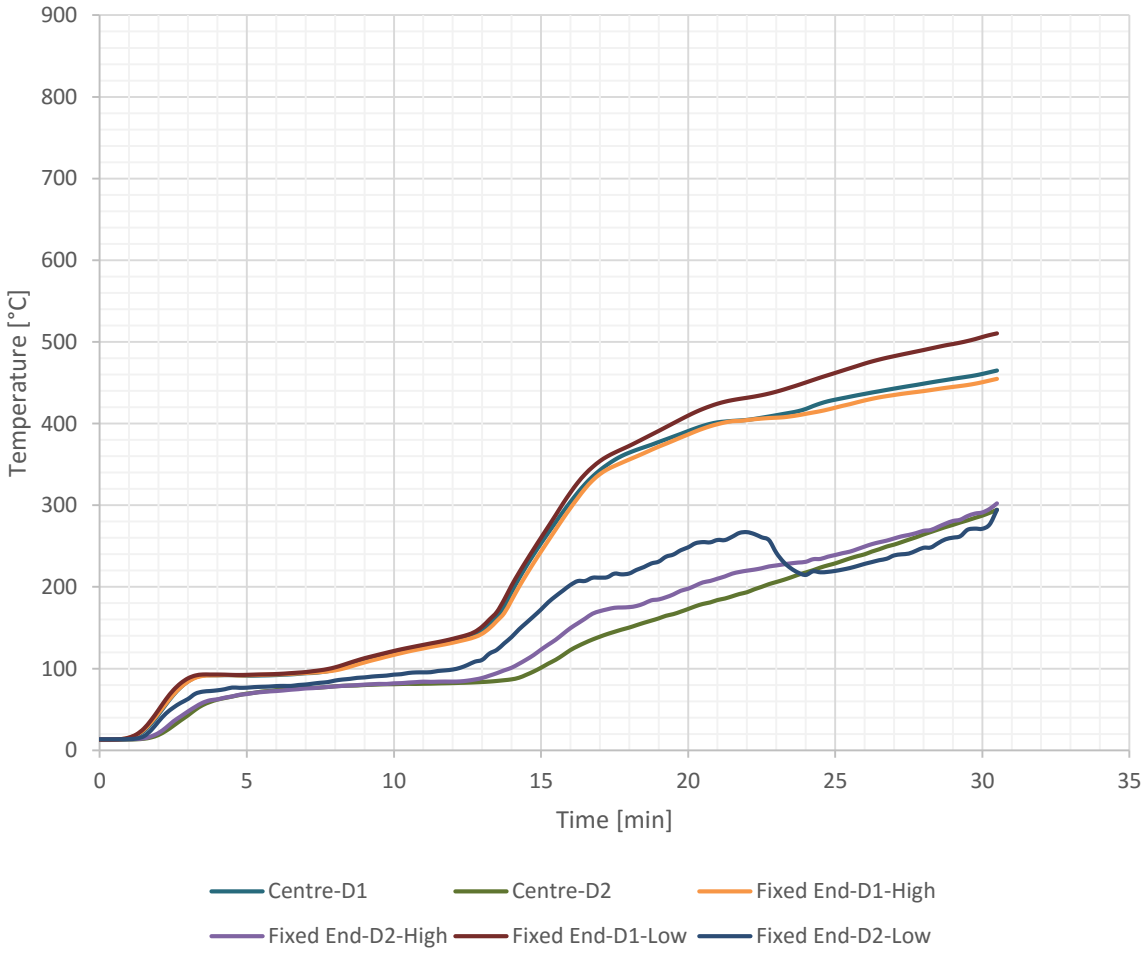

Figure 5-56 – Experiment #1 fire-rated wall cavity side temperature of linings

Figure 5-57 shows the outside face temperature of the unexposed lining on the fire-rated wall. The temperature does not exceed 100°C at any of the measurement locations and therefore remains below the failure criteria defined in AS 1530 Part 4 as described in Section 2.4.3.

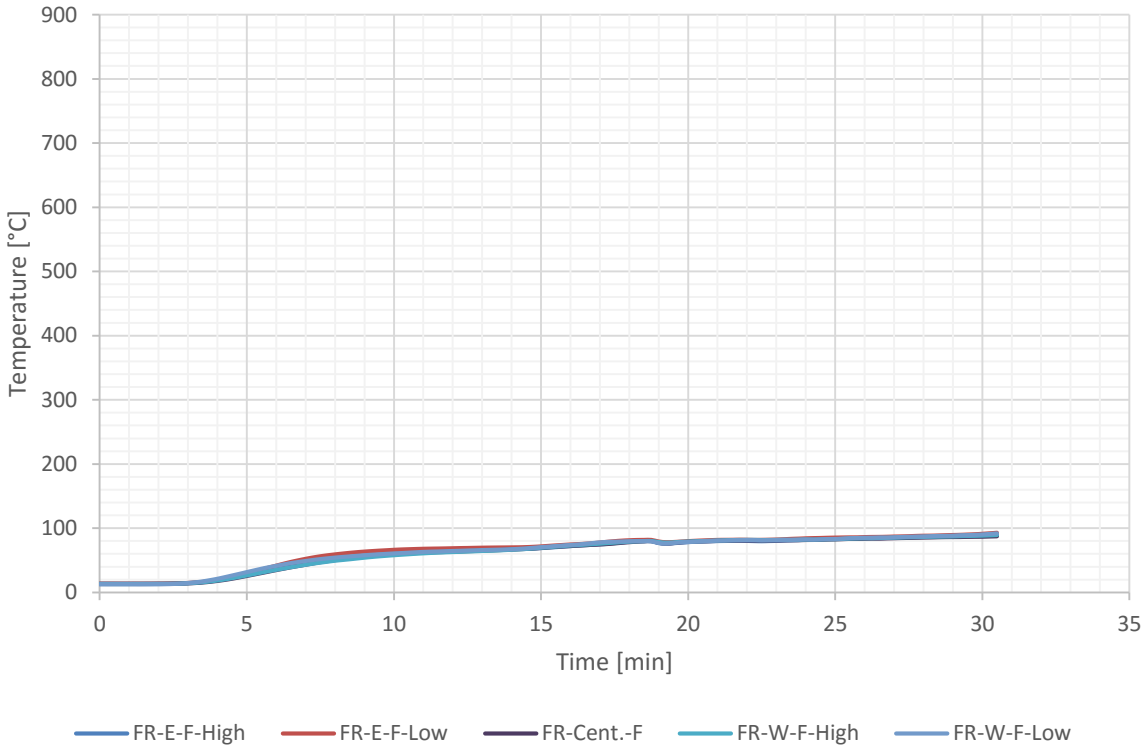

Figure 5-57 – Experiment #1 fire-rated wall unexposed lining outside surface temperature

5.4.5 Compartment Temperature Distribution

There was evidence of non-uniform compartment temperature distribution with a suggestion that burning intensity in the furnace may have been more severe in the lower half of the wall compared to the upper half. After the experiment, cuts were taken through a number of stud members and it was noted that generally more charring had occurred at a lower level than higher up. A photo showing cuts from three different studs at various wall locations is shown in Figure 5-58. The left side specimen of each pair is a cut taken 200 mm from the top plate, and right hand side is a cut taken from 200 mm above bottom plate

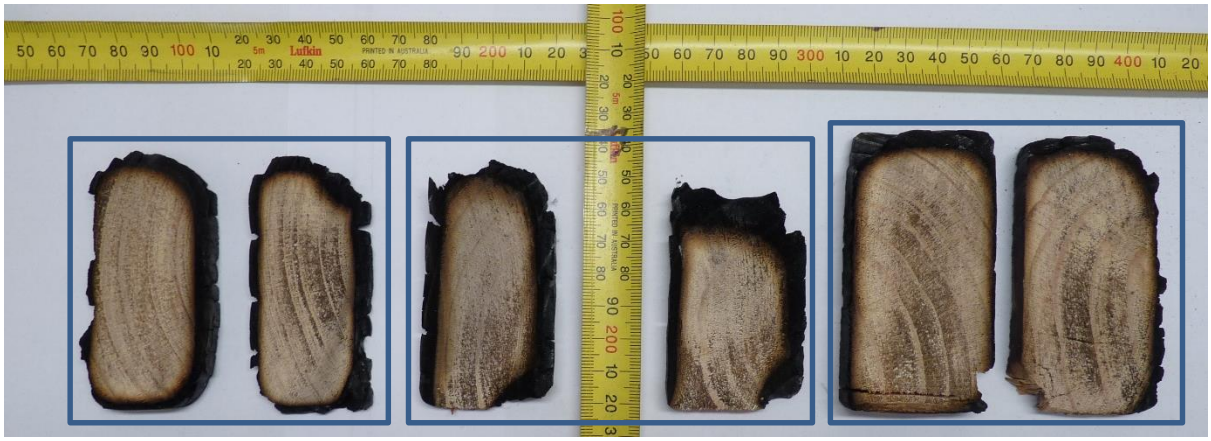

Figure 5-58 – Experiment #1 example of stud charring from three studs

Figure 5-59 shows a comparison of the adiabatic surface temperature measured for the walls and ceiling with the temperature measured by the furnace thermocouples, and the ISO 834 standard fire curve. It is noted that the adiabatic surface temperature measuring devices are of different construction for the walls and ceiling. A comparison of these devices is beyond the scope of this report and the temperature measurements are taken at face value. Both the wall and ceiling adiabatic temperature measurements are lower than the furnace temperature and standard fire curve at all times during the experiment. The wall and ceiling adiabatic surface temperature measurements are similar, except for in the early stages of the experiment where the ceiling was more severe. This is not unexpected given the ceiling plates face the burner flames below the notional floor level and therefore have a better 'view' of these flames than the wall plates, which face the compartment walls. Noting that the ceiling failed after approximately 16 min the validity of the surface temperature measurements taken after this point could be questioned, however it is noted that the ceiling temperature trends remain consistent with the plates on the walls, and these wall devices stayed in place much longer. At the end of the experiment, the ceiling adiabatic surface temperature measurement plates were found to be hanging in the compartment, suspended from the wires to which they were attached. The measurements are considered reasonable and have been used in analysis for fire severity in Section 5.5.1.

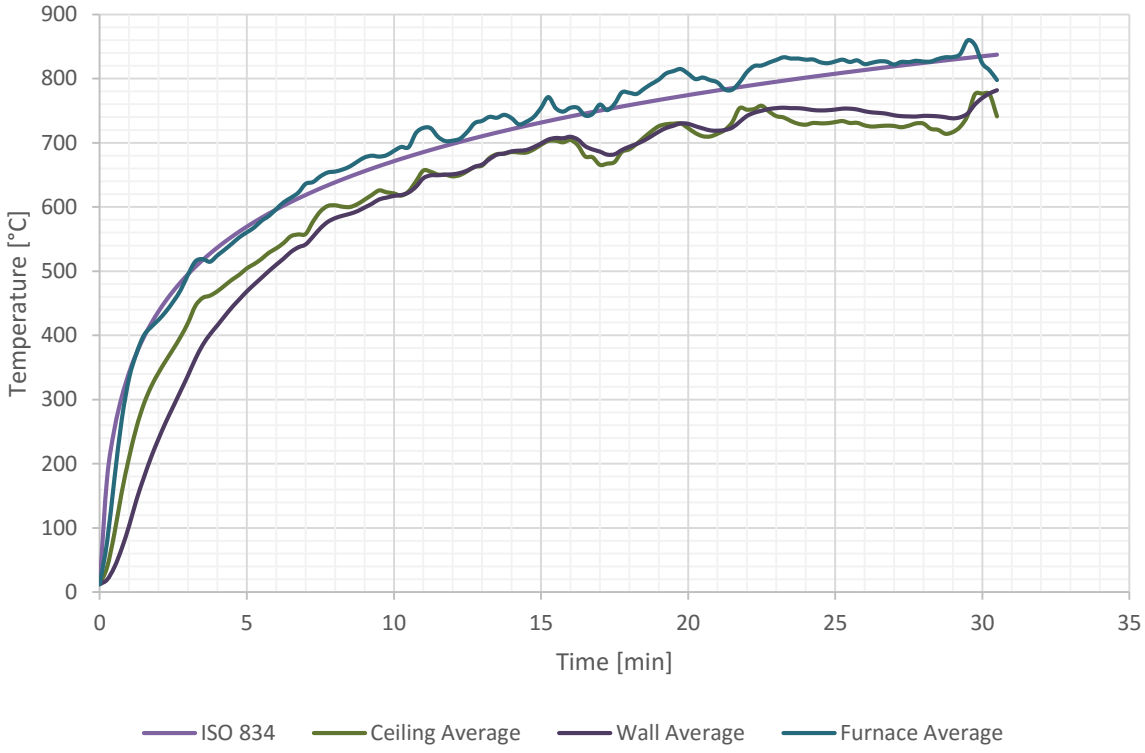

Figure 5-59 – Experiment #1 average wall and ceiling adiabatic surface temperature measurements compared to furnace thermocouple average and ISO 834

5.4.6 Dummy Chord

The dummy chord was directly exposed to the furnace fire when the ceiling failed after 16 min. Figure 5-60 shows temperature measurements from the dummy chord. Thermocouple B1 at the centre of the dummy chord, 5 mm from the underside, was unresponsive from the start of the experiment and has been discarded. Thermocouple A3 (nail-plate side of stud, 20 mm from bottom) seemed to have

an unreasonably long delay in rising temperature given that it was the same distance from the side surface of the chord as A4, therefore this value was ignored.

All thermocouple temperature measurements exhibited a plateau at 100°C which would coincide with moisture being driven away from the area of wood local to the thermocouple, as that area is heated. The deeper areas of wood appear to have extended plateaus, likely due to slower heating but possibly due to moisture being driven toward these areas from the fire exposed area as described in Section 4.3.3. The fastest temperature rise occurs on the thermocouples at 5 mm from the underside of the dummy chord (row 1), and occurred slightly sooner on the non-nail-plate side. This is followed by a coincident temperature rise in thermocouples A2 and A4, located on the nail-plate side of the dummy chord.

Charring is considered to occur when the wood reaches a temperature of 300°C as described in Section 4.3. The first thermocouple to indicate the presence of charring was C1 at 19 min, approximately 2.5 min after ceiling failure. Approximately 1 min later, A1 reached 300°C, 3.5 min after the ceiling failed. The temperature at thermocouples A2 and A4 increase at a similar rate and reach 300°C after 22 and 22.5 min respectively. Thermocouples C2, C3 and C4 all begin to increase above 100°C between 19.5 to 20.5 min. C2 is the last of these to start increasing and increases at the fastest rate, indicating charring at this point after 23.75 min, C4 follows at 24.25 min and then C3 at approximately 25 min.

As expected, the central thermocouples on column B at the centre-line of the timber member lag behind the others. The temperature at B2 begins to climb above 100°C at around 21 min, and reaches 300°C after 26 min. B3 starts to rise above 100°C after 27 min but never exceeds 200°C during the experiment, and B4 never exceeds the 100°C plateau.

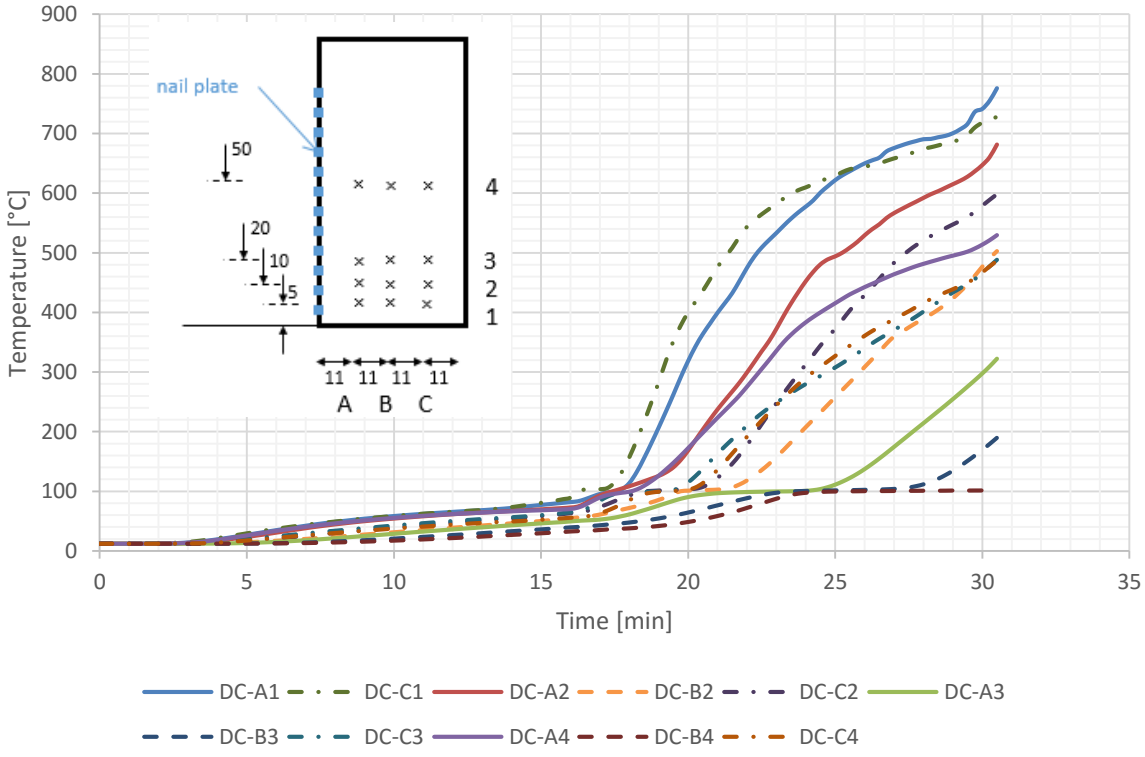

Figure 5-60 – Experiment #1 dummy chord thermocouple temperature measurements

5.4.7 Fire-rated Wall Deflection

Figure 5-61 shows the deflection measurements for the fire-rated wall taken during the experiment. Deflection measured by the potentiometers is less than 5 mm for the first 25 min of the experiment. Displacement of the drums at this time was 15 mm, 16 mm and 10 mm for the fixed, centre and free end loading points respectively. It is worth noting the discrepancy between the free end deflection measurements and the nearest drum deflection measurement, possible explanations for this are discussed in Section 5.5.3.

At 30 min there is a notable increase in displacement measured at the drums, the fixed, centre and free end increased to 17, 28 and 38 respectively. Soon after these measurements were taken, at approximately, 30.5 min, the wall failed away from the compartment, as shown in the deflection measurements by the potentiometers. Note that the wall remained fixed to one end wall and did not fail 'catastrophically'. The experiment was designed such that the weighted drums would rest on the ground as run-away deflection occurred as described in Section 5.2.9, thereby relieving the wall of any lateral load. The residual strength in the wall framing and connection at the fixed end allowed it to remain standing.

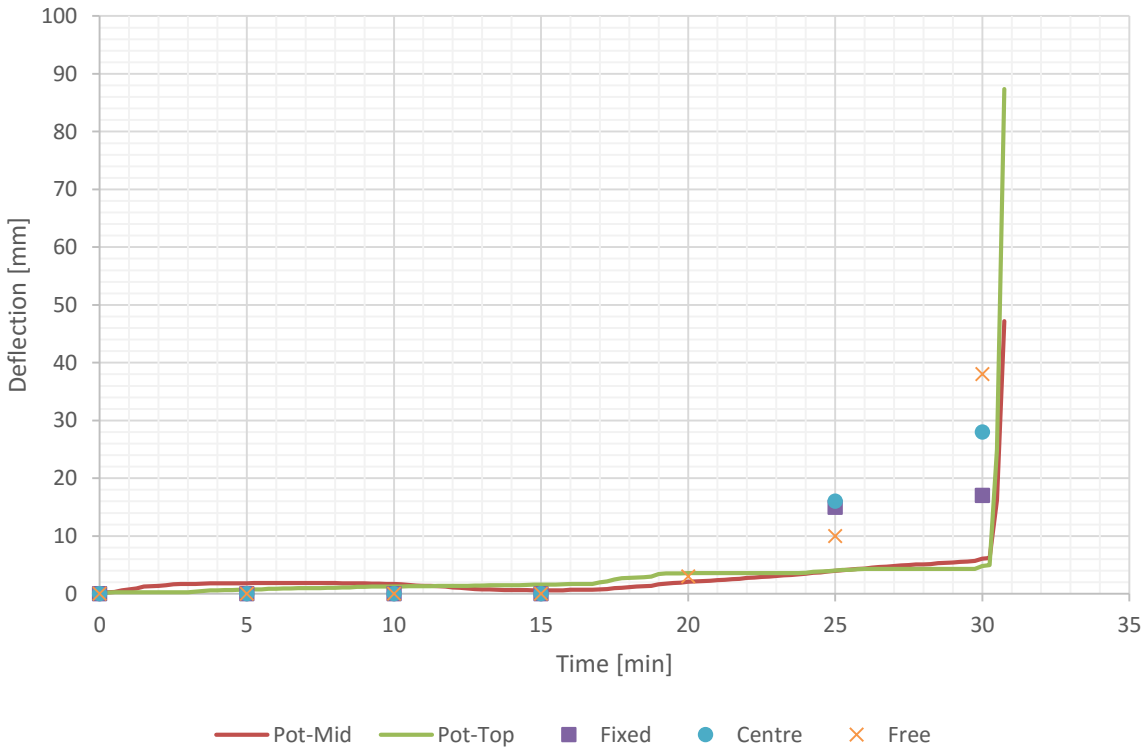

Figure 5-61 – Deflection measurements for fire-rated wall

Inspection after the experiment indicated that the main mechanism of failure was the splice in the bottom chord of each of the intermediate (load-carrying) roof trusses, as shown in Figure 5-62, Figure 5-63 and Figure 5-64.

Figure 5-62 – Experiment #1 photo of centre truss (T3) failure after experiment

Figure 5-63 – Experiment #1 photo of free end truss (T4) failure after experiment

Figure 5-64 – Experiment #1 photo of fixed end truss (T2) failure after experiment

5.5 Analysis and Discussion

5.5.1 Fire Severity

As described in Section 5.4.5 there is an indication from experiment measurements and observations that the compartment temperatures may not have been uniform. This will have affected the fire severity experienced by various elements throughout the compartment. Nyman's (2002) cumulative radiant energy (CRE) method for equivalent fire severity as described in Section 2.5.5 is applied to the experiment results to estimate failure times had various compartment elements been exposed to the standard ISO fire time-temperature. As described in Section 2.4.3, AS 1530 Part 4 does not require the use of plate thermometers measuring adiabatic surface temperature to be used to drive a furnace temperature during testing.

Figure 5-65 shows a comparison of the cumulative radiant energy (CRE) exposure (Nyman, 2002) for the standard fire time-temperature curve, the average furnace temperature as measured by the furnace thermocouples, and the average adiabatic surface temperature for the walls and ceiling. The furnace measured temperatures equate to an equivalent fire severity greater than the standard fire, while the ceiling and wall measured adiabatic temperatures are less severe. The difference between the CRE for the walls and ceiling compared to the standard fire increases as the experiment progresses. The CRE for the walls and ceiling is similar throughout the experiment.

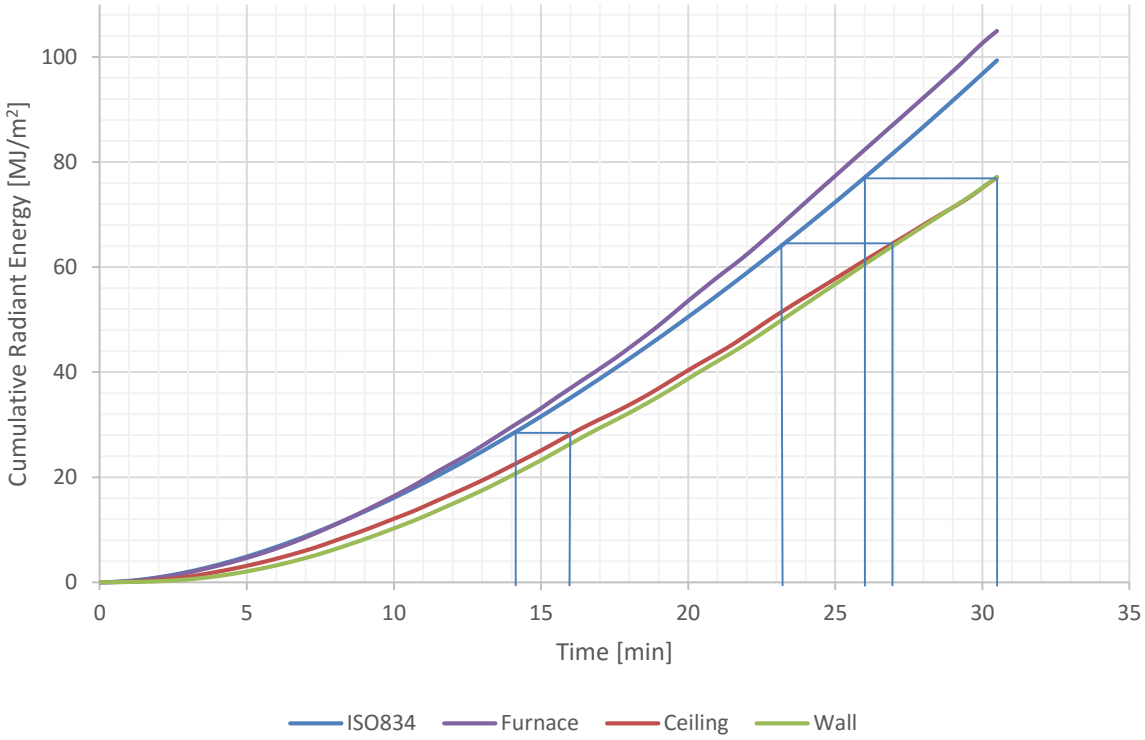

Figure 5-65 – Experiment #1 cumulative radiant energy comparison based on time temperature histories for ISO 834 fire, average adiabatic ceiling and average adiabatic wall measurements

If temperature measuring devices (for example, plate thermometers) located at ceiling height were used to drive the furnace temperature, then the gas temperature near the ceiling would be closer to that of the standard fire time-temperature. By comparing the cumulative radiant energy at the time various elements failed, an assessment can be made of the expected failure time if the furnace had been driven using temperature measuring devices located near the ceiling height in the compartment. Table 5-2 compares the observed failure times of the ceiling lining, standard plasterboard wall linings and the roof truss with predicted failure times using the CRE method to adjust the fire severity.

Applying the CRE to the performance of the laterally loaded fire-rated wall, that failed due to failure in the splice in the roof truss, suggests that if exposed to standard fire time-temperature the failure would have occurred slightly earlier at 26 min. This is less than the minimum 30-min FRR required by C/AS1 Acceptable Solutions for external walls. Note that the test standard AS 1530 Part 4 as referred to in the NZBC does not consider specimens configured as a full-scale compartment and further research may be necessary to define a suitable methodology for driving the furnace given the non-uniform temperature distribution that is likely to occur.

Table 5-2 – CRE time equivalence comparison for Experiment #1 failure times

Element	**Experiment failure observed [min]**	**Time Equivalent failure – Exposed to standard time-temperature at ceiling [min]**
Ceiling lining	16	14
Wall linings	27	23
Fire-rated wall failure due to lateral load	30.5	26

5.5.2 Plasterboard Lining Performance

The measured temperature rise of the plasterboard on the cavity side of the exposed lining shown in Figure 5-54 can be compared with calculation methods given by Ostman (2010) as described in Section 4.4.5. Using the equation for "basic protection value" given in Equation 4-4 gives a predicted time of 18 min for a 10 mm thick plasterboard to have an average temperature rise of 250°C on the unexposed side of the lining. Figure 5-54 shows that a temperature rise of 250°C occurred after approximately 14-15 min for the wall linings in the experiment. As previously discussed in Section 4.2.3 there are a number of factors that affect the fire performance of plasterboard, including but not limited to board thickness, density, composition and any additives. Taking this into consideration the observed failure time for wall and ceiling linings seems to be within reasonable tolerances for experimental error.

Although the wall and ceiling linings were the same thickness and type of plasterboard, fall-off of the ceiling system before the wall linings is not unexpected. As discussed in Section 4.2.3, ceiling linings tend to fall off sooner than wall linings due to gravity loads. This is consistent with the experiment observation and results that showed ceiling failure occurring after 16 min, compared to 27 min for walls.

5.5.3 Fire-rated Wall Performance

Stability failure of the fire-rated wall was observed at approximately 30.5 min in the experiment, this was evidenced by the inability to carry the lateral load imposed by the weight of the drums resulting in the wall being pulled away from the compartment until the drums rested on the ground. The failure occurred suddenly and the deflection results at the free end of the wall suggest there was relatively small deflections leading up to the point of failure.

AS 1530 Part 4 has failure criteria for axially loaded elements and vertically loaded elements as described in Section 2.4.3. It is recognised that this failure criteria was not intended to test for failure of a structural system consisting of a vertical element restrained laterally by a horizontal element, i.e. a fire-rated wall supported laterally by a roof truss system. However it can provide one way of establishing a failure criteria definition for the experiment. It is important to keep in mind that the failure criteria for AS 1530 Part 4 would have been developed with specific objectives considered, and it is very unlikely these would have been for the purpose of assessing lateral stability of a fire-rated wall protecting other property. It may be reasonable to allow an external fire-rated wall to deflect further than the failure criteria of AS 1530 Part 4, and this could be the subject of further research.

The fire-rated wall framing was 90 mm deep and 2400 mm high. Using Equation 2-1, the limiting deflection is calculated to be 160 mm, and using Equation 2-2 the limiting rate of deflection is 7 mm/min. There was not sufficient allowable movement in the weighted drums to assess the limiting deflection case, however run-away deflection was expected and this would be captured by the limiting rate of deflection failure criteria. The limiting rate of deflection measured over 1 min intervals was exceeded at 30.5 min, with the wall deflecting at an average rate of 21 mm/min between 29.5 and 30.5 min. This calculated failure time is consistent with the observed failure time.

Another approach for defining failure for the fire-rated wall would be to consider the intent of the NZBC to limit unprotected openings within 1 m of a boundary. C/AS2 permits small unprotected (non-fire-rated) openings up to 0.1 m^2; C/AS1 does not have the same concession, it is unclear if this has intentionally been omitted or was an oversight. Beyond this limited allowable unprotected area, integrity failure of the fire-rated wall could be considered to constitute a failure. This should be

considered in the context of the NZBC requirement of preventing spread of fire to neighbouring property and also keeping in mind that all the structure around building elements other than the fire-rated wall are permitted to fail or collapse. The failure of a roof or end walls is likely to be a more significant exposure risk than small gaps that occur between building elements due to deflection of the fire-rated wall. Integrity failure was not assessed during the experiment due to inaccessibility of the fire-rated wall (for safety reasons), and also noting that the gap between the roof and top plate of the wall was not sealed, so hot gases and flames were allowed to escape at that location throughout the experiment.

There was a difference between the free end deflection measurements and the nearest drum deflection measurement as shown in Figure 5-61, particularly from 25 min onward there was noticeably more deflection in the drums than measured by the linear potentiometer at the free end of the wall. There are at least two possible reasons for this:

i. The drums were connected on a long metal cable and anchored into fire-rated wall with mild steel eye bolts, and the cable was hung over a steel bar supported by a timber-frame. There are a number of factors that could have contributed to elongation in the load system rather than the wall and this could include thermally induced stresses that would contribute to a deflection of the drum.
ii. One possible explanation is that this could be a result of bowing of the wall, either the fire-wall or non-rated long wall, or both. For the fire-rated wall this bowing would tend to have a maximum deflection at the drum fixing locations and the least deflection at the truss fixing points and the fixed end wall. For the non-rated long wall, the deflection may be a maximum somewhere near the middle of the length of the wall and would be negligible at the end walls. This seems less likely given the brittle behaviour of timber as described in Section 4.3.2 and relatively small associated deflections.

5.5.4 Truss Performance

Failure of the roof truss system at the truss connector plate occurred at 30.5 min, resulting in lateral deflection of the loaded fire-rated wall. An analysis of the failure sequence is performed by comparing the observed behaviour with estimates of the residual capacity of the structural system by examining charring rates of the bottom chords of the trusses.

Figure 5-66 shows the set-out of the roof trusses and locations where the lateral load was applied to the top plate of the wall; locations W1, W2 and W3 indicate the loading points. The lateral load was applied to represent a uniform load across the top plate of the wall, however the truss spacing was not uniform and therefore each truss was carrying a different load. Truss T1 is above the fixed end wall and effectively is a zero load member as the fire-rated wall is fixed into the end wall at the top plate. Truss T2 is an intermediate truss near the fixed end of the compartment, T3 is an intermediate truss near the centre, and T4 is an intermediate truss near the free end. The three intermediate trusses T2, T3 and T4 are all carrying a tensile load transferred from the top plate of the fire-rated wall. T5 sits above the free end wall and was installed to accept the roof cladding, it is not connected to the fire-rated wall and does not carry any tension load.

Calculations are carried out to find the loading on each truss, assuming pinned connection between the top plate of the wall to each truss, and assuming the top plate behaves as a non-continuous

member. The minimum residual cross-sectional truss area required to carry the load is calculated, and a time for failure for a truss without a splice is estimated.

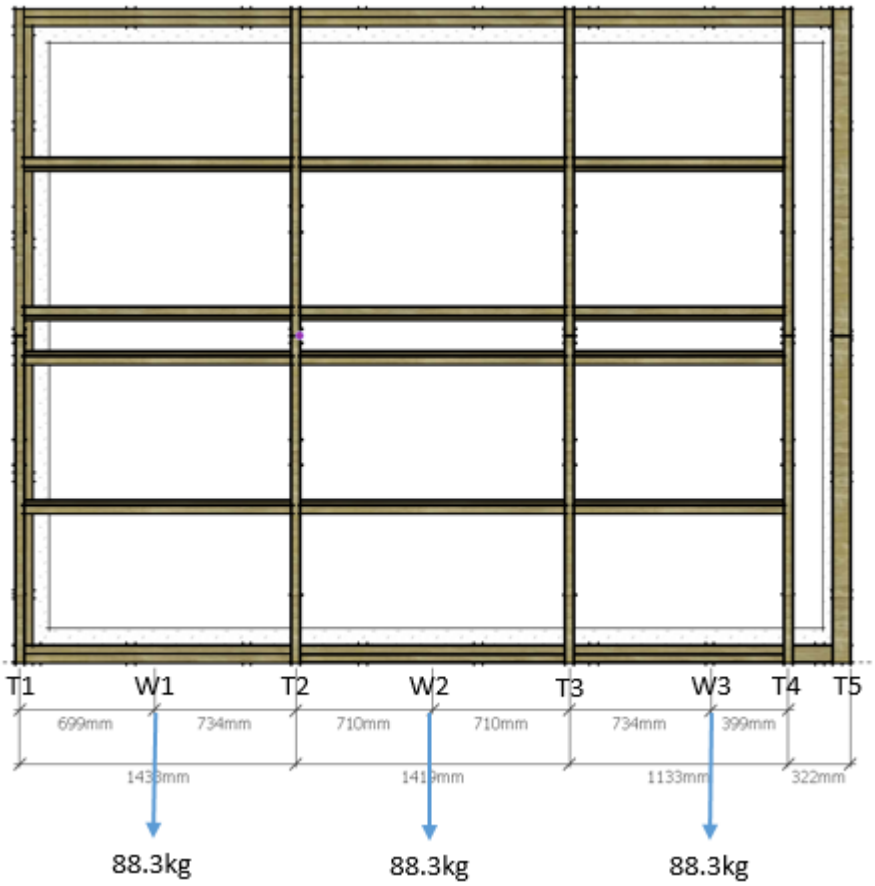

Figure 5-66 – Truss and lateral load layout

The truss properties are stated in Table 5-3. The modulus of elasticity and tension strength are taken from characteristic values for SG8 dry timber given in NZS 3603:1993 Table 2.2. It is recognised that characteristic values are a design value based on statistical analysis of timber properties with suitable adjustment for design purposes, and may not be representative of an 'average' value.

Table 5-3 – Truss bottom chord dimensions and mechanical properties

Depth	0.090	m
Width	0.045	m
Cross-sectional area	0.0041	m^2
Modulus of elasticity, E	8.0	GPa
Tension strength, f_t	6.0	MPa

The stress in each truss member's bottom chord, σ, is calculated using Equation 5-1; the strain in a given member, ε, is calculated using Equation 5-2; and the elongation of that member, Δl, is calculated using Equation 5-3.

Stress $$\sigma = \frac{F}{A}$$ *Equation 5-1*

Strain $$\varepsilon = \frac{\sigma}{E}$$ *Equation 5-2*

Elongation $$\Delta l = L \times \varepsilon$$ *Equation 5-3*

The tension load in each truss can be calculated by considering a free body force diagram as shown in Figure 5-67. Equation 5-4 and Equation 5-5 describe how to solve for the forces in the supporting trusses, assuming pin joint connections.

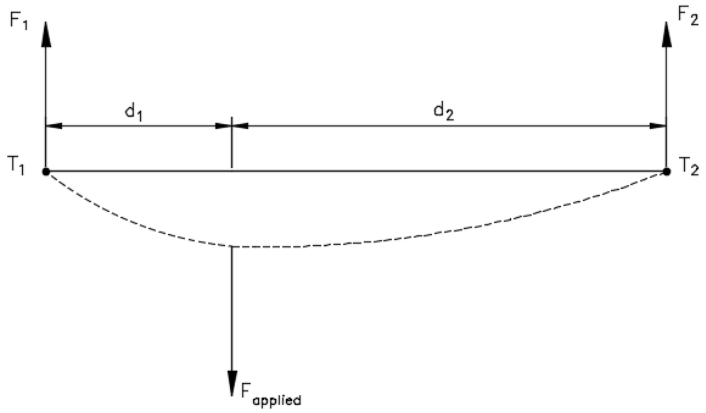

Figure 5-67 – Member force diagram for bottom chords in tension

$$F_1 = F_{applied} \frac{d_2}{d_1 + d_2}$$ *Equation 5-4*

$$F_2 = F_{applied} \frac{d_1}{d_1 + d_2}$$ *Equation 5-5*

The calculation results for the load being carried, stress, strain and elongation of truss members T2, T3 and T4 in the cold design condition is shown in Table 5-4.

Table 5-4 – Experiment #1 calculation of tensile load, stress, strain and elongation for each truss in cold design condition

	Proportion of load being carried						
Truss	W1	W2	W3	Tensile Load [N]	Stress [× 10^5 Pa]	Strain [× 10^{-5} mm/mm]	Elongation [mm]
T2	0.49	0.50	0.0	855	2.11	2.64	0.09
T3	0.0	0.50	0.35	738	1.82	2.28	0.08
T4	0.0	0.0	0.65	561	1.39	1.73	0.06

Section 5.4.6 presented results for the temperature measurements in the dummy chord. A nominal charring rate was calculated by taking values from when the ceiling failed to when 300°C was reached at a specified thermocouple on the nail plate and non-nail plate sides of the dummy bottom chord. Thermocouple rows 1 and 2 were expected to be affected by corner rounding and the effects of being exposed from two sides and were therefore discarded for this analysis. Thermocouple A3 appears to have a delayed response and without being able to explain this behaviour, a decision was made to discard this thermocouple. The rate of char excluding corner rounding effects was determined based on thermocouples A4 and C4, C3 is also included for comparison purposes. The values used to calculate char rate and the calculated char rates are shown in Table 5-5.

Table 5-5 – Experiment #1 calculation of nominal charring rates for dummy chord

Thermocouple Location	Time 300°C reached [min]	Time Elapsed since ceiling failed [min]	Depth of thermocouple [mm]	Char Rate [mm/min]
A4 (nail-plate)	22.5	6.5	11	1.7
C4 (non-nail-plate)	24.25	8.25	11	1.3
C3 (non-nail-plate)	25	9	11	1.2

At the end of the experiment, the temperature readings of A4, B4 and C4 were 530°C, 102°C and 486°C respectively. The char depth on the nail plate and non-nail plate sides of the dummy chord at the end of the experiment can be approximated by linearly interpolating between each outer thermocouple (i.e. A4 and C4) and the central thermocouple, B4. An average charring rate can be determined using this estimated depth of char for the nail-plate and non-nail-plate sides of the dummy chord. The results of this analysis is shown in Table 5-6. The char rates are slower than those in the early stages, which is not unexpected given that the char itself forms a protective layer to the wood.

Table 5-6 – Experiment #1 estimate of depth of char at end of experiment and average charring rate

Thermocouple Location	Temperature at end of experiment [°C]	Estimated char depth [mm]	Equivalent char rate [mm/min]
A4 (nail-plate)	530	16.9	1.2
C4 (non-nail-plate)	486	16.3	1.1

After the experiment, cuts were taken in the bottom chord of trusses at a distance of approximately 200 mm from the splice. Note that this distance was selected due to damage that occurred at the nail plate connection when the building was demolished, and also due to the ends of the timber continuing to char. Photos of the cuts from the free end, centre and fixed end intermediate (i.e. load-carrying) trusses are shown in Figure 5-68, Figure 5-69 and Figure 5-70.

Figure 5-68 – Experiment #1 photo of cut from free end intermediate truss (Truss T4)

Figure 5-69 – Experiment #1 photo of cut from centre truss (Truss T3)

Figure 5-70 – Experiment #1 photo of cut from fixed end intermediate truss (Truss T2)

The calculated equivalent char rates and estimated char depths can be compared to estimates from cross-sections taken after the experiment. This comparison is shown in Table 5-7. Char rates are based on those 'averaged' values at completion of the experiment as shown in Table 5-6, i.e. 1.2 mm/min for the nail plate area and 1.1 mm/min for the non-nail plate side. Note that measurements for residual cross sectional area from section cuts were estimated to the nearest multiple of 2.5 mm. Corner rounding effects are taken into account for the calculated values and not the measured values.

It can be seen the calculated char rate based on dummy chord temperature measurements tends to over-predict the reduction in section area when compared to experiment results. This could be due to charring rates being faster in the early stages and more thermocouples may have been required to better capture the char profile in the timber.

Table 5-7 – Experiment #1 comparison of measured and estimated char depths

	Free end truss (T4)	Centre Truss (T3)	Fixed end truss (T2)	Calculated (with nail plate)	Calculated (non-nail plate)
Depth remaining [mm]	52.5	55	60	55.2	58.0
Width remaining [mm]	22.5	20	22.5	10.2	13.0
Cross section area remaining [mm^2]	1181	1100	1350	498	706
Effective charring rate (depth) [mm/min]	1.3	1.2	1.1	1.2	1.1
Effective charring rate (width) [mm/min]	0.8	0.9	0.8	1.2	1.1

Table 5-8 shows the elongation of each truss for the cold condition and elongation based on the residual cross-section areas at the end of the experiment, measured from cuts taken and calculated from the dummy chord charring rates. Note that the 'averaged' char rate value based on the dummy chord temperature readings at the end of the experiment was used, i.e. 1.1 mm/min. The table also shows the minimum cross-sectional area required to carry the load, based on the design characteristics of the truss. These calculations do not take into account the nail plate connection in the bottom chord of the truss, which governed failure in Experiment #1, but allow an assessment to be made of performance without a nail plate connection.

Table 5-8 – Summary of load, elongation and minimum required cross-section area for each truss

	Cross section area [mm^2]			Elongation [mm]		
Truss	Minimum to carry load	Fire – Measured from cuts taken after experiment	Fire – Calculated from char rate in dummy chord (non-nail-plate)	Cold	Fire – Calculated using measured residual cross-section area	Fire – Calculated based on char rate in dummy chord
T2	143	1350	708	0.09	0.27	0.51
T3	123	1100		0.08	0.28	
T4	94	1181		0.06	0.20	

The results show that there was sufficient cross-sectional area of unaffected timber to support the lateral load being applied to the fire-rated wall and the predicted elongation of the trusses remains negligible. It is not unreasonable that the nail plate failed much earlier than the timber member would have been expected to fail in tension. Truss T2 is most critical with respect to loading (i.e. carries the greatest load) and therefore requires the largest residual cross sectional area, 143 mm^2. Applying a 1.1 mm/min charring rate to the 90 mm × 45 mm bottom chord member and ignoring corner rounding effects (refer Section 5.4.6), it can be estimated that after 19 min of fire exposure the truss cross-section area would have been reduced to approximately 143 mm^2. This compares to the observed failure time of 14.5 min from the time when the ceiling system failed and the bottom chord was exposed directly to the fire.

A detailed analysis on the failure of the splice is beyond the scope of this report, and there appears to be limited research into the performance of such connections when directly exposed to fire. One method for calculating a predicted failure time of the splice could be to consider that when the char depth has exceeded the depth that the tooth of the truss connector plate penetrates the timber, failure will occur. For the truss plates used this would be approximately 8 mm. Using the 1.2 mm/min charring rate, the char layer would exceed the depth of the teeth on the truss connector plates after approximately 6.5 min of direct fire exposure. Actual failure of the splice occurred 14.5 min after the ceiling failed and this method would seem to be a poor predictor of performance.

The aforementioned charring assumption could be considered to be non-conservative because a minimum depth of tooth in unaffected timber would be required to carry a tensile load. However the result does not support this as failure occurred after the char depth exceeded the length of the tooth. One possible explanation for this could be that char itself provided more residual strength than the zero strength assumed, sufficient to hold the connection for a period of time. Another could be contribution from other factors in the building construction. These two possible explanations are further described:

- Wire dogs – As previously described in Section 5.2.3; these are metal timber fasteners used in the construction of trusses to connect truss members, as shown in Figure 5-71. These likely would have provided a tensile strength after failure of the nail plate and this contribution is difficult to quantity.
- As previously described in Section 5.2.4 there is a roof bracing element consisting of a metal strap fixed to the four corners of the compartment, effectively pulling the roof down onto the wall and also applying a load to pull the walls inward toward the compartment. This strapping may have contributed to some load sharing. Although it is noted the truss failure appears to be the cause of the fire-wall failure and the strapping did not appear to have any ability to resist this failure after the roof truss failed and this seems a less likely explanation.

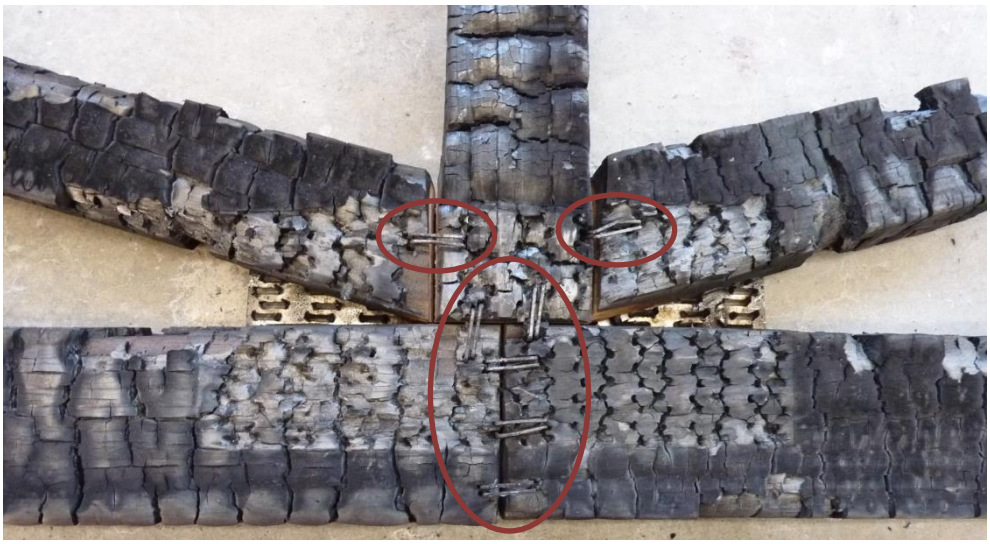

Figure 5-71 – Photo of fixed end truss (non-load-carrying) after the experiment, with wire dogs visible

5.5.5 Performance of an Unlined Compartment

The expected performance of an unlined compartment can be predicted by applying the CRE method to the results from Experiment #1. A CRE value is calculated from the adiabatic surface temperature measurements recorded from the time of ceiling failure to the time of fire-rated wall lateral stability failure, starting with a value of 0 MJ/m^2 at the time of ceiling failure. The calculated CRE value is compared to the CRE curve of the ISO 834 time-temperature curve from time 0 min. The predicted time of failure is the time when the CRE of the ISO 834 time-temperature equals the CRE value calculated from the adiabatic surface temperature measurements recorded during the experiment. The effects of pre-heating the bottom chord and other structure members before the ceiling failed are ignored. Similarly, any differences in char rate due to different furnace gas temperature is not taken into account.

The ceiling failed at 16 min in the experiment, and the roof truss system supporting the fire-rated wall failed at 30.5 min. The cumulative radiant energy for this 14.5 min period based on the ceiling adiabatic surface temperature measurements (Type B devices) is calculated to be 48.7 MJ/m^2. The ISO time-temperature curve takes 19.5 min to reach this same CRE, as shown in Figure 5-72. The calculated stability failure time for the laterally loaded wall in an unlined building configured as in Experiment #1 is approximately 19.5 min if exposed to the standard fire time-temperature heating regime.

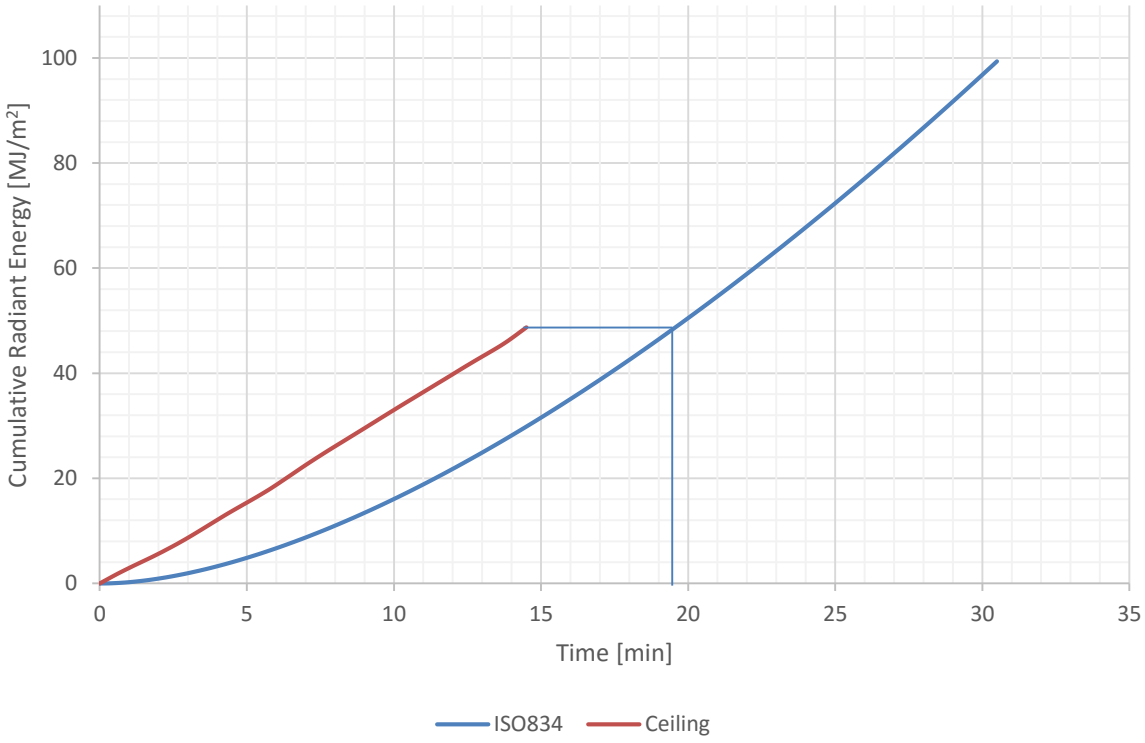

Figure 5-72 - Experiment #1 CRE from time of ceiling failure to time of wall stability failure compared to standard fire CRE

5.6 Experiment #1 Summary

A furnace experiment was carried out on a laterally loaded light timber-framed compartment. The furnace temperature was driven by the furnace thermocouples to follow the ISO 834 standard time-temperature curve, and was within the tolerances given by AS 1530 Part 4. The ceiling system lined with 10 mm standard plasterboard provided a level of protection to the roof truss system in the experiment until failure at 16 min.

The bottom chord of the roof truss failed at the spliced connection in tension after 30.5 min in the experiment, this was 14.5 min after the ceiling failed. An analysis of the observed failure time applying the criteria specified in AS 1530 Part 4 for limiting rate of deflection is consistent with the observed failure time. The results show there was a non-uniform temperature distribution in the compartment, which is not unexpected given the heat loss that will have occurred from the external walls and roof of the compartment. The observed failure time of 30.5 min is equated using the CRE method to a failure time of 26 min if the furnace had been driven using temperature measuring devices located at ceiling height level (instead of below notional floor level) and following the ISO 834 time-temperature curve.

An analysis of the results of the dummy chord temperatures determined an average charring rate of 1.2 mm/min for timber behind the nail-plate, and 1.1 mm/min for timber not behind a nail plate. These were used to determine residual cross-section areas for the bottom chord of the trusses, and compared to cuts taken from samples of bottom chords after the experiment. The results show that there was sufficient cross-sectional area of unaffected timber to support the lateral load being applied to the fire-rated wall and the predicted elongation of the trusses remains negligible. It is not unreasonable that the nail plate failed much earlier than the timber member would have expected to fail. Without the splice in the roof truss system, it is expected that for this experiment the wall would have been sufficiently restrained for an estimated additional 4 min. An adequately protected splice could also be designed to achieve sufficient restraint for this additional time, such that the failure occurs due to charring of timber away from the splice.

The toothed nail plate connection performed better than would be expected or predicted if it is assumed there is no residual strength in the connection once charring of the timber exceeds the depth that the nails penetrate the timber. As previously discussed there may have been contribution from other construction elements which provided sufficient residual capacity to withstand the applied load, after the truss connector plate would have otherwise failed. There is likely to be a contribution of strength to the connection from the wire dogs connecting the spliced bottom chord and this was not quantified. Similarly, the effect of the roof bracing has not been quantified although it is considered less likely this contributed significantly to the strength of the system in fire.

The expected performance of an unlined compartment was predicted by applying the CRE method to the results from the experiment. The CRE based on furnace temperature from the time of ceiling failure (16 min) to the time of bottom chord failure (30.5 min) is compared to the CRE of ISO 834 time-temperature curve. The calculated stability failure time for the laterally loaded wall in an unlined building configured as in Experiment #1 is approximately 19.5 min if exposed to the standard fire time-temperature heating regime and therefore would not meet the C/AS1 30-minute FRR requirement.

6 Experiment 2

6.1 Introduction

Experiment #2 was a compartment experiment with the fire conditions provided by burning a fixed fuel load inside the compartment. A key difference between this and the furnace experiment in terms of building design is that an initial ventilation opening size was designed and included in the building construction. A number of ventilation configurations were modelled in B-RISK. Due to the ventilation openings the spatial temperature distribution was not expected to be uniform. The fuel characteristics were also expected to influence the compartment fire behaviour and were selected with consideration for ventilation openings, ensuring flashover, and aligning with a fuel load specified by the NZBC for a residential building.

Part of the purpose of the full-scale burn experiment is to provide data for Wade's research to understand how the building elements progressively fail during a post-flashover (fully developed) fire. This progressive failure leads to changing ventilation conditions in the compartment due to wall and/or roof cladding failure. The fire severity within a compartment will be affected by changing ventilation. A simple compartment was modelled using B-RISK (introduced in Section 2.3.4) to understand how changing ventilation may influence fire severity. The influence of the changing ventilation conditions on fire severity is assessed from the experiment with measurements of compartment temperature, surface temperatures and adiabatic surface temperatures.

6.2 Building Design

6.2.1 Building Set-out, Framing, Cladding, Internal Linings and Ceiling System

Compartment dimensions including width, length and stud height were the same as those in Experiment #1. There was a minor change to framing layout on the non-fire-rated wall to accommodate an anticipated requirement to move assembled wood cribs from outside into the compartment; the framing layout change is not considered to affect results. There were two changes to the framing of the end walls. One was a minor change to framing layout with the stud set-out being essentially a mirror image compared to the construction in the first experiment. This was unintentional and simply due to the way in which the builder laid the framing out before assembling the walls. The second change was to incorporate openings in end walls, measuring 535 mm wide × 1375 mm with a sill height 627 mm above notional floor level. Figure 6-1 shows the framing and window opening layout in an elevation, viewed from the outside of the 'free' end wall.

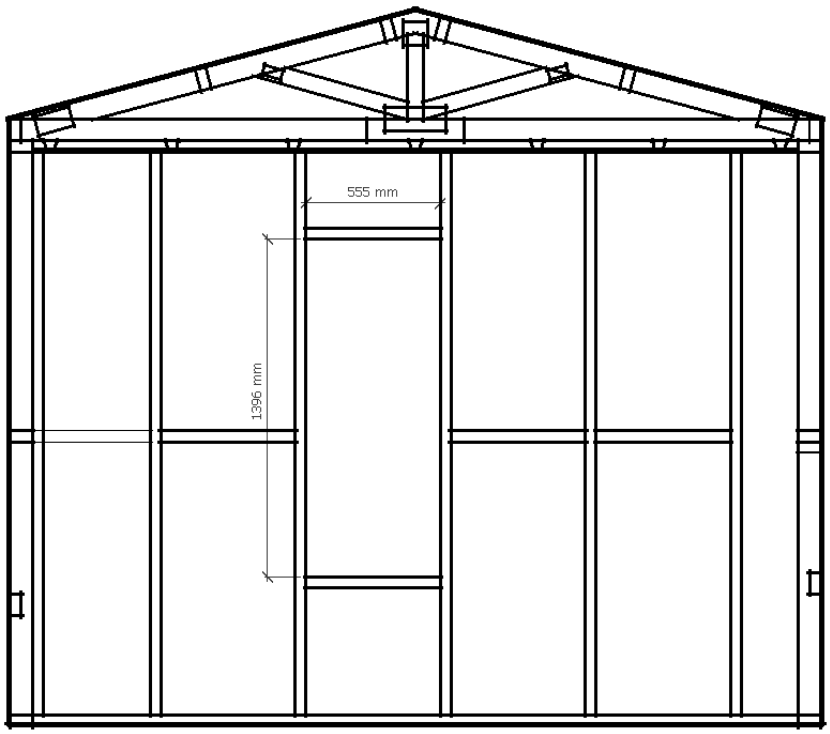

Figure 6-1 – Experiment #2 outside view of free end wall framing and window opening for Experiment #2

The fire-rated wall construction was the same including framing, linings and fixing method. Similarly, the internal wall linings and ceiling system construction were consistent with Experiment #1. Internal wall linings on the end walls were cut to suit the window layout. The faces of the timber framing forming the window opening were protected with 10 mm fibre-reinforced plasterboard.

The outside cladding on non-rated long wall changed including moving the plywood to the centre panel of the wall and the plasterboard to left hand side as shown in Figure 6-2. Due to the framing layout change described in Section 6.2.1, a 'step' was also formed in the wall cladding so that joints between cladding sheets remained over solid timber. Cladding was cut to suit the window openings in the end walls.

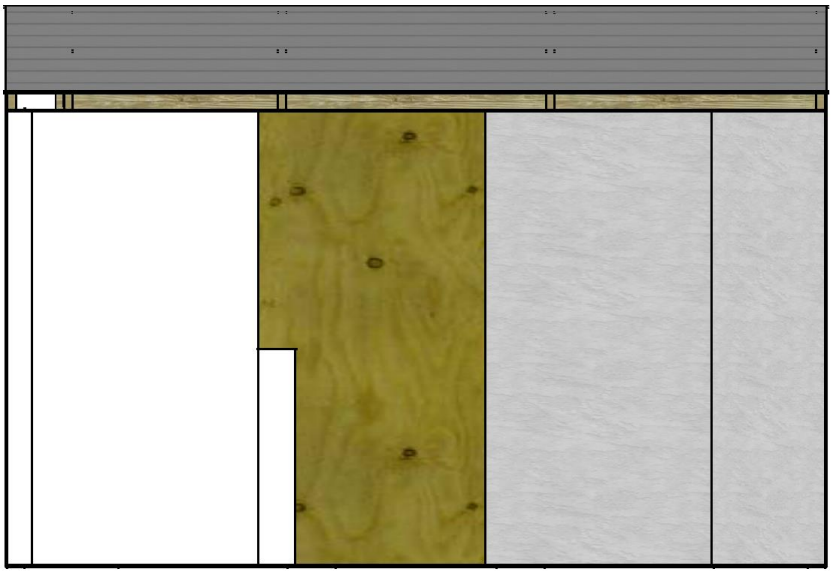

Figure 6-2 – Experiment #2 non-rated long wall lining layout

6.2.2 Roof Truss and Bracing

For unknown reasons the truss manufacturer used a different connector plate size to connect the trusses compared to what was used in Experiment #1, despite the truss dimensions being otherwise identical. A connector plate measuring 175 mm × 150 mm was used to connect the two halves of the bottom chord, and this also connected the three web members. Connector plates measuring 75 mm × 150 mm connected the top chords to the bottom chords at each end of the truss members. The sloping web members were connected to the top chords with truss connector plates measuring 50 mm × 100 mm. The top chords were joined at the apex to each other and to the vertical web member with a 100 mm × 100 mm truss connector plate. Beyond these changes, the roof truss manufacture was consistent with Experiment #1.

A key change made in Experiment #2 was the addition of protection to the nail plate connector at the splice in the centre of the bottom chord of the roof trusses. Timber blocking consisting of 90 mm × 45 mm SG8 timber, approximately 400 mm long, was fixed with two nails at each end of the blocking into the bottom chord of the roof truss. Blocking was fixed on both sides of the splice, as shown in Figure 6-3 and Figure 6-4.

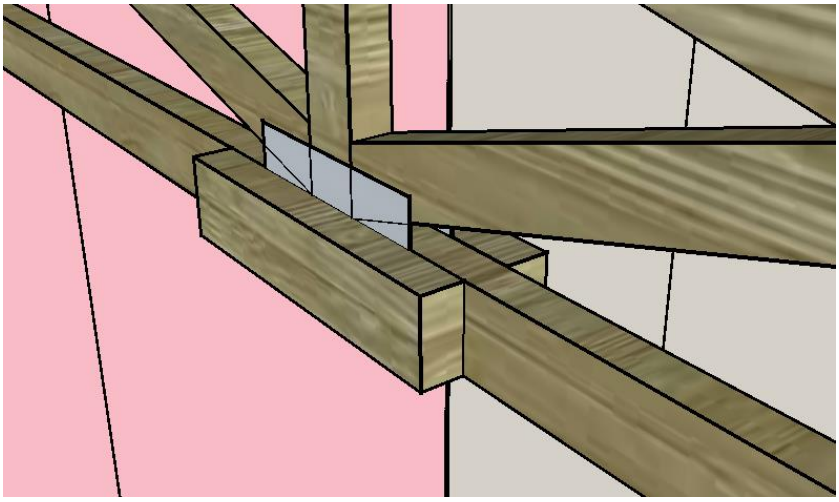

Figure 6-3 – Experiment #2 3D sketch of roof truss with timber blocking protecting nail plate connection in truss

Figure 6-4 – Experiment #2 Photo of roof truss construction with timber blocking protecting nail plate connection in truss

The roof bracing strap configuration was the same as Experiment #1 and is described in Section 5.2.4.

6.2.3 Lateral Load

The lateral load system remained the same as Experiment #1 including fixing locations, fixing hardware and suspended weight as described in Section 5.2.9. A photo of the lateral setup for Experiment #2 is shown in Figure 6-5.

Figure 6-5 – Experiment #2 Photo of lateral load setup

6.3 Preliminary Compartment Fire Design

6.3.1 Fuel Load and Geometry

The basis of the fuel load selection-was the NZBC C/VM2 stipulated requirement of 400 MJ/m^2 for a residential dwelling including garages. It is noted that energy densities in the New Zealand Building Code may be relatively low compared to overseas as discussed in Section 3.2.3; however this is not an area of investigation in this research. Wood cribs were used to make up the quantity of fuel required. It was expected that more than one crib would be required, and the intent was to have the geometry of each crib consistent, and the fuel load relatively evenly distributed throughout the compartment. The surface area of the fuel needed to be sufficient such that ventilation controlled burning would occur in the compartment.

Figure 6-6 shows a typical wood crib geometry, where D is the width and height of each stick, S is the spacing between the sticks in each layer, and h_c is the height of the crib. The number of sticks in each layer, the width of the sticks and their spacing determines the overall width and length of the crib. The number of layers of sticks and the height of each stick determines the overall height of the crib. The total mass of wood and the energy density of the wood determines the total fuel load. Note that the stick cross sections are square, i.e. the width and height dimensions are equal.

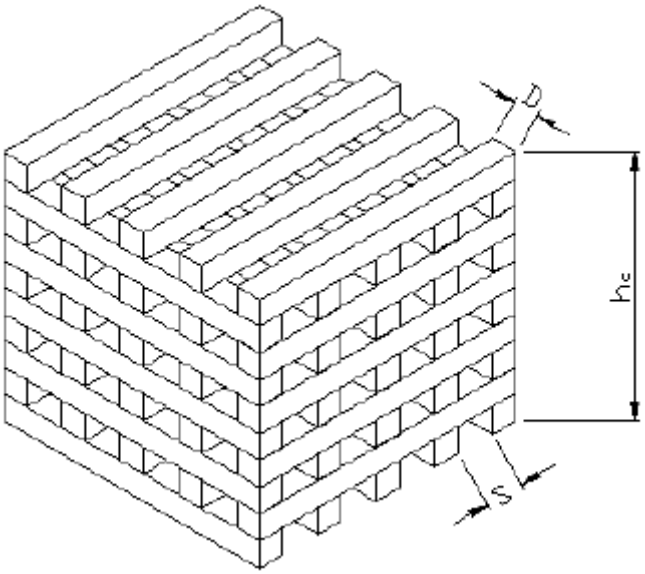

Figure 6-6 – Wood crib fuel geometry (taken from Nyman, 2002)

Preliminary calculations and modelling was carried out to obtain a sense of what a reasonable wood crib geometry and size would be, and considered two different wood crib configurations; herein referred to as 'configuration A' and 'configuration B'. An effective heat of combustion of 12 MJ/kg was used, as suggested by Babrauskas (2002). A timber density of 497 kg/m^3 was assumed for these initial calculations based on the average density of timber used for cribs in Nyman's (2002) experimental research. The two trial crib geometries and properties are summarised in Table 6-1.

Table 6-1 – Summary of trial wood crib configuration values for Experiment #2

Parameter	**A**	**B**	
Width of stick of timber, *D*	0.05	0.045	m
Spacing between sticks, *S*	0.1	0.07	m
Number of sticks per layer, *n*	5	8	sticks
Width and length of crib	0.65	0.85	m
Number of layers of sticks	20	12	layers
Height of wood crib, h_c	1.0	0.54	m
Effective heat of combustion of wood	12	12	MJ/kg
Density of wood	497	497	Kg/m^3
Mass per crib, m_0	81	82	kg
Number of cribs (rounded up)	6	6	cribs
Calculated FLED	401	408	MJ/m^2

6.3.2 Ventilation

A suitable compartment ventilation area needed to be determined for the experiment. The key criteria were:

- Ensuring flashover occurred in the compartment and a ventilation-controlled burning state is reached.
- Having compartment temperatures exceeding those attained in the standard fire time-temperature curve in the first 30 min
- A fire duration sufficiently long to compromise the internal linings as a minimum
- As far as practicable have a relatively even temperature distribution in the compartment

- Be within the bounds of what would be expected for common residential buildings in NZ.
- Be easily constructible for the experiment compartment geometry

As described in Section 2.3.2; the compartment geometry and ventilation opening size and location will affect the temperature distribution in the compartment. It was decided that in an effort to try to achieve a reasonable level of uniformity in temperature distribution along the long dimension of the compartment, that two evenly sized openings would be placed at opposite ends of the compartment in the short walls.

Section 2.3.2 described research by British Steel in cooperation with the Fire Research Station at Cardington, United Kingdom (BS/FRS) in which experimental research showed comparable maximum temperatures for single opening areas 25% or greater than the individual wall area, and a much lower maximum temperature for 12.5% opening area. With this in mind, it was considered important the compartment was not overly starved of oxygen.

To establish the bounds of what range of opening sizes would be expected for common residential buildings, NZBC H1/AS1 *Energy Efficiency* (MBIE, 2011) and G7/AS1 *Natural Light* (MBIE, 2014b) were referred to. H1/AS1 provides information for thermal performance of a compartment, provided that vertical glazing areas are limited to maximum of 30% of the total wall area. Since many residential buildings are designed in accordance with the Acceptable Solution it seemed reasonable to use this as an upper bound. For the Experiment #2 compartment, the total wall area is 37 m^2 and therefore the upper limit for ventilation openings based on 30% is 11 m^2. G7/AS1 provides a reasonable lower bound by requiring a minimum window area to provide natural light and awareness of the outside environment. G7/AS1 requires a window area in external walls of at least 10% of the floor area. For the Experiment #2 compartment, 10% of the floor area equates to a window opening size of 1.45 m^2.

There was an initial round of preliminary modelling and calculation; this found that for ventilation areas much greater than 5 m^2 the fire quickly became fuel controlled and there was a limited period of ventilation controlled burning occurring followed by a decay, it also resulted in relatively short fire durations. Following this initial modelling, two ventilation configurations were further investigated; these are summarised below and in Table 6-2.

Table 6-2 – Preliminary ventilation opening areas for Experiment #2

Parameter	**1**	**2**	
Ventilation opening area	1.45	2.12	m^2
Number of openings	2	2	
Opening height	1.37	2.0	m
Opening width	0.53	0.53	m
Sill height	0.63	0.0	m
Head height	2.0	2.0	m

Vent Configuration 1 was based on a glazed ‘window’ type opening meeting the minimum area requirements of G7/AS1. This consisted of two evenly sized openings at opposite ends of the compartment with a 1.45 m^2 opening area. For ease of construction the opening width was designed to align with the space between studs less any protective plasterboard, i.e. 530 mm and this dictated that the height be approximately 1370 mm. The sill height was selected so that at least half the opening was above 900 mm as per G7/AS1 requirements; the sill height selected was 630 mm.

Vent Configuration 2 is based on providing a 'door' type opening at each end of the compartment that is 2.0 m high and the width of the space between adjacent studs. This equates to a 2.12 m^2 opening area.

6.3.3 Wood Crib Mass Loss Rate

Babrauskas (1979) developed equations for calculating the mass loss rate of wood cribs burning in a post-flashover environment in a compartment, and a model for calculating post-flashover fire temperatures (COMPF2). The method presented by Babrauskas (1979) is based on calculating three mass loss rates for the burning cribs; a ventilation controlled mass loss rate, a fuel surface area controlled mass loss rate and a crib porosity controlled mass loss rate. The smallest of the three mass loss rates is considered to govern the crib pyrolysis rate. The input parameters that affect the fuel surface controlled burning rate and crib porosity controlled mass loss rate are the characteristic stick thickness, stick spacing, and the height of the cribs.

Equation 6-1 gives Babrauskas' equation for calculating the mass loss rate for a wood crib in the fuel surface controlled regime, and Equation 6-2 for crib porosity control. The mass loss rate for ventilation controlled burning is given by Equation 6-3. For rooms with multiple vents, the $A_v\sqrt{h_v}$ term is summed for each vent. It is assumed that all vents open to outside.

Fuel surface control

$$\dot{m}_p = \frac{4}{D} v_p \left(\frac{m}{M_0}\right)^{1/2} M_0 \qquad \textit{Equation 6-1}$$

Crib porosity control

$$\dot{m}_p = 4.4 \times 10^{-4} \left(\frac{S}{h_c}\right) \frac{M_0}{D} \qquad \textit{Equation 6-2}$$

Room Ventilation control

$$\dot{m}_p = 0.12 A_v \sqrt{h_v} \qquad \textit{Equation 6-3}$$

The regression velocity for wood was taken from Babrauskas (2002) as $2.2 \times 10^{-6}\ D^{-0.6}$. It is worth noting that this value is different to that given by Babrauskas (1979) in the COMPF2 technical note of $1.7 \times 10^{-6}\ D^{-0.6}$.

The pre-flashover growth rate was calculated using Equation 6-4 and Equation 6-5 (Babrauskas, 2002). Equation 6-4 calculates the time for flame spread of a centre-ignited crib to reach the edge of the crib (t_0), and Equation 6-5 calculates the mass loss rate during this period of radially spreading fire growth. Equation 6-5 is in the form of an 'alpha t-squared' fire growth rate, whereby the alpha coefficient is a function of M_0, v_p, n and D. It was assumed that there would be simultaneous ignition of all cribs in the compartment and therefore the growth rate coefficient for one crib was simply multiplied by 6 to represent the number of cribs. The growth rates were found to be 1.57 kW/s^2 for Crib A and 0.74 kW/s^2 for Crib B. These were also used as input to B-RISK model described in Section 6.3.4.

$$t_0 = 15.7n \qquad \textit{Equation 6-4}$$

$$\dot{m} = 0.0254 M_0 \frac{v_p {t_{ig}}^2}{n^2 D} \qquad \textit{Equation 6-5}$$

Babrauskas' equations were applied to the trial wood crib configurations A and B as described in Section 6.3.1 with the two ventilation configurations 1 and 2 as described in Section 6.3.2. The results are shown in Figure 6-7 and show that configurations with 'door' sized ventilation openings (2A and 2B) had a greater mass loss rate in the early stages of the fire which is expected during the ventilation controlled phase of burning. This faster consumption rate of the fuel results in a decay into a fuel surface area controlled phase earlier. The smaller ventilation opening area resulted in a fire duration between 10 and 15 min longer.

Wood crib configuration A becomes fuel surface controlled slightly earlier than configuration B for both ventilation scenarios. The decay during the fuel surface area controlled phase is more rapid for configuration B. The change in wood crib geometry appears to be less significant on the overall result than the different ventilation configuration. This suggests the experiment will be more sensitive to selection of ventilation openings than the geometry of the wood cribs, provided it is similar to or within the bounds of the crib sizes modelled.

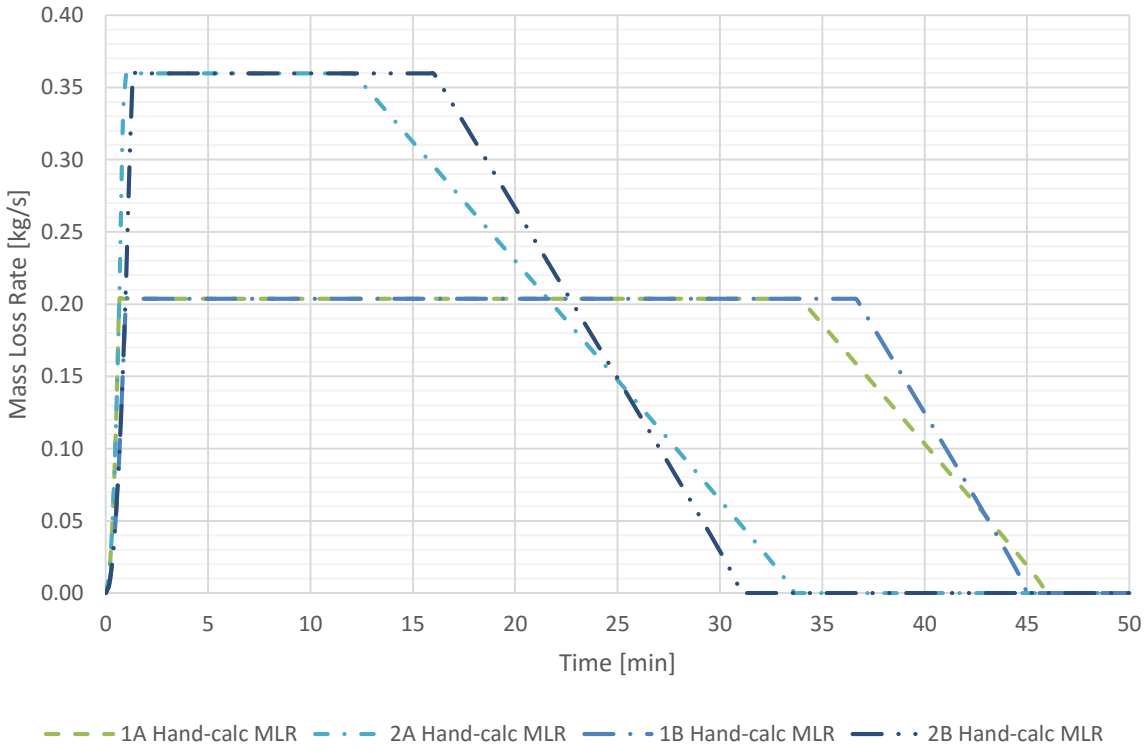

Figure 6-7 – Predicted mass loss rate for wood cribs based on preliminary ventilation area

6.3.4 B-RISK Modelling

Four configurations were modelled consisting of ventilation configurations 1 and 2 as shown in Figure 6-8 and Figure 6-9 respectively; with each of wood crib configurations A and B. The compartment was modelled with wall and ceiling thermal properties based on 10 mm plasterboard, this is assumed to stay in place throughout the duration of the fire with respect to calculating thermal properties and heat transfer from the compartment. Any possible contribution of timber framing as fuel load was ignored.

The B-RISK zone model has the capability to model changing ventilation conditions during the simulation; and failure of elements can be progressive and based on a time equivalence method to calculate the time of failure. Failure of the plywood cladding was included in the model with the

plywood cladding assigned an FRR of 29 min based on results from Experiment #1, as described in Section 5.4.1. Nyman's CRE method is used in the B-RISK model to calculate the time of failure due to exposure to the compartment's upper layer gases. The plywood cladding is split into 4 vents; two upper vents measuring 1155 mm high × 555 mm wide each and two lower vents measuring 1180 mm high × 555 mm wide each, as shown in Figure 6-8. Based on observations from Experiment #1 and an estimate of performance, the vent is opened to 80% of its original area over a period of 5 min.

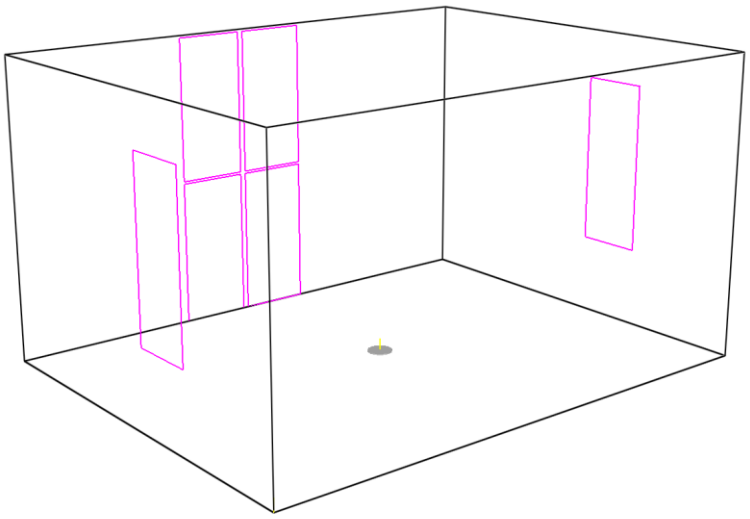

Figure 6-8 – Experiment #2 image of compartment showing openings for ventilation configuration 1

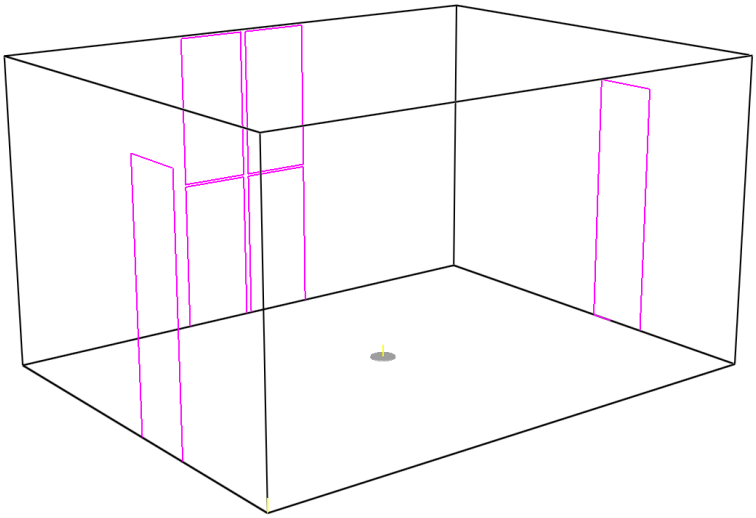

Figure 6-9 – Experiment #2 image of compartment showing openings for ventilation configuration 2

B-RISK has a built in post-flashover subroutine for burning of wood cribs, based on Babrauskas' COMPF2 model (Babrauskas, 1979). This was used in the simulations with wood crib geometry as previously described. The energy content of the wood has been assumed to be 12 MJ/kg as before. It has been observed experimentally that a wood crib does not burn more than approximately 30 to 40 percent fuel rich (Babrauskas, 2002). An excess fuel factor of 30% was used, meaning that the ventilation constrained mass loss rate in the post-flashover phase is multiplied by 1.3 to account for fuel that is pyrolised but not burnt in the compartment; this is combusted outside as a 'vent fire' in B-RISK.

Figure 6-10 shows a comparison of mass loss rate calculated by B-RISK and predicted by the spreadsheet calculation for ventilation configuration 1 with both wood crib configurations. Comparing the spreadsheet calculated mass loss rate with the B-RISK model; the initial ventilation controlled burning phase is similar, until failure of the plywood vent occurs in the B-RISK model at approximately 17 min. There is a sharp increase in mass loss rate over a period of 1-2 min before the burning becomes fuel controlled. Crib configuration B has a faster fuel controlled burning rate than configuration A, and as a result of this has a higher peak mass loss rate and a faster decay. In the context of the uncertainties expected with experiment; the difference in wood crib behaviour seems negligible.

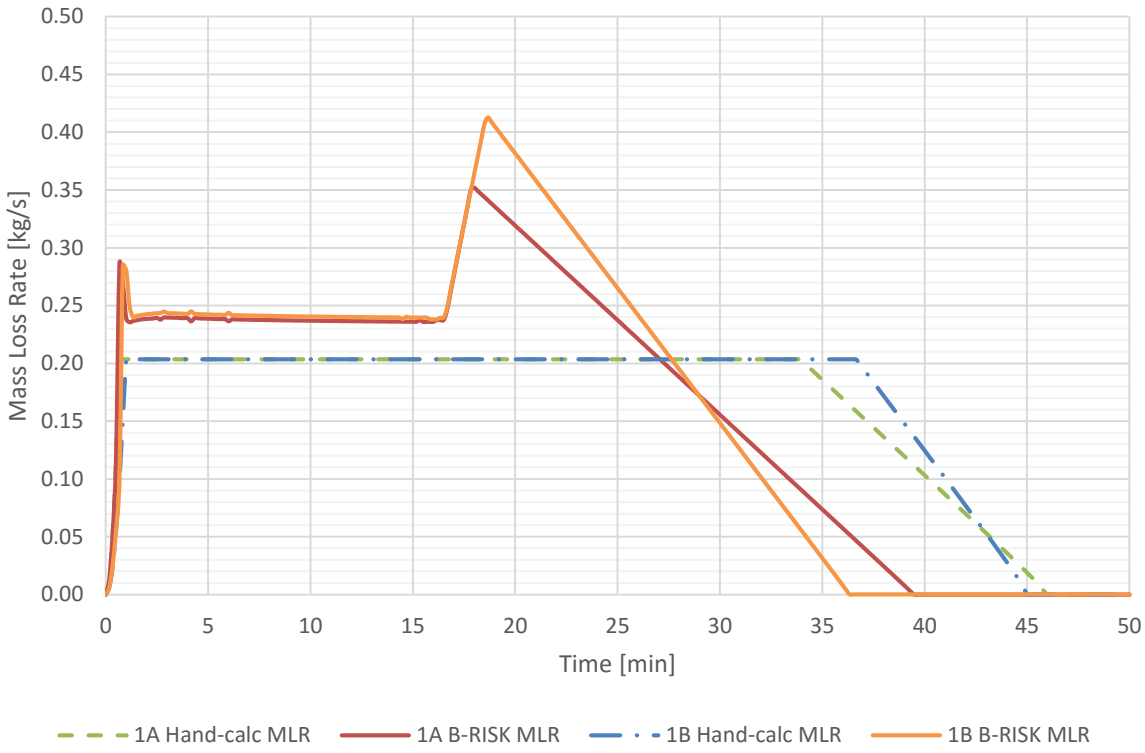

Figure 6-10 – Experiment #2 comparison of mass loss rate for ventilation configuration 1 (window openings)

Figure 6-11 shows a comparison of mass loss rate calculated by B-RISK and predicted by the spreadsheet calculation for ventilation configuration 2 with both wood crib configurations. Comparing the spreadsheet calculated mass loss rate with the B-RISK model; the initial ventilation controlled burning phase is similar, however crib configuration A enters the fuel controlled burning phase after approximately 8 min, significantly before the plywood vent begins to fail at 11 min. Crib configuration B enters the fuel controlled phase at the same time as the plywood vent fails and has a steeper decay than crib configuration A. The predicted fire duration is approximately 30 min for both configurations, and a significant portion of this is in the fuel controlled decay phase of the fire.

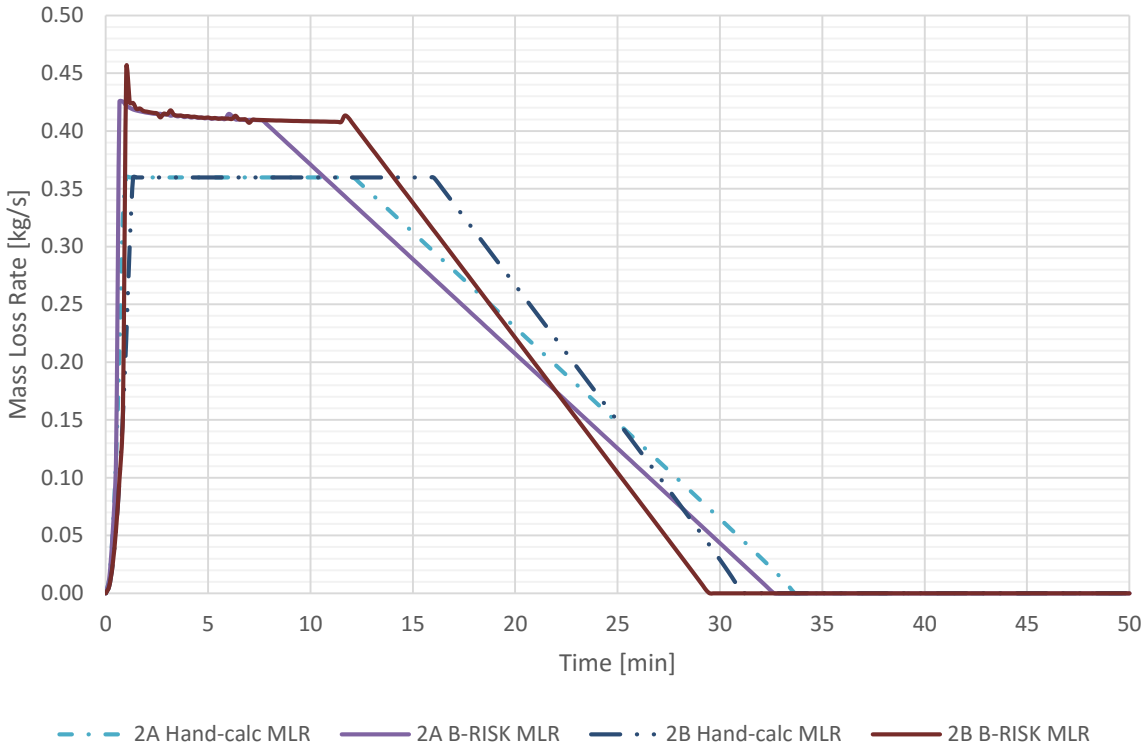

Figure 6-11 – Experiment #2 comparison of mass loss rate calculated by B-RISK and predicted by the spreadsheet calculation for ventilation configuration 2 with both wood crib configurations

Figure 6-12 shows the upper layer temperature predictions from the B-RISK simulations for each ventilation and wood crib configuration, also shown is the ISO 834 time-temperature curve. The wood crib configuration does not appear to have a significant effect on the upper layer temperature during the fully developed phase of the fire, and only has a small effect on the peak temperature reached. There is a more noticeable effect on temperatures in the decay phase of the fire, with the type of crib affecting the rate of temperature decay. During the decay phase, configuration B results in a slightly more rapid rate of temperature decay.

The different ventilation configurations have a more significant influence on the compartment time-temperature curve. The initial temperature increase is similar for both configurations, however once the upper layer temperature reaches approximately 730°C for ventilation configuration 1 the rate of temperature increase slows significantly. It continues to increase until about 17 min where it has reached close to 1000°C, at which time the plywood vent begins to fail. This results in a further sharp increase in compartment temperature to approximately 1100°C during a 2-3 min period, followed by a steady decay in temperature as the fire becomes fuel controlled.

The door ventilation (configuration 2) results in a higher peak temperature compared to configuration 1; increasing to approximately 1100°C after approximately 12 min. Failure of the plywood vent results in a small temperature increase and this is more pronounced for crib configuration B. The upper layer temperature declines immediately after the plywood failure as the burning becomes fuel controlled. The rate of temperature decay is similar as for configuration 1, however it occurs more than 10 min earlier in the simulation.

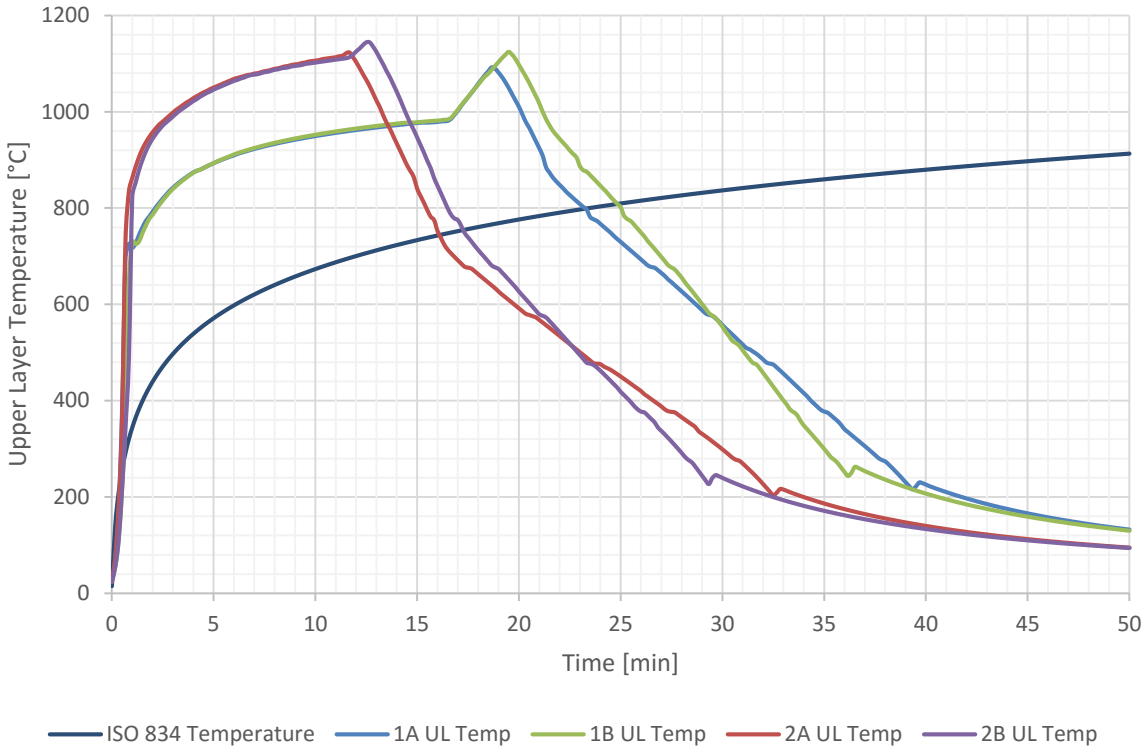

Figure 6-12 – Comparison of upper layer temperature results from B-RISK modelling

Based on the modelling and spreadsheet calculation results, it was decided that ventilation configuration 1 would be the basis for the experiment design as this more closely aligned with the objectives as described in Section 6.3.2. Nyman's cumulative radiant energy method (CRE) as described in Section 2.5.5 was used to compare the expected compartment fire severity using the upper layer temperature results from B-RISK modelling with the standard fire time-temperature curve. Figure 6-13 shows the cumulative radiant energy for each of the ventilation and wood crib configurations modelled in B-RISK with a comparison to the standard fire time-temperature curve.

The observed times of ceiling failure and fire-rated wall failure from Experiment #1 are used in conjunction with the CRE method and the upper layer temperature from the B-RISK model to predict failure times in the compartment experiment. For the purpose of the analysis it was assumed that the fire severity in Experiment #1 was that of the ISO 834 standard fire. This means that the observed failure times have not been adjusted to account for non-uniform temperature distribution in the compartment as described in Section 5.5.1. The standard fire time-temperature curve has been used to calculate the equivalent CRE.

In Experiment #1 the ceiling system failed after 16 min, using the CRE method in conjunction with the B-RISK results for upper layer temperature predicts a failure time of 7 min for the compartment experiment. The fire-rated wall failed after 30.5 min in Experiment #1, and if the splice was not protected this is predicted to occur at 15 min in the compartment experiment. The plywood failed after 29 min in Experiment #1, using the CRE method this is predicted to occur after 14.5 min.

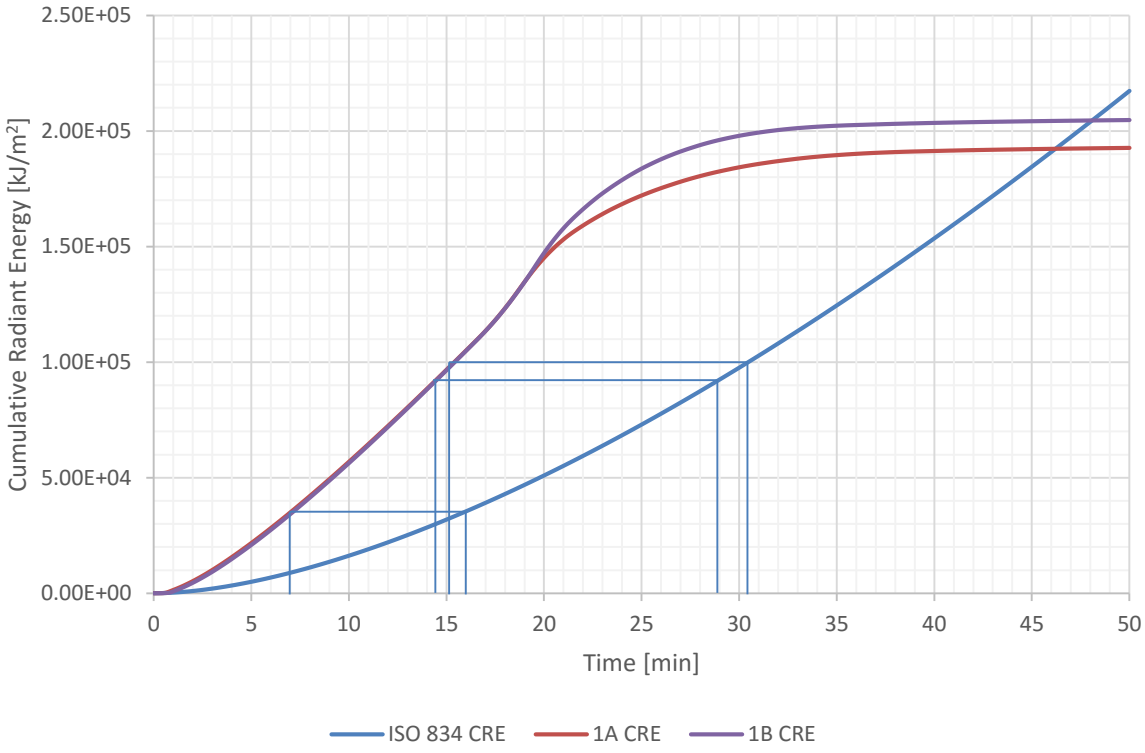

Figure 6-13 – Comparison of cumulative radiant energy using Nyman's method

The actual experiment configuration was closest to configuration 1B. Figure 6-14 shows the B-RISK prediction for heat release rate in the compartment and combustion occurring outside the compartment (vent fire), compared to the hand-calculation predicted heat release rate. Also shown is the B-RISK predicted upper layer temperature comparted to the standard time-temperature curve.

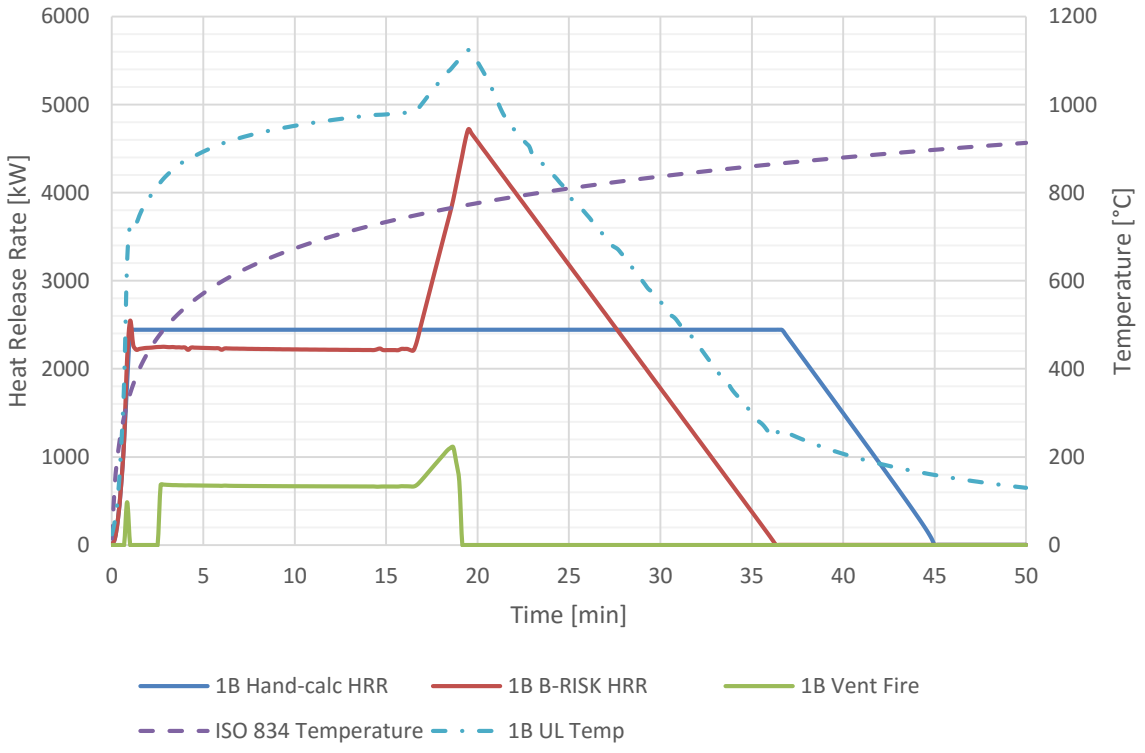

Figure 6-14 - Experiment configuration 1B, comparison of B-RISK predicted results with hand calculation and ISO 834 curve

6.4 Experiment Fuel Load and Configuration

6.4.1 Wood Crib Geometry

There were two existing wood cribs available for use at BRANZ with dimensions shown in Table 6-3. For cost reasons it was decided that these were to be used, with the additional fuel load made up with new cribs. Due to limitations on availability of untreated timber and cost constraints, the timber size obtained for this experiment was 42 x 42 mm. The new cribs were sized to be similar to the existing BRANZ cribs, within the bounds of the preliminary calculations carried out, and to achieve the required FLED and fuel surface area to ensure ventilation controlled burning as described in Section 6.3.2.

Table 6-3 – Experiment #2 wood crib geometry

Parameter	New	Existing	
Width of stick of timber, D	0.042	0.045	m
Spacing between sticks, S	0.08	0.07	m
Number of sticks per layer, n	8	8	sticks
Width and length of crib	0.90	0.85	m
Number of layers of sticks	14	15	layers
Height of wood crib, h_c	0.59	0.675	m

The timber was untreated radiata pine (structural grade). The sticks in the cribs were nailed at the ends with two nails at each end. Each nail weighed approximately 4 grams and there were less than 250 used in each crib. A total nail weight of approximately 1 kg has been assumed per crib and is considered to be negligible in the context of the experimental results and analysis. Figure 6-15 shows a photo of the wood cribs used for the experiment.

Figure 6-15 – Photo of wood cribs used for Experiment #2, top two on right hand side are the existing cribs from BRANZ, and the remaining four are the new cribs

6.4.2 Wood Crib Moisture Content

Samples of the timber used to construct the wood cribs were kept with the wood cribs leading up to the experiment. On the day of the experiment, these were taken to a laboratory to have the moisture content assessed. The mass and dimensions of the samples were measured before they were placed in a drying oven. Drying was carried out over 72 hours, with weight readings taken every 24 hours. The moisture content of the crib sticks was calculated and the results are shown in Table 6-4. The average of all measurements is 11.2%

Table 6-4 – Experiment #2 wood crib moisture measurements from samples sent away for oven drying

	Initial mass [g]	Mass after 24 hours [g]	Mass after 48 hours [g]	Mass after 72 hours [g]	Total mass loss [g]	Moisture content [%]
New crib timber sample 1	243.0	215.1	214.8	214.7	28.3	11.6
New crib timber sample 2	180.0	158.9	158.7	158.6	21.4	11.9
Existing crib timber sample 1	264.0	235.4	235.1	235.0	29.0	11.0
Existing crib timber sample 2	248.0	220.7	220.4	220.3	27.7	11.2
Existing crib timber sample 3	233.0	208.9	208.7	208.7	24.3	10.4

In addition to the samples sent away for moisture content measurements, spot measurements were taken from each crib on the morning of the experiment; using a calibrated *Protimeter Surveymaster SM* 'pin type' resistance based wood moisture meter. The results of these measurements are shown in Table 6-5. The average of all measurements is 9.9%, which compares well with the oven drying sample determined moisture content of 11.2%.

Table 6-5 – Experiment #2 wood crib moisture measurements from moisture meter, taken on morning of experiment

	Reading No.					Average
Crib #	1	2	3	4	5	[%]
1	11.3	11.4	9.2	7.4	8.2	9.5
2	9	9.2	9.8	9.8	10.2	9.6
3	11.8	11.3	10.1	9.9	11	10.8
4	10.2	10.2	8.4	8.7	8.5	9.2
5	9.6	9.4	10.7	10.2	9	9.8
6	10	9.6	12.3	9.4	10.1	10.3

6.4.3 Experiment Fuel Layout

The cribs were evenly spaced throughout the compartment, leaving sufficient room for movement of people between the cribs to complete the experiment setup. To maintain a level of symmetry, the two existing cribs were placed in the centre row of the compartment, and the four new cribs in the rows closest to the end walls. The crib layout is shown in Figure 6-16. Cribs 1 and 5 are the existing cribs (labelled Crib A), and cribs 2, 3, 4 and 6 (labelled Crib B) are the new cribs.

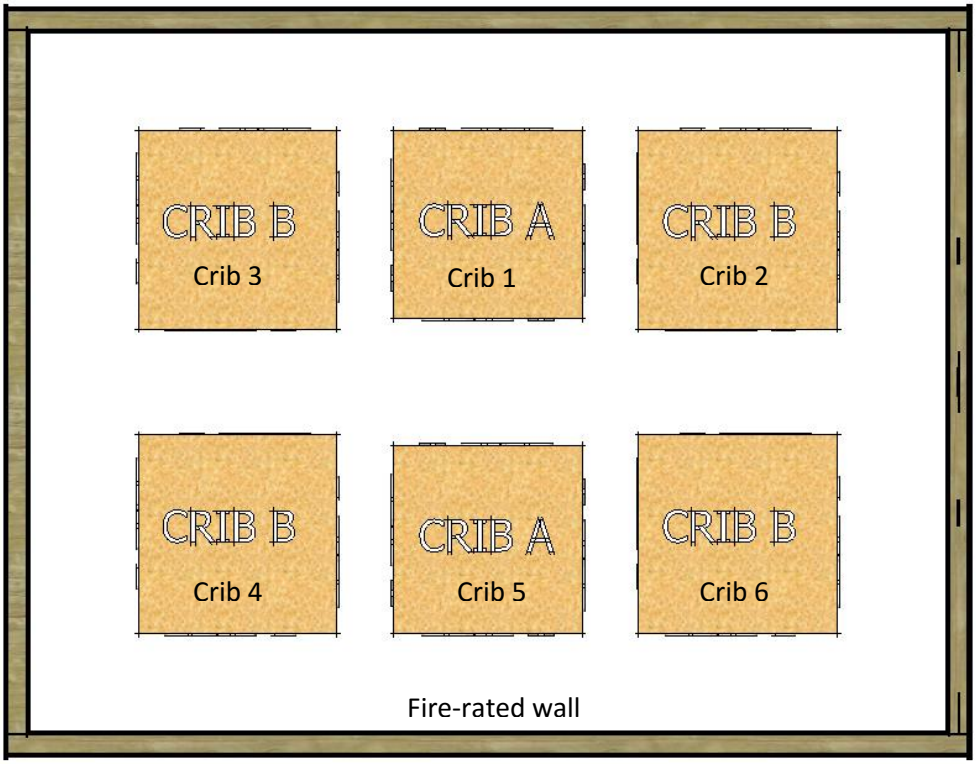

Figure 6-16 – Experiment #2 crib layout

6.4.4 Fuel Quantity

The total fuel quantity in mega joules is calculated based on the total mass of each wood crib and an effective heat of combustion, Δh_{eff} of 12 MJ/kg (Babrauskas, 2002). The total mass of the wood cribs was measured by the load cells before the experiment started and continuously after ignition. The total mass can also be calculated based on the volume and weight of timber samples sent for oven drying as described in Section 6.4.2. The results of this analysis is summarised in Table 6-6:

Table 6-6 – Summary of wood crib mass and fuel load

	Crib 1	Crib 5	Crib 2	Crib 3	Crib 4	Crib 5	Units
Mass measured by load cell	95	98	82	85	85	91	kg
Volume of drying sample	0.00149		0.000767				m^3
Mass of sample before drying	0.745		0.423				kg
Calculated density of timber	500		550				kg/m^3
Volume of timber in crib	0.207		0.177				m^3
Mass of crib calculated from density	103		97				kg
Mass used for fuel load calculation	100		85				kg
Effective heat of combustion	12						MJ/kg
Fuel load per crib	1200		1020				MJ/crib
Total fuel load	6480						MJ
Compartment FLED	450						MJ/m^2

The mass used to calculate the compartment fuel load is based on the load cell weight measurements. Based on this analysis it was considered that the fuel load designed for the experiment was 50 MJ/m^2 greater than 400 MJ/m^2 prescribed by the NZBC C/VM2 document as described in Section 3.2.3.

6.5 Instrumentation

6.5.1 Temperature Measurements – Devices

Surface temperatures and adiabatic surface temperature measurements were recorded at a number of locations on the internal walls, ceiling and cladding. The types of devices used to measure temperature are listed in Table 6-7 with the same naming convention as Experiment #1 as described in Section 5.3. The only change to the description is that the device Type G were installed on the unexposed side of the ceiling lining, rather than in the air in the ceiling space.

Table 6-7 – Measurement device types and descriptions (Experiment #2)

Device Type	Description
A	The thin steel plate devices consisted of a 75 mm × 75 mm square mild steel plate approximately 0.6 mm thick, painted on the front (fire exposed surface) with high temperature black paint as shown in Figure 5-35. A 24g bare thermocouple wire bead was welded to the centre of the back face of the steel plate (back face of plate in contact with the panel surface; measuring exposed face surface temperature of internal linings (Figure 5-36 and Figure 5-37).
B	Thin steel plate with affixed thermocouple and ceramic fibre insulation backing, compressed thickness approximately 10 mm; measuring adiabatic surface temperature of internal linings (Figure 5-38).
C	Plate thermometers constructed in accordance with ISO 834-1 (1999) and EN1363-1 (2012). The plate thermometers are made from a 0.7±0.1 mm thick nickel alloy sheet. The 150 × 100 mm sheet is folded to form a plate thermometer with a face of 100 x 100 mm. A K-type thermocouple was secured to the centre of the back face of the nickel alloy sheet by a small (25 × 6 mm) steel strip and two 2 mm diameter screws. A 97 mm × 97 mm × 10 mm thick) pad of inorganic insulation material was fitted behind the thermocouple; measuring adiabatic surface temperature (Figure 5-39).
D1	Copper disk thermocouple covered by insulated pad; measuring cavity surface temperature of exposed lining.
D2	Copper disk thermocouple covered by insulating pad; measuring cavity surface temperature of unexposed lining or cladding.
E	Fibreglass insulated, Type K, thermocouple wire with twisted ends, measuring air temperature in roof space.
F	Copper disk thermocouple; measuring outside surface temperature of unexposed plasterboard, plywood or fibre cement. Fiberglass insulated, Type K, thermocouple wire with twisted ends used (held with a screw) on metal cladding.
G	Copper disk thermocouple covered by insulated pad; measuring cavity surface temperature of exposed ceiling lining.

6.5.2 Dummy Chord

A dummy chord with an array of twelve thermocouples was installed in the roof space of the compartment, at the same height and similar location to the bottom chords of the roof trusses. The thermocouple layout is shown in Figure 6-17. Mineral insulated metal sheath (MIMS) thermocouples were used. In addition to the internal thermocouples, Type B devices were installed on the underside and two vertical faces of the dummy chord, as shown in Figure 6-18.

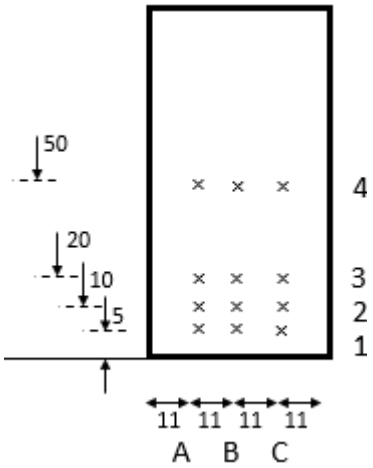

Figure 6-17 – Experiment #2 dummy chord thermocouple layout

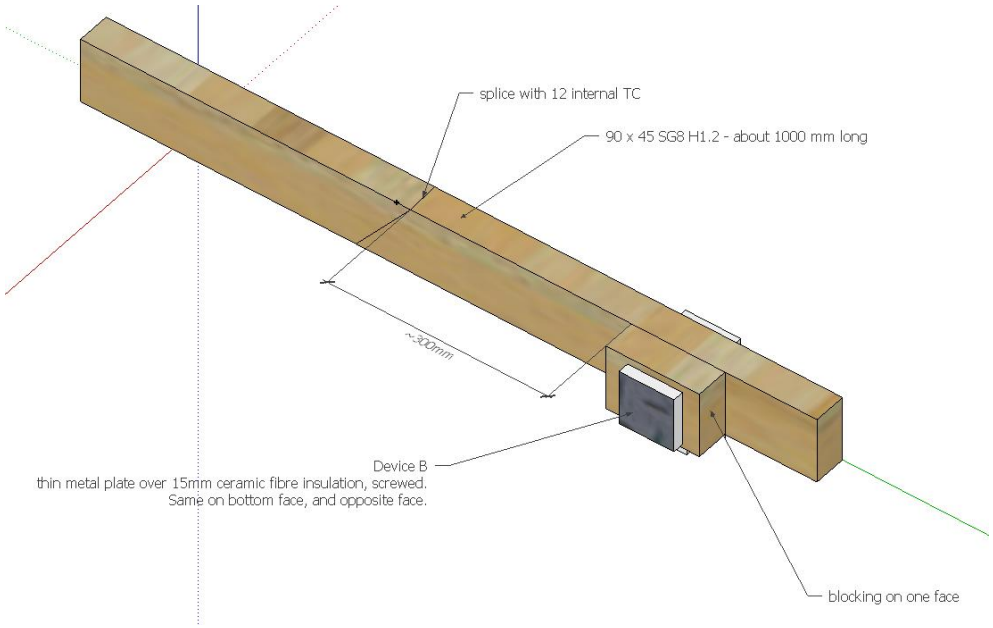

Figure 6-18 – Experiment #2 depiction of dummy chord with Type B devices

The general location of the dummy chord in the ceiling space is depicted in Figure 6-19 and Figure 6-20, and Figure 6-21 shows a photo. The dummy chord was suspended from the roof purlins, so as not to impart any significant additional loading on the ceiling system. The additional load on the roof purlins and therefore the trusses was considered negligible in the context of the experiment.

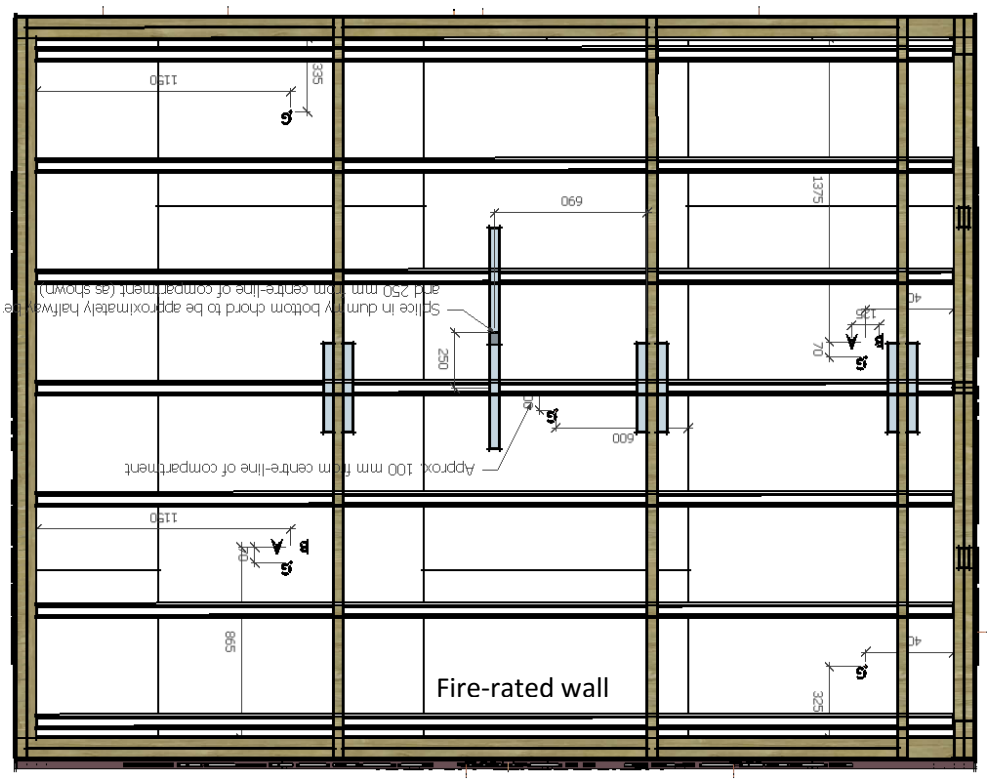

Figure 6-19 – Experiment #2 dummy chord general location

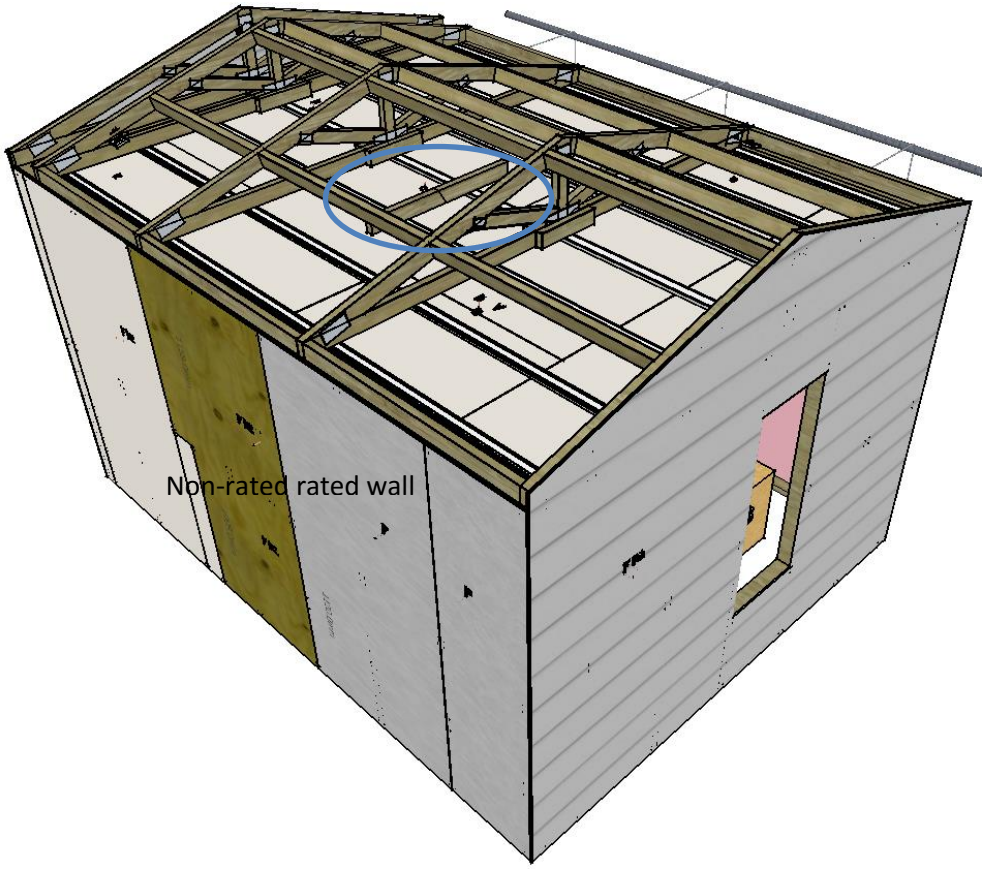

Figure 6-20 – Experiment #2 3D image showing general location of dummy chord

Figure 6-21 – Experiment #2 photo of dummy chord

6.5.3 Adiabatic Surface Temperature Measurement – Intermediate Trusses

Type B devices were installed on the underside and two vertical faces of each of the three (load-carrying) intermediate trusses. Figure 6-22 and Figure 6-23 show a view of the devices from below and above respectively.

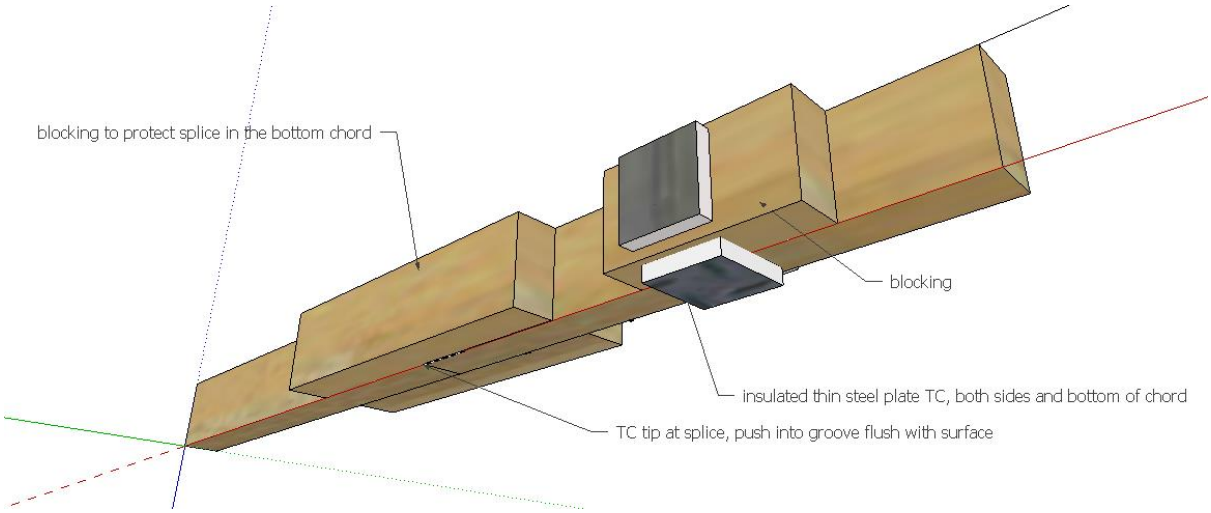

Figure 6-22 – Experiment #2 schematic view from below of intermediate truss with protected splice and Type B device

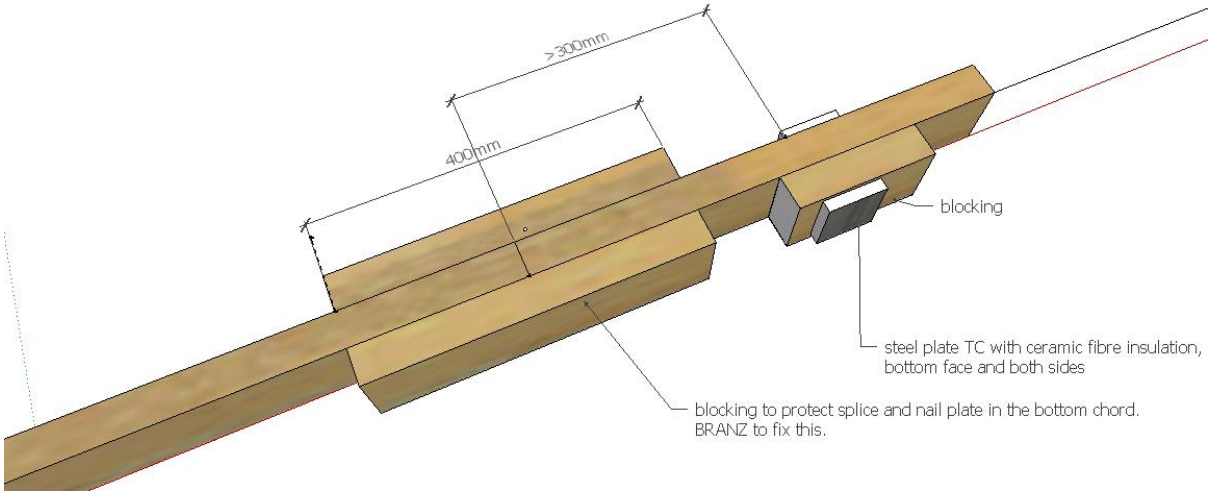

Figure 6-23 – Experiment #2 schematic view from above of intermediate truss with protected splice and Type B device

6.5.4 Temperature Measurement – Roof

The surface temperature on the unexposed side of the roof was measured in two places (Type F) as shown in Figure 6-24, and adjacent to this adiabatic surface temperature measurements on the exposed side of the roof were taken using Type B devices. Figure 6-25 shows the set-out of the Type F and Type B devices in relation to each other, and Figure 6-26 shows a view from inside the ceiling space of a Type B device on the underside of the roof.

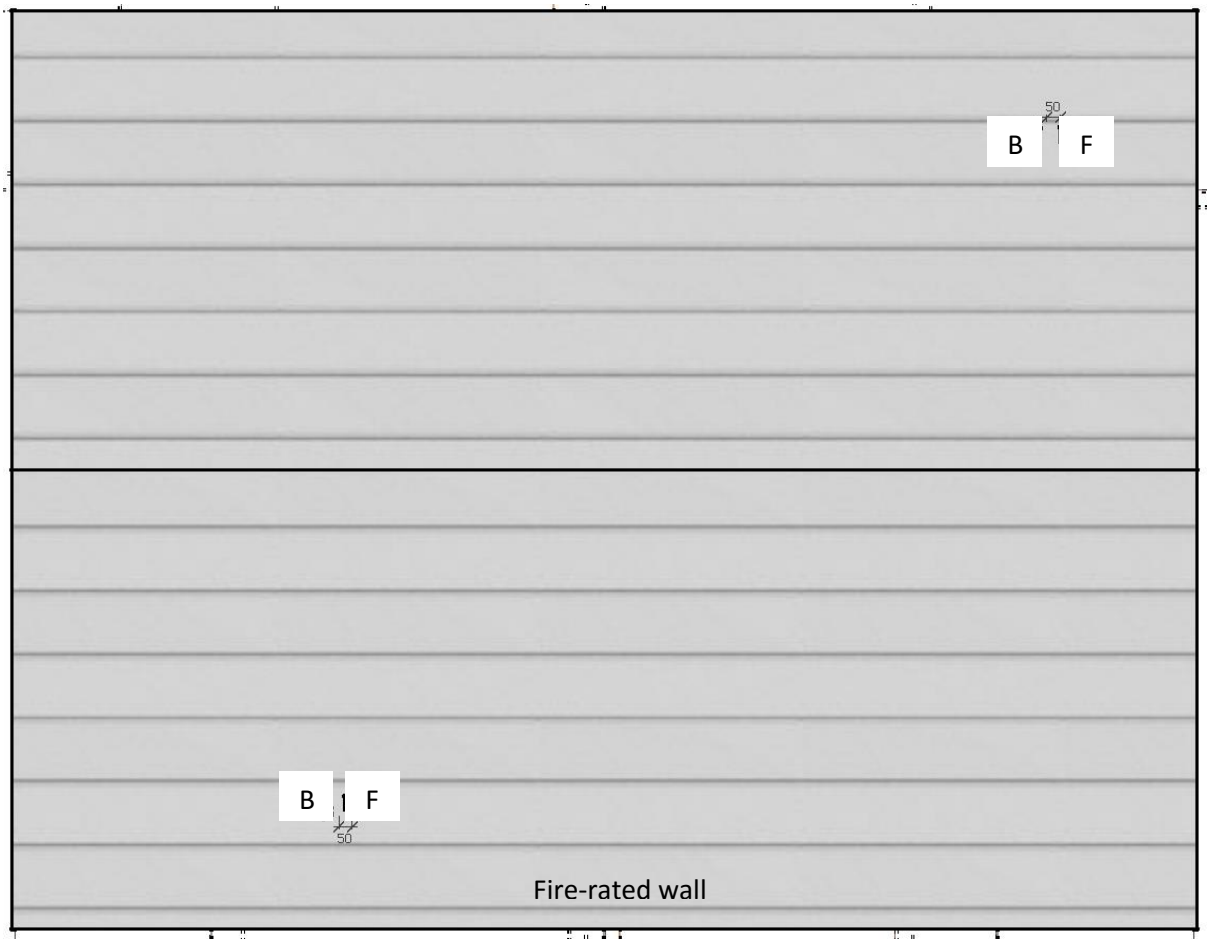

Figure 6-24 – Experiment #2 roof thermocouple locations, plan view

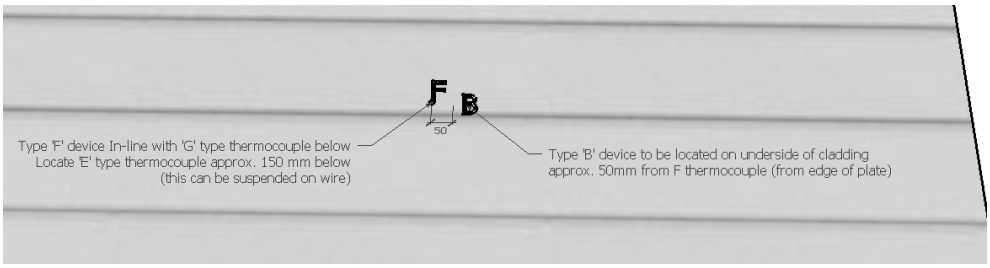

Figure 6-25 – Experiment #2 Roof thermocouple locations, detail view

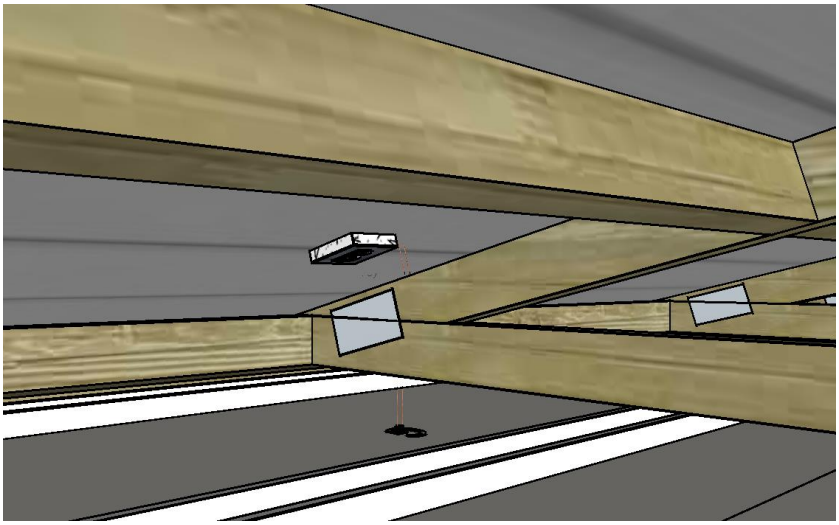

Figure 6-26 – Experiment #2 Detail view of Type B device measuring adiabatic surface temperature on underside of roof

6.5.5 Temperature Measurement – Ceiling

The surface temperature and adiabatic surface temperature on the exposed side of the ceiling linings were measured with device Type A and B respectively. These thermocouples were located in two places on the ceiling as shown in Figure 6-27. Five Type G devices were used to measure the plasterboard surface temperature on the unexposed side of the ceiling, their locations are shown in Figure 6-27.

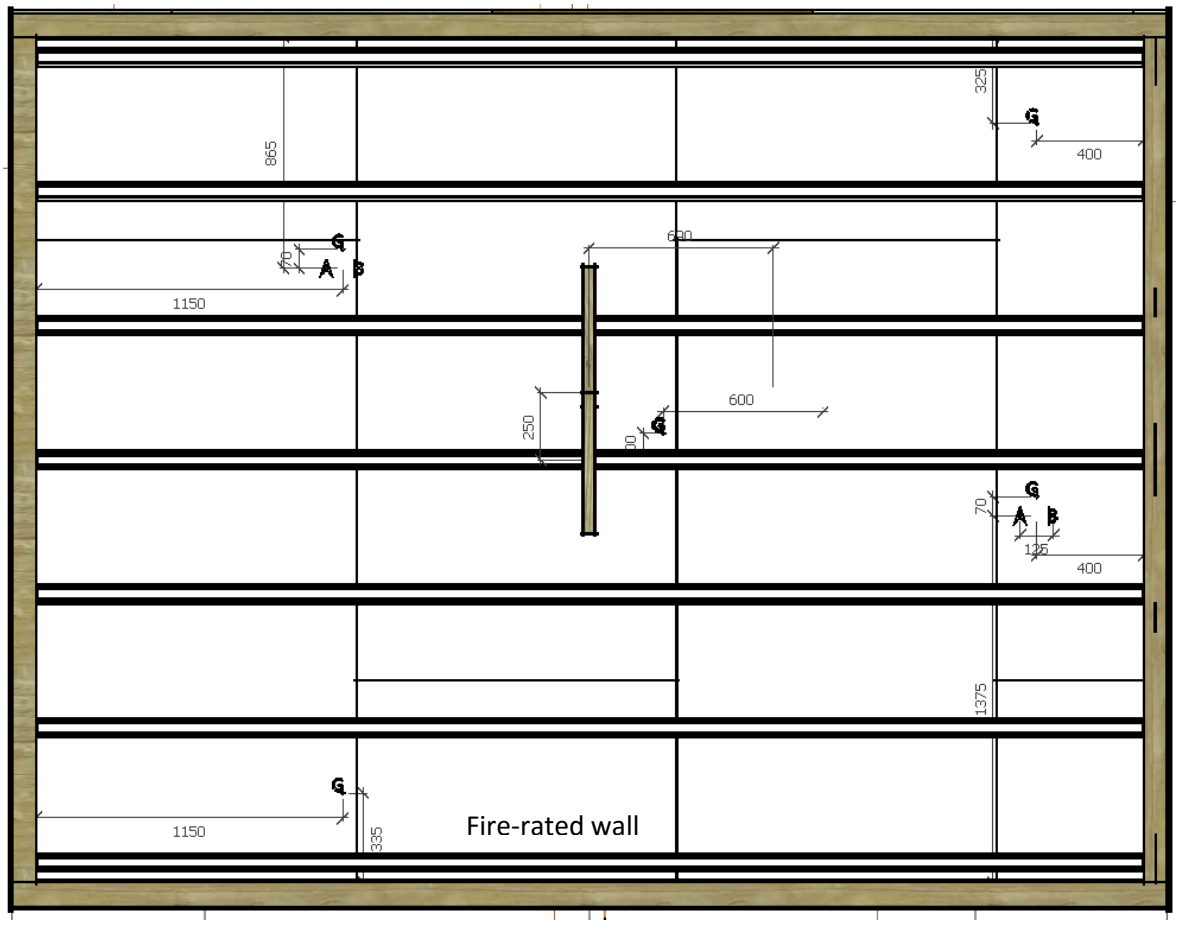

Figure 6-27 – Experiment #2 Ceiling thermocouple locations, viewed from above (ceiling void side)

6.5.6 Temperature Measurement – Walls

Temperature measurements were taken at a number of locations on each wall, on the exposed surface, in the cavity and on the outside of the wall. The fire-rated wall had six measurement locations, with various measurements taken in each location. The general layout of the thermocouples on the exposed and unexposed linings is shown in Figure 6-28 and Figure 6-29 respectively. The cavity side temperature of the exposed lining was measured in all six locations (D1). In the central location the exposed surface temperature was measured at high and low locations (A), and the adiabatic surface temperature measured at these same locations (B). A Type C device was also used to measure adiabatic surface temperature at the central high location, and this was used for comparison purposes with the Type B device in the same location.

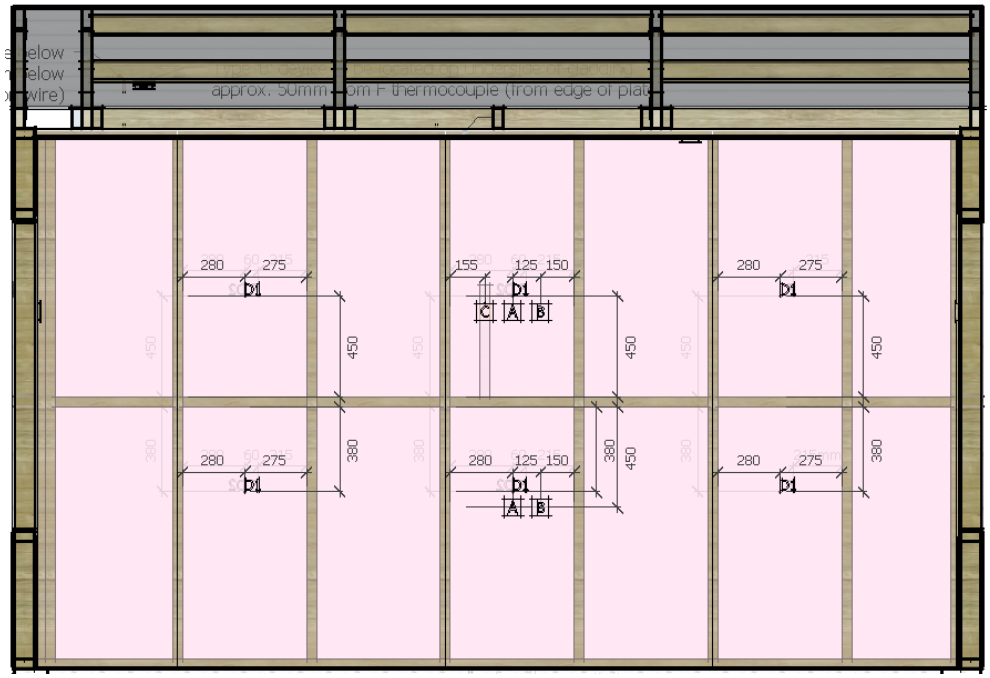

Figure 6-28 – Experiment #2 general layout of thermocouples on fire-rated wall exposed lining (viewed from inside)

Type F devices were used to measure the surface temperature on the outside face of unexposed linings at all six locations as shown in Figure 6-29. The cavity side temperature of the unexposed lining was measured at low and high locations at the centre of the wall, and in a plasterboard sheet near the free end of the compartment using Type D2 devices.

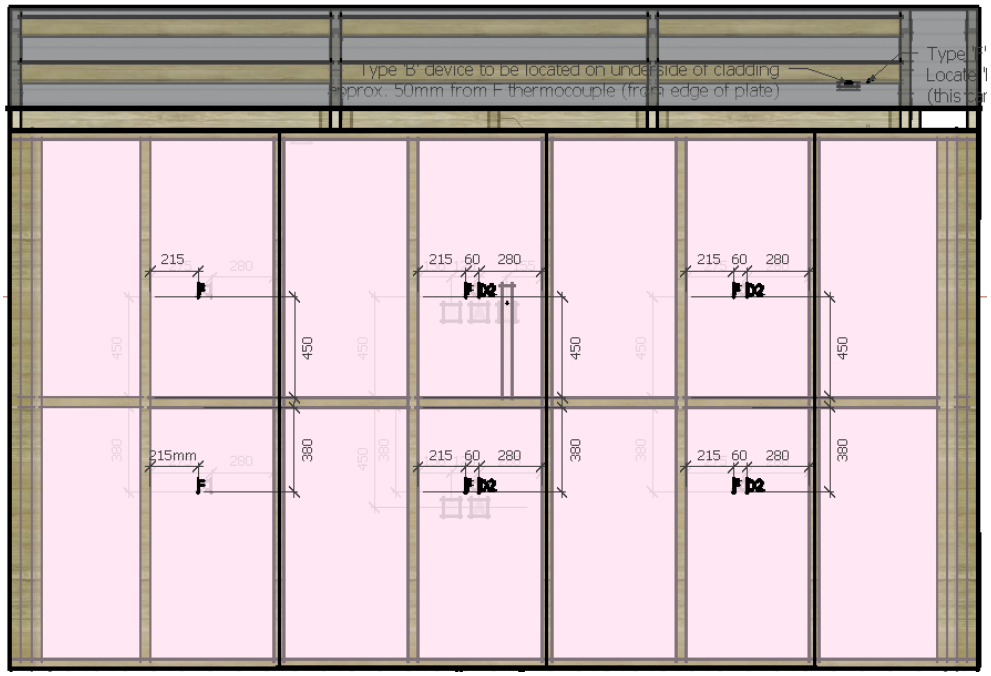

Figure 6-29 – Experiment #2 general layout of thermocouples on fire-rated wall unexposed lining (viewed from outside)

Figure 6-30 shows the general layout of thermocouples on the exposed lining in the non-rated long wall clad with plasterboard, plywood and fibre cement. In each of the three cladding systems, the fire side and cavity side surface temperatures were measured in the upper half of the wall, using Type A and Type D1 devices respectively. The adiabatic surface temperature at these same locations was measured using Type B devices. On the plywood clad segment of the wall, the adiabatic surface temperature was also measured using a Type C device; for the purpose of comparing with the Type B device results. The adiabatic surface temperature and cavity side surface temperature were measured in the lower half of the plywood segment, using Type B and D1 devices respectively.

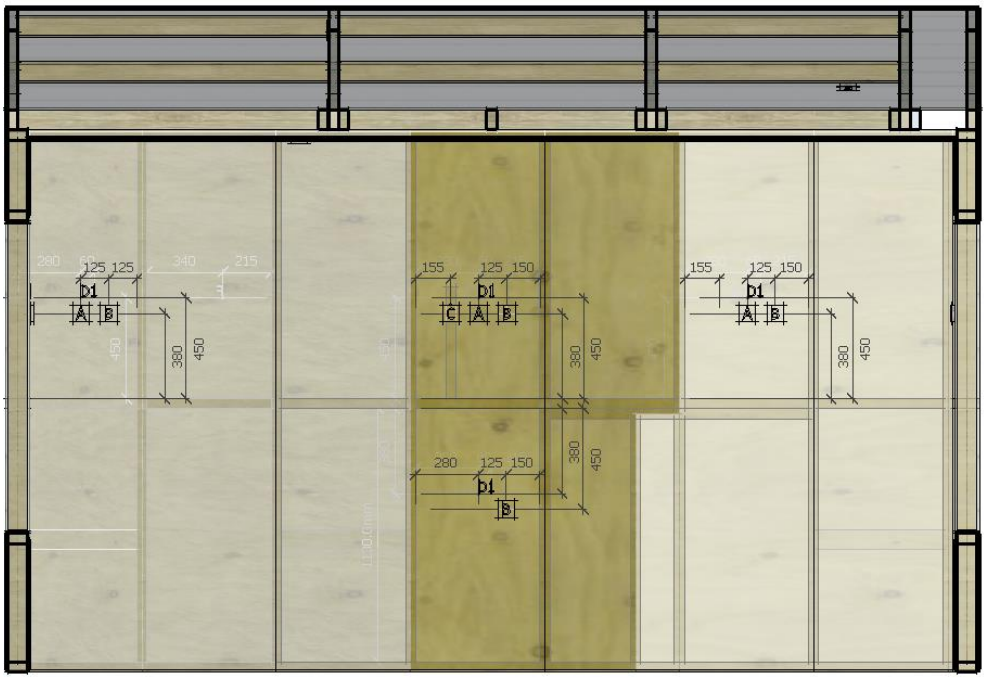

Figure 6-30 – Experiment #2 general layout of thermocouples on non-rated long wall exposed lining (viewed from inside)

Figure 6-31 shows the general layout of thermocouples on the unexposed cladding in the non-rated long wall clad with plasterboard, plywood and fibre cement. The outside face temperature was measured in the four locations that correspond to the exposed lining measurements previously described, and a fifth Type F device was installed in the end sheet of fibre cement to measure outside face temperature. The cavity side temperature was measured using Type D2 devices in the upper segment of the plasterboard, and both the upper and lower segments in the plywood.

Figure 6-31 – Experiment #2 general layout of thermocouples on non-rated long wall cladding (viewed from outside)

Figure 6-32 shows the general layout of thermocouples on the exposed lining in the fixed end wall. The cavity side surface temperature of the lining was measured in the upper half of the wall in two locations using Type D1 devices. The exposed surface temperature and adiabatic surface temperature were measured adjacent to the Type D1 device closest to the non-rated long wall (right of image).

Figure 6-33 shows the general layout of thermocouples on the unexposed cladding on the fixed end wall. The cavity surface temperature of the cladding was measured in the upper half of the wall to coincide with where the exposed lining temperature measuring devices were located. The cladding outside surface temperature was also measured in this location.

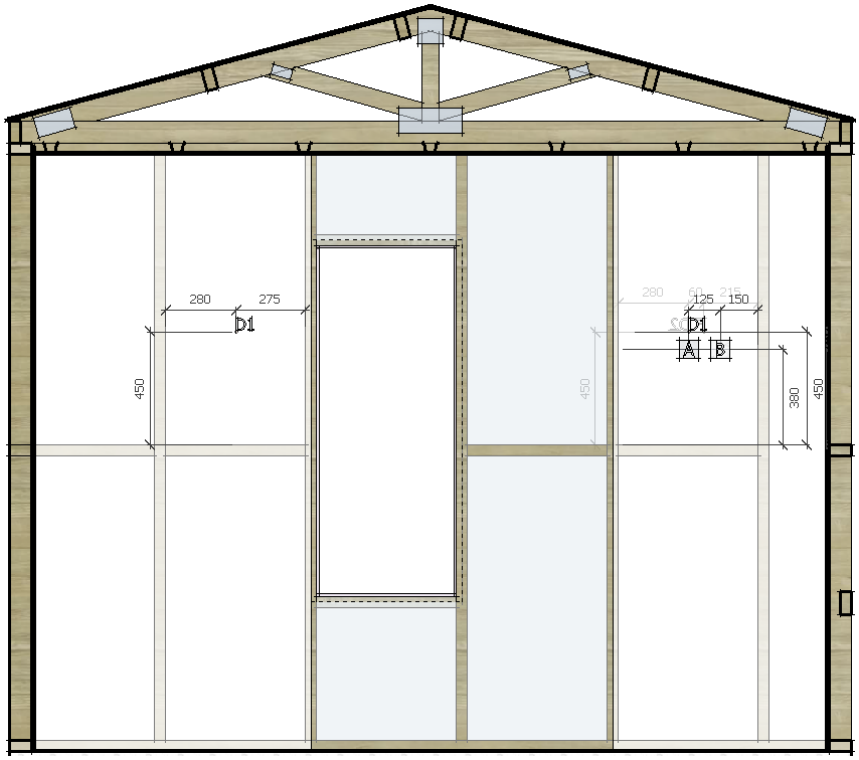

Figure 6-32 – Experiment #2 general location of thermocouples on fixed end wall lining (viewed from inside)

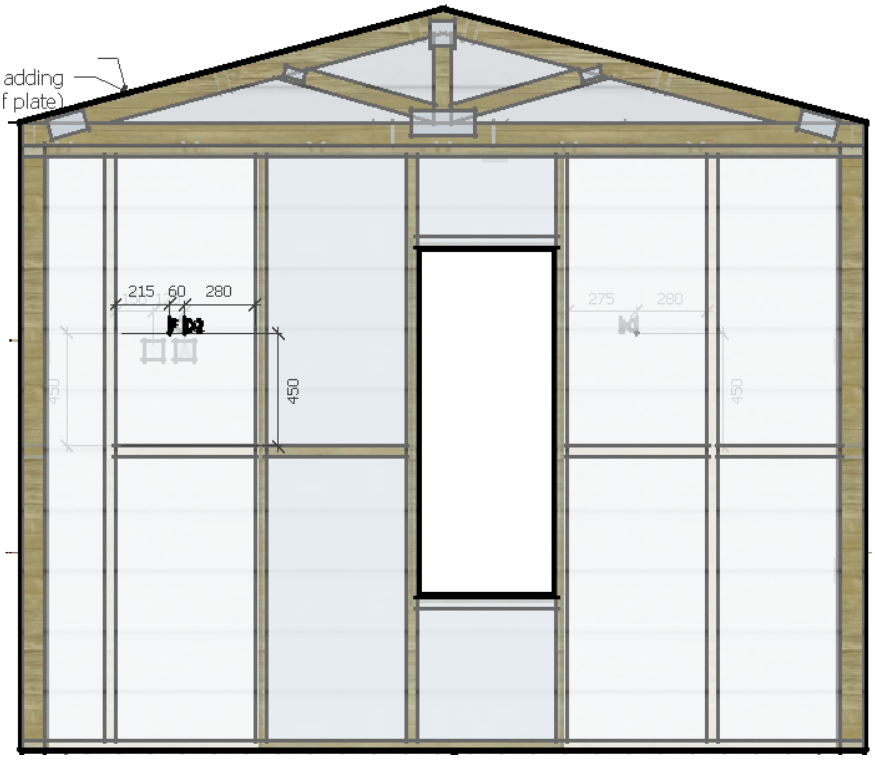

Figure 6-33 – Experiment #2 general location of thermocouples on fixed end wall cladding (viewed from outside)

Figure 6-34 shows the general layout of thermocouples on the exposed lining in the free end wall. The cavity side surface temperature of the lining was measured in the upper half of the wall in two locations using Type D1 devices. The exposed surface temperature and adiabatic surface temperature were measured adjacent to the Type D1 device closest to the non-rated long wall (left of image).

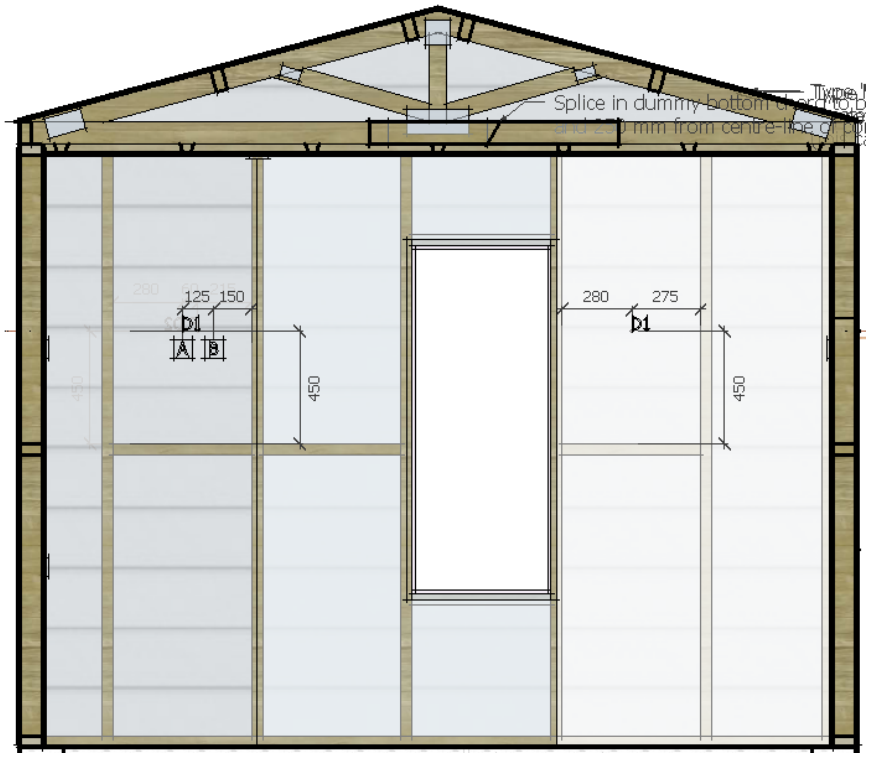

Figure 6-34 – Experiment #2 general location of thermocouples on free end wall lining (viewed from inside)

Figure 6-35 shows the general layout of thermocouples on the unexposed cladding on the free end wall. The cavity surface temperature of the cladding was measured in the upper half of the wall to coincide with where the exposed lining temperature measuring devices were located. The cladding outside surface temperature was also measured in this location.

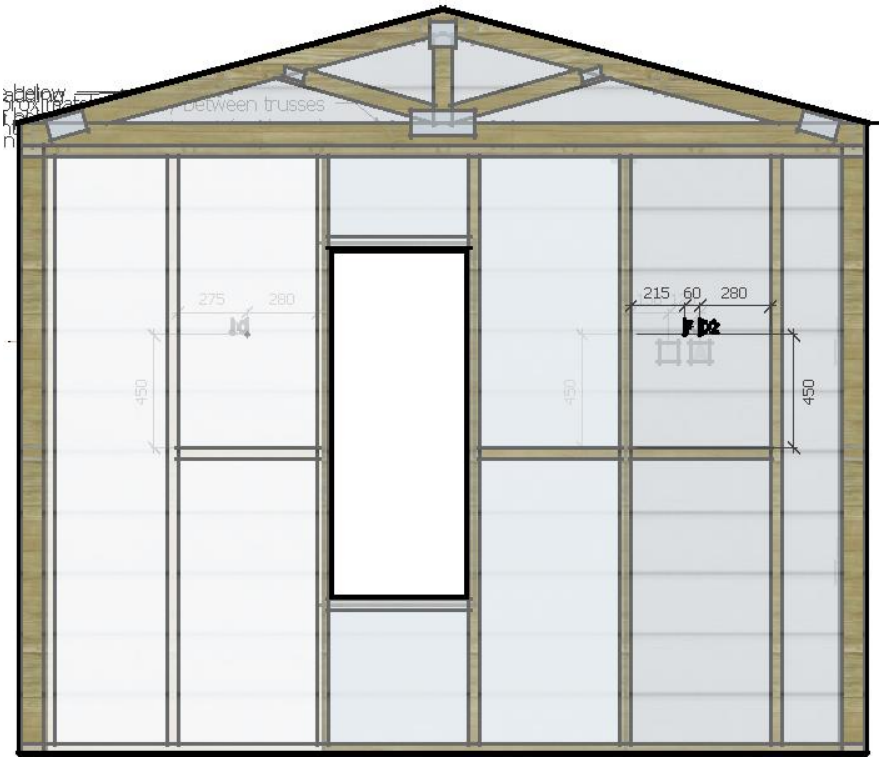

Figure 6-35 – Experiment #2 general location of thermocouples on free end wall cladding (viewed from outside)

Figure 6-36 – Photo of 360° view inside Experiment #2 compartment with surface temperature measurement devices visible

6.5.7 Fire-rated Wall Deflection

The deflection of the laterally loaded fire-rated wall was measured at the nogging and top plate heights at six locations along the wall, using linear potentiometers fixed on a frame. Figure 6-37 shows the general locations on the wall at which the deflection of the fire-rated wall was measured using linear potentiometers. Figure 6-38 shows a detail schematic of an example location in relation to the wall framing. Figure 6-59 is a photo of the typical setup of a linear potentiometer measuring deflection of the fire-rated wall.

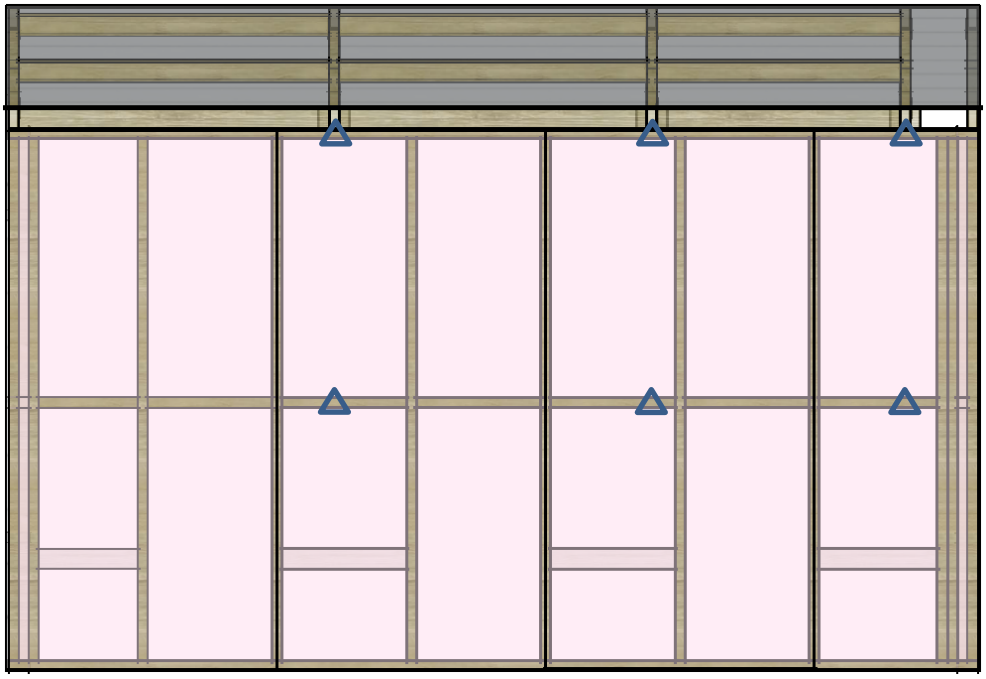

Figure 6-37 – Experiment #2, schematic of linear potentiometer layout to measure deflection of fire-rated wall

△ = linear potentiometer locations

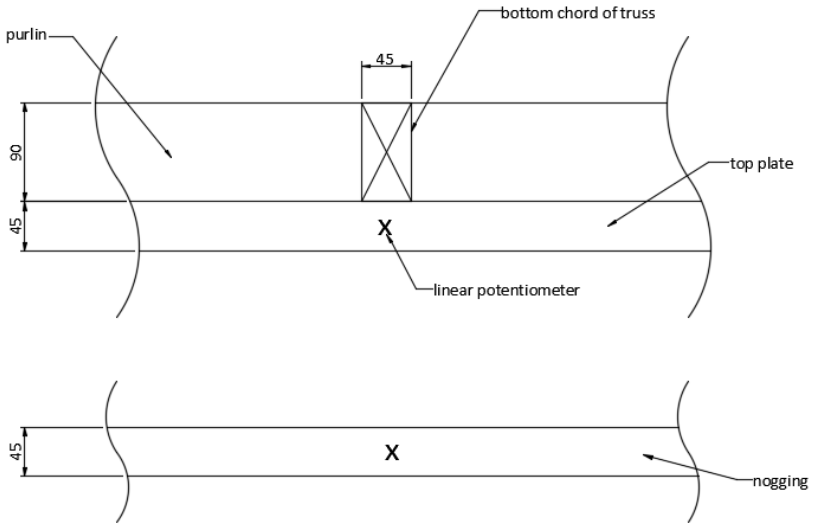

Figure 6-38 – Experiment #2, detail of location of linear potentiometers measuring deflection of fire-rated wall

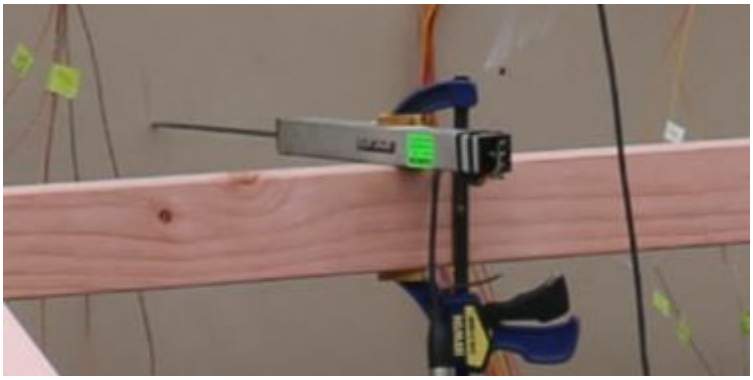

Figure 6-39 - Experiment #2, photo of typical setup for linear potentiometer

6.5.8 Temperature Measurement – Compartment

A thermocouple tree was installed in the compartment below the ceiling, suspended from the roof purlins. Thermocouples were Type K Alumel/Chromel, 24 gauge, 0.5 mm diameter, glass braid insulated and sheathed thermocouple wire with crimped tip. These thermocouples were located at distances 100 mm, 300 mm and 1200 mm below the ceiling. A weight was hung from the bottom of the tree to keep it straight, as shown in Figure 6-40. At the start of the experiment, the weight was unintentionally left resting on the corner of a wood crib and therefore the height of the measurements would have varied slightly from the intended locations. Thermocouples were installed approximately 100 mm above the bottom sill of each window opening, and 100 mm below the head of each opening.

Figure 6-40 - Experiment #2 view into compartment showing central thermocouple tree with weight suspended at bottom

6.5.9 Load Cells

Six electronic load cells were used to measure the mass loss rate of each crib during the experiment. The load cells were fixed to custom-built steel frames with adjustable feet to level them, as shown in Figure 6-41. The load cell unit had a load capacity up to 100 kg with a safe overload of 150 kg and ultimate overload of 250 kg. The operating temperature range is -30 to +70 °C, and the compensated range is -10 to +40°C. The load cells were calibrated before the experiment using weights of a known mass, up to 100 kg. The load cells and the frames were protected from the effects of fire with a custom-built platform as shown in Figure 6-42. The wood cribs rested on top of the protection platforms. High temperature ceramic fibre was affixed to the sides of the platform and draped to the ground to protect the platform. Cables were protected with high temperature ceramic fibre. Figure 6-43 shows the load cells in the compartment with the ceramic fibre protection and cribs on top.

Figure 6-41 – Experiment #2 photo of load cells used

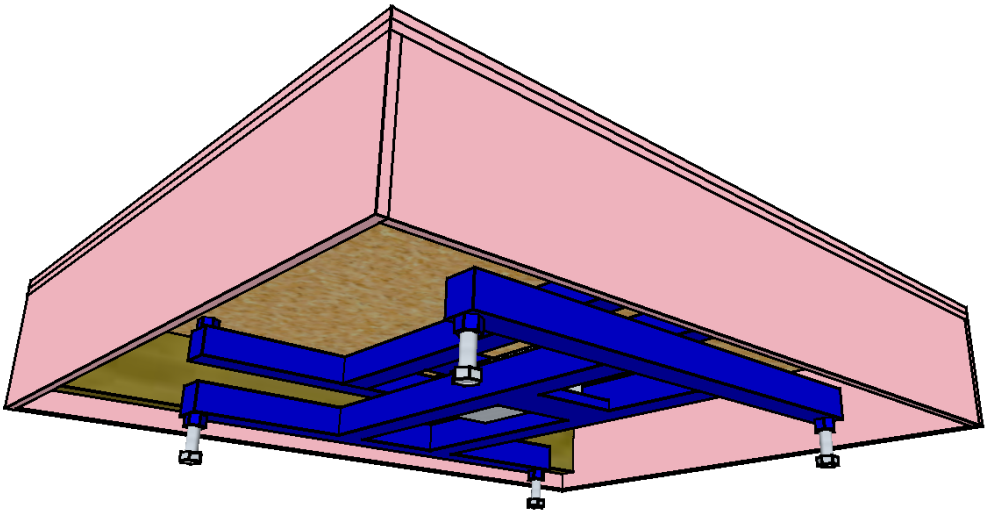

Figure 6-42 - Experiment #2 load cell protection platform resting on load cell frame

Figure 6-43 – Experiment #2 photo showing load cells in the compartment with the ceramic fibre protection and cribs on top

6.5.10 Crib Ignition

Section 2.3.2 described research by British Steel in cooperation with the Fire Research Station at Cardington, United Kingdom (BS/FRS) that different ignition modes resulted in little difference in the maximum temperatures reached or the duration of high temperatures compartment temperatures. With this taken into consideration it was determined that the key focus for crib ignition was to ignite all cribs simultaneously as far as could be achieved practically, and to ensure that flaming in the cribs was self-sustaining from early on in the experiment.

Six lengths of cotton wool were soaked in heptane to form a wick, and inserted underneath each wood crib with a 'tail' hanging out to be within reach for ignition. In total; 1.2 litres of heptane was used in soaking of the cotton wool. The time between soaking the cotton wool and ignition was minimised to limit the evaporation of heptane. Ignition was achieved using two poles each with a flaming cotton pad attached to the end. They were inserted through the openings at opposite ends of the compartment and each pole ignited three of the cribs over a period of about 5 seconds as shown in Figure 6-44 and Figure 6-45.

Figure 6-44 - Photo from Experiment #2 showing ignition of cribs at start of experiment

Figure 6-45 - Experiment #2 wood cribs after ignition, burning wicks visible

6.6 Results

6.6.1 Observations

There was a light breeze from the South toward the free end short wall when the cribs were ignited, Figure 6-46 shows a photo of the wood cribs during the initial growth period. During the first 4 min of the experiment there was little smoke visible from the compartment openings, and at about 4.5 min the smoke became noticeably more visible with increasing density, darkness and volume. At 6 min there was soot and small debris observed to be coming out of the south window. After 6.5 min there was a noticeable increase in the smoke leakage from the roof eave (i.e. gap between the top plate of the wall and underside of roof) on the fire-rated wall side. At about 10 min there was a notable increase in the quantity of smoke being emitted from both windows, and the mass flow from the south window appears to be slightly greater than that from the north. Figure 6-47 and Figure 6-48 show photos of the compartment viewed from the fire-rated wall side at 5 and 10 min respectively.

Figure 6-46 - Experiment #2 view of cribs during initial fire growth, t ≈ 3 min

Figure 6-47 - Experiment #2, view of fire-rated wall after 5 min

Figure 6-48 - Experiment #2, view of fire-rated wall after 10 min

Between 12 and 13 min there was a large increase in quantity of smoke rising from the compartment, including from the windows and eaves as shown in Figure 6-49; as the plasterboard ceiling is observed to progressively fail and fall from the ceiling battens. There was a brief period of steady burning and then at about 14 min the quantity of smoke increased, the smoke was darker from the south window and lighter from the north. At 14.5 min the first external flaming was observed coming out of the free end window.

Figure 6-49 - Experiment #2 photo of compartment near time of ceiling failure, t ≈ 13 min

Figure 6-50 - Experiment #2, view of the free end wall after ceiling failure, t ≈ 14 min

Figure 6-51 - Experiment #2, view of fire-rated wall after 15 min

At 16 min the wind from the south increases, and at around 17 min there was a notable increase in external flame projection from the window to the south, with a decrease in smoke quantity. At 17.5 min there were flames projecting from the flashing at the ridge of the roof.

Figure 6-52 - Experiment #2, view of free end wall with external flaming visible, t ≈ 16 min

Figure 6-53 - Experiment #2, view of fire-rated wall after 20 min

At approximately 24 min there was noticeable scorching on the outside face of the top left panel of plywood cladding, and at 24.8 min the panel began to flame. At 25 min there were pieces of plywood debris falling from the wall to the ground, and scorching on other quadrants of the ply cladding was occurring. Shortly after this the fire spread to the adjacent top right panel of the plywood cladding and also the adjacent bottom left, and external flaming was occurring from the newly formed opening. After approximately 27 min both top halves of the plywood cladding were almost completely open and the last large remaining pieces of ply had fallen from these openings. The lower half of the plywood cladding had approximately a 50 % opening area after 27.5 min, and after 28.2 the plywood cladding was almost completely degraded such that the area of wall was more than 80% open as shown in Figure 6-56. By 29 min there was no significant area of plywood cladding remaining.

Figure 6-54 - Experiment #2, view of fire-rated wall after 25 min

Figure 6-55 - Experiment #2 photo of non-rated long wall and free end wall after plywood failure, t ≈ 28 min

Figure 6-56 - Experiment #2, view of non-rated long wall after plywood failure, t ≈ 28 min

Shortly after 25 min there were flames projecting from between the top plate of the fire-rated wall and the underside of the metal roofing. At 27 min, flames projected from the gable end wall/roof junction. Soon after this there were flames projecting from joints in the roof cladding. At 27.8 min the feet of the centre barrel appeared to touch the ground, while the feet of the other barrels remain suspended above the ground. At 28.6 min both the free and fixed end barrels dropped significantly and the roof collapsed inwards to the compartment. The end barrels remained suspended above the ground with their weight supported by the compartment. There was a visible gap between the fire-rated wall and the free end wall, and flames projected from this opening, as shown in Figure 6-57 and Figure 6-58.

Figure 6-57 - Experiment #2, photo of free end wall (approx. 29 min) after fire-rated wall failure, visible on left of photo

Figure 6-58 - Experiment #2, photo of fire-rated wall free end after failure (approx. 29 min)

There appeared to be little or no deflection in the fire-rated wall at the fixed end of the fire-rated wall as shown in Figure 6-59. The wall appears to be connected at the fixed end, also it can be seen that the gable end truss has collapsed inward toward the compartment centre. There was notable bowing along the length of the fire-rated wall and this appears to have the largest deflection near the middle of the wall as shown in Figure 6-60.

Figure 6-59 - Experiment #2, photo of fire-rated wall after failure (approx.31 min)

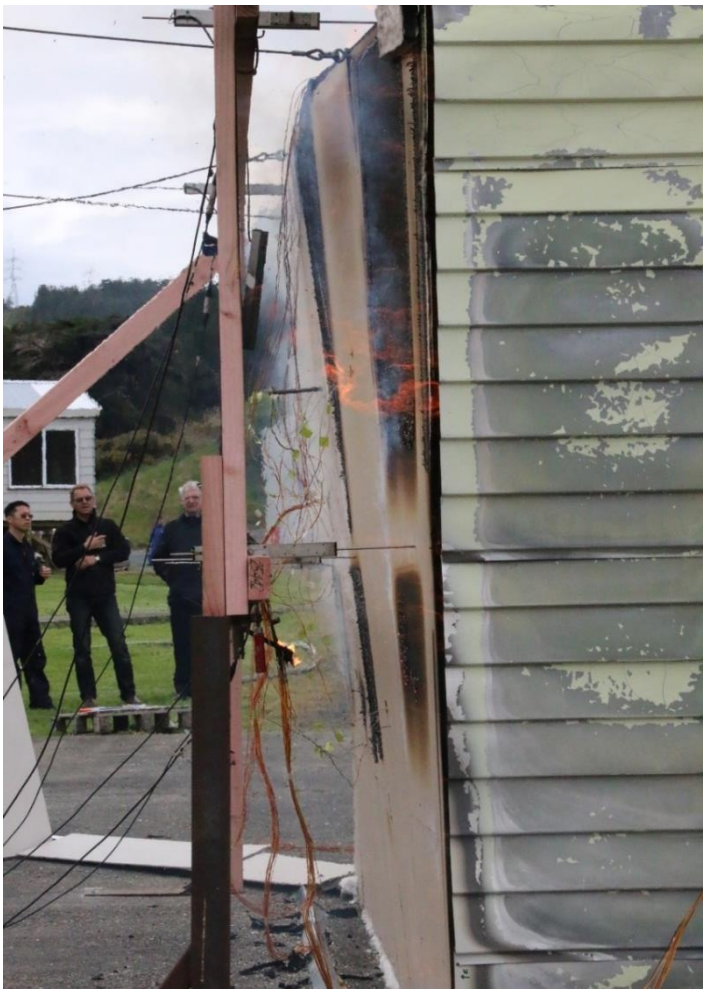

Figure 6-60 - Photo of fire-rated wall taken approx. 31 min, viewed from free end

Figure 6-61 - Experiment #2 view of fire-rated wall and free end wall after failure under lateral load, t ≈ 30 min

At 32 min the external flaming recedes and the fire appears to be fuel controlled with no flaming outside openings visible as shown in Figure 6-62. The paper facing on the outside of the fire-rated wall lining is scorched, and the scorch patterns indicate that the internal linings failed at the free end before the fixed. The scorching occurred at the top half of the wall before the bottom, indicating that the fire was more severe higher up in the compartment.

Figure 6-62 - Experiment #2 photo of opening in non-rated long wall where plywood cladding has failed, t ≈ 32 min

At 38 min the experiment is ended and water is applied to extinguish the fire. The compartment walls are forcibly collapsed.

Figure 6-63 - Experiment #2, photo looking into compartment from plywood opening, t = 35 min

Figure 6-64 - Experiment #2, photo at end of experiment facing compartment from non-rated long wall side, t ≈ 38 min

6.6.2 Mass Loss

Figure 6-65 shows the mass measurements for each load cell during the experiment. As previously described in Section 6.5.9; load cells 1 and 5 are the BRANZ cribs and load cells 2, 3, 4 and 6 were the new cribs. Window openings are at opposite ends of the building in the short walls, slightly offset toward the fire-rated wall (i.e. closest to cribs 4, 5 and 6).

It is observed that load cells 4, 5 and 6 follow a similar mass loss rate gradient during the fully developed phase of the fire, and load cells 1, 2 and 3 follow a different, but similar to each other, mass loss rate gradient during the fully developed phase of the fire. Load cell 6 has a greater starting mass than 2, 3 and 4 which may have been due to moisture content in the load cell protection platform, due to rain-fall the night before the experiment.

Between 30 and 31 min the reference voltage on the data logger indicated that there was a short circuit in one of the channels; which was likely due to falling debris severing a connection. Mass readings recorded after this time have been discarded.

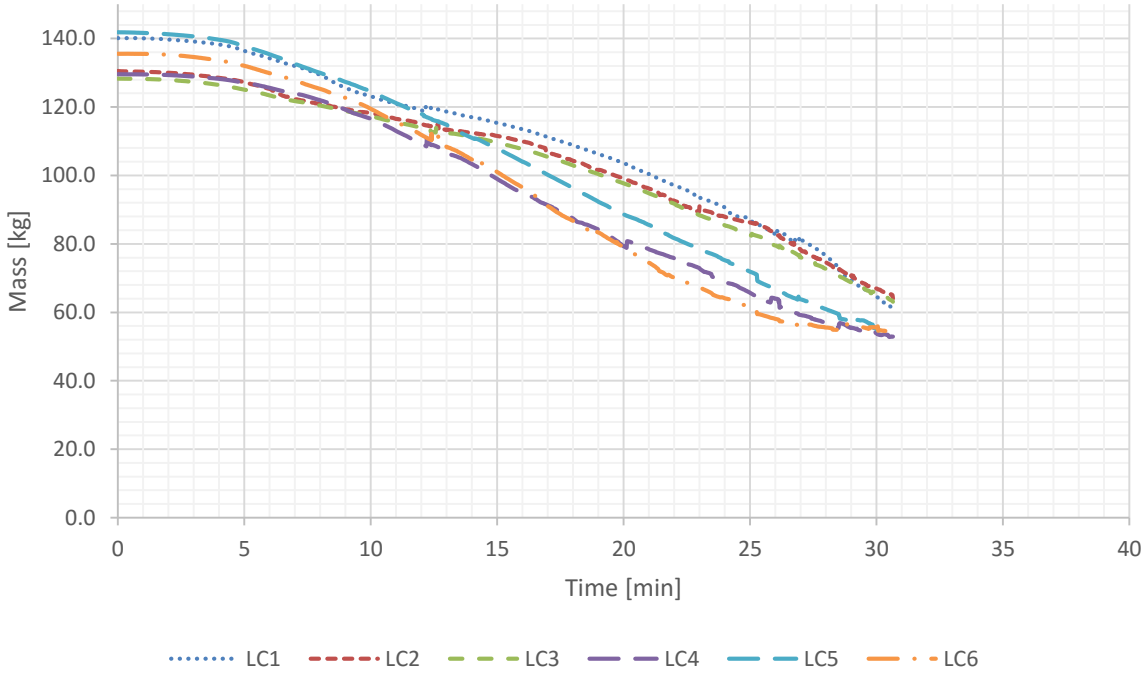

Figure 6-65 - Experiment #2 mass loss results based on load cell measurements

6.6.3 Compartment Temperatures

Figure 6-66 shows compartment gas temperature measurements. As described in Section 6.5.8 the end of the thermocouple tree was initially resting on top of a wood crib - initial temperature results may be at slightly different heights than intended, particularly for the lower thermocouples, however the effects are not considered to be significant in the context of the experiment.

In the experiment, the compartment temperature climbs steadily during the first 5 min to approximately 800°C. It oscillates about this value until about 25 min, at which time it climbs to approximately 900°C, coinciding with the partial failure of the plywood cladding which resulted in additional ventilation for the compartment. At approximately 31 min the measured compartment temperature begins to decay, due to the fire transitioning from the ventilation controlled phase to the fuel controlled phase.

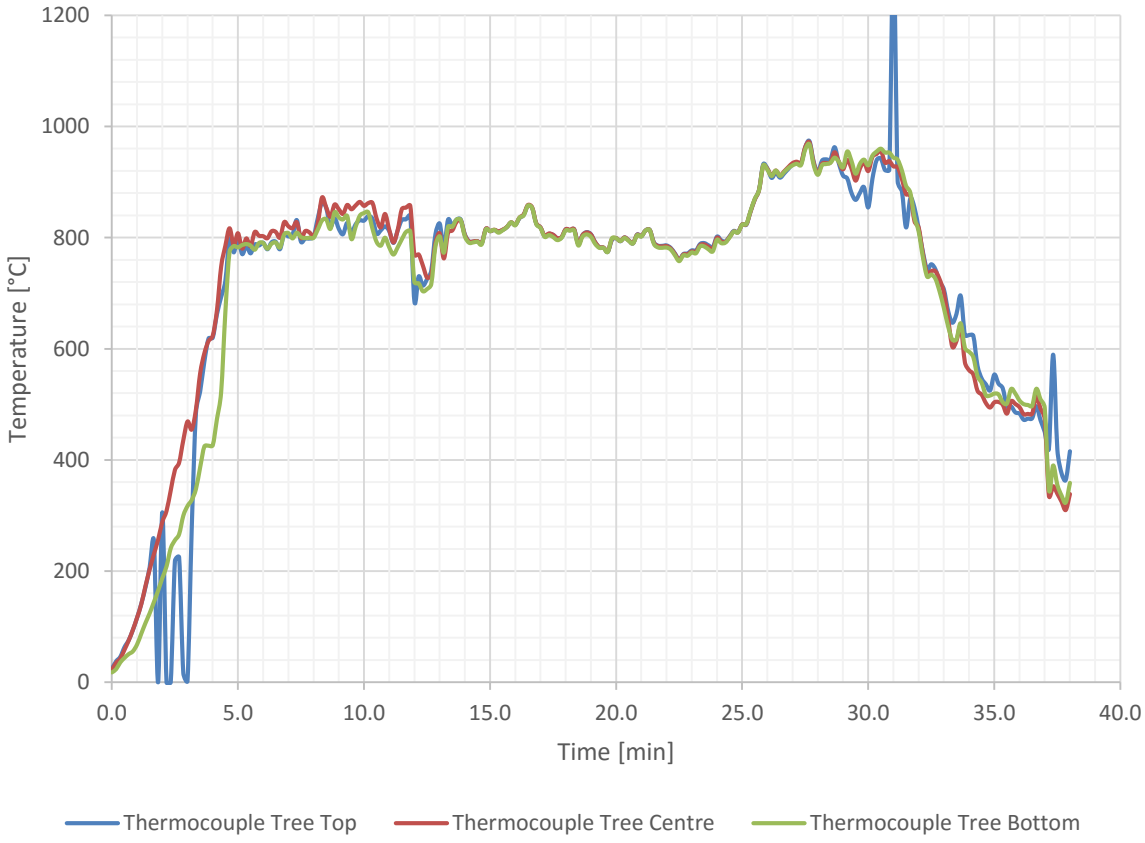

Figure 6-66 - Experiment #2 compartment gas temperature measurements

Figure 6-67 shows the temperature measurements taken 100 mm above the bottom sill of each window opening, and 100 mm below the head of each window opening. Note that the data has been truncated at various times due to failure of instrumentation during the experiment. The temperature at the bottom of each window is significantly lower than at the top. This is expected due to airflow behaviour through the vents, which typically draw cold air in from the bottom and exhaust hot gases and products of combustion at the top. The temperature at the top of the openings is comparable to the compartment temperature measurements as shown in Figure 6-66, approximately 800°C. Note that 'East' refers to the side of the compartment with the 'fixed' end wall, and 'West' refers to the side of the compartment with the 'free' end wall. This convention is used throughout the results.

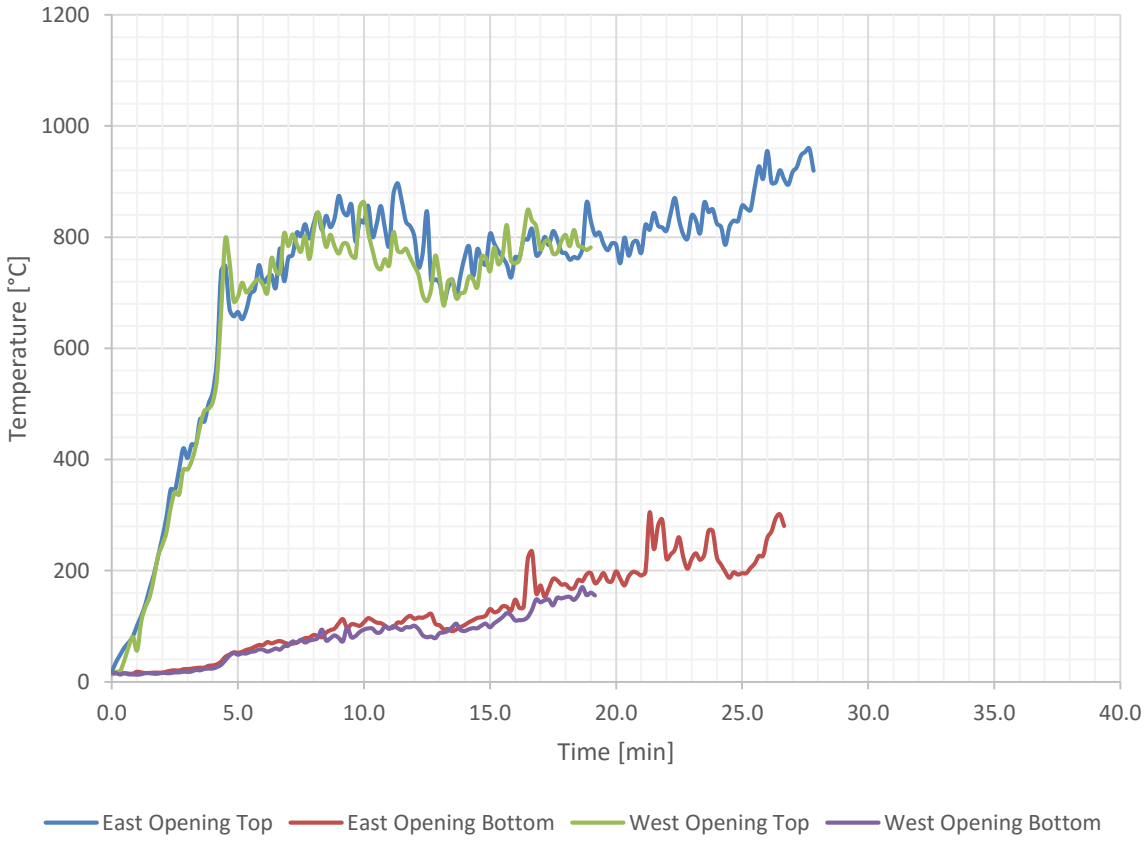

Figure 6-67 - Experiment #2 temperature measurements from top and bottom of openings

6.6.4 Ceiling Lining and Roof

Figure 6-68 shows ceiling lining temperature measurements on the exposed and unexposed sides. Exposed surface temperature and adiabatic surface temperature measurements at two locations as recorded by Type A and Type B devices respectively are shown, and the unexposed surface temperature measurements in five locations. The exposed side temperature rises as the compartment temperature increases, and the unexposed side plateaus at 100°C after approximately 5 min as moisture is driven from the plasterboard. There is a sharp increase in the unexposed face temperature at approximately 12 min and this coincides with the observed ceiling failure.

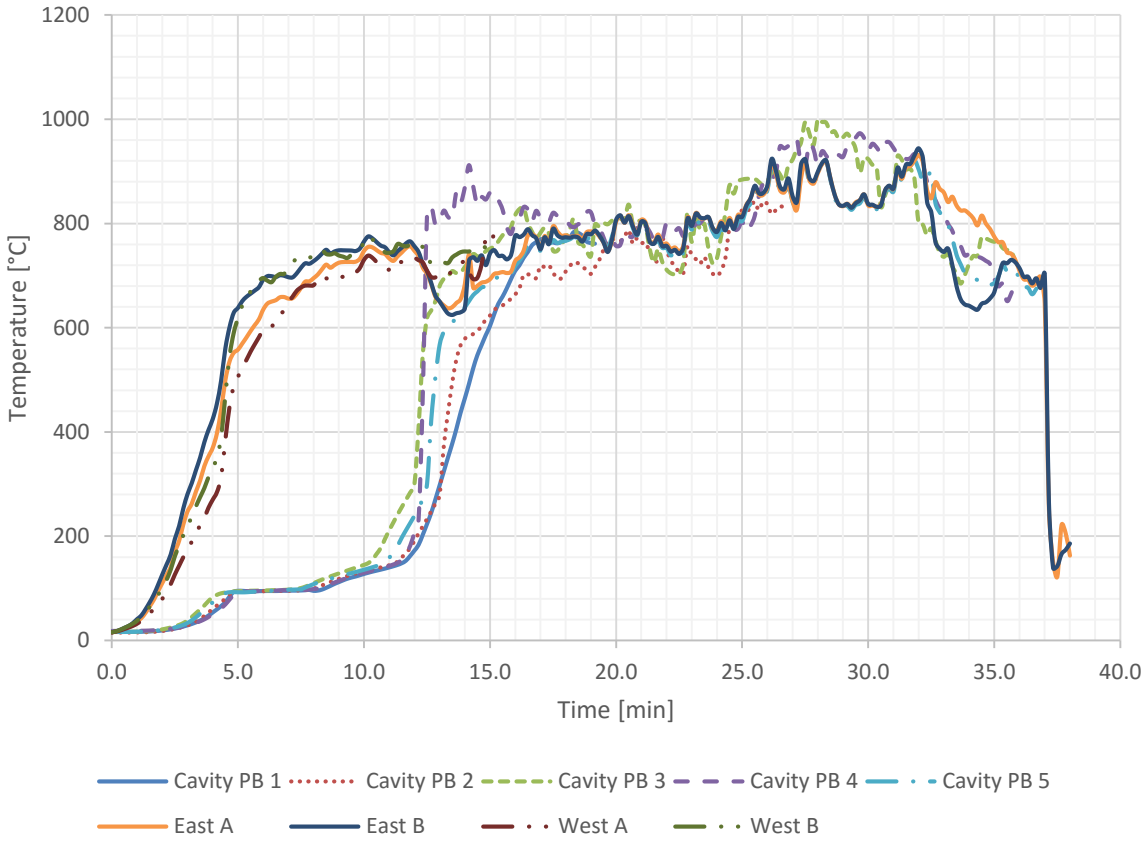

Figure 6-68 - Experiment #2 ceiling lining temperature measurements on the exposed and unexposed sides

6.6.5 Bottom Chord Temperatures

Figure 6-69 shows the adiabatic surface temperature measurements taken on the bottom and both sides of the intermediate bottom chord near the fixed end of the compartment (Type B devices), as well as the quick tip thermocouple temperature measurement; these thermocouple locations were described in Section 6.5.3. The results show that temperature measurements from these four devices were comparable and differences are negligible in the context of experimental uncertainty. Temperatures remain below 100°C until 12 min, at which time failure of the ceiling exposes the bottom chord of the trusses to the elevated compartment temperatures.

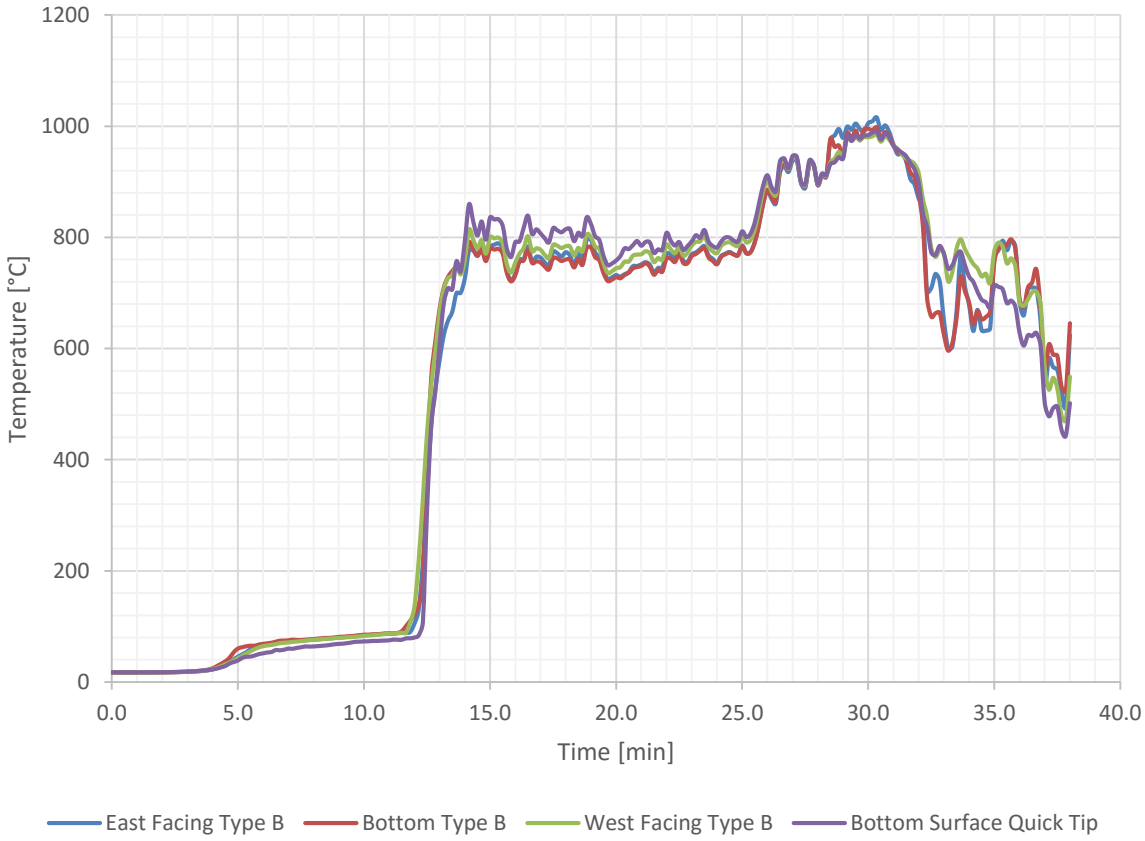

Figure 6-69 - Experiment #2, adiabatic surface temperature measurements on intermediate bottom chord near fixed end of compartment, and quick tip thermocouple temperature measurement from underside of bottom chord

Figure 6-70 shows the adiabatic surface temperature measurements taken on the bottom and both sides of the intermediate bottom chord near the centre of the compartment, as well as the quick tip thermocouple temperature measurement; these thermocouple locations were described in Section 6.5.3. The results show that temperature measurements from these four devices were comparable and differences are negligible in the context of experimental uncertainty. Temperatures remain below 100°C until 12 min, at which time failure of the ceiling exposes the bottom chord of the trusses to the elevated compartment temperatures.

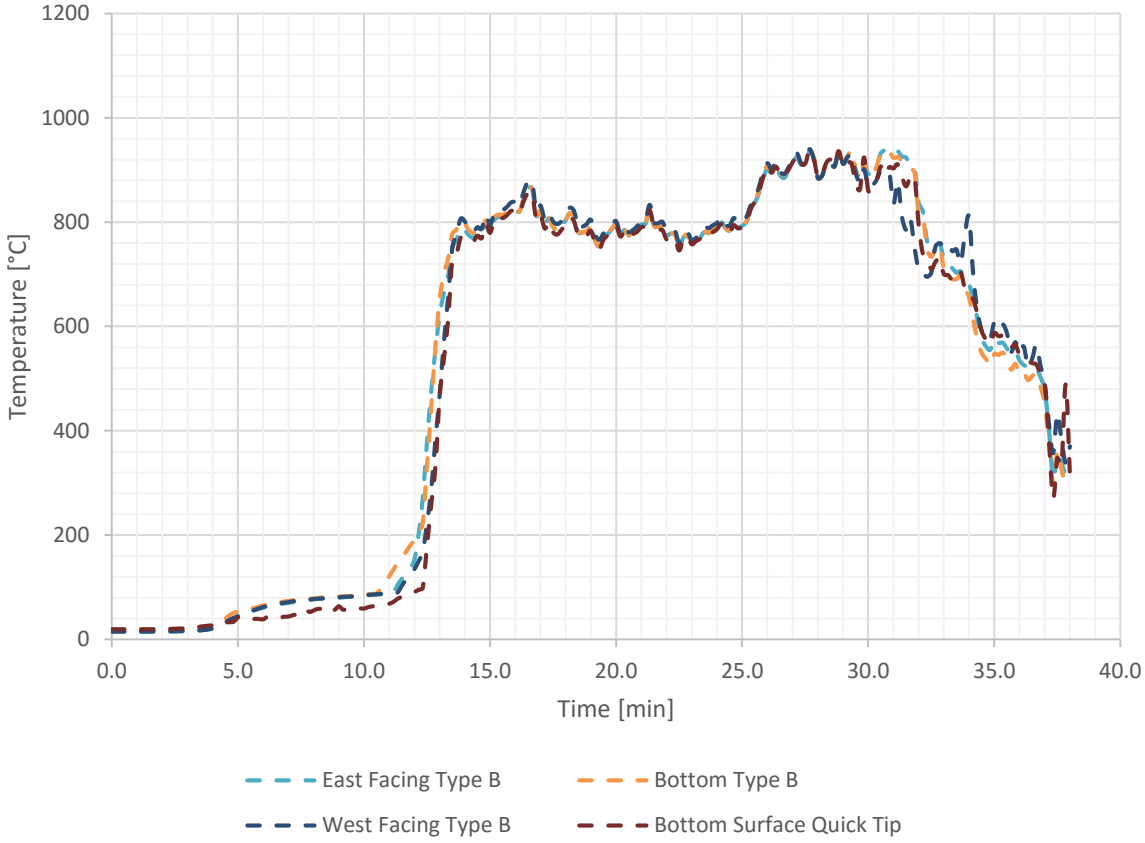

Figure 6-70 - Experiment #2, adiabatic surface temperature measurements on intermediate bottom chord near centre of compartment, and quick tip thermocouple temperature measurement from underside of bottom chord

Figure 6-71 shows the adiabatic surface temperature measurements taken on the bottom and both sides of the intermediate bottom chord near the free end of the compartment, as well as the quick tip thermocouple temperature measurement; these thermocouple locations were described in Section 6.5.3. The data has been truncated at 17.5 min due to failure of measurement equipment during the experiment that resulted in unusable data. The results show that temperature measurements from these four devices varied and there was temperature difference of up to 100°C at the time the devices failed (17.5 min). Temperatures remain below 100°C until 12 min, at which time failure of the ceiling exposes the bottom chord of the trusses to the elevated compartment temperatures.

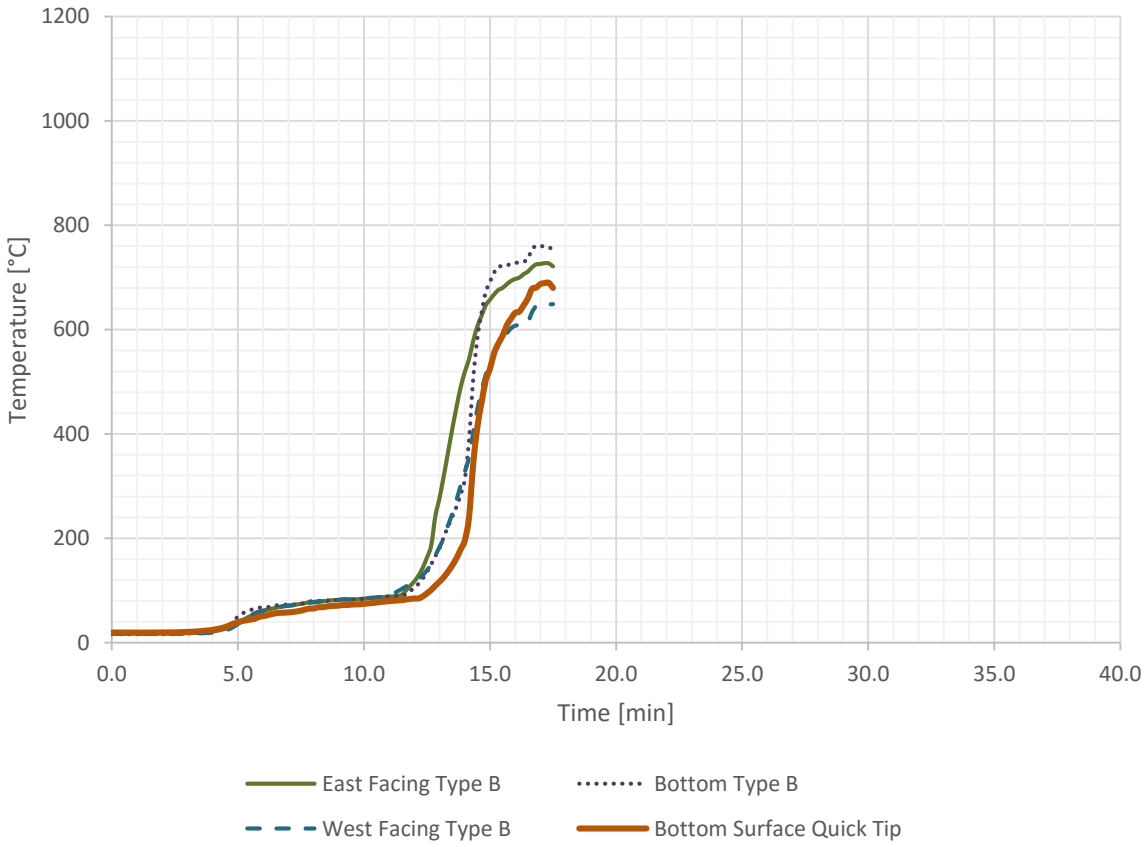

Figure 6-71 - Experiment #2, adiabatic surface temperature measurements on intermediate bottom chord near free end of compartment, and quick tip thermocouple temperature measurement from underside of bottom chord

6.6.6 Dummy Chord

Figure 6-72 shows the adiabatic surface temperature measurements taken on the bottom and both sides of the dummy chord near the free end of the compartment, as well as the quick tip thermocouple temperature measurement; these thermocouple locations were described in Section 6.5.2. The graph shows a significant increase in temperature on the surface of the dummy chord, corresponding to when it was directly exposed to the compartment fire temperatures due to the progressive ceiling failure between 12 and 13 min. The ceiling failure time is considered to be 12 min for the purposes of calculation and analysis throughout this report.

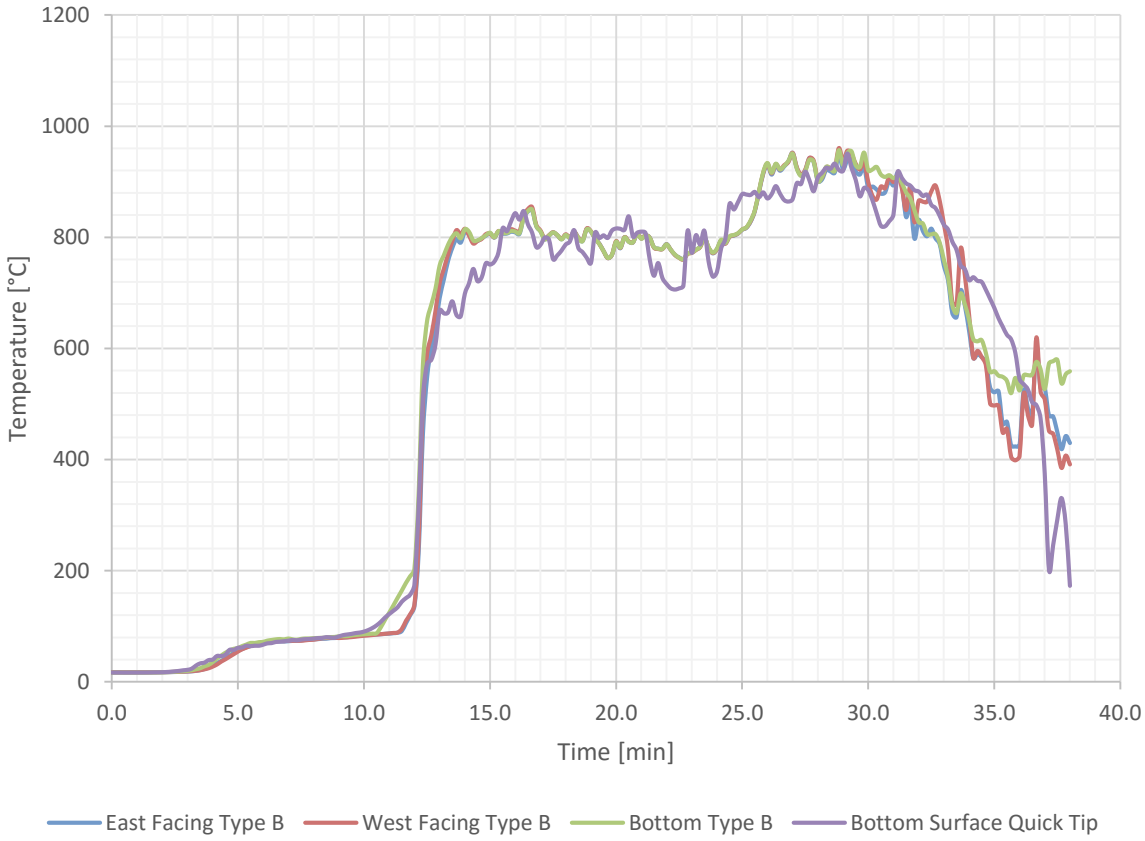

Figure 6-72 - Experiment #2, adiabatic surface temperature measurements on dummy chord, and quick tip thermocouple temperature measurement from underside of dummy chord

Figure 6-73 shows temperature measurements from the dummy chord, the data has been truncated between 27 and 28 min due to failure of instrumentation during the experiment. Thermocouple A1 located on one side of the dummy chord, 5 mm from the underside, was dead from the start and has been discarded. All thermocouple temperature measurements exhibited a plateau at 100°C which would coincide with moisture being driven away from the area of wood local to the thermocouple, as that area is heated. The deeper areas of wood appears to have extended plateaus, likely due to slower heating. The fastest temperature rise occurs on the thermocouples at 5 mm from the underside of the dummy chord.

Charring is considered to occur when the wood reaches a temperature of 300°C as described in Section 4.3. The first thermocouples to indicate the presence of charring were A1 and C1 at just after 14 min, approximately 2 min after ceiling failure. Approximately 1 min later, B1 reached 300°C, 3 min after the ceiling failed. The temperature at the other thermocouples in columns A and C all reach 300°C between 17 and 20 min, with C2 being the first of this group and C4 being the last the reach 300°C. Thermocouple B2 also reaches 300°C during this period, after approximately 19 min and at a similar time to thermocouples A2, A4 and C3. This seems reasonable as all these thermocouples are located approximately 11 mm from an exposed surface.

As expected, the central thermocouples closest to the centre of the dummy chord lag behind the others. The temperature at B3 begins to climb above 100°C at around 20.5 min, and reaches 300°C after 24 min. The temperature at B4 start to rise slightly after B3 but the data is truncated due to an instrumentation failure before reaching 100°C.

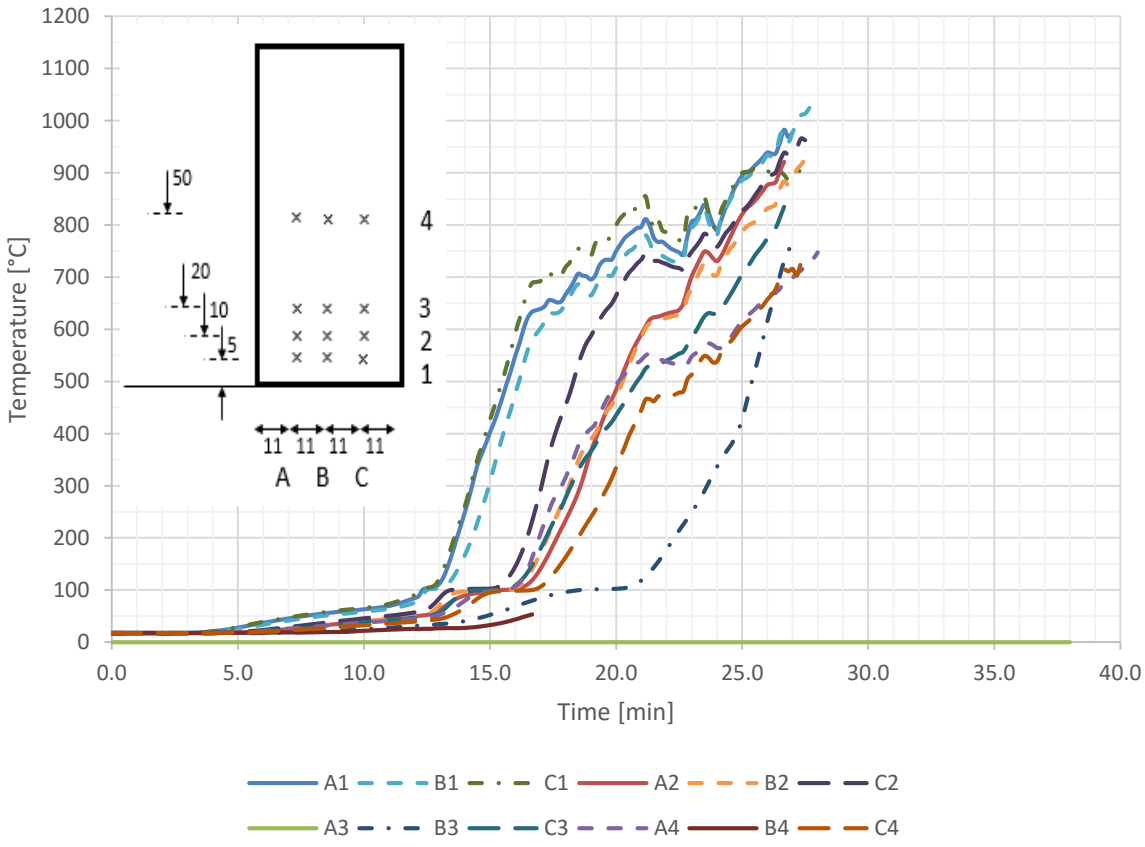

Figure 6-73 - Experiment #2, dummy chord thermocouple temperature measurements

A nominal charring rate was calculated by taking values from when the ceiling failed to when 300°C was reached at specified thermocouples on each side of the dummy bottom chord. The time for each thermocouple to reach 300°C and the char rate calculated based on this time and the depth of thermocouple is shown in Table 6-8. The highlighted values are those that have been used for the char rate analysis to determine a char value for this research.

Table 6-8 – Calculation of nominal charring rates for dummy chord

Thermocouple	Time 300°C reached [min]	Time Elapsed since ceiling failed [min]	Depth of thermocouple [mm]	Char Rate [mm/min]
A1	14.3	2.3	5	2.1
A2	18.7	6.7	10	1.5
A3	Failed	-	-	-
A4	18.0	6.0	11	1.8
C1	14.3	2.3	5	2.1
C2	17.2	5.2	10	1.9
C3	18.3	6.3	11	1.7
C4	19.8	7.8	11	1.4
B1	15.0	3.0	5	1.7
B2	18.2	6.2	10	1.6
B3	23.7	11.7	22	1.9
B4	Failed	-	-	-

The calculated char rate ranged from 1.4 mm/min to 2.1 mm/min, and an effective average value is required for further analysis of the performance of the truss in Section 6.7.4. Char rates are also expected to be faster closer to the surface of the wood as the char itself needs to build up a thickness to provide protection to the timber behind. Thermocouple rows 1 and 2 were expected to be affected by corner rounding and the effects of being exposed from two sides and were therefore discarded for this analysis. Thermocouples A3 and B4 failed either before or early in the experiment and have been discarded. The analysis has considered thermocouples B3, C3, A4 and C4, which had char rates of 1.9, 1.7, 1.8 and 1.4 mm/min respectively. This equates to an average char rate of 1.7 mm/min; this value is used for further analysis in this report.

6.6.7 Fire-rated Wall Lining Performance

Figure 6-74 shows the adiabatic surface temperature measurements for the fire-rated wall. The results show that the fire exposure was more severe on the upper part of the wall than the lower; particularly during the first 15 min of the experiment. The adiabatic surface temperatures for the lower and upper wall converge between 15-20 min, and the difference is noticeable again between 20-25 min, before they converge again until about 30 min. The upper wall adiabatic surface temperature is more severe throughout the fully developed ventilation controlled phase of burning. The adiabatic surface temperature measured by the Type B and Type C devices compares closely.

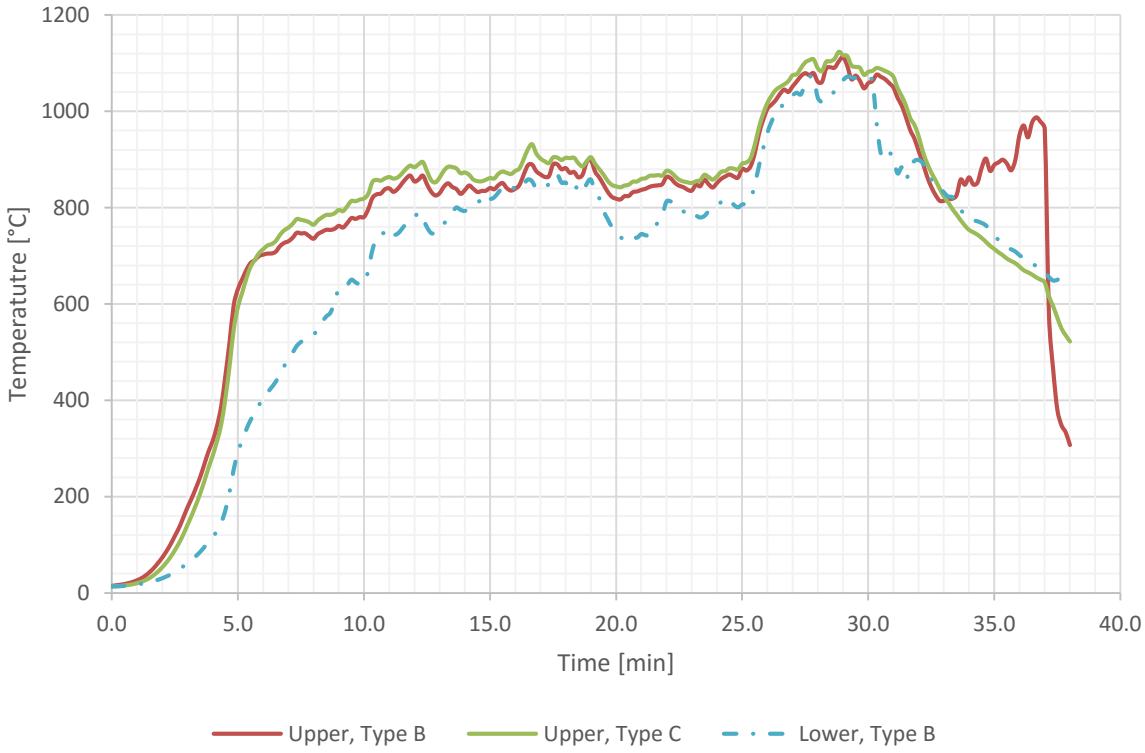

Figure 6-74 – Experiment #2, fire-rated wall adiabatic surface temperature

Figure 6-75 shows the cavity side temperature measurements for the exposed and unexposed linings of the fire-rated wall. Devices D1-1, D1-3 and D1-5 are on the cavity side of the exposed lining in the top half of the fire-rated wall, and devices D1-2, D1-4 and D1-6 are in the lower half. Devices D2-1, D2-2, D2-3 and D2-4 are located in the same section of wall as devices D1-1, D1-2, D1-3 and D1-4 respectively. The data has been truncated at 30 min due to failure of instrumentation during the experiment.

There is an initial temperature rise to approximately 100°C of the exposed lining and at this temperature there is a plateau, due to chemical change and moisture removal from the board as described in Section 4.2.3. The rate of temperature rise on the upper portion of the exposed lining increases significantly at approximately 13 min, and reaches 400°C between 14 and 15 min. The lower portion exhibits similar behaviour and lags behind the upper wall. The 100°C plateau extends from approximately 7 min to between 12 and 13 min, after which time the temperature rises to 400°C between 16 and 17 min.

The temperature of the unexposed lining exhibits a similar behaviour to the exposed lining, however the 100°C plateau is more pronounced and the rate of temperature rise is generally more gradual and linear. Temperature rise above 100°C begins to occur for the upper portion of the wall after approximately 12 min, and after approximately 14 min for the lower portion. Both the upper and lower portion temperatures climb steadily toward 400°C until about 27 min.

After approximately 27 min there is a noticeable increase in the rate of temperature rise of both the exposed and unexposed lining. It is likely that this coincides with failure of the exposed lining of the fire-rated wall. The unexposed lining remained in place at this time.

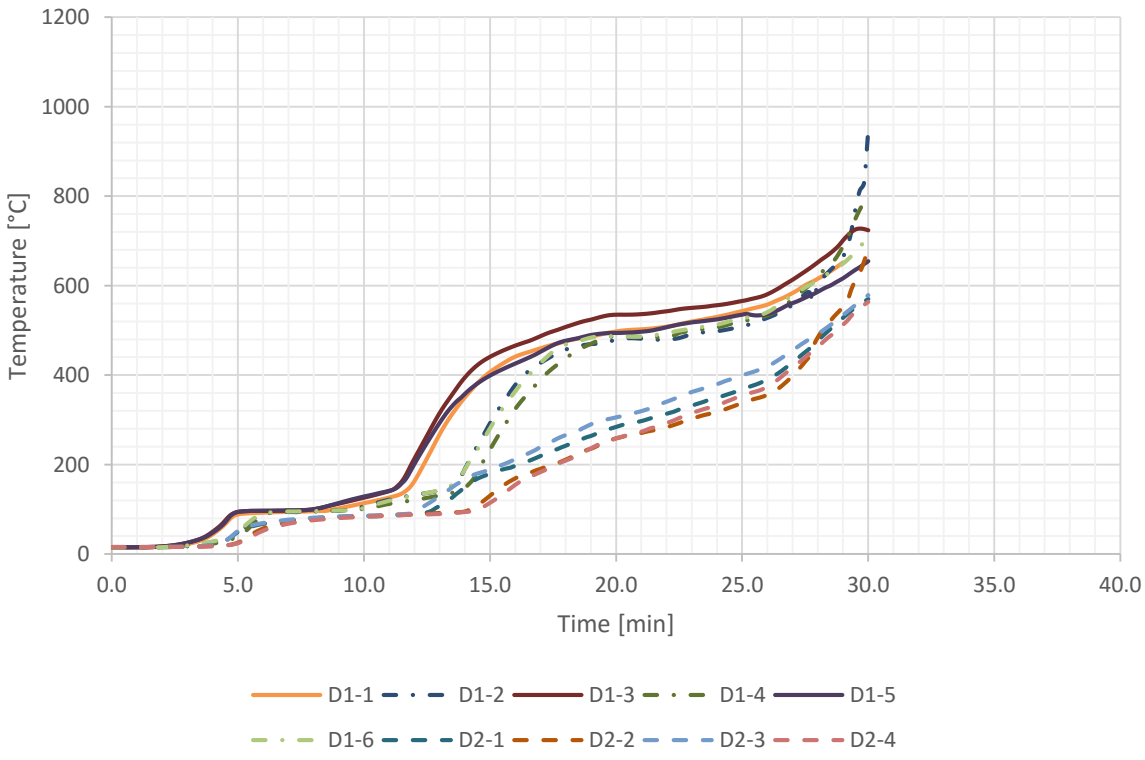

Figure 6-75 - Experiment #2 Fire-rated wall cavity side temperature of linings

Figure 6-76 shows the outside face temperature of the exposed lining on the fire-rated wall. The ambient temperature during the experiment was 14°C and therefore the failure criteria based on AS 1530 Part 4 is a maximum temperature at any location of 194°C and an average temperature of no more than 154°C. The results show that the maximum temperature rise is exceeded after 32.7 min by thermocouple F2 and the average temperature rise is exceeded after 33.0 min.

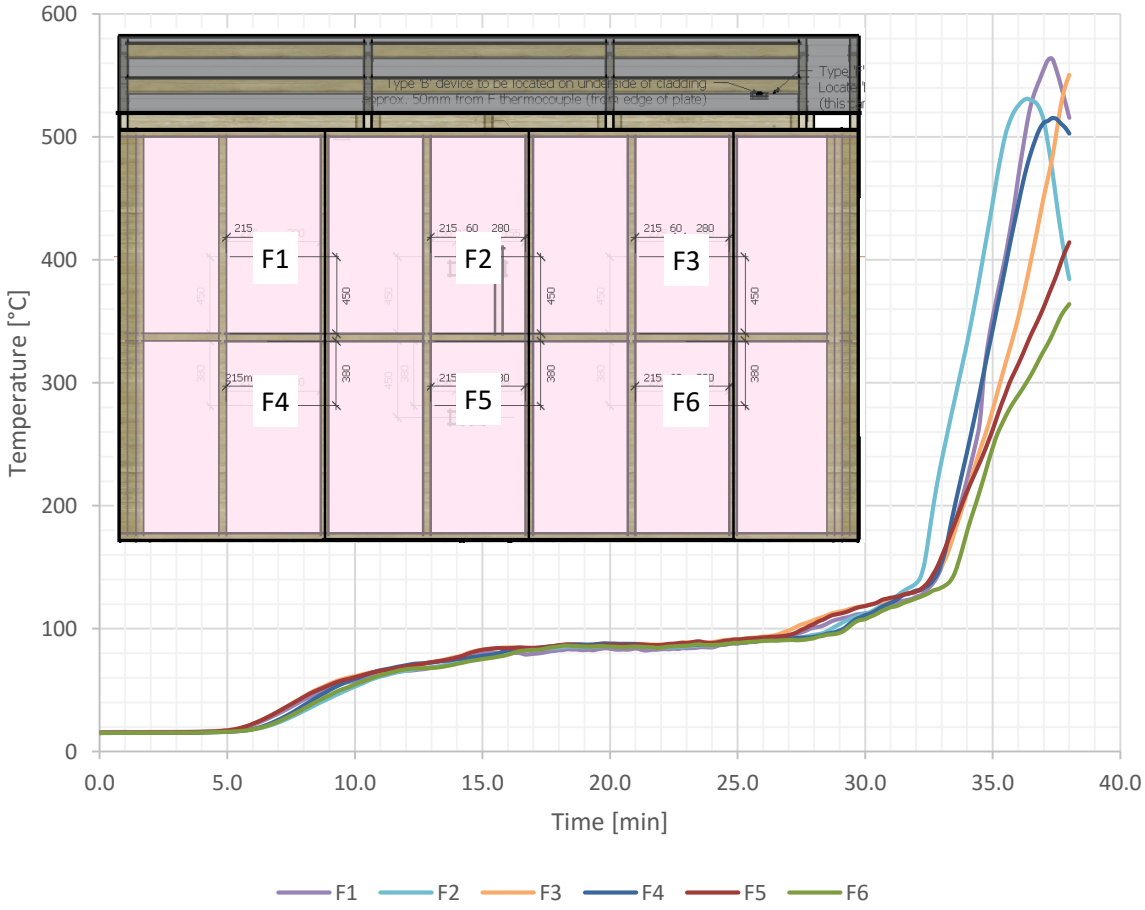

Figure 6-76 – Experiment #2 Fire-rated wall unexposed lining outside surface temperature

6.6.8 Fire-rated wall Lateral Performance

Figure 6-77 shows the deflection measurements for the fire-rated wall taken during the experiment. After about 12 min the 'fixed' and 'mid' walls start to deflect at a similar rate, the 'free' wall also starts to deflect at this time. Until about 25 min the wall deflection rate is reasonably linear, and at around 25 min there is a noticeable increase in the rate of the deflection across the length of the wall. The observations noted that at approximately 27.8 min the feet of the centre weight barrel rested on the ground. At approximately 28.5 min run-away deflection occurs at the fixed and middle intermediate trusses, while the free end wall continues to increase in deflection at a controlled rate. At 30.5 min the reference voltage was lost due to a suspected short circuit, readings after this time are not of use and the data has been truncated.

The deflections appear to be consistent with experimental observations as described in Section 6.6.1. These observations noted that deflection was most significant near the intermediate trusses, with the fire-rated truss end having a smaller deflection, and the fixed end having no notable deflection. Note that deflection at the fixed end was not measured.

The event of the centre barrel resting on the ground in the time leading up to the rapid deflection of the fire-rated wall will have influenced the time of failure. The effect of this is difficult to quantity and the rapid deflection of the fire-rated wall occurred very soon after the centre barrel rested on the ground, i.e. 27.8 min to 28.5 min, a time elapsed of less than 1 min. For the purposes of carrying out failure calculations in this report a failure time of 28 min has been used. This is considered reasonable and within the bounds of experimental uncertainty given the other uncontrolled variables in the experiment.

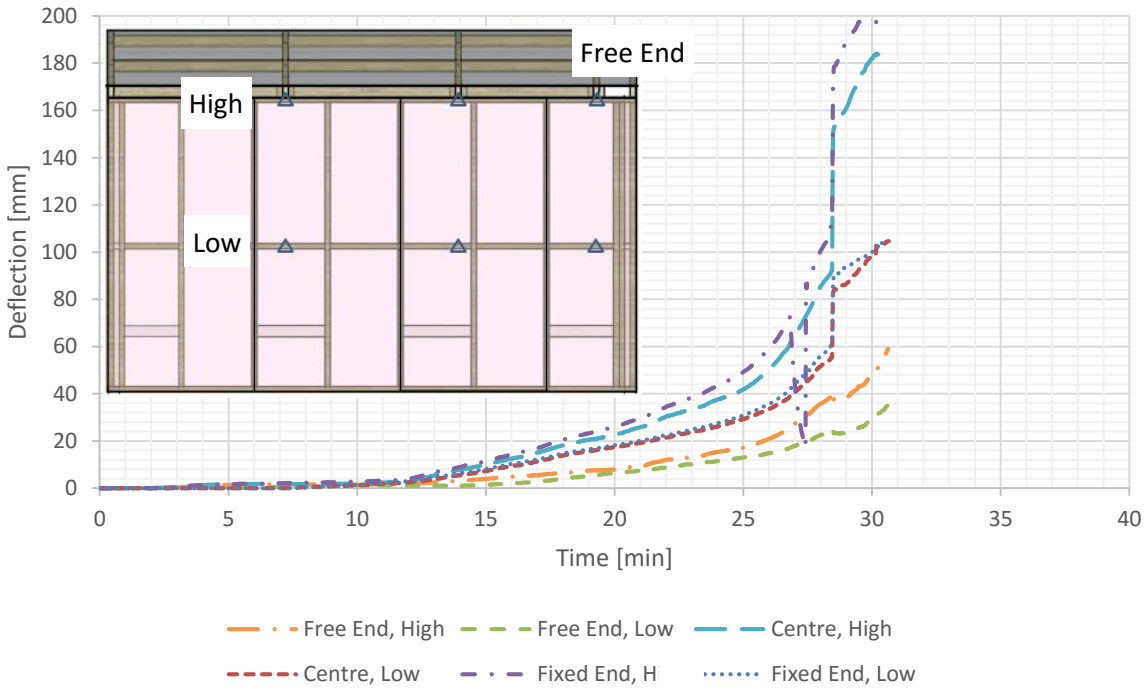

Figure 6-77 - Experiment #2 fire-rated wall deflection measurements

6.7 Analysis and Discussion

6.7.1 Mass Loss

Table 6-9 compares the B-RISK wood crib geometry with the experiment crib geometry. It can be seen that the existing BRANZ cribs used are similar to crib configuration B, except the height of the BRANZ cribs was 0.675 m compared to 0.59 m due to having 3 additional layers of sticks. The 'new' cribs used for Experiment #2 had a smaller stick size of 0.042 m compared to crib configuration B stick size of 0.045 m. The spacing was slightly greater at 0.08 m and the crib height was slightly taller at 0.59 m. The crib weight of the BRANZ cribs was 100 kg and the new cribs were 85 kg, the configuration B crib was calculated to have a weight of 82 kg.

Section 6.3.4 described the differences in upper layer and mass loss rate predictions using B-RISK for wood crib configurations A and B. It was found that the crib geometry made little difference during the fully developed phase, but became more important in the decay phase. This is explained by considering Babrauskas' crib mass loss rate calculation methodology described in Section 0, which requires the lowest of three calculated values to be used. For a fully developed fire constrained by ventilation, the room ventilation control (Equation 6-3) governs, and the crib mass loss rate is a function of the opening area and height of the compartment only. Noting that the fully developed phase of the compartment fire accounts for the period of highest fire severity and compartment temperatures, it is considered reasonable to compare the B-RISK predictions with experimental results, despite the slight differences in crib geometry.

Table 6-9 - Comparison of wood crib geometry used for preliminary compartment design with that used in Experiment #2

Parameter	A	B	New	Existing	
Width of stick of timber, D	0.05	0.045	0.042	0.045	m
Spacing between sticks, S	0.1	0.07	0.08	0.07	m
Number of sticks per layer, n	5	8	8	8	sticks
Width and length of crib	0.65	0.85	0.90	0.85	m
Number of layers of sticks	20	12	14	15	layers
Height of wood crib, h_c	1.0	0.54	0.59	0.675	m
Effective heat of combustion of wood	12				MJ/kg
Density of wood	497	497	550	500	kg/m^3
Mass per crib, m_0	81	82	85	100	kg
Number of cribs (rounded up)	6	6	4	2	cribs
Calculated FLED	401	408	450		MJ/m^2

Figure 6-78 shows a comparison of the total measured mass loss with the mass loss predicted by the B-RISK simulation for scenario 1B described in Section 6.3.4, the B-RISK result has been offset by 3 min to account for the slower initial fire growth in the experiment. The result shows that between 5 and 17 min the mass loss rate in the experiment was closely aligned with that predicted by the B-RISK simulation. Between 15 min and 17 there is an increasing rate in the mass loss rate observed during the experiment, this coincides with the observation of increased external flaming and quantity of smoke as described in Section 6.6.1. During the 5 to 15 min period of the experiment, the mass loss rate is approximately 0.23 kg/s. Following the aforementioned increase in mass loss rate between 15 and 17 min, the mass loss rate is approximately 0.32 kg/s between 17 and 29 min.

The B-RISK model predicted a plywood failure time of approximately 19.5 min, with the plywood failing open to 80% of its area over 5 min as described in Section 6.3.4. The mass loss rate in the B-RISK

simulation increases notably after approximately 20 min, this coincides with the predicted plywood failure. The B-RISK model uses the CRE method to predict failure of the plywood based on the failure time of plywood in Experiment 1 as previously described in Section 6.3.4, which followed the ISO 834 time-temperature fire. In Experiment #2, the plywood began to fail at approximately 25 min as described in Section 6.6.1. There is no significant notable increase in measured mass loss rate at this time.

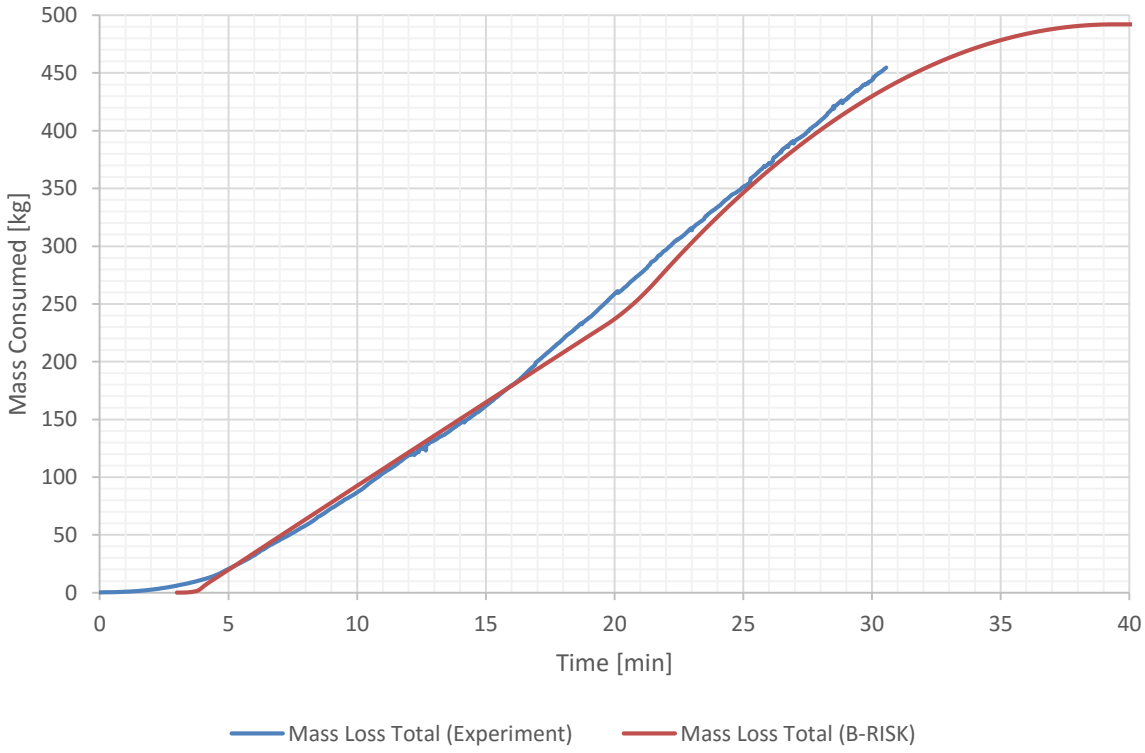

Figure 6-78 - Experiment #2 comparison of measured mass loss with prediction from B-RISK simulation, note that B-RISK result has been offset by 3 min to account for the slower initial fire growth in the experiment

6.7.2 Fire Severity and Time Equivalence

As described in Section 2.5 the fire severity experienced by building elements will be different in a 'real' compartment fire to those experienced in a standard fire furnace test. In addition to this, Figure 6-74 showed that the compartment temperature distribution was not uniform over the height of the compartment and therefore different elements in the compartment will have experienced different fire severity.

The Eurocode time equivalence method described in Section 2.5.4 is one way of relating compartment fire severity to standard furnace test. Four scenarios are considered for Experiment #2 based on a combination of two ventilation scenarios and two lining material scenarios. One ventilation scenario is based on a vertical vent area equal to initial window openings, area: 1.45 m^2. The second ventilation scenario is a vent area calculated from the area windows plus the area of plywood clad wall: 1.45 + 2.3 = 3.75 m^2. The two lining material scenarios considered were one with plasterboard ceiling and walls and one with a thin steel roof. For these two scenarios the Eurocode states k_b factors of 0.09 and 0.04 respectively.

The FLED calculated based on weight of fuel = 450 MJ/m^2 as described in Section 6.4.4 and the contribution of timber framing has been ignored. The results of this calculation using Equation 2-4 are

shown below in Table 6-10. The material modification factor k_m has been taken as 1.0 for all scenarios for a material that is not unprotected steel as described in Section 2.5.4. The compartment height is calculated as the stud height (2.42 m) plus half the height of the roof truss (0.54/2 = 0.27 m) and equates to 2.69 m.

Table 6-10 - Experiment #2 time equivalence calculation summary (Eurocode method)

	k_b = 0.09	k_b = 0.04
Initial openings only, A_v = 1.45 m^2	70 min	31 min
Initial openings plus plywood area as vent, A_v = 3.75 m^2	34 min	15 min

The maximum time equivalent value calculated is 70 min; this is based on the ventilation area being the initial window area only and the compartment linings being plasterboard wall and ceiling. The minimum calculated time equivalent value is 15 min; this is based on the ventilation area being the window area plus the plywood clad wall area fully open and the compartment ceiling/roof being thin steel. The actual time equivalence value for compartment experiment is expected to be between these bounding scenarios. It is acknowledged that this is a large range, and this highlights the significant effect the assumptions in regards to ventilation and bounding material properties have on the calculated time equivalence values using the Eurocode method.

To apply the CRE method the compartment gas temperatures are required. Figure 6-79 shows the average of the compartment temperature measurements compared to B-RISK prediction for scenario 1B and ISO 834 time-temperature curve. The B-RISK temperature predictions have been offset by 3 min due to the difference in initial fire growth rate. Although the mass loss prediction by B-RISK and the measured mass loss in the experiment were similar (refer Figure 6-78); the B-RISK simulation predicted higher compartment temperatures. There could be a number of reasons for this including:

- There was a slight but not insignificant cross-wind through the compartment, which may have increased the heat loss due to convection and also through the introduction of additional fresh cool air. The B-RISK simulation did not account for any cross-wind effects and assumed no outdoor wind.
- There was a brief period of overnight rain the night before the experiment, and it was noted that the floor of the compartment was slightly damp and the ceramic fibre protection to the load cell enclosures had absorbed significant amounts of moisture. The evaporation of this moisture may have kept temperatures lower than otherwise expected, and was not included in the B-RISK simulation.
- For the purposes of calculating heat transfer through walls, the B-RISK simulation implicitly assumes that internal wall and ceiling linings remain in place throughout the fire. In the experiment the wall and ceiling linings failed and exposed the cladding materials, which would be expected to change the heat loss characteristics from the compartment. In particular the metal roof and wall claddings would be expected to have a significantly higher heat transfer rate than plasterboard linings.
- The compartment was leaky with hot gases escaping from gaps at the roof ridge, gable ends, between roof and top plates of the wall. This additional leakage was ignored in B-RISK. The

compartment volume also effectively increased after failure of the ceiling which was also ignored.

The experiment compartment temperature was initially lower than the standard fire temperature, and after 4 min all thermocouples had exceeded the standard fire temperature. For the majority of the experiment the compartment temperature remains greater than the standard fire temperature curve, until reaching the decay phase. At approximately 32 min the experiment compartment temperature drops below the standard fire and remains below. There is one short period during which the temperature is below that of the standard fire, between 22 and 25 min.

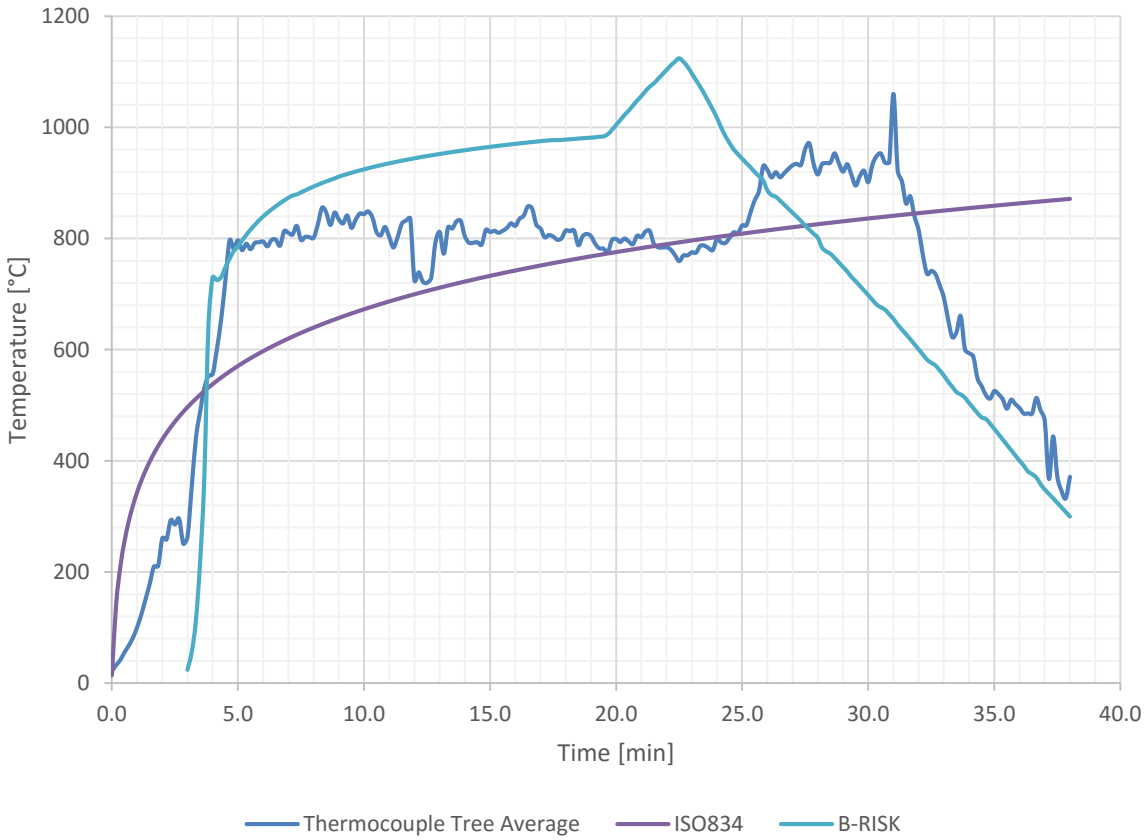

Figure 6-79 - Experiment #2 compartment temperature average measurements compared to B-RISK prediction for scenario 1B and ISO 834 time-temperature curve

Nyman's (2002) cumulative radiant energy (CRE) method for equivalent fire severity as described in Section 2.5.5 is applied to the results to estimate failure times had elements been exposed to the standard ISO fire. Figure 6-80 shows a comparison of the cumulative radiant energy (CRE) exposure using Equation 2-5 applied to the standard fire curve, the average thermocouple tree temperature measurements, and the B-RISK predicted upper layer temperature. The B-RISK CRE curve has been offset by 3 min, to account for the difference in initial fire growth between the model and the experiment as described earlier. The increase in fire severity at approximately 25 min due to failure of the plywood and the resulting additional ventilation can be seen in the CRE results, which shows that CRE rate increasing at this time.

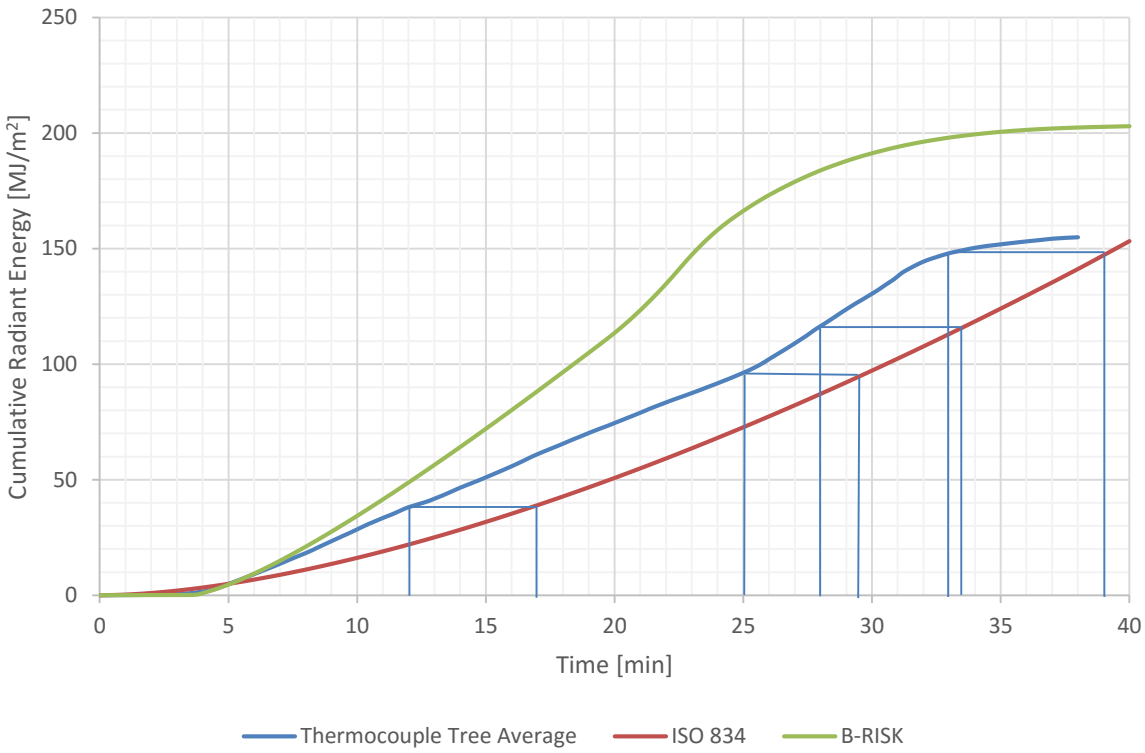

Figure 6-80 – Cumulative radiant energy comparison based on time temperature histories for ISO 834 fire, average compartment thermocouple tree measurement for Experiment #2, and B-RISK predicted upper layer temperature

By comparing the cumulative radiant energy at the time various elements failed, an assessment can be made of the equivalent failure time if exposed to standard fire conditions. Table 6-11 compares the observed failure times (column 2) of the ceiling lining, fire-rated wall insulation failure and the fire-rated wall lateral stability failure with predicted failure times if exposed to the standard fire using the CRE method (column 4). Also compared are the predicted failure times using the CRE method with compartment gas temperatures from the B-RISK modelling (described in Section 6.3.4) and observations from Experiment #1 (column 3). Note these values are offset by 3 min to account for the slower initial fire growth in the experiment as described earlier. It can be seen that the compartment fire temperatures and subsequently the CRE were more severe than the standard fire, and less severe than those predicted by the B-RISK modelling.

Table 6-11 – CRE time equivalence comparison for Experiment #2 failure times

Column	2	3	4
Element	**Experiment #2 observed time [min]**	**Failure predicted using B-RISK gas temperatures and results from Experiment #1 with CRE method [min]**	**Time Equivalent failure – Exposed to standard time-temperature [min]**
Ceiling lining	12	10	17
Plywood failure	25	17.5	29.5
Fire-rated wall lateral stability failure	28	18	33.5
Fire-rated wall insulation failure	33	Did not occur in Exp. #1	39

Applying the CRE to the performance of the laterally loaded fire-rated wall, that failed due to failure in the splice in the roof truss, suggests that if exposed to standard fire time-temperature curve the failure would have occurred at approximately 33.5 min. This is greater than the 30-min FRR required by C/AS1 Acceptable Solution. These results are compared to Experiment #1 results in Section 7.1.

6.7.3 Fire-rated Wall Performance

As described in Section 6.6.8 the fire-rated wall deflection steadily increased between 12 and 25 min, with the free end measuring less deflection than the fixed and centre measurements. From 25 min the rate of deflection increased at all wall locations, and was more pronounced at the fixed and centre locations. A run-away type of deflection was observed just after 28 min, and this coincided with an inwards roof collapse. The inwards roof collapse was caused by the failure of the trusses supporting the roof. The way in which the roof collapsed at the apex suggests that this failure was in the bottom chord of the trusses. Although there was clearly a failure of the lateral support to the fire-rated wall at this time, it is useful to investigate how this failure could be defined by a failure criteria.

AS 1530 Part 4 has failure criteria for axially loaded elements and vertically loaded elements as described in Section 2.4.3. As described in Section 5.5.3, using the AS 1530 Part 4 failure criteria may not be entirely appropriate for defining failure for laterally loaded external walls but it provides one means of comparing observed failure with a defined criteria.

Using Equation 2-1, the limiting deflection is calculated to be 160 mm, and using Equation 2-2 the limiting rate of deflection 7 mm/min. There was not sufficient allowable movement in the weighted drums to assess the limiting deflection. The limiting rate of deflection measured over 1 min intervals was exceeded at 25.5 min measured at the top plate at the fixed end truss (T2). Less than 0.25 min after this, the limiting rate of deflection of 7 mm/min was exceeded at the top plate at the centre truss (T3). The free end truss (T4) deflection measurement exceeded the limiting rate after approximately 27.25 min. This calculated failure time is slightly less than the observed failure time of 28 min as described in Section 6.6.1 and Section 6.6.8.

As described in Section 6.6.7, the fire-rated wall did not fail the AS 1530 Part 4 criteria for insulation failure until after 33.5 min; after the time the wall failed to remain upright due to the applied lateral load. The insulation failure of the fire-rated wall is not the subject of this research, beyond noting that it exceeded the performance of the lateral stability of the wall and its support system.

6.7.4 Truss Performance

The failure mode of the trusses was not able to be visually confirmed due to severely degraded state of the building elements at completion of experiment. Roof collapse and truss failure occurred, but whether this was at the splice or elsewhere in the bottom chord of the truss was unclear from experimental observation alone. An analysis of the failure sequence is performed by comparing the observed behaviour with estimates of the residual capacity of the structural system by examining charring rates of the bottom chords of the trusses.

As discussed in Section 6.2.3, the lateral load and truss layout for Experiment #2 was consistent with Experiment #1. Section 5.5.4 showed calculations for the tensile stress, strain and elongation in each truss in the cold design condition and these results are restated below in Table 6-12 for ease of reference.

Table 6-12 – Calculation of tensile load, stress, strain and elongation for each truss in cold design condition

	Proportion of load being carried						
Member	W1	W2	W3	Tensile Load [N]	Stress [$\times 10^5$ Pa]	Strain [$\times 10^{-5}$ mm/mm]	Elongation [mm]
T2	0.49	0.50	0.0	855	2.11	2.64	0.09
T3	0.0	0.50	0.35	738	1.82	2.28	0.08
T4	0.0	0.0	0.65	561	1.39	1.73	0.06

A char rate of 1.7 mm/min as described in Section 6.6.6 can be used to calculate an expected residual cross-section area for a truss member at the time the fire-rated wall failed due to the lateral load. The results of these calculations are shown in Table 6-13 based on an assumption of even charring on four sides of the member and includes corner rounding effects. The calculations show that based on the nominal 1.7 mm/min charring rate; a 90 mm × 45 mm timber member would be expected to have no residual cross-sectional area after 13 min. In the experiment, the roof trusses were estimated to be exposed for 16 min before failing, based on the ceiling failing at 12 min and the rapid deflection of the fire-rated wall occurring at 28 min.

Table 6-13 – Experiment #2 estimated char depths

Char rate	1.7	mm/min
Fire exposure time	16	min
Depth of char	27.2	mm
Depth remaining	35.6	mm
Width remaining	-9.4	mm
Rectangular area remaining	-335	mm^2
Area lost due to corner rounding	159	mm^2
Cross section area remaining fire exposure	-494	mm^2
Time to reach zero cross-sectional area	13	min

An analysis of failure is carried out based on a hypothesis that the nail plate connection was sufficiently protected such that the failure of the bottom chord of the truss occurred at a location other than the splice. The time to reach the minimum residual cross section area in the truss was calculated using NZS 3603 charring rate, the charring rate from Experiment #1 and Experiment #2 dummy chord thermocouple measurements. Table 6-14 shows a summary of these calculations.

Table 6-14 – Summary of minimum required cross-section area for each truss and time to reach these based on char rates

		Time to reach minimum cross section area [min]			Experiment #2 roof truss time exposed before observed failure [min]
Truss	Minimum section area to carry load [mm^2]	NZS 3603 charring	Using charring rate calculated from Experiment 2 dummy chord	Using charring rate calculated from Experiment 1 dummy chord	
T2	143	31	12	19	16
T3	123	31	12	19	
T4	94	32	12	19	

The predicted time to reach the minimum section area with sufficient capacity for the applied load is 12 min based on the Experiment #2 charring rate of 1.7 mm/min, which is less than the observed failure time of 16 min. This may suggest that the char rate is over-predicted in the analysis of dummy chord results. This char rate was based on the time for thermocouples 11 mm from the surface of the

dummy chord to reach 300°C as described in Section 6.6.6. It is not unreasonable that the char rate may have been over-predicted given that char itself forms a protective layer on the timber which reduces the charring rate below the surface as described in Section 4.3.3. Charring rate is also a function of timber density as described in Section 4.3.4 and this introduces further uncertainty given the expected variation in light timber framing.

The predicted time to reach the minimum section area based on the Experiment #1 char rate of 1.1 mm/min is 19 min. This is close to the observed failure time of 16 min, but may be coincidental rather than significant given the difference in fire exposure as described in Section 6.7.2.

The NZS 3603:1993 charring rate is 0.65 mm/min and results in a much slower rate of reduction in section area compared to the 1.1 mm/min and 1.7 mm/min charring rates based on results from Experiments #1 and #2 respectively. The time to reach the critical section area is predicted to be 31 min for truss T2. The NZS 3603:1993 charring rate is based on heavy timber with minimum 100 mm × 100 mm section dimensions, and relies on a 25 mm protective char layer being developed as previously discussed in Section 4.3.4.

The elongation in the cold condition and at the minimum residual cross-section area are calculated. These are compared to the observed deflection of the fire-rated wall in Table 6-15. It can be seen that the measured deflection at the top plate of the fire-rated wall was greater than the calculated elongation in the truss before ceiling failure and any significant charring had occurred, and significantly greater 15 min into the experiment, i.e. 3 min after ceiling failure.

Table 6-15 - Experiment #2 Summary of elongation of truss members and deflection of fire-rated wall

	Calculated Elongation [mm]		Measured deflection [mm] at various experiment times (time since ceiling failure in brackets)					
Truss	Cold	Min. residual section	10 min (-2 min)	12 min (0 min)	15 min (3 min)	20 min (8 min)	25 min (13 min)	28 min (16 min)
T2	0.09	2.5	2.8	4	12	26	49	101
T3	0.08		2.0	3	10	23	42	85
T4	0.06		1.6	2	4	8	17	36

Deflection is largest at the fixed end truss (T2), closely followed by the centre truss (T3), and the free end truss (T4) exhibits significantly less deflection than T2 and T3. Assuming the cross-section area of the trusses is comparably similar to one another during the experiment, a reason for the difference in measured deflection at each point could be due to difference in elongation in each truss. As described previously, the elongation is proportional to the load applied. The measured deflection at each truss at 28 min from Table 6-15 is divided by the load carried by that truss taken from Table 6-12. The resulting ratio is 0.12 for both T2 and T3, and 0.06 for T4. The significant difference between trusses T2/T3 and T4 suggests that there may have been contribution to deflection of the fire-rated wall other than due to truss elongation.

The results show that there was likely to be insufficient cross-sectional area of unaffected timber to support the lateral load being applied to the fire-rated wall at the time of failure. Failure of the bottom chord of the roof truss could have been one reason for lateral failure of the fire-rated wall. However the measured deflections being much greater than the timber elongation are not conducive to brittle timber behaviour and suggests that there were one or more other mechanisms providing support to

the fire-rated wall that failed in a ductile manner. Elongation is unlikely to be a significant contributor to fire-rated wall deflection. There are a number of possible contributing factors that could result in load sharing and the ductile behaviour observed and evident in the measured results. These include:

- There may have been ductile behaviour in the protected splice / nail plate connection. The blocking itself would have provided some limited contribution to the tensile strength of the spliced connection. There may have been some ductile behaviour/elongation occurring due to yielding of nails of the protective blocking and some slippage in the nail plate connection itself.
- Both the non-rated long wall and the fire-rated wall top plates will have been bowing to some extent due to the lateral load. The top plates of the walls both will have degraded due to fire exposure, and the extent of this is unknown. For the fire-rated wall this bowing would be expected to have a maximum deflection at the drum fixing locations and the least deflection at the truss fixing points and the fixed end wall. For the non-rated long wall, the deflection may be a maximum somewhere near the middle of the length of the wall and would be negligible at the end walls. This seems less likely given the brittle behaviour of timber as described in Section 4.3.2 and relatively small associated deflections.
- Slip between framing connections would contribute to deflection of the fire-rated wall. This for example may have occurred at the connection between the bottom chord of trusses and the top plate of walls. These effects have not been quantified.
- As previously described in Section 5.2.4 there is a roof bracing element consisting of a metal strap fixed to the four corners of the compartment, effectively pulling the roof down onto the wall and also applying a load to pull the walls inward toward the compartment. This strapping may have contributed to some load sharing although this seems less likely.

It could be that one or more of these factors contribute to the behaviour observed. These are all areas which cannot be answered from this research.

6.7.5 Performance of an Unlined Compartment

The expected performance of an unlined compartment is predicted by applying the CRE method to the results from Experiment #2. A CRE value is calculated from the compartment temperature measurements recorded between the time of ceiling failure and the time of bottom chord failure, starting with a value of 0 MJ/m^2 at the time of ceiling failure. The calculated CRE value is compared to the CRE curve the of ISO 834 time-temperature curve from time 0 min. The predicted time of failure is the time when the CRE of the ISO 834 time-temperature equals the CRE value calculated from the compartment temperature measurements. The effects of pre-heating the bottom chord and other structure members before the ceiling failed are ignored. Similarly, any differences in char rate due to different furnace gas temperature is not taken into account.

The ceiling failed at 12 min in the experiment, and the roof truss system supporting the fire-rated wall failed at 28 min. The cumulative radiant energy for this 16 min period based on the thermocouple tree temperature measurements is calculated to be 77.9 MJ/m^2. The ISO time-temperature curve takes 26 min to reach this same CRE, as shown in Figure 6-81. The calculated stability failure time for the laterally loaded wall in an unlined building configured as in Experiment #2 is approximately 26 min if exposed to the standard fire time-temperature heating regime.

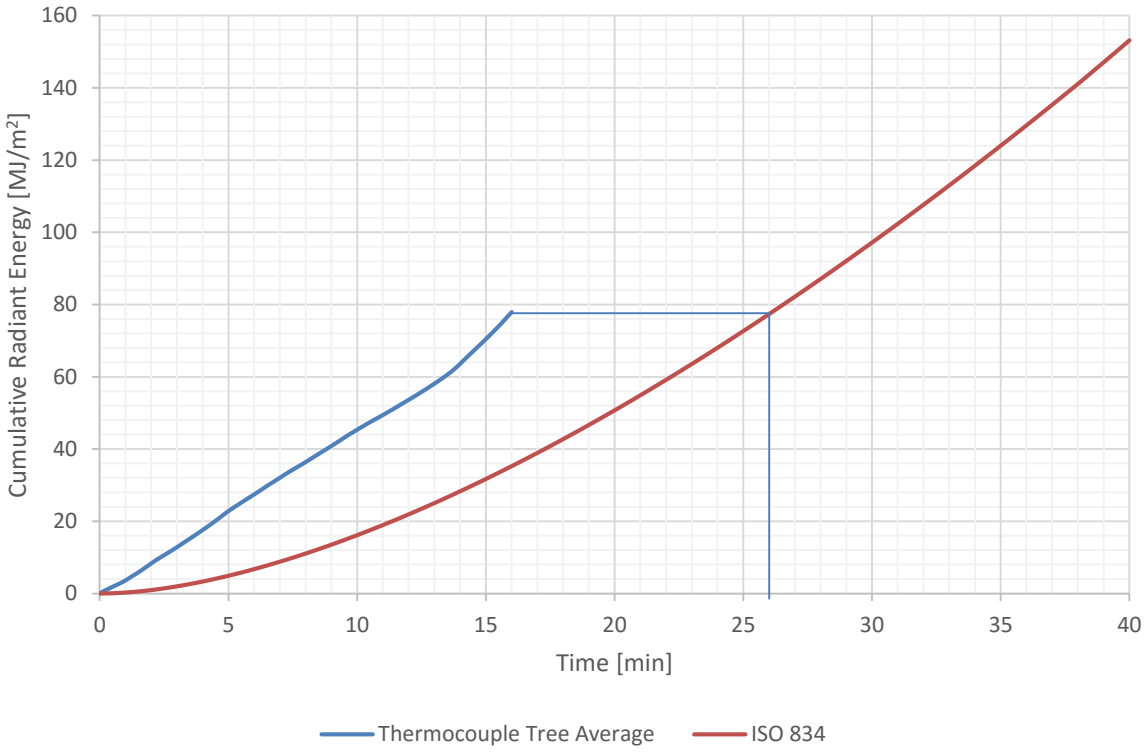

Figure 6-81 - Experiment #2 CRE from time of ceiling failure to time of wall stability failure compared to standard fire CRE

6.8 Experiment #2 Summary

A compartment experiment was carried out on a laterally loaded light timber-framed compartment with a fuel load of approximately 450 MJ/m^2 and an initial ventilation opening area of 1.45 m^2. There was a plywood element in the cladding system that progressively failed from 25 min, resulting in an increase in ventilation. The ceiling system lined with 10 mm standard plasterboard provided a level of protection to the roof truss system in the experiment until failure at 12 min.

The bottom chord of the roof truss failed in tension after 28 min in the experiment, this was 16 min after the ceiling failed. An analysis of the observed failure time applying the criteria specified in AS 1530 Part 4 for limiting rate of deflection suggests that some parts of the wall may have failed the limiting rate of deflection criteria slightly earlier than the observed failure time. A failure time of between 25.5 and 27.25 min was calculated using the criteria of AS 1530 Part 4.

The fire severity in the compartment was calculated as being more severe than the standard fire time-temperature curve for the 28 min, with this failure time equating to a failure time of 33.5 min in the standard fire. The results suggest a protected spliced connection in a truss protected behind standard plasterboard 10 mm ceiling system may provide sufficient restraint to achieve a 30 min FRR when supporting an external fire-rated wall laterally loaded to NZBC B1/VM1 0.5 kPa load requirement.

The bottom chord of the truss appears to have maintained sufficient section area to carry the required load longer than the time predicted based on the char rate measured in the dummy chord of 1.7 mm/min. It could be that there was load sharing occurring and the lateral load was being

supported by contributions from the roof bracing, the fixed wall and possibly the roofing itself. The effects of these are difficult to quantify and would need to be studied individually.

The expected performance of an unlined compartment was predicted by applying the CRE method to the results from the Experiment. The CRE based on furnace temperature from the time of ceiling failure (12 min) to the time of bottom chord failure (28 min) is compared to the CRE of ISO 834 time-temperature curve. The calculated stability failure time for the laterally loaded wall in an unlined building configured as in Experiment #2 is approximately 26 min if exposed to the standard fire time-temperature heating regime.

7 Summary

7.1 Experiment Analysis

Table 7-1 compares failure times of the ceiling lining, fire-rated wall insulation failure as defined in AS 1530 Part 4, and the fire-rated wall stability failure for Experiment #1 and #2. Also shown are equivalent times of failure calculated using the CRE method and the expected performance of an unlined compartment.

For Experiment #1 the bottom chord of the roof truss failed at the spliced connection in tension after 30.5 min in the experiment, this was 14.5 min after the ceiling failed. The observed failure time of 30.5 min is equated using the CRE method to a failure time of 26 min if the furnace had been driven using plate thermometers located at ceiling height level and following the ISO 834 time-temperature curve. The CRE based on furnace temperature from the time of ceiling failure (16 min) to the time of bottom chord failure (30.5 min) is compared to the CRE of ISO 834 time-temperature curve. The calculated stability failure time for the laterally loaded wall in an unlined building configured as in Experiment #1 is approximately 19.5 min if exposed to the standard fire time-temperature heating regime.

For Experiment #2 the bottom chord of the roof truss failed in tension after 28 min in the experiment, this was 16 min after the ceiling failed. The fire severity in the compartment was calculated as being more severe than the standard fire time-temperature curve for the 28 min, with the Experiment #2 failure time equating to a failure time of 33.5 min in the standard fire. The calculated stability failure time for the laterally loaded wall in an unlined building configured as in Experiment #2 is approximately 26 min if exposed to the standard fire time-temperature heating regime.

Table 7-1 – Comparison of experiment failure times, observed and predicted, all times in min

		Ceiling lining failure	**Fire-rated wall insulation failure**	**Fire-rated wall stability failure**
Exp. #1	Observed	16	Did not occur	30.5
	Predicted using CRE based on exposure to standard time-temperature at ceiling	14		26
	Unlined compartment, predicted using CRE applied to results from Experiment #1 and standard fire time-temperature	N/A		19.5
Exp. #2	Observed	12	33	28
	Predicted using CRE applied to gas temperatures from B-RISK model and results from Experiment #1	10	Not calculated	18
	Time Equivalent failure – Exposed to standard time-temperature	17	39	33.5
	Unlined compartment, predicted using CRE applied to results from Experiment #2 and standard fire time-temperature	N/A		26

Comparing the results and analysis for Experiment #1 and #2 it can be seen that protecting the splice in the bottom chord of the roof truss has improved the stability performance of the laterally loaded fire-rated wall restraint system. Based on a CRE comparison to the ISO 834 time-temperature curve the time of lateral stability failure increases from 26 min to 33.5 min from Experiment #1 to Experiment #2. The performance of an unlined compartment was also predicted, and for Experiment #1 a stability failure time for the fire-rated wall of 19.5 min was predicted, and 26 min for the Experiment #2 compartment.

A dummy chord was used to record temperatures at various depths in a timber member. For Experiment #1 an analysis of the results of the dummy chord temperatures determined a charring rate of 1.2 mm/min for timber behind the nail-plate, and 1.1 mm/min for timber not behind a nail plate. For Experiment #2 an average char rate of 1.7 mm/min was calculated based on results from the dummy chord. An analysis of the tensile load in each truss bottom chord member was carried out, and the expected elongation for both cold and fire conditions. The fire condition elongation was based on the residual cross-section area of truss, calculated from the depth of char in each experiment.

Table 7-2 shows a summary of the calculated minimum required cross-section area for each truss to resist the applied lateral load. Note that this excludes the effects of the toothed nail plate. The time for the bottom chord of each truss to reach these residual section areas was calculated for each experiment based on dummy chord charring rates, and is compared to the observed failure times.

Table 7-2 – Summary of minimum required cross-section area for each truss and predicted and observed failure times

Truss	Minimum section area to carry load [mm^2]	Time to reach minimum cross section area [min]		Experiment #1 truss time of direct fire exposure before failure [min]	Experiment #2 truss time of direct fire exposure before failure [min]
		Using charring rate calculated from Experiment 1 dummy chord	Using charring rate calculated from Experiment 2 dummy chord		
T2	143	19	12	14.5	16
T3	123	19	12		
T4	94	19	12		

For Experiment #1 the results show that there was likely to be sufficient cross-sectional area of unaffected timber to support the lateral load being applied to the fire-rated wall; a predicted failure time of 19 min is compared to the actual failure time of 14.5 min. It is not unreasonable that the nail plate failed earlier than the timber member would have expected to fail, and this is consistent with the experiment observations. Without the splice in the roof truss system, it is expected that for Experiment #1 the wall would have been sufficiently restrained for an estimated additional 4 min. An adequately protected splice could also be designed to achieve sufficient restraint for this additional time, such that the failure occurs due to charring of timber away from the splice.

For Experiment #2 the bottom chord of the truss appears to have maintained sufficient section area to carry the required load longer than the time predicted based on the char rate measured in the dummy chord of 1.7 mm/min. The predicted failure time based on a charring rate determined from the dummy chord was 12 min of direct fire exposure and the actual failure time was 16 min of direct fire exposure. It could be assumed that load sharing occurred and the lateral load was being supported

by contributions from the fixed wall, roof bracing and possibly the roofing itself. The effects of these are difficult to quantify and would need to be studied separately.

There was a noticeable difference in behaviour between the first and second experiments. The first had a sudden failure of the fire-rated wall, representative of brittle behaviour, the second had large deflections that occurred slowly before sudden failure, exhibiting ductile behaviour. Elongation of the truss bottom chord is unlikely to be a significant contributor to fire-rated wall deflection. There are a number of possible contributing factors that could result in load sharing and the ductile behaviour observed and evident in the measured results:

- There may have been ductile behaviour in the protected splice / nail plate connection. The blocking itself would have provided some limited contribution to the tensile strength of the spliced connection. There may have been some ductile behaviour/elongation occurring due to yielding of nails of the protective blocking and some slippage in the nail plate connection itself.
- Both the non-rated long wall and the fire-rated wall top plates will have been bowing to some extent due to the lateral load. The top plates of the walls both will have degraded due to fire exposure, and the extent of this is unknown. For the fire-rated wall this bowing would be expected to have a maximum deflection at the drum fixing locations and the least deflection at the truss fixing points and the fixed end wall. For the non-rated long wall, the deflection may be a maximum somewhere near the middle of the length of the wall and would be negligible at the end walls. This seems less likely given the brittle behaviour of timber as described in Section 4.3.2 and relatively small associated deflections.
- Slip between framing connections would contribute to deflection of the fire-rated wall. This for example may have occurred at the connection between the bottom chord of trusses and the top plate of walls. These effects have not been quantified.
- As previously described in Section 5.2.4 there is a roof bracing element consisting of a metal strap fixed to the four corners of the compartment, effectively pulling the roof down onto the wall and also applying a load to pull the walls inward toward the compartment. This strapping may have contributed to some load sharing although this seems less likely.

7.2 Conclusion

An experimental investigation of the fire performance of laterally loaded light timber-framed compartments was carried out. Performance has been assessed for a fire-rated wall laterally restrained by a roof truss system spanning between the fire-rated wall and non-rated wall. The equivalent of a 0.5 kPa lateral load was applied to the fire-rated wall.

The toothed nail plate connector and wire dog splice connection system in the bottom chord providing lateral restraint to the fire-rated wall was found to perform better than predicted. This is based on the observed performance in comparison to a calculated performance using the assumption that failure occurs when the depth of char exceeds the depth of the teeth embedded into the timber. It is expected that the contribution of wire dogs is significant in the tensile performance of the splice connection. It was found the performance of the spliced connection was less than that would be predicted for a non-spliced connection. The performance of a spliced connection was significantly improved by protecting with solid timber blocking nailed to the truss. The bracing capacity of the 0.35 mm thick mild steel cladding was found to be sufficient in both experiments, however the bracing performance of other cladding systems in fire was not determined.

The char rates found in the experiment were greater than those commonly used for heavy timber, such as the 0.65 mm/min given in NZS 3603:1993. This is not unexpected given the small cross-section does not have sufficient material to build up a 25 mm thick protective layer. For Experiment #1 charring rates were found to be 1.2 mm/min for timber behind the nail-plate, and 1.1 mm/min for timber not behind a nail plate. The 1.1 mm/min char rate was found to be reasonably consistent with depth of char measurements taken from cuts of timber after the experiment. The nail plate was found to increase the charring rate of timber behind it. For Experiment #2 the charring rate was found to be 1.7 mm/min. The different charring rates found in Experiment #1 and #2 suggest that the compartment temperatures have a significant effect on charring rates for light timber-frame members.

The B-RISK model provided a reasonable prediction of mass loss rate using the Babrauskas wood crib equations, particularly during the fully developed post-flashover phase before the plywood cladding failed and resulted in additional ventilation. After the plywood vent opened up in the B-RISK model, the rate of mass loss predicted was slightly faster than that measured. The fire growth rate used for centre ignited cribs based on equations given by Babrauskas (2002) significantly over-predicted the fire growth rate (mass loss rate) compared to the experimental results.

The B-RISK model tended to over predict compartment temperatures. There were a number of effects in the experiment that were not captured in the model that will have contributed to this. For example ambient conditions leading up to and during the experiment that included rainfall and cross-wind effects respectively. The B-RISK model also assumed the plasterboard wall and ceiling linings remain in place, whereas in the experiment these failed exposing steel roofing and other wall cladding. This would influence the rate of heat loss from the compartment. The compartment was also leaky after ceiling failure with hot gases escaping from gaps at the roof ridge, gable ends and between roof and top plates of the wall. This additional leakage of hot gases was ignored in B-RISK and therefore increased the compartment temperatures predicted in the model.

The cumulative radiant energy method was used to calculate a standard fire equivalent time of failure for the plasterboard ceiling using the observed failure time in Experiment #2. This predicted failure time was 17 min and compares closely to the failure time in the Experiment #1 standard fire furnace experiment of 16 min. The CRE was also used to calculate the expected lateral stability performance of a fire-rated wall laterally restrained by a roof truss system with a protected splice. Because the spliced connection configuration was different in Experiment #1 and #2, the accuracy of this prediction cannot be assessed.

In the furnace experiment the compartment was heated to the standard time-temperature curve. It was found there was non-uniform temperature distribution in the compartment, with the temperatures being lower toward the top of the compartment. This occurred due to greater heat losses from the walls and roof of the enclosure and because the furnace gas thermocouples were located below notional floor level, closer to the location of the gas burners. The standard AS 1530 Part 4 does not envisage a test on a full-sized compartment such as this and if similar experiments were carried out in the future then there should be additional consideration given for where the furnace thermocouples are located and how the furnace is driven.

AS 1530 Part 4 provides failure criteria for a vertically loaded element in bending such as a beam or floor system. The rate of deflection failure criteria for vertically loaded elements was applied to the experiment results and compared to observations of stability failure of the fire-rated wall. The rate of deflection criteria compared favourably to the experiment observations and appeared to be a reasonable way of assessing failure of the wall. The failure criteria worked better for Experiment #1 in which the deflections leading up to failure were relatively small, and the roof truss failure mechanism resulted in runaway deflection. The absolute failure criteria of AS 1530 Part 4 was not compared as the lateral load setup did not allow for sufficient deflection to assess this.

Based on the experimental results, a small timber-framed compartment with 10 mm standard plasterboard linings and a suitable roof truss structure providing lateral support to a fire-rated wall could be designed to achieve stability for a 30-min FRR equivalent duration. This can be achieved without the need for providing moment-resisting fixity at the connection between the studs and bottom plate of the fire-rated wall. An unlined compartment of otherwise similar construction and lateral load configuration is unlikely to achieve a nominal 30-min FRR.

7.3 Limitations

The results of this research are specific to the experiments undertaken and this work had certain characteristics which may have an effect on the results. These include construction details and other building configurations for which the effect on performance has not been assessed. Examples include:

- The ceiling system had no penetrations; any non-fire-rated penetrations may allow fire spread into the roof cavity at an earlier stage and cause an earlier failure of the roof truss system.
- The lateral load was applied parallel to the direction of the trusses that provided lateral restraint to the fire-rated wall. The research has not assessed if the lateral load had been applied to a gable end wall. This is quite a different loading scenario as the bottom chord of trusses can no longer be relied on to restrain the wall, instead there would be a load in the direction of the roof purlins. This scenario would likely produce quite different results.
- A pushing load would impose a compression load on the bottom chord of the roof truss system and its performance is expected to be worse in compression than tension. However it is worth noting that in compression there would be support provided by both end walls, and the distance between these walls would be important for this scenario.
- Only one cladding system was used on the end walls (thin metal sheeting). End wall bracing performance is likely to be sufficient for metal clad systems provided cladding remains fixed in place. It was noted that in the experiment the steel sheeting remained intact longer than the plywood, plasterboard and fibre cement cladding systems on the non-rated long wall. Performance of other cladding systems for providing bracing during fire is unknown.

The cumulative radiant energy method has been used throughout the analysis to compare the observed failure times with expected failure times of various building configurations exposed to the ISO 834 standard time-temperature curve. The CRE method of equivalent fire severity has been well researched for predicting insulation and integrity failure of plasterboard linings on light timber-framed walls. The suitability of this method for assessing the performance of timber and structural performance of roof truss is largely unknown and this introduces a level of uncertainty.

There was a noticeable difference in behaviour between the first and second experiments. The first had a sudden failure of the fire-rated wall, representative of brittle behaviour and sudden loss of stability, the second had large deflections that occurred slowly before sudden failure, exhibiting ductile behaviour. More research is required for establishing failure mechanisms with protected trusses, contribution of other members, load sharing, different building geometry, and ventilation and fuel configurations. The results of this research are specific to the experiments undertaken.

7.4 Further Research

There are two distinct and related main parts to research into the lateral stability of light timber-framed compartments. One is the performance requirements / acceptance criteria and the other is the building performance. The key areas for further research that were identified during this research predominantly relate to the context of the performance requirements and how these should be applied to common residential light timber-framed buildings.

In regards to building performance, further research is required for establishing failure mechanisms with protected trusses, contribution of other members, load sharing, different building geometry, and ventilation and fuel configurations. The scenario where a load is applied to a gable-end wall needs specific consideration as it is distinctly different from the scenario that this research investigated. The suitability of the cumulative radiant energy method for equating fire severity experienced by timber members in charring should be investigated. Further research is needed for suitable char rates for light timber-frame members directly exposed to compartment fires.

There is scope to improve prediction of fire growth rates in wood cribs. The equations used in this research over-predicted the fire growth rate. Further research should be carried out in applying zone models (e.g. B-RISK) to compartments in which progressive failure of wall linings and also cladding occurs. There is likely to be opportunities to improve the model if changing thermal properties for bounding surfaces of the compartment can be taken into account.

Furnace testing of full-scale compartments appears to be feasible, however there needs to be consideration for non-uniform temperature distribution in the compartment. Current test standards (e.g. AS 1530 Part 4) do not consider such a test specimen configuration. A method for driving furnaces and assessing performance of construction elements in the specimen given these non-uniform temperature conditions could be investigated.

The performance requirements for stability of structural elements in fire need to be clarified. There appears to be inconsistency between NZBC Clause B performance criteria which requires all structural elements to be stable during and after fire, and the Clause C performance criteria which require only fire rated primary elements and those which support them to remain stable. There are also conflicting design assumptions. In NZ fire-rated walls in residential buildings may not be the most conservative and the performance criteria in Clause C3 for prevention of horizontal spread of fire implicitly recognises that there may need to be Fire Service intervention to prevent horizontal fire spread in some instances. In the same Building Code regulatory requirements, a fire-rated wall in a light timber-framed building is seemingly required to remain stable and serviceable ‘after-fire’ by Clause B1.

The test for stability is unclear and may be unduly onerous for a light timber-framed building. A 0.5 kPa lateral load equates to a 100 km/h wind and approximately 2 times the self-weight of a typical light timber-framed wall. Perhaps more importantly, the purpose of applying this lateral load and after-fire stability is unclear. The protection of firefighters is important, however it should be clearly noted that light timber-framed residential buildings more than 1 m from a property boundary need not have any fire-rated elements and seemingly collapse is permitted under the NZBC Clause C requirements. Prevention of collapse onto other property is another argument for providing stability of fire-rated walls, however in this case it would seem reasonable to permit inwards collapse. The risk associated with timber-framed building collapse seems to require further consideration.

8 References

Babrauskas, V. (1979). *COMPF2: A Program for Calculating Post-Flashover Fire Temperatures* (Technical Note No. NBS TN 991) (p. 76). Springfield, VA 22161: National Technical Information Service (NTIS), Technology Administration, U.S. Department of Commerce.

Babrauskas, V. (2002). *Heat Release Rates, Section 3/Chapter 1, in the SFPE handbook of fire protection engineering* (3rd ed.). Quincy, Mass. : Bethesda, MD: National Fire Protection Association ; Society of Fire Protection Engineers.

Barnett, C. R. (2007). A New T-equivalent Method for Fire Rated Wall Constructions using Cumulative Radiation Energy. *Journal of Fire Protection Engineering*, *17*, p113–127.

Barnett, C. R., & Wade, C. A. (2002). A Regulatory Approach to Determining Fire Separation between Buildings based on the Limiting Distance Method. In *Paper presented, 4th International Conference on Performance Based Codes and Fire Safety Design Methods*. Melbourne, Australia.

Blackmore, J., Brescianini, C., Collins, G., Delichatsios, M. A., Everingham, G., Hooke, J., Ralph, R., Thomas, I., Beever, P. (1999). *Fire Code Reform Centre, Project 3: Fire Resistance and Non Combustibility, Part 3: Room and Furnace Tests of Fire Rated Construction*. NSW, Australia: Fire Code Reform Centre Ltd ; CSIRO Division of Building, Construction and Engineering.

BSI. (1987). BS 476: Parts 20-24, Fire Tests on Building Materials and Structures. British Standards Institution, United Kingdom.

BSI. (2004). BS EN 520:2004 Gypsum plasterboards – Definitions, requirements and test methods. European Committee for Standardization.

BSI. (2012). BS EN 1363-1:2012 Fire resistance tests. General requirements. British Standards Institution, United Kingdom.

Buchanan, A. H. (2001). *Structural design for fire safety*. Chichester, England ; New York: Wiley.

Buchanan, A. H. (2008). The Challenges of Predicting Structural Performance in Fires. *Fire Safety Science*, *9*, 79–90.

CEN. (1999). EN 1364-1:1999 Fire resistance tests for non-loadbearing elements. Walls. British Standards Institution, United Kingdom.

CEN. (2002). Eurocode 1: Actions on Structures - Part 1-2: General Actions - Actions on structures exposed to fire, European standard EN 1991-1-2.

CEN. (2004). EN 1995-1-2:2004, Eurocode 5. Design of timber structures – Part 1-2: General – Structural fire design. British Standards Institution, United Kingdom.

CIB. (1986). Design Guide - Structural Fire Safety, CIB-W14. *Fire Safety Journal*, *No. 10*(No. 2), p75–p138.

Collier, P. (1996). A model for predicting the fire-resisting performance of small-scale cavity walls in realistic fires. *Fire Technology*, *32*(2), 120–136.

Collier, P. C. R. (1992). *Charring Rates of Timber* (Study Report No. 42). Porirua, New Zealand: Building Research Association of New Zealand.

Collier, P. C. R. (2000). *Fire Resistance of Lightweight Framed Construction, Fire Engineering Research Report 00/2*. Department of Civil Engineering, University of Canterbury, Christchurch, New Zealand.

Cote, A. E., Hall, J. R., Powell, P., Grant, C. C., Solomon, R. E. (Eds.). (2008). *Fire protection handbook* (20th ed.). Quincy, Mass: National Fire Protection Association.

Cramer, S. M. (1995). Fire Endurance Modelling of Wood Floor/Ceiling Assemblies. In *Proceedings of the Fire & Materials Conference* (p. pp 105–114). Washington DC.

Cramer, S. M., Shrestha, D., & Mtenga, P. V. (1993). Computation of Member Forces in Metal Plate Connected Wood Trusses. *Structural Engineering Review*, *Vol. 5*(No. 3), pp 209–217.

Drysdale, D. (2011). *An introduction to fire dynamics* (3rd ed.). Hoboken, N.J: Wiley InterScience.

Dumont, F. (2010). *Summarised report of the Egolf round robin nr. TC2 09-1 in fire resistance testing*. Fire testing laboratory, University of Liège.

England, J. P., Young, S. A., Hui, M. C., & Kurban, N. (Eds.). (2000). *Guide for the Design of Fire Resistant Barriers and Structures*. Melbourne, Vic. Dandenong South, Victoria, Australia: Building Control Commission ; Warrington Fire and Research (Australia) Pty Ltd.

Friquin, K. L. (2011). Material properties and external factors influencing the charring rate of solid wood and glue-laminated timber. *Fire and Materials*, *35*(5), 303–327.

Gerlich, J. T. (2015a). Boundary walls. *BRANZ Build Magazine*, (146), p8–p9.

Gerlich, J. T. (2015b). Structural Adequacy vs Stability (Fire Resistance). *GIB News*, (2), p6–p7.

Harman, K. A., & Lawson, J. R. (2007). *A study of metal truss plate connectors when exposed to fire*. US Department of Commerce, Technology Administration, National Institute of Standards and Technology.

ISO. (1993). ISO 9705:1993 Fire tests -- Full-scale room test for surface products. International Organization for Standardization.

ISO. (1999). ISO 834-1:1999(en) Fire-resistance tests — Elements of building construction — Part 1: General requirements. International Organization for Standardization.

ITM. (2012). Know Your Timber Grades? Retrieved 5 January 2016, from http://www.itm.co.nz/Article?Action=View&Article_id=24

Karlsson, B., & Quintiere, J. G. (2000). *Enclosure fire dynamics*. Boca Raton, FL: CRC Press.

King, A. (2003). What's behind timber strength and stiffness? *Build Magazine*, *Build 74*, 12–13.

Kirby, B. R. (2004). Calibration of Eurocode 1: actions on structures - Part 1.2: actions on structures exposed to fire. *The Structural Engineer*, *82*, p38–43.

Kirby, B. R., Wainman, D. E., Tomlinson, L. N., Kay, T. R., & Peacock, B. N. (1999). Natural fires in large scale compartments. *International Journal on Engineering Performance-Based Fire Codes*, *1*(2), pp 43–58.

König, J. (1998). Structural Stability of Timber Structures in Fire - Performance and Requirements. In *Proceedings of COST Action E5 Workshop on Timber Frame Building Systems*. Building Research Establishment, U.K.

König, J., & Walleij, L. (2000). *Timber Frame Assemblies Exposed to Standard and Parametric Fires. Part 2: A Design Model for Standard Fire Exposure* (Report No. I 0001001). Stockholm: Trätek, Swedish Institute for Wood Technology Research.

Law, M. (1971). *A Relationship Between Fire Grading and Building Design and Contents - Fire Research Note* (No. 877). Fire Research Station. UK.

MBIE (2011). Compliance Document for New Zealand Building Code Clause H1 Energy Efficiency – Third Edition (Amendment 2). Ministry of Business, Innovation and Employment, Wellington, New Zealand.

MBIE, (2013a). Commentary for Acceptable Solutions C/AS1 to C/AS7. Ministry of Business, Innovation and Employment, Wellington, New Zealand.

MBIE, (2013b). Commentary for Building Code Clauses C1–C6 and Verification Method C/VM2. Ministry of Business, Innovation and Employment, Wellington, New Zealand.

MBIE. (2014a). Acceptable Solutions and Verification Methods For New Zealand Building Code Clause B1 Structure (Amendment 12). Ministry of Business, Innovation and Employment, Wellington, New Zealand.

MBIE, (2014b). Acceptable Solutions and Verification Methods For New Zealand Building Code Clause G7 Natural Light (Third Edition, Amendment 2)

MBIE, (2014c). C/AS1 Acceptable Solution for Buildings with Sleeping (residential) and Outbuildings (Risk Group SH) (Amendment 3). Ministry of Business, Innovation and Employment, Wellington, New Zealand.

MBIE, (2014d). C/AS2 Acceptable Solution for Buildings with Sleeping (non institutional) (Risk Group SM) (Amendment 3). Ministry of Business, Innovation and Employment, Wellington, New Zealand.

MBIE, (2014e). C/VM2 Verification Method: Framework for Fire Safety Design (Amendment 4). Ministry of Business, Innovation and Employment, Wellington, New Zealand.

MBIE, (2014f). New Zealand Building Code Handbook (Amendment 13). Ministry of Business, Innovation and Employment, Wellington, New Zealand.

MiTek Holdings, Inc. (2011). Lumberlok® Timber Connectors.

New Zealand Government. (2004, August 24). Building Act 2004, Public Act No 72. Ministry of Business, Innovation and Employment.

New Zealand Government. (2012a, April 10). New Zealand Building Code Clause A3 Building Importance Levels in Schedule 1 of the Building Regulations 1992. Wellington, New Zealand.

New Zealand Government. (2012b, April 10). New Zealand Building Code Clauses C1-C6 Protection from Fire in Schedule 1 of the Building Regulations 1992. Wellington, New Zealand.

New Zealand Government. (2015a). Acceptable Solutions and Verification Methods. Retrieved 3 January 2016, from http://www.building.govt.nz/blc-compliance-documents

New Zealand Government. (2015b). How the Building Code and Acceptable Solutions and Verification Methods work together. Retrieved 3 January 2016, from http://www.building.govt.nz/how-the-building-code-asvm-work-together

New Zealand Government. (2015c). New Zealand Standards. Retrieved 3 January 2016, from http://www.building.govt.nz/blc-nzstandards

New Zealand Government. (2015d). The Building Code and compliance. Retrieved 1 March 2016, from http://www.building.govt.nz/the-building-code

Nyman, J. F. (2002). *Equivalent fire resistance ratings of construction elements exposed to realistic fires*. Christchurch: Department of Civil Engineering, University of Canterbury.

NZ Wood. (2016). Light Timber Framing. Retrieved 10 January 2016, from http://www.nzwood.co.nz/learning-centre/lc-applications-and-products-sawn-timber/

Ostman, B. (Ed.). (2010). *Fire safety in timber buildings: technical guideline for Europe*. Boras, Sweden: SP Technical Research Institute of Sweden.

Quintiere, J. G. (2008). Compartment Fire Modeling. In *The SFPE Handbook of Fire Protection Engineering* (4th ed., pp. p3–195 – p3–203). One Batterymarch Park, Quincy, Massachusetts 02269: National Fire Protection Association ; Society of Fire Protection Engineers.

Richardson, L. R., & McPhee, R. A. (1996). Fire Resistance and Sound-Transmission-Class Ratings for Wood Frame Walls. *Fire and Materials*, *Vol 20*, pp 123–131.

SAA. (2005). AS 1530: Part 4: Fire Resistance Tests of Elements of Construction. Standards Association of Australia, NSW, Australia.

SANS. (2011, March). SANS 10400-T:2011, The application of the National Building Regulations, Part T: Fire protection (Edition 3). SABS Standards Division, 1 Dr Lategan Road Groenkloof, Pretoria 0001.

Schneider, U., Morita, T., & Franssen, J.-M. (1994). A Concrete Model Considering the Load History Applied to Centrally Loaded Columns under Fire Attack. In *Proceedings of the Fourth International Symposium on Fire Safety Science* (pp. 1101–1112).

Shrestha, D., Cramer, S. M., & White, R. H. (1994). Time Temperature Profile across a Lumber Section Exposed to Pyrolytic Temperatures. *Fire and Materials*, *Vol. 20*, pp 211–220.

Shrestha, D., Cramer, S., & White, R. (1995). Simplified models for the properties of dimension lumber and metal-plate connections at elevated temperatures. *Forest Products Journal*, *45*(7, 8), 35.

Spearpoint, M. (Ed.). (2008). *Fire engineering design guide* (3rd ed.). Christchurch, N.Z: New Zealand Centre For Advanced Engineering.

Standards New Zealand. (1988). *NZS 3631:1988 New Zealand timber grading rules*. Wellington, New Zealand.

Standards New Zealand. (1991). *Fire Properties of Building Materials and Elements of Structure* (No. Miscellaneous Publication No. 9). Wellington, New Zealand: Standards New Zealand.

Standards New Zealand. (2003). *NZS 3602:2003 Timber and wood-based products for use in building*. Wellington, New Zealand.

Standards New Zealand. (2004). *NZS 3622:2004 Verification of timber properties*. Wellington, New Zealand.

Standards New Zealand. (2005). *NZS 3603:1993 Timber Structures Standard (Amendment 4)*. Wellington, New Zealand.

Standards New Zealand. (2006). *NZS 3101:Part 1:2006 Concrete Structures Standard*. Wellington, New Zealand.

Standards New Zealand. (2010). *AS/NZS 4063.2:2010 Characterization of structural timber - Determination of characteristic values*. Wellington, New Zealand.

Standards New Zealand. (2011a). *AS/NZS 1748.1:2011 Timber - Solid - Stress-graded for structural purposes - General requirements*. Wellington, New Zealand.

Standards New Zealand. (2011b). *AS/NZS 1748.2:2011 Timber - Solid - Stress-graded for structural purposes - Qualification of grading method*. Wellington, New Zealand.

Standards New Zealand. (2011c). *NZS 3604:2011 Timber-framed buildings*. Wellington, New Zealand.

Sultan, M. A. (2000). Fire Spread via Wall / Floor Joints in Multi-Family Dwellings. *Fire and Materials*, *Vol. 24*(No. 1), pp 1–8.

Technical Committee ISO/TC 92. (2008). ISO 13943:2008(en) Fire safety -- Vocabulary. International Organization for Standardization.

Thomas, G. C. (1996). *Fire Resistance of Light Timber Framed Walls and Floors.* (Fire Engineering Research Report 97/7). Department of Civil Engineering, University of Canterbury, Christchurch, New Zealand.

Thomas, I. (2008). Enclosure Fire Temperature-Time Estimation. In *The SFPE Handbook of Fire Protection Engineering* (4th ed., pp. p4–208 – p4–227). One Batterymarch Park, Quincy, Massachusetts 02269: National Fire Protection Association ; Society of Fire Protection Engineers.

Thomas, P. H. (1986). Design guide: Structure fire safety CIB W14 Workshop report. *Fire Safety Journal*, *10*(2), 77–137.

Wade, C. A. (2015). FQ0712 RQ07 - Temperature Measurement using Plates. BRANZ, Porirua, New Zealand.

Wade, C. A., Baker, G., Frank, K., Robbins, A., Harrison, R., Spearpoint, M., & Fleischmann, C. (2013). B-RISK User Guide and Technical Manual. BRANZ Study Report 282. BRANZ, Porirua, New Zealand.

Wade, C. A., Gerlich, J. T., & Abu, A. (2014). The Relationship Between Fire Severity and Time-Equivalence. BRANZ Study Report 314. BRANZ, Porirua, New Zealand.

Walker, S. (2011). Roof trusses. *Build Magazine*, (Build 124).

White, R. H., & Cramer, S. (1994). Improving the fire endurance of a wood truss system (Vol. 1, pp. 582–589). Presented at the Pacific Timber Engineering Conference, Australia.

Winstone Wallboards Ltd. (2012). GIB® Fire Rated Systems - Specification and Installation Manual. GIB.